NUM 01

INTERNATIONAL JOURNAL OF **NUCLEAR MEDICINE** AND MOLECULAR IMAGING

WORLD FEDERATION OF NUCLEAR MEDICINE AND BIOLOGY CONGRESS ABSTRACTS

VOL 2 • JANUARY - APRIL 2015

PUBLISHING DIFFERENT

NUCLEAR MEDICINE

INTERNATIONAL JOURNAL OF **NUCLEAR MEDICINE** AND MOLECULAR IMAGING

EDITORIAL

CANCUN AND THE WORLD CONGRESS OF NUCLEAR MEDICINE

The World Congress of Nuclear Medicine will take place in a perfect site to know the last advances in our medical specialty and found out the most innovative technology in the field; as well as, for the exchange of ideas and sharing experiences with our peers. This place is Cancun, México! This tourist destination of the beautiful caribbean beaches and hotels of great infrastructure are ready to receive you in the best event of its kind this year.

This destination offers the perfect combination of sun & beach, fun, and culture along with the best facilities. You will see all the spectacularity that awaits us after daily conferences!

The world class tourist zone of Cancun, the spectacular landscapes in front the turquoise sea and memorable sunsets at Nichupte lagoon have been the perfect setting for superb medical meetings. Now it is the turn of the World Congress of Nuclear Medicine. If you come with a companion, there will be a lot of great amenities for them. We know...you will like to come again!

So, for these and many others reasons; It is a pleasure invite you to the XI Congress of the World Federation of Nuclear Medicine and Biology.

We will see you in Cancun this summer!!!

Best Regards.

Dr. Enrique Estrada Lobato
Current President WFNMB

INDEX

TERAPHY

TECHNOLOGIST

NEFROUROLOGY / GENITOURINARY

ONCOLOGY / HEMATOLOGY

RADIOPHARMACY

MUSCULOSKELETAL

PHYSICS / INSTRUMENTATION

MOLECULAR IMAGING

CARDIOVASCULAR

ENDOCRINOLOGY

RESPIRATORY

PEDIATRICS

GASTROINTESTINAL

INFECTION / INFLAMMATORY

NEUROLOGY

VALUE OF ELECTROENCEPHALOGRAMS FOR PET SCAN INTERPRETATION IN PATIENTS WITH SEIZURE DISORDER
Isis Gayed, Osagi Ighile, Mina Fanous, Synda Vandenmooter, Usha Joseph, Takijah Heard.

UNITED STATES

The importance of electroencephalopgram (EEG) localization of seizure focus in conjunction with PET scans interpretation has been scarcely investigated. We evaluated the correlation of EEG and PET findings in patients with refractory seizure disorders. Methods: We retrospectively included consecutive adult patients who underwent PET scans and MRI orMagnetoencephalography (MEG) between May, 2010 to November, 2011. EEG as well as MRI and/or MEG findings were correlated with blindly read PET scans for localization of the epileptogenic focus. Both ictal and interictal EEG was available in 33 patients and interictal EEG in 2 patients. MRI was performed in 29 patients and MEG in 4 patients. Two patients had neither MRI nor MEG scans.Results: 35 patients (17M, 18F) with an average age of 38.9 yr were included. Seizure types were complex partial seizures in 27 patients, generalized seizures in 6, simple partial seizures in one and status epilepticus in one. A correlation of the site of seizure origin between EEG and PET scan was achieved in 22 patients (63%). Discordant results were noted in 13 patients (37%) with 3 out of 13 patients (9%) showing good clinical correlation to PET and non-localizing EEG findings. Nine out of 29 patients (31%) had also correlating MRI findings while 7 had discordant findings (24%) and 13 normal MRI (45%) results. Conclusion: There is good correlation for seizure site detection between PET and EEG and/or clinical findings. PET scan is more sensitive than MRI in seizure site detection.

99MTCSPECT/CTVOLUMETRICQUANTIFICATIONCORRELATESWITHCLINICALMEASURESINADVANCEDPARKINSON´SDISEASE.
Artur Martins Novaes Coutinho Coautores: Etchebehere P, Santos AO, Vicente A, Ghilardi MG, Cury RG,Martinez RCR, Fonoff ET, Camargo EE.

BRAZIL

Introduction: ^{99m}Tc-TRODAT is a pre-synaptic dopamine transporter (DAT) SPECT radiotracer used for differential diagnosis between Parkinson's disease (PD) and non-Parkinsonian motor dysfunctions such as essential tremor. Semi-quantitative analysis of ^{99m}Tc-TRODAT uptake with the help of manually drawn volumetric regions of interest (VOI) in SPECT/CT equipments could be a reliable way of measuring the progression of PD, since the lower the uptake in the basal ganglia, the greater the motor dysfunctions. Clinical scales, such as the Unified Parkinson's Disease Rating Scale (UPDRS) and Hoehn and Yahr scale (H&Y), are widely used by clinicians to measure PD function and disability. UPDRS is a numeric scale that measures the disability related to PD, including motor and cognitive symptoms (the higher the numeric score, the greater the disability). The UPDRS scale has also sub-scales that measure exclusively motor symptoms (UPDRS III) or axial motor dysfunctions (UPDRS axial). The H&Y scale measures qualitatively the progression of PD, divided by progressive qualitative stages. Objective: to correlate the basal ganglia uptake of ^{99m}Tc-TRODAT quantified with SPECT/CT and VOI with the clinical scales in patients with advanced stage PD.-Methods: sixteen patients (9 male; 7 female) with advanced stage PD were prospectively enrolled. All patients signed an informed consent prior to the studies. ^{99m}Tc-TRODAT uptake in the basal ganglia was quantified by the following equation: (target area VOI – occipital cortex VOI)/ occipital cortex VOI). The numeric results of left and right striatum and from each nucleus (left and right putamen and caudate) were then correlated with the clinical scales (UPDRS III, UPDRS axial and H&Y) using Pearson's (variables with a "normal" distribution) or Spearman's coefficients (variables without a "normal" distribution) ($p \leq 0.05$).Results: The mean time from initial symptoms to the ^{99m}Tc-TRODAT SPECT/CT study was 10.1 ± 3.8 years. The mean values of the VOI were 0.36 ± 0.25 for right striatum and 0.43 ± 0.25 for the left striatum. There was a significant inverse correlation of left striatum uptake with UPDRS III (R= -0.57; p = 0.0215), UPDRS axial (R= -0.54; p = 0.033) and H&Y (R= -0.61; p = 0.011). The left putamen also demonstrated a significant inverse correlation with UPDRS III (R= -0.63; p = 0.0094), axial UPDRS (R= -0.64; p = 0.0079) and time from initial symptoms (R= -0.48; p = 0.057). Other less significant inverse correlations were found with clinical scales in other nuclei. Conclusion: ^{99m}Tc-TRODAT uptake in the basal ganglia using SPECT/CT and semi-quantitative VOI analysis showed an inverse correlation with PD clinical scales and time from initial symptoms. These results suggest that, as previously hypothesized, the lower the ^{99m}Tc-TRODAT uptake in the basal ganglia the higher the impairment in the clinical scales. ^{99m}Tc-TRODAT SPECT/CT is a potentially reliable tool to evaluate disease status.

CONCORDANCE BETWEEN THE SPECT AND SPECT-CT IN THE EVALUATION OF PATIENTS WITH PARKINSONISM USING 99MTC-TRODAT-1"

Cristián Montalba[1] , Arturo Baeza López[2] ,María PazMartínez[2], Ricardo Castillo[1] , Víctor Díaz[1] .
[1] *Escuela de Tecnología Médica, Facultad de Medicina, Universidad del Desarrollo.*
[2] *Departamento de Imagenología, Servicio de Medicina Nuclear, Clínica Alemana Santiago,Chile.*

CHILE

One alternative to diagnose Parkinsonism, is SPECT image with the radiopharmaceutical 99mTc-TRODAT-1. For this, it is necessary to measure the intensity value of 99mTc-TRODAT-1 in ROIs uptake them in the basal ganglia. However, to select the correct ROI is difficult, because the quality of the reference image is low and it has not good definition of the anatomical structure edges. The resolution of the reference image can be achieved by using an hybrid image generate by SPECT-CT technique. This hybrid images provides an improve SPECT image, with anatomic information give it by CT. This allows to define a more precisely ROI. For this propuse 20 subjects (11 men, 9 women) with a clinical diagnosis of Parkinsonism were studied according to UPDRS scale. For the acquisition of the images all subjects were injected intravenously with a dose of 25 mCi (925 MBq) in a 2ml volume of 99mTc-TRODAT-1. The imaging was performed 4 hours later using a SPECT-CT Symbia T with 4 detectors, double head camera equipped with ultrahigh resolution fabeam collimators. First, SPECT images were acquired and in the same position, we obtained the CT images. Later the hybrid image was obtained fusing the SPECT and CT images. The image analysis was performed by one Nuclear Medicine Physician and two Nuclear Medicine Technologists. The ROI were drawn on the SPECT and SPECT-CT images in the following anatomic regions: the putamen, caudate nucleus, and the striatum of both brain hemispheres (area of the specific striatal uptake) and occipital lobe (area of nonspecific striatal uptake) in a transversal slice with the highest activity of the radiopharmaceutical in the basal ganglia. Finally, we compared the methods by the statistical method Bland And Altman, which determines the concordance between both methods. From the results, we can determine there is no concordance between the values obtenied by SPECT and SPECT-CT. Finally, with the use of SPECT-CT we can obtain a precise uptake value by improving the anatomical structure of the basal ganglia. Therefore, the contribution of the anatomical reference by the CT scan in the acquisition of the images, allows a more accurate measurement and precise the quantification of the ROI.

ALTERED BRAIN METABOLIC PATTERN DEPICTED BY 18F FDG PET AND ITS CLINICO-ANATOMICAL CORRELATION: A CASE REPORT

Dr, Ivan E. Diaz Meneses and Dra. Nora E. Kerik Rotenberg.
PET/CT Molecular Imaging Unit, National Institute of Neurology and Neurosurgery of Mexico.

MEXICO

The metabolic findings in brain 18F-FDG PET studies performed for oncological purposes must be reported in an integral manner and go beyond of just mentioning the metabolic tumoral activity; besides it, there are many purely funtional alterations -with out anatomical correlation- that have a clinical significance by a neurological approach.

We present a case report of a patient with a tumoral mass which stars with altered alterness, bradylalia, campimetric visual alterations, right thoracic an d pelvic extremities weakness that progressed to a dense pyramidal syndrome (right hemiplegia), and sphincter incontinence. A Magnetic Resonance was performed and reveal a mass that comprises the white matter of the left temporal lobe and extended to the posterior arm of the ipsilateral internal capsule. In the 18F-FDG PET study the mass was hypermetabolic, but there were brain end cerebellar cortical zones with generalized hypometabolism. The patient was diagnosed with primary central nervous system lymphoma and underwent its oncologic treatment.It is known, that the neurological clinical impairment not always have an structuralexplanation and some pathophysiological events only have a functional manifestation, as in this case report.It is important that the reporting nuclear medicine physician knows the neurologicalsemiology and be capable of make a correct correlation between the clinical manifestion and the PET findings.

ASSESSMENT OF STRIATAL DOPAMINERGIC UPTAKE IN PATIENTS WITH MODERATE- TO ADVANCED-STAGE PARKINSON'S DISEASE COMPARED TO CONTROLS BY MEANS OF CO-REGISTERED 18F-DOPA PET/CT AND MRI IMAGES

MD Maria Bastianello[1]. Argentina, MD Danny Mena[1], MD Martin Aguilar[2], RT Hugo Corradini[1], Ph Amalia Pérez[3], PhD Alejandro Valda[3], MSc Federico Biafore[3], MD Cecilia Peralta[4]

[1] *Molecular Imaging and Metabolic Therapy Section. Hospital Universitario CEMIC*
[2] *Neuroradiology. Hospital Universitario CEMIC*
[3] *Escuela de Ciencia y Tecnología. Universidad Nacional de San Martin*
[4] *Movement Disorders. Neurology Department. Hospital Universitario CEMIC*

Objectives
To evaluate the striatal dopaminergic function using *6-[F-18]Fluoro-L-dopa (FDOPA)* PET/CT scan along with MRI in patients with Parkinson's disease (PD) and controls.Material and MethodsPatients: n=11; mean age=66 y.o. (41–80); male/female=8/3; mean PD duration=9.2 y (6–14): H&Y stage III (n=9), IV (n=2), UPDRS=32 ON (21–48). Controls: n=5; mean age=55 y.o. (37–81); male/female=3/2. All subjects gave written informed consent from Institution and National Authorities prior to procedures.

PET/CT scanning was performed after injection of 18F-DOPA (0.05–0.07 mCi/kg.) to patients and controls. All subjects received carbidopa, 100 mg 60 minutes and 50 mg 5 minutes before administration of 18F-DOPA. Acquisition was performed 75 minutes post-injection in a PET/CT Philips Gemini 64 TF. They were also subjected to volumetric MRI. After normalization to a Hammers's atlas, the MR image was segmented in the structures of interest caudate, putamen and cerebellum. The resulting segmentation was applied to a co-registered PET-MRI for quantification of volume, count density and total number of counts per structure. Concentration uptakes in caudate and putamen were normalized to cerebellum. Mean and standard deviation of normalized uptakes were calculated for patients and controls. From this, a relative loss index was calculated as the percentage of patient uptake decrease with respect to controls. For each patient, left vs. right normalized uptake was evaluated.

Results For patients, the mean normalized uptake in caudate and putamen were 1.26 (sd=0.28) and 1.34 (sd=0.11) respectively while for controls they resulted in 1.65 (sd=0.25) and 2.19 (sd=0.20). These values show significant differences for putamen between both populations. Patient loss index for putamen is 39% and for caudate 24%. In the left-right asymmetry analysis, 7 patients showed increased uptake in the right caudate. In the same patient group, 4 of them also showed increase in right putamen. The only patient diagnosed with initial symptoms on the left side consistently showed a slight increase uptake in left caudate and putamen.

Conclusions: It was possible to reliably determine uptake values of 18F-DOPA in the striatal structures of interest based on co-registered PET/CT and MRI images. These preliminary results show significant lower uptake in patients compared to controls, giving the possibility to use 18F-DOPA as a useful biomarker for dopamine-deficient Parkinsonism. The observed left-right asymmetry is more pronounced for caudate than for putamen and correlates with clinical symptoms of initial disease development. On the one hand, this is the first study in Argentina on biomarkers for PD with PET/CT. On the other, it is the first to incorporate advanced segmentation and quantification techniques based on the combination of MRI and molecular imaging modalities.

DECREASED BRAIN UPTAKE OF ^{18}F-FDG IN LYMPHOMA PATIENTS WITH EXTENSIVE TUMORAL OR BONE MARROW UPTAKE. REPORT OF THREE CASES

Daniel Vicentini.

CHILE

In oncologic positron emission tomography with computed tomography (PET/CT) studies with ^{18}F-fluorodeoxyglucose (^{18}F-FDG), a rare phenomenon has been described in which extensive areas of abnormally increased glucose metabolism are associated with very low background activity and decreased normal tissue uptake in some organs, such as the brain. This pattern is called "metabolic superscan" and has been described in patients with lymphoma, lung cancer, prostate cancer, renal adenocarcinoma and renal neuroectodermal tumor.

In this report we describe three patients with lymphoma that showed a metabolic superscan pattern on PET/CT, in which brain uptake comparison with follow up study was performed. Two patients showed intense and homogeneous metabolic activity in bone marrow, suggesting chemotherapy induced bone marrow hyperplasia. The third patient showed extensive bone, hepatic and splenic tumoral involvement with high glucose uptake. All patients showed low brain uptake in a diffuse pattern, with relatively preserved striatum activity and without any CT abnormality. None of these patients reported neurological symptoms or use of medications that could modify brain metabolism. In the follow up study, all patients showed resolution of the intense tumor or bone marrow metabolic activity and normal brain uptake.

Patients with metabolic superscan show an abnormal brain uptake pattern that is probably explained by ^{18}F-FDG redistribution, with no actual brain functional abnormality. This pattern is reversible and must be identified to avoid misdiagnosis.

INCIDENTAL BRAIN FINDINGS IN ONCOLOGIC PET/CT: DESCRIPTION OF A CASE SERIES

Daniel Vicentini.

CHILE

The usual field of view of the oncological FDG PET/CT protocol is from skull base to upper third of the thighs, excluding most part of the brain. The rationale for this approach is the high gray matter physiological activity may hinder metastases identification. However, it has been described that in a small percentage of patients, PET/CT shows previously unknown abnormalities in the brain, which in some cases lead to changes in management. This prospective case series study describes incidental brain findings in oncologic PET/CT studies performed from the top of the head to the upper third of the thighs, using proper windowing and PET color scale for brain visualization. Within 235 oncologic FDG PET/CT studies in a four month period, we identified 9 studies with incidental brain abnormalities (3.8%). These included 4 patients with metastases, 1 with a benign primary lesion (meningioma), 3 with brain infarction and 1 with a dementia pattern. Case 1: Patient in evaluation for restaging of cervicouterine cancer. The computed tomography showed a 10 mm extraaxial frontal lesion with the characteristics of a meningioma. Case 2: Post-treatment evaluation of a lung cancer patient. Three metastatic lesions were found in the brain, with no other sites of dissemination. Case 3: patient in follow up for a treated sarcoma of the thigh. Three metastatic lesions were found, two in the lungs and one in the brain. Case 4: staging of a newly detected lung tumor. The study showed multiple thoracic lymph node involvement, bilateral pulmonary metastases and two brain metastases. Case 5: patient with suspicious pleural effusion. Findings were consistent with a primary pleural neoplasm with mediastinal lymph node involvement, bone metastases and intracranial metastases in gray matter and leptomeninges. Case 6: patient with lymphoma in post-treatment evaluation. The study showed a large infarction in the territory of right middle cerebral artery, with crossed cerebellar diaschisis. Case 7: staging of a non-Hodgkin lymphoma. There was diffuse bilateral frontal and anterior temporal hypometabolism, suggestive of frontotemporal dementia, and an old brain infarction. Case 8: patient with suspicious pulmonary nodules. An old left occipital infarction was found. Case 9: staging of a newly diagnosed colorectal cancer. PET showed diffuse bilateral frontal and temporal hypometabolism, suggestive of frontotemporal dementia, and unilateral occipital hypometabolism without anatomic correlation.

In spite of the high metabolic activity of gray matter, the evaluation of the brain in oncologic PET/CT studies is possible. It can lead to identification of metastases and other incidental findings, which may change patient management.

BRAIN DEACTIVATION DIMINUTION OBSERVED AFTER A MOTH OF COCAINE ABSTINENCE IN DEPENDENT PATIENTS PERFORMING EXECUTIVE TASKS.

JC Quintana, T Massardo. Chile, R Jaimovich, C Ibáñez, J Véliz, J Pallavicini, P Flores, R Chandía, G Castro, R Fernández, M. Servat, J Pereira.

HOSPITAL CLÍNICO UNIVERSIDAD DE CHILE AND HOSPITAL CLÍNICO PONTIFICIA UNIVERSIDAD CATÓLICA DE CHILE.

INTRODUCTION: Executive functions are commonly impaired in chronic cocaine consumers, who present difficulties in take-decision tasks. Wisconsin Card Sorting Test (WCST) is able to measure perseverative behavior in these patients. WCST should activate in healthy subjects prefrontal, dorsolateral, superior parietal and anterior cingulated areas.The aim of the study was to evaluate brain activation using WCST after recent cocaine consumption and after a month of strict controlled in-hospital abstinence.METHOD: We studied 27 cocaine DSM-IV criteria dependent patients (mean age: 31 y.o; gender: 89% males; mean education: 14 years; mean cocaine consumption: 6.9 years with a mean: 1.87 g/day).Cocaine was their main drug of dependency and all have proved presence of cocaine in urine analysis. Brain perfusion SPECT with ^{99m}Tc-ECD was acquired at baseline and after a month of in-hospital cocaine abstinence at rest and neuroactivated. Perseverative errors (PE), non-perseverative errors (NPE) and perseverative answers (PA), normalized to age and education, were expressed as z scores. Statistical Parametric Analysis (SPM8) was applied to evaluate the regional cerebral blood flow (rCBF) activation using the WCST parameters as covariates.

RESULTS: At baseline 10/27 patients presented more than expected PE (3 mild, 5 moderate and 2 severe) and after abstinence 9/27 (5 mild, 3 moderate and 1 severe); they were able to reach a mean of 4.25 and 5.03 out of 6 WCST categories, respectively (p=ns). PE, PA and NPE did not change significantly with abstinence; however, total errors diminished (p=0.0207). At baseline, we observed bilateral parietal cortical perfusion activation extending slightly to prefrontal areas and also deactivation of prefrontal ventrolateral cortex including anterior cingulated area. After detoxification, the amount and extension of ventral prefrontal and anterior cingulate deactivation decreases. The activation areas did not change significantly. PE, PA and NPE, introduced as covariates in the change of activation after a month of cocaine deprivation, did not demonstrate significant association.
CONCLUSIONS: After cocaine detoxification, abnormal executive task results persisted without improvements in the rCBF activation pattern of dependents. Nevertheless, abnormal prefrontal and anterior cingulate deactivation was less than the observed at base-

line, which might be a sign of some sort of recovery. This work support that longer withdrawal periods of cocaine are necessary to recover brain functions, as is observed clinically.

USE OF 99MTC-TRODAT-1 IN PATIENTS WITH MACHADO-JOSEPH DISEASE – A PRELIMINARY STUDY

Paulo Henrique Silva Monteiro.

BRAZIL

INTRODUCTION: Machado-Joseph's disease (spinocerebellar ataxia type 3) is a dominantautossomic neurodegenerative disease being the most common dominant autossomic ataxia.Studies with 99mTc-TRODAT-1 brain SPECT have shown a reduced expression of dopamine receptors in these patients, including asymptomatic patients.

OBJECTIVE: This preliminary study aims to evaluate 99mTc-TRODAT-1 uptake in patients withMachado-Joseph's disease.METHODS: Three patients with a known diagnostic of Machado-Joseph's disease and a healthycontrol patient (for quality control and comparison) were selected. Each patient was injectedwith approximately 740 MBq (20 mCi) of 99mTc-TRODAT-1 and performed brain SPECT imaging(128 views, 128 X 128 matrix, 50 seconds per frame) four hours post-injection. An iterativemethod was used for image reconstruction (OSEM, 4 subsets, 4 iteration), along with a 9,85 Gaussian filter for noise attenuation. Quantification was performed by drawing regions-of interest(ROI) on the left and right striate nuclei and on the occipital region (which serves as background), according to this formula: (area-of-interest ROI – occipital ROI)/ occipital

ROI. RESULTS: Visual and quantitative analysis of the control individual image presented expected values for normal patients (right striatum 0.98; left 1.12; normal: 1.1 + 0.25). Visual analysis of the Machado-Joseph patients showed bilaterally decreased striatal uptake and quantitative analysis presented lower values: case A – right striatum 0.64 and left 0.72; case B – right striatum 0.31 and left 0.28; case C – right striatum 0.17 and left 0.15.

DISCUSSION: TRODAT is a tropane derivative which, when labeled with technetium-99m,crosses the blood-brain barrier and binds in pre-synaptic dopamine transporter terminalswhich is reduced in motor syndromes like Parkinson's disease. Machado-Joseph's disease has five clinical subtypes, with primarily motor symptoms, often leading to death through aspiration pneumonia. Its clinical diagnosis, due to phenotypical variation, is difficult, allowing for confusion with other motor syndromes. Studies with 99mTc-TRODAT-1 brain SPECT have shown a reduced expression of dopamine receptors in these patients, including asymptomatic patients. However, the number of patients in these studies is small, making differentiation by clinical phenotypes or disease stages difficult. In this preliminary study 99mTc-TRODAT-1 brain SPECT also presented lower basal ganglia radiotracer uptake in patients with Machado-Joseph's disease, like other studies in literature. However, further studies with more patients are required to confirm these findings and to correlate different phenotypes and disease stages to visual and quantitative 99mTc-TRODAT-1 uptake patterns.

THERAPY

OPTIMIZATION OF RADIO-IODINE 131 DOSE IN TREATMENT OF CHILDREN WITH DIFFUSE LUNG METASTASIS FROM THYROID CARCINOMA- LOCAL EXPERIENCE AT AL-ASSAD UNIVERSITY HOSPITAL, DAMASCUS

Majdi Zein Institution: Al-Assad University Hospital Address: 17th Nissan Street, Damascus, Syria, P.O.Box: 10967.

SYRIA

Objective:Children with diffuse lung metastasis considered to be a challenge for radio-Iodine treatment, due to critical difference between the effective treatment dose and side effects expected after long -term treatment with several radio-iodine 131 doses Material and Methods: 11 children suffering from Diffuse Lung Metastasis from Thyroid Carcinoma were admitted to the department of nuclear medicine at Al-Assad University Hospital, Damascus at the period between May 2010 until March 2012.

Age of patients was from 7 to 14 years, five males and six Females.General medical evaluation was done for all patients physically and psychiatrically. Also , WBC – blood test for renal function-Thyoglobulin level- Ultrasound image for the anterior neck and chest x-ray were obtained. After discontinue of thyroid hormone for 3-4 weeks and withdrawing foods containing iodine for enough time a doses of Radio-active iodine between 30 -60 mCi (depending at the patient age and weight) were given at the department, admission prolonged for 3-5 days according to residual activity in the body. Whole body scans were performed at the 5th day after radio-iodine treatment dose.Six months after radio-iodine treatment second total evaluation was done for all patients. All patients showed residual metastasis at the lungs, without any residual tissue at the neck.According to initial results all patients were given a second radioactive-iodine dose of 70-100 mCi.

Another repeated doses were given according to results of general evaluation until total remission of the disease in 5 children.No significant side effect nor respiratory symptoms were noted except for some dyspinia in 3 children.

Results: 7 of 11 patients revealed total remission after three to five cycles of radio-iodine treatment including negative Iodine WBS and thyroglobulin level around zero, while 4 patients showed no significant improvement after the fifth dose. Where the whole body iodine whole body scan still positive in the lungs, also Thyroglobulin level remained in high levels with mild decrease writhen two month after treatment. Conclusions:Diffuse lung metastasis from thyroid cancer can be treated safely using a doses of radioactive-iodine between 70-100 mCi without significant side effects, and the treatment overall results were acceptable.Name of presenter: Prof. MAJDI ZEIN.

STUDY ON CLINICAL APPLICATION OF IODINE-131 RADIOTHERAPY COMBINED WITH LEUCOGE IN POST-OPERATED PATIENT WITH DIFFERENTIATED THYROID CANCER

Rong Fu Wang. China, Fei Wang, Ying Li, Yonggang Cui, Yuan Zhao, Qian Wu.

DEPARTMENT OF NUCLEAR MEDICINE, PEKING UNIVERSITY FIRST HOSPITAL, BEIJING 100034, CHINA

Objective: To investigate the feasibility of combined radioactive iodine [^{131}I] and Leucoge curing the differentiated thyroid carcinoma after operation and in order to enhance the therapeutic compliance and efficacy in the thyroid cancer patients during therapy period. Methods: The information was collected and then had a retrospective analysis in 167 differentiated thyroid cancer patients (01/2007 - 03/2013) with postoperative residual thyroid tissue, local recurrence or lymph node and systemic metastases.

The therapeutic effectiveness of ^{131}I. combined with Leucoge was evaluated during therapy period. Results: 167 patients divided into A group(N=47), B group(n=54) and C group(n=66) had no change ($P>0.05$) in sample size, age, WBC and PLT before curing of ^{131}I. The level of WBC and PLT had selective change after curing of ^{131}I in three groups patients in which WBC and PLT had significantly decreased ($P<0.05$)in A, B group and C group has no effect ($P>0.05$). The efficacy of ^{131}I on differentiated thyroid carcinoma with postoperative residual thyroid tissue, local and distant metastases was confirmed in this study. Conclusion: The combination of ^{131}I and Leucoge is an effective cure on postoperative differentiated thyroid carcinoma to prevent the decrease of WBC and PLT as well as bone marrow suppression.

[Kyeword] Differentiated thyroid cancer; Radioiodine; White blood cell; Platelet; Leucogen.

EVALUATION OF ^{188}RE-HEDP EFFICACY IN METASTATIC BONE PAIN PALLIATION THERAPY

Davood Beiki[1]. Iran, Babak Fallahi[1], Maryam Tajik[1], Peiman Haddad[2], Amir Mohammad Arefpour[2], Hamidreza Mirzaei[3], Armaghan Fard-Esfahani[1], Alireza Emami-Ardekani[1], Mohammad Eftekhari[1].

[1] Research Center for Nuclear Medicine, Tehran University of Medical Sciences, Tehran, Iran.
[2] Department of Radiation Oncology, Cancer Research Center, Cancer Institute, Tehran University of Medical Sciences, Iran.
[3] Radiation Oncology Department, Cancer Research Center, Shohada-E-Tajrish Hospital, Shaheed Beheshti University of Medical Sciences, Tehran, Iran.

TEHRAN, IRAN

Objective: Bone metastases are the most common cause of cancer-related pain in various primary malignant tumors, most often, breast and prostate. ^{188}Re-hydroxyethylidene diphosphonate (^{188}Re-HEDP) is a new and less expensive bone seeking radiopharmaceutical with favorable physical characteristics of the radionuclide such as short half life of 16.9h, maximal - energy of 2.1 MeV with a 15% - component of 155 keV and easily available from an in-house ^{188}W/^{188}Re generator. The aim of this study is to evaluate the therapeutic efficacy and safety profile of bone palliative therapy following administration of ^{188}Re-HEDP.

Materials and Methods: Seventeen patients (7 men, 10 women; mean age, 57.1±13.3 years) with painful metastatic bone lesions were included in the study. Before and after treatment with 1 mCi/kg of ^{188}Re-HEDP, the patients were followed at weekly intervals for the first months and every two weeks thereafter for as long as four months using standardized sets of questions including Karnofsky index and ECOG (Eastern Cooperative Oncology Group) performance status. Hematologic profiles were recorded before therapy and weekly for 8 weeks after treatment.

Results: Significant pain relief was found in 68.8% of our patients. Decreased from 8.34±2.10 to 5.55±2.45 at visual analogue scale was observed 4 weeks after the treatment. The osteoblastic lesions (breast and prostate) showed rather similar response to the treatment. Mean platelet counts decreased in 6th week and returned to baseline level in 8th week. Mean leukocyte counts in 6th week were lower than baseline (4913±2210/ml vs. 6502±2410/ml; p=0.02) and one patient showed grade III leukopenia without any serious complication.

Conclusions: ^{188}Re-HEDP is an effective radiopharmaceutical in metastatic bone pain palliation. Side effects include mild and transient thrombocytopenia and leucopenia and no life threatening side effect is observed.

METHOD FOR COMPARING THE INDUCTION OF TSH SECRETION WITH rhTSH VS METHIMAZOLE FOR THE TREATMENT WITH 131I IN GOITER MULTINODULAR. ANATOMO-FUNCTIONAL COMPARISON.

Alberto E. Hardy Pérez[1-3], México, Consuelo Arteaga De Murphy[2]. Eleni Mitsoura[3]. Keila Isaac Olivé[3]. Martha Pedraza López [2].

[1] Centro Oncológico Estatal-Issemym (Coe).
[2] Instituto Nacional De Ciencias Médicas Y Nutrición "Salvador Zubirán".
[3] Facultad de Medicina Uaemex.

MEXICO

INTRODUCTION Underactive thyroid nodules, large volume are frequent pathology associated with iodine deficiency and other factors. Aesthetic and cause compression of neck structures and risk of hyperthyroidism problems. Treatment is usually surgical, but there can be contraindication or patient no acceptance and is chosen to reduce the volume with 131I. This is used for more than three decades in European and Latin American countries ago.The administration dose of 0.01-0.03 mg recombinant thyroid stimulating hormone (rhTSH) uptake increases double or more and produce a homogeneous distribution of 131I. However, induction of uptake rhTSH is expensive and prohibitive for some countries. Researchers Brazilians and Mexicans reported increased release of endogenous TSH induced methimazole therapy. 131I uptake increased from 21 to 78% average increase endogenous TSH 11.7 ± 5.4 mIU / L and decreased volume thyroid of 46% after administration of radioactive iodine.

OBJECTIVE Design a method to compare, in patients with multinodular goiter, TSH levels, T3, T4, before and after induction with methimazole or rhTSH, randomized into two groups and measures both rates of uptake and elimination 131I, valuing the change in volume of the thyroid gland to 6 months of treatment.

RESULTS Approval of the Research Ethics Committee of the Cancer Center-State ISSEMyM Select 10 patients with multinodular goiter not candidates for surgical treatment and obtaining informed consent Profile and thyroid echosonography.

Randomize: Group I methimazole induced or rhTSH group II Manage the group I methimazole, 10-15 mg / day for 4 weeks titrated to maintain levels above 9.0 pmol / L free T4 monitored each week. Profile thyroid. Manage rhTSH group II, intramuscular, two doses of 0.9 mg, separated by a 24-hour period Profile thyroidIn both groups: Manage 18.5 MBq (500 Ci) of 131I orally Perform dynamic scintigraphic study of iodine uptake by the thyroid Acquiring, as specific protocol, static images thyroid, 1, 4, 8 and 24 hours, 4 and 8 days Managing ablative dose of 1110 MBq (30 mCi) of 131I schemes together with propranolol and prednisone. Profile thyroid before administration and every 15 days for two months or when required, as symptoms of hypothyroidism. Ecosonagrafía 3 and 6 months post-administration of 131I. Analyze data obtained from descriptive and statistical comparison of groups.
Significance level <0.05.

CONCLUSIONS Submit to empirical test method designed.

RADIATION DOSE RATE AFTER RADIOIODINE THERAPY CORRELATES WITH RESIDUAL DISEASE IN PATIENTS WITH DIFFERENTIATED THYROID CANCER

Gulin Ucmak.

TURKEY

The aim of this study was to evaluate the factors effecting radiation dose rate (DR) measured on the day of discharge after administration of radioiodine therapy in patients with differentiated thyroid cancer (DTC). Method: 144 patients who received radioidoine ablation (RIA, n:103, dose range: 100-200 mCi) or radioiodine therapy (RIT, n:41, dose range: 200-300 mCi) for DTC and have iodine –avid tumors on post-therapy scan were included in this retrospective study. Patient height, weight, body surface area (BSA), serum Thyroglobulin levels were measured. Optimal hydration and premedication for possible side-effects of radioiodine was given to all patients who were hospitilized for administration of RIA/RIT. DR was measured 72 hours after the administration of radioiodine, on the day of discharge and post-therapy whole body scans (WBS) were acquired. On WBS, ROIs were drawn on neck, thorax and abdominopelvic regions after background corrections, ratios were obtained. Patients were grouped according to distribution of radioiodine -avid tumor uptake as; Group1: uptake limited to neck, Group2: uptake in neck plus one additional distant metastasis and Group3: widespread uptake. Measured DR were compared between groups. In addition, DR were correlated with the dose given, neck/whole body(WB), thorax/WB, abdomen/WB, serum Tg and BSA. Results: Measured dose rate was 2±2.2 mR/sa (0.2-11 mR/h). DR was significantly differed among groups 1,2 and 3 (1.5±1.2 mR/h vs. 2.9±2.1 2 vs. 4.8±4.1 mR/h respectively, p=0.003). We observed a positive correlation between serum Tg levels and DR (p=0.0001). DR was comparable between patients who received RIA and RIT (1.7±1.5 vs. 2.6±3.3 mR/h). The radioiodine dose administered was not correlated with the measured DR (p>0.05). We found that thorax/WB ratio were correlated with DR due to lung and/or thorasic vertebra metastasis, however neck/WB and abdomen/WB ratios were not correlated with DR. Conclusion: Neither the residual tyhroid tissue nor the administered dose alone have correlation with DR measured 72 hours after radioiodine ablation/therapy. In DTC patients treated with radioiodine therapy, DR significantly associates with the extent of radioiodine-avid disease which is- in part- reflected by serum Tg levels.

DO THE PATIENTS SUBMITTED TO RADIOIODINE THERAPY CAN BE DISCHARGED ON THE SAME DAY OF ADMISSION BASED ON THE NEW BRAZIL CNEN RULES

Thiago Souza Rocha Alves.

BRAZIL

ObjectiveTo evaluate the exposures rates of patients treated with ^{131}I dose and the time until hospital discharge with appropriate radiometric levels based in new CNEN rules for discharging lesser than 0,03 mSv/h measured two meter far.Materials and MethodsIt is a cross-sectional prospective study of 38 patients diagnosed with differentiated thyroid carcinoma (DTC), submitted to total thyroidectomy (TT) and radioiodine therapy with ^{131}I (RIT) doses between 3700- 5550 MBeq (100-150mCi), between February to April 2014. The exposure's rates were measured immediately after receiving ^{131}I oral dose during the same day until 12 hours and with 24 hours in the cervical region with one and two meters far the patients.

Results Twenty nine patients received 3700 MBeq of ^{131}I, the exposure's rate immediately after dosing, showed average 0,155 mSv/h (one meter far) and 0.058 mSv/h (two meters far). In the mean-time interval of 7.11 hours after administration, the exposure's rate was 0.098 mSv/h (one meter far) and 0.0310 mSv/h (two meters far). Eighteen (62%) of these 29 patients had appropriate radiometric levels (two meters far) to hospital discharge in the time interval described (mean 7.11 h), and all of them until 12 hours. Nine patients received doses of 5550MBeq of ^{131}I, the exposure's rate immediately after dosing, showed average 0.242 mSv/h (one meter far) and 0.083 mSv/h (two meters far). In the meantime interval of 6.40 hours after administration, the exposure's rate had an average of 0.146 mSv/h (one meter far) and 0.049 mR/h (two meters far). No one of the 9 patients that received dose of 5550 MBeq had appropriate radiometric levels to left the hospital within 12 hours.Discussion The international community and the radiation protection agencies from different countries developed restricted rules and restricted treatment protocols. In Brazil, we required mandatory hospitalization of all RIT patients with doses above 1.1 GBq (30 mCi). These hospitalizations are not always guided by clinical criteria, disregarding the patients' socioeconomic status, generating high costs and limiting the access to these procedures. Usually the hospitalization period was at least one day. In December 2013, Brazilian´s National Nuclear Energy Commission (CNEN) changed some rules allowing the release of RIT patients with exposure rate less than 0.03 mSv/h, measured two meters far and that study aimed evaluate the possibility to discharge on the same day of admission.Conclusion. Based on the new CNEN rules, we conclude that it is possible to hospital discharge patients who receive doses of 3700MBeq of ^{131}I on the same day of admission and it can reduce costs and perhaps making the treatment more accessible.

EFFICACY OF RADIOIODINE TREATMENT IN WELL-DIFFERENTIATED THYROID CANCER IN CHILDREN

Emerita A. Barrenechea MD.
emieab@yahoo.com

PHILIPPINES

Institution: Veterans Memorial Medical Center/ St. Luke's medical Center
Address: Quezon City

Well-differentiated thyroid cancer in children is the third most common solid tumor malignancy and the most frequent endocrine malignancy in children. They are more aggressive at the time of diagnosis and with metastases and have a higher risk for recurrence. The objective of this paper is to determine the efficacy of radioiodine treatment after five to six years from therapy. Fifteen (15) pediatric patients with a diagnosis of thyroid carcinoma, aged below 18 years of age were included in a six-year follow-up after treatment. They underwent thyroidectomy, followed by RAI ablation.

The predominantly female population (74%) had papillary TCA (13 patients) and (2) had follicular. Nodal metastases were seen in 53% and lung metastases were seen in 20% of the cases. Of the 13 who underwent RAI ablation, 3 cases of lung metastases while two cases with lymph node metastases needed repeat treatment. On follow-up after an average of six years, all the 13 patients who underwent RAI ablation are doing well with the lifetime thyroid hormone treatment. WDTCA in children is rare and the biological behavior differs from that of adults.
Their presentation is quite aggressive and may be recurrent. Total or near total thyroidectomy with I-131 ablation reduces mortality making RAI necessary.

TAILORING THERAPY FOR BENIGN THYROID DISEASE IN PRIVATE PRACTICE

Dr Masha Maharaj.
drmasha@yahoo.co.uk

SOUTH AFRICA

Institution: Department of Nuclear Medicine, Westridge PET/CT Oncology Centre, Durban, South Africa

Address: 39 Cassia Road, Lotusville, Verulam, 4340, Kwa-zulu Natal, South Africa

Objective:Targeted radionuclide therapy has the potential to selectively deliver radiation to diseased cells with minimal toxicity to

surrounding tissues. The cost of radiopharmaceutical, travel, pre and post management have serious implications on the private patient's pocket. The aim is to reduce the costs by providing effective single dose therapy outcome. The average cost for benign thyroid therapy inclusive of pre and post management is an estimate R20000 per patient. This comes out of the patients own Medical Aid savings or salary. Previously in this region patients were treated for Benign thyroid disease by Oncologists. Thyroid uptake scans were not included in this protocol. The doses applied were 148Mbq followed by 296MBq and 444MBq, depending on the patient's clinical response. In retrospect, at least 50% of patients were administered therapy doses upto the 2nd and 3rd doses.

Material and Methods: 10 patients were referred to our Centre for thyroid uptake scans and subsequently for benign thyroid therapy for hyperthyroidism. Five criteria were used to tailor the dose: size of gland, distribution of activity, percentage thyroid uptake, sex of patient, age of patient. Using these criteria the minimum dose given would be 185MBq and maximum 555MBq. Concurrent control studies were not done. Response of therapy was confirmed clinically and on biochemistry.

Results: There was confirmed single dose response in 9 of the 10 patients. The one patient confirmed response after the 2nd capsule.

Conclusions: There appears to be a benefit in tailoring radionuclide therapy for benign thyroid disease.

TELEMEDICINE: NEW APPROACH TO ON-LINE MONITORING OF PATIENTS WITH DIFFERENTIATED THYROID CARCINOMAS (DTC) AND NEUROENDOCRINE TUMORS (NET) TREATED WITH HIGH DOSES OF RADIONUCLIDE THERAPY (RNT)

Milovan Matović, Serbia.
mmatovic1955@gmail.com

SERBIA

Name of presenter and co-authors: Milovan Matović, Marija Jeremić, Vlade Urošević, Miroslav Ravlić, Marina Vlajković, Zoran Tasic

Institution: Department of Nuclear Medicine, Clinical Center Kragujevac and Faculty of Medical Sciences, University of Kragujevac, Serbia

Address: Zmaj Jovina 30, 34000 Kragujevac, Serbia

Objective:Following RNT of DTC and NET, patients must usually remain hospitalised in special premises with restricted access, until radiation in their body drops below the legally defined effective dose limit. During hospitalisation, these patients may experience complications or adverse reactions, so it is of vital importance that doctors and nurses have audio-visual contact with patients, and follow-up their vital functions as well as the decline of radiation in their body. Telemedicine could be a potential solution for monitoring such cases. Material and Methods:We have developed a telemedicine system which encompasses three important aspects: continuous on-line remote monitoring of the patient's vital functions and radiation level in the patient's body, and video surveillance of the patient's room. Our system consists of custom-developed hardware/software solutions for data acquisition and processing, and enables communication via the Internet and related services.Results:Our custom-developed telemonitoring system has been in use for the last 4 years, helping us treat more than 300 patients who received RNT. It has helped us detect and react to various instances of patients' vital function or behavioural changes. Furthermore, the continous monitoring of radiation levels in the patient's body achieved with our own custom-developed sotware has helped us predict when the patient will be released from the hospital and optimise the use of limited hospital space allotted to radionuclide therapy. Conclusions:Four years of experience in telemonitoring patients who receive radionuclide therapy suggest that this technological aspect of the treatment ensures a high level of safety for the patient, as well as a significant reduction of overall treatment costs.

OUTCOME OF LOW RADIOIODINE DOSE FOR THE POSTOPERATIVE ABLATION OF THYROID REMNANT IN PATIENTS WITH LOW-RISK DIFFERENTIATED THYROID CARCINOMA

Zvezdana Rajkovaca, Bosnia.

BOSNIA

Name of presenter and co-authors: Zvezdana Rajkovaca, Sonja Bobic, Davor Golic, Jovana Brstilo
Institution: Clinical Centre, Department of Nuclear Medicine
Address: 12 beba 6, 78000 Banja Luka, Bosnia and Herzegovina

Objective:This study aimed to evaluate the success rate of low dose radioiodine remnant ablation (RRA) on the outcome of low-risk differentiated thyroid carcinoma (DTC) patients.

Material and Methods: We retrospectively analyzed 512 patients, 143 (27.93%) of whom received low dose RAI, 1724+/-270 MBq. The patients consisted of 14 males and 129 females, mean age 47.7+/-12.9 years, 93 stage pT1N0, 35 pT2N0 and 15 pT3N0.

Results:Successful RRA was achieved in 131 patients (91.6%). 11 patients (7.69%) needed additional RAI treatment. Only 1 patient (0.7%) needed RAI treatment three times.

Conclusions:Good outcomes were achieved with the low dose of 1724+/- 270 MBq RRA.

177LU-DOTA-HIS2-MG11: EVALUATION FOR CCK-2 RECEPTOR TARGETED THERAPY

Trindade, V.; Reyes, L.; Vasilskis, E.; Oliver, P.; Balter, H.; Engler, H.

URUGUAY

We describe the radiolabelling with 177Lu of the Minigastrin analogue His2-MG11 (His-His- Glu-Ala-Tyr-Gly-Trp-Met-Asp-Phe-NH2) for detection of tumours overexpressing CCK-2 receptors: medullary thyroid carcinoma, gastroenteropancreatic neuroendocrine tumours, lung carcinoid and small cell lung cancer. Quality control methods, in vitro stability, radiolysis effects and biological behaviour are also considered.Labelling of DOTA-His2-MG11 with 177Lu (ITG and Perkin-Elmer gift) was optimized including peptide to activity ratio, 1-80 µg and 43-264 MBq, incubation at 80oC during 10-30 min and reaction pH: 3.5-6.0 adjusted with NaOAc-gentisic acid buffer.Radiotracer's radiolysis and effect of gentisic acid (GA) as antioxidant were followed up to 7 days. Radiochemical purity was evaluated by RP-HPLC in a C18 column, solvent gradient of A (0.1% TFA in water) and B (0.1% TFA in acetonitrile) and by ITLC-SG in NH4OH:EtOH:H2O (2:10:20) to evaluate the radiocolloid formation.Biodistribution studies were performed at 0.5, 1, 2 and 24 h post-injection in normal mice injected with 3-12 MBq (ID) of 177Lu-DOTA-His2-MG11 (n=3 for each condition).

Xenographic tumour models were induced in two nude mice by inoculation of 1.0x107 and 2.5x106 AR42J cells in the left deltoideus muscle. SPECT/CT images were acquired 27 days later and authoradiography was also done.Yield for 177Lu-DOTA-His2-MG11 was >94% at pH 4.5 in NaOAc 0.4M with GA 0.24M, incubation at 80oC during 20 min and 200MBq / 30µg of peptide (specific activity about 10 MBq/nmol). Higher temperatures or longer incubation times increased the amount of the oxidized methionine species (Met-Ox) with decreased receptor affinity.Optimization studies demonstrate that 20-30 µg of DOTA-His2-MG11 were enough to avoid the presence of free 177Lu in the solution, but 10% of Met-Ox was found. Reaction pH: 4.5 or higher is necessary to chelate 177Lu to DOTA. Higher pH increases Met-Ox; reaching 10% at pH 4.4-5.0 and 15% at pH 5.5-6.0. Probably due to the lower amount of GA (antioxidant) added at higher pH. This evidenced a direct relation between pH and amount of GA added, thus giving more stability at lower pH, where GA concentration is higher.The addition post labelling of GA, three times higher than usual, concomitantly increasing the final volume, improves the stability of 177Lu-DOTA-His2-MG11.In normal mice a rapid blood clearance with high urinary excretion (90% of ID in 24h) and low renal uptake (1.9% of ID at 0.5h to 0.4% of ID at 24h) was observed. In other organs and tissues the uptake was negligible. In mice with induced tumours, the T/B (Tumour/Blood) ratio was 25, five days post injection.These results open new possibilities for molecular targeted radiotherapy of tumours expressing CCK-2 receptors.
Radiolysis studies revealed the conditions required to minimise the presence of oxidized methionine which alters the biodistribution pattern.

DIFFERENTIATED THYROID CANCER (PAPILLARY). BRAIN TUMOR METASTASIS AS CLINICAL ONSET. SURGICAL TREATMENT AND 131I. 9 YEARS SURVIVAL AND 7 YEARS DISEASE-FREE.

Dr. Danny Mena; Dr. Hernán García del Río, Dr. Oscar Bruno, Tmn. Liliana Alvarez.

ARGENTINA

Objetives:The differentiated thyroid cancer is the most common endocrine neoplasia. The major manifestation belongs to the papillary variant (65 - 90%). The prognosis tends to be very favorable, with a mortality rate of 1.8% and a disease-free rate up to 10 years of around 90-95%. The distant metastasis in brain accounts for 0.1 - 5%. There are no established protocols for the management of brain metastasis.

Therapeutic options are: surgery, stereotactic radiotherapy / radiosurgery, and 131I. The successful management of this case is an option for brain metastasis from thyroid papillary carcinoma. Methods: A 69 year-old female begins with double vision (diplopia). She underwent twice a surgery for brain tumor with a histopathological report on thyroid papillary tissue. The endocrine evaluation determines euthyroid state except TG 2300 ng/mL. Total thyroidectomy with classic thyroid papillary carcinoma. A diagnostic 131I scan shows for first time brain metastasis uptake. The patient receives 25 mCi of 131-I as initial therapeutic dose, and subsequent therapeutic doses (50, 50, 75, 75, 50 mCi) in 2 years, in accordance with the evolution of magnetic resonance, clinic, endocrine lab, hematological analysis, and 131I scintigraphy.The follow-up was carried out by means of a clinical control, thyroglobulin values, U.S., 131I scans, and magnetic resonance.

Results: The patient is at the present time over 9 years survival and 7 years disease-free.Discussion: Even though the distant metastasis is not very common in brain and is generally associated with aggressive variants of tumor, our case started with a metastatic brain tumor in an euthyroid patient with no thyroid pathology background and with low-risk post-thyroidectomy criterion.The 131I scan turned positive in brain metastasis when the patient was thyroidectomized. This detail must be considered important, since it makes it possible to understand the behavior of the metastatic lesions when the primary thyroid tissue is present or absent.

Conclusion:We presented a case involving a patient with brain metastasis from thyroid papillary carcinoma. The management of this disease was: previous surgeries to improve the initial neurological clinic, thyroidectomy, and 131| with therapeutic doses in stages and in a fractional manner with an initial therapeutic dose of 25 mCi 131I, and an accumulated dose of 325 mCi.

TECHNOLOGIST

USE OF TECHNETIUM-99M PERTECHNETATE INJECTION TO OBTAIN BODY OUTLINES FOR OPTIMAL LOCALIZATION IMAGE IN BREAST LYMPHOSCINTIGRAPHY

Nicolas Niell.

URUGUAY

Objective. Several methods have been used for outlining the body for breast sentinel node imaging before radioguided removal. One of the most popular is the use of a transmission ^{57}Co flood source (backlighting), while another is outlining the boundaries of the patient's body by hand with a ^{99m}Tc point source during image acquisition. More complex methods include the acquisition of a scatter image using a lower energy window and produce a fusion image with the photopeak and more recently, the use of SPECT/CT. However, all these methods are time consuming and are associated with some technical, economic, or dosimetric challenges. Our purpose was to investigate the advantages of producing a complete body background with the injection of a very low dose of ^{99m}Tc-pertechnetate.Methods. A total of 10 patients with breast cancer were studied, who were submitted for lymphoscintigraphy with sentinel node detection. A subareolar, intradermal injection of ^{99m}Tc-albumnin nanocolloid (0,2- 1 mCi) was given to each patient, with the maximum dose depending on whether surgery was performed the same or the following day. Immediately after, 1-2 mCi of ^{99m}Tc-pertechnetate were injected intravenously. Planar images were then obtained for 5 min in a dual-head camera with the detectors in 90°, simultaneously acquiring anterior and lateral projections in a 128x128 matrix, using LEHR collimators and a 140 keV ± 10% energy setting. Results. Imaging was completed in only 5 min after injection, including both planar projections with body outline. The quality of the images was excellent, with sentinel nodes clearly depicted over a weak, homogeneous background. Physiologic uptake in salivary glands, thyroid and stomach was noted, as well as faint blood pool activity. In all cases, intraoperative identification of target nodes was not affected by the presence of background activity and all were successfully removed. Effective dose estimates for ^{99m}Tc-pertechnetate is about 0.4 mSv per mCi injected, while for a ^{57}Co source (3 min transmission scans) is in the order of 0.01-0.015 mSv, depending on the strength of the source, and for a standard low-dose CT it is close to 3 mSv, although in newer scanners it can be <1 mSv.

Conclusions. The proposed protocol for body delineation in breast lymphoscintigraphy is simple, fast, very low-cost, and is associated with marginal increment in the effective dose to the patient. Preliminary results demonstrate no effect on the rate of intraoperative sentinel node detection. Potentially, it can also be used for SPECT imaging allowing fusion with remote-acquired CT if available.

CURRENT SITUATION AND PROSPECTS OF NUCLEAR MEDICINE IN PARAGUAY

Pedrozo MG, Giménez G, Velázquez G, Galván P.

PARAGUAY

Instituto de Investigaciones en Ciencias de la Salud (IICS), Universidad Nacional de Asunción (UNA)

Introduction: Currently, nuclear medicine has an essential function worldwide in diagnosis, staging, treatment, prognosis and follow-up of many diseases. Among all diagnostic and therapeutic procedures, nuclear medicine is unique, as it is based on physiopathological and molecular mechanisms and uses cells, biological molecules and drugs marked with radiotracers to study the physiopathology of the body organs and systems and treat diseases.

Objective: To establish a baseline of the situation of nuclear medicine in Paraguay.Methodology:We present a brief outline of the beginning, current situation and prospects of Nuclear Medicine concerning diagnosis and treatment in Paraguay, based in bibliographic reviews and documents of the previous service of nuclear medicine of the Health Sciences Research Institute of the National University of Asunción (IICS–UNA in Spanish) and personal communications with private centers. The training of the professionals involved in the new service of nuclear medicine was financed by the Program of Technical Cooperation of the Atomic Energy International Agency (IAEA) within the frame of national and regional projects with Paraguay as member state.Results:Nuclear Medicine started in Paraguay in the IICS-UNA in 1983 with the support of IAEA, where oseum, renal, gastric, pulmonary, cardiac and endocrinology scintigraphic studies were carried out using 99mTc for diagnosis and later treatment of thyroid cancer using 131I. These services were offered until 2009 because the only one-head plane gamma chamber reached the end of its useful life without possibility of being replaced at that time. On the other hand, there are three private centers that provide diagnosis services with 99mTc and treatment of thyroid pathologies with 131I, oriented to the diagnosis of the diseases prevailing in the country.

The radiopharmaceuticals used are mainly those marked with 99mTc and 131I for the treatment of thyroid metastasis. Besides, one of these centers has a PET/CT that uses 18FDG. The generators of 99Mo/99m Tc, 131I and 18 FDG are imported from neighboring countries.In 2011, the IAEA presented a report about Paraguay to the Ministry of Public Health and Social Welfare, called "Integrated Missions of PACT" (imPACT, 2011) where the lack of coverage of the assistance with techniques of nuclear medicines to patients of

public sector was shown. Considering this, the UNA, through the IICS, is developing the National Project PAR 6014 “Strengthening of nuclear medicine in diagnostic and therapeutic areas in Paraguay” with the support of IAEA which preliminary and important achievements are: formation of human resources in areas of nuclear medicine, , radiochemistry, medical physics and clinical engineering in regional reference centers apart from scientific visits and expert missions. The project also included the donation of a dual-head single-photon emission computed tomograph (SPECT) to replace the image equipment previously mentioned.

Conclusion: The future prospect is documented by national and regional investment projects of public and private institutions with the support of IAEA towards the expansion of the use of nuclear medicine, which are directed to strengthen the quality of the practice of nuclear medicine by the training of human resources, acquisition of equipment with advanced technology and application with diagnostic and therapeutic purposes. It should be emphasized the commitment and support of the IICS – UNA by considering a physical space assigned to the service of Nuclear Medicine in its new facilities of the campus of the UNA according to international requirements.

TRENDS, INFLUENCES AND CHALLENGES IN HARMONIZING TRAINING THROUGH E-LEARNING: THE EXPERIENCE OF DISTANCE ASSISTED TRAINING (DAT) FOR NUCLEAR MEDICINE PROFESSIONALS

Heather Patterson NMT.

AUSTRALIA

The rapid growth trend in nuclear medicine (NM) and hybrid molecular imaging increases the need for structured vocational training and continuing professional development (CPD). Even in places where established higher education courses are available, these do not necessarily cater to the practical component of training and the ever-changing technology that is central to medical imaging. Not only is training to understand new concepts limited but often there is inadequate training in the basics of NM and this can be a major constraint to the effective use of developing technology. To meet the expanding needs, initially in economically disadvantaged countries, the Distance Assisted Training (DAT) program commenced 20 yrs ago under the auspices of the International Atomic Energy Agency (IAEA). It has more recently evolved through several revisions and peer reviews, extending to SPECT-CT and PET-CT and has been available On-Line (DATOL) since 2009 with interest from all levels of the profession. The program is currently used in 30 countries with varying degrees of success. The main influences on successful implementation have been the level of commitment of local management and students as well as time available to study whilst working. A critical factor is good communication between in-country management and course participants whilst adhering to timetables and deadlines. Challenges include the availability of national or regional professionally recognized certificates for assessed graduates. Countries have varying needs and requirements and are encouraged to approach Higher Education Institutions to either implement the DATOL program or utilize materials to ‘fill any gaps’ in their current curricula. DATOL is proving to fulfill the goal of harmonizing nuclear medicine training globally through sustainable e-learning delivery and offers a benchmark for introducing an internationally consistent basic standard of practice. Open access to training materials for personal study, CPD activities and general use in teaching and training, without formal assessment, will be available soon through IAEA Human Health (NAHU) website.

INFLUENCE OF BACKGROUND ON THE CALCULATION OF RELATIVE RENAL FUNCTION RENAL SCINTIGRAPHY STATIC

Elizabeth Huanca Sardinas, María Rita Vasquez Ibáñez, Marcelo Torrez Cabero, Orlando Castro Sacci, Greta Vargas Pinto.

BOLIVIA

Institute of Nuclear Medicine - Universidad Mayor, Real y Pontificia de San Francisco Xavier de Chuquisaca, Sucre-Bolivia.

INTRODUCTION One of the roles of professional nuclear medical technologist is to process the acquired Nuclear Medicine studies , among which is the purpose of the calculations of relative renal function (RRF) of static renal scintigraphy studies, important information whenmedical decision making . For comfort or time pressure usually these prosecutions and calculations were performed with the automatic programs.OBJECTIVEThe aim of this study is to quantify and analyze the influence of BKG in the calculationof Relative Renal Function in studies of static renal scintigraphy.

MATERIALS AND METHODSFrom a total of 230 studies of static renal scintigraphy , a random sample of 50 studies corresponding to 27 women and 23 men was made, these studies were acquired in Gamma Camera Planar Mediso , with the following parameters : four projections AP ,PA , OPD , OPI , 400 kilocuentas for projection, 128 x 128 matrix , 20 % window , lowenergy collimator all purpose (LEAP). Were processed in the anterior and posterior projections using a DIAG Digital Image Analizar for Gama Camera V.2.000E, Split kidney program without taking into account bkg and manually taking into account bkg, were processed 100 studies; maintaining the

same areas of interest of the kidneys in bothmethods.

RESULTS The results of the relative kidney function (RRF) in posterior projection showed an average 53.4% of the left kidney, and right kidney 46.6 % with macro. In relation those obtained manually from 53.5% in left kidney and 46.5 in the right kidney. In the anterior projection showed an average in the left kidney of 53.4 % in the right kidney of 46.5 % with macro, in relation those obtained manually from 51.8 % in the left kidney and 48.2 % in kidney right. The standard deviation of RRF obtained both macro and manual in posterior projection of the left kidney was 3.77 compared to 3.80 in the right kidney. While in the anterior projection with both methods the RRF of the left kidney was 3.60 compared to 3.23 of the right kidney.

CONCLUSION The variation of the relative renal function obtained both manual and automatic background without background is significant, so the operator must be aware of the processing performed taking into account the data provided can help an effective and
timely treatment.

DUAL-ISOTOPE (I-123/TC-99M SESTAMIBI) SPECT/CT PRIOR TO REOPERATION IN POSTOPERATIVE RECURRENT PRIMARY HYPERPARATHYROIDISM

Donald R. Neuman.

UNITED STATES

OBJECTIVE: Imaging localization studies are considered essential prior to reoperation in patients with postoperative recurrent primary hyperparathyroidism. The purpose of this study was to directly compare the sensitivity and the positive predictive value of dual isotope (I-123/Tc-99m sestamibi) SPECT and SPECT/CT for the localization of parathyroid lesions in postoperative recurrent primary hyperparathyroidism.

MATERIALS AND METHODS: A total of 109 consecutive surgical patients (87 females and 22 males, with mean age +/- SD 58.8 +/- 15.1 years) with primary hyperparathyroidism who had previously undergone parathyroid surgery were studied. All patients underwent both I-123/Tc-99m sestamibi subtraction SPECT and SPECT/CT imaging using a hybrid SPECT/CT instrument prior to reoperation. The subtraction SPECT images and coregistered SPECT/CT images were interpreted separately, with images scored on a 5-point scale. The reoperative surgical and histopathologic findings were used as the standard of comparison.

RESULTS: At reoperative surgery, 94 parathyroid adenomas (single adenoma in 90 patients, double adenomas in 2 patients), 39 hyperplastic parathyroid glands (single gland in 7 patients, 3 glands in 4 patients, 4 glands in 5 patients), and 1 parathyroid carcinoma were resected. Of these 134 parathyroid lesions, SPECT/CT correctly localized 103 (76.9%) compared to 97 (72.4%) for SPECT ($p=0.18$). SPECT/CT was associated with 1 false finding, compared to 18 false positive findings for SPECT. 99% (103/104) of the positive SPECT/CT findings were associated with parathyroid lesions, compared to 84% (97/115) of the positive SPECT findings ($p<0.001$).

CONCLUSIONS: Although the sensitivities of SPECT and SPECT/CT for the detection of parathyroid lesions in postoperative recurrent primary hyperparathyroidism were comparable, SPECT/CT resulted in fewer false positive findings and had a higher positive predictive value than SPECT. Incorporating CT with SPECT using hybrid SPECT/CT technology has the advantage of improving the positive predictive value of the test without affecting its ability to correctly localize parathyroid lesions in postoperative recurrent primary hyperparathyroidism.

CONTRAST MEDIA-RADIOPHARMACEUTICAL PHARMACOKINETIC INTERACTION IN A BASIC RADIO RENOGRAM

Portillo Mariano Gastón, Tesán FC, Giaquinta Romero D, Costa J, Zubillaga MB, Salgueiro MJ.

ARGENTINA

It has long been known about the existence of drug-drug interactions and the mechanisms involved, affecting the kinetic, the efficacy and the toxicity of conventional medications. On the other hand, it is a common Nuclear Medicine (NM) practice to use some drugs to enhance diagnostic procedures, so-called interventional NM. Nevertheless, in the last years there has been an increasing interest in evaluating and recognizing drug-radiopharmaceutical interactions, and systematically report them. In this sense, the study reports the modification of the results in the radionuclide basic renogram (RBR) in control animals after the administration of iodine contrast media. The context of contrast media administration deals with some common facts at NM departments such us when patients came for health controls during their cancer treatment, or when multimodality imaging is employed (even in small animals). We used 9 healthy Sprague-Dawley rats (average weight 250 mg) to perform RBR with 99mTc-DTPA (37 MBq) under control conditions. Dynamic studies

were acquired using a small-field-of-view- gamma-camera equipped with a high-resolution collimator and dedicated software for small animals taking 1 frames/1 second during the first minute and then 1 frames/15 seconds until at least 30 minutes for each study. After 1 week, we repeated the RBR but this time it was perform 1 hour after the intravenous administration of iodine contrast media (1mg/Kg body weight) as Iopamidol (iodine 370 mg/ml). The results showed that RBR under control conditions displayed functional curves with the 3 phases of perfusion-function-elimination within the expected normal patterns. Average Tmax (2.3 min) and T50% (8 min) were obtained as well as right and left relative renal functions within normal range (45-55%). On the contrary, qualitative and quantitative changes affected functional curves after iodine contrast media administration. Although the 3 phases were visualized changes in the functional phase that prolonged Tmax (8 min) was sometimes recorded and in all cases the elimination phase was significantly prolonged (T50 % > 30 min). In these cases, relative renal function was always observed in the normal range and resumed images showed that elimination of 99mTc-DTPA was being accomplished. In conclusion, iodine media contrast interfered with normal renal function as demonstrated by results obtained in BRR. The consequences and significance of these findings highlights the importance of considering the effect of iodinated contrast media on renal function, derived from their own physicochemical characteristics. The pharmacokinetic interactions with other radiopharmaceuticals which biodistribution depends on renal function should also be studied and enlightened.

RADIONUCLIDE BASIC RENOGRAM IN BACK TRANSLATIONAL RESEARCH. THE RELEVANCE OF RADIOPHARMACEUTICAL ADMINISTRATION

Portillo Mariano Gastón. Argentina, Tesán FC, Giaquinta Romero D, Zubillaga MB, Salgueiro MJ.

ARGENTINA

The evaluation of renal function may be of interest in the framework of many research protocols. In this context, back translational research may benefit from a valuable tool such as radionuclide basic renogram (RBR). To date there is scarce data about RBR protocols in animal models therefore the objective of this work is to evaluate the applicability of BR with 99mTc-DTPA in rats. The main variables analyzed are the route of administration and the anesthesia effects on diuresis. The usefulness of this kind of dynamic study is highly dependent of the success of intravenous bolus administration of 99mTc-DTPA. Then, we employed the tail vein and the retroorbital sinus as injection accesses for the radiopharmaceutical (37 MBq). Immobilization of rats was achieved by ketamine/xilazine anesthesia in standard doses for rats. Tail vein injections were performed by means of a catheter that was placed under anesthesia and correct placement was assumed when blood reflux was observed. Retroorbital sinus injections were performed in a direct way also under anesthesia. Independently of the route, the bolus injection was initiated a few seconds after image acquisition started. Dynamic studies were acquired using a small-field-of-view- gamma-camera equipped with a high-resolution collimator and dedicated software for small animals taking 1 frame/1 second during the first minute and then 1 frames/15 seconds until at least 30 minutes for each study. The results showed that, independently of the route, infiltration of injections rendered the loss of valuable information (i.e. Tmax is too much long or even absent). Although retroorbital sinus administration is an easy, rapid and thus attractive route for the direct intravenous access of radioactive material, infiltration of the administered material is possible if it is not performed technically perfect. Thus, although the elimination phase is observed, it is too prolonged and results either in an increment of T50% or in the inability to determine it within the time of the study. Even when intravenous administration was successful, a disturbance on the elimination phase was also observed in some cases, probably caused by anesthesia effect on retardation of diuresis. Additionally, diuresis may be a source of contamination of the animals during the study if they do not have a foley catheter, as ROIs are drawn on an image that is a sum of the whole study. This urine contamination may introduce pitfalls in the results, such as a prolonged elimination phase and T50%, if it is not evidenced and corrected.

Conclusion: BR protocols may be useful in back translational research. Bolus administration of the radiopharmaceutical and diuresis interference correction are crucial to successfully achieve a reliable result avoiding possible pitfalls as described.

BONE SCINTILOGRAPHY WITH SPECT-CT: BETTER CLINIC RESOLUTION

Allan Vieira Barlete.

BRAZIL

INTRODUCTION: A bone scan is a test of high sensitivity, but has relatively low specificity, often requiring additional studies with other imaging methods. SPECT added to the X-ray computed tomography (Single Photon Emission Computed Tomography and Computed Tomography, SPECT-CT) combines the functional information with one from a low-dose CT anatomical images. Some studies suggest that the addition of techniques increases the clinical impact of the exam and speeds up the therapeutic decision making.

OBJECTIVE: The aim of this study is to evaluate the role of bone scintigraphy with SPECT-CT in clinical practice, especially because of

it´s hability to be conclusive without requiring additional investigations.

MATERIALS AND METHODS: Seventy consecutive patients from January to December 2013 that performed bone scintigraphy with SPECT-CT in our institution were chosen. Scintigraphy of the whole body, lateral skull and SPECT CT (low-dose CT) of the chest and abdomen were performed 3 hours after intravenous administration of 925 Mbq 99mTc-MDP in equipment Symbia T2 Siemens. The cases were grouped according to clinical indications, scintigraphic findings, incremental value of CT image and the need for investigations by methods additional image. RESULTS: Of the 70 patients, the majority were male (41), mean age 55 +/- 25 years. The most frequent clinical indications were: evaluation in cancer patients (43 cases); reviews of orthopedic complaints (13 cases); suspected infection (10 cases); suspected metabolic disease (4 patients). The SPECT-CT was useful in the evaluation of 59 of the 70 patients (84%). Of the 70 examinations, it has been necessary to request additional imaging exams to complement the diagnosis in 19 cases (27%): 12 cases were cancer, 5 cases were infectious disease,1 case was metabolic suspicious and 1 case was orthopedic disease. In 14 cases (74%) further investigation with anatomical methods was necessary: 3 cases (16%) with MRI and 2 cases (10%) with scintigraphy with labeled leukocyte/marrow. Among oncological patients, in 19 cases were identified low probability/absence of bone metastases. The higher incidence of bone metastatic sites were in thoracic spine, ribs, pelvis, lumbar and sacral spine and femur.

CONCLUSION: Bone scintigraphy with SPECT-CT is extremely useful in clinical practice, especially because of it's greater resoluteness therefore significantly reduces the need for additional investigations.

BIODISTRIBUTION OF NASAL NEBULIZED AEROSOL USING A PULSATING SYSTEM (PARI SINUS ®).

Sonia Neubauer1. Chile, Gloria Ribalta2, Catalina Gutiérrez2, Isabel Largo2, Jacqueline Cornejo1, Pamela Lovera1

1Dpt. of Nuclear Medicine
2Dpt. of Otorhinolaryngology. Clínica Las Condes. Santiago-Chile

CHILE

Introduction: Chronic rhinosinusitis and secondary pulmonary infection has a very high prevalence among Cystic Fibrosis (CF) patients. Direct paranasal sinus nebulization with antibiotics is one of the important therapeutic interventions. We evaluated the efficacy of the Pari Sinus vibrating system to deliver a nebulized radioactive solution to the maxillary sinuses and its whole body biodistribution in normal volunteers and in CF patients with chronic sinusitis (CR) and FESS (Functional Endoscopic sinus surgery).

Material and Method: Prospectively nasal nebulizations in 4 normal volunteers and in 2 CF patients with CR and FESS were done by means of the Pari Sinus® pulsating aerosol system. Tc99m-phytate, in a concentration of 10 mCi in 2 ml, was continously administered during 1 minute through each nostril. Anterior and posterior static images of the head and whole body were obtained on a Siemens dual head ECAM with LEHR collimators. Biodistribution analysis was done using regions of interest to whole body, lungs, head and sinus (head minus nose). Some cases also had SPECT images of the head for extemporary SPECT-CT image fusion using the OSIRIX program.Results: Mean activity in the paranasal sinuses was 9%, in the lungs 11%, in the abdomen (gastrointestinal) 32% in the normal volunteers. In the CF patients the radioactivity deposition was 4% in paranasal sinuses for both, 37% and 46% in the lungs and 32% and 31% in the abdomen (gastrointestinal) respectively. The two patients were regulary using nasal nebulization with a method that differs from the manufacturers recommendations. The volunteers and the patients applied that same method in this experimental setting.

Conclusion: A small percentage of the nebulized solution is deposited in the paranasal sinuses in healthy volunteers and even less in the CF patients with FESS. Our finding of important lung deposition may account for the effectivity of the nasal nebulization to prevent lung infection in CF patients. Also gastrointestinal absortion may give a systemic effect of the nebulized medication.The manufacturers recommended nasal nebulization method showed to be unfeasible and thus was not applied.

HIGH RESOLUTION PARALLEL PROJECTION SPECT IMAGING TECHNOLOGIES AND CLINICAL PERFORMANCES

1,2Bela Kari. Hungary, 3Gabor Hesz, 3Akos Szlavecz, 4Andras Wirth, 4Laszlo Papp,
4Tamas Bukki, 4Laszlo Nagy, 2Tamas Gyorke, 4Balazs Benyo.

1Semmelweis University, Dept. of Radiology and Oncotherapy, Budapest, Hungary
2Semmelweis University, Dept. of Nuclear Medicine, Budapest, Hungary
3Budapest University Of Technology and Economics Dept. Of Control Engineering and Information Technology, Hungary
4Mediso Ltd. , Budapest, Hungary

HUNGARY

High resolution SPECT imaging has great impact in the diagnosis of functional abnormalities in the investigated organ and plays important role in the functional biology. Various hardware and software solutions are presented in order to improve both physical and clinical performances of the SPECT imaging. Till nowadays, mainly parallel projection based Large Field Of View (LFOV) imaging systems are used in daily clinical applications. The image quality of these systems suffer from non-linear image blur effects and low sensitivity (i.e. high noise level) due to the contradiction between the system resolution and the sensitivity. Simultaneous image blur reduction and sensitivity improvement is possible to perform by designing imaging geometry adapting more suitably to the size and shape of the imaged object. XRing/4R four head dedicated brain SPECT system (Mediso Ltd.) with extra high intrinsic resolution (<2.2mm within the 230*220mm^2 field of view) NaI(Tl) based detectors as well as LEHR/LEUHR parallel collimator set deliver a feasible solution for high resolution brain SPECT imaging by ^{99m}Tc/^{123}I radiopharmaceuticals. 1mm and 2mm isotropic voxel-size can be applied for both phantom and clinical studies. Simple MTF^{-1} based 2D pre-filtering on the projection data with FBP reconstruction produces morphologically highly detailed artefact free images 3D Ordered Subset Expected Maximization (OSEM) iterative reconstruction method has been developed for conventional LFOV parallel projection imaging as another approach, in order to reduce the non-linear image blur effect and compensate the photon absorption. Dedicated calibration procedure has been worked out for the Point Spread Function (PSF) modelling of the image blur effect. Gamma photon attenuation map is determined by co-registered and resampled CT imaging (SPECT/CT multi-modality method).

Forward projection step of the 3D reconstruction includes both the PSF modelling and the photon absorption effect. Due to the intensive computation demand of 3D procedure a high performance Graphic Processor Unit (nVidia) based algorithm has been implemented. AnyScan™ SC (SPECT/CT, Mediso Ltd.) was considered for both physical phantom and patient studies. 3D reconstruction method was also tested by the XRing/4R SPECT studies without CT based attenuation correction (Chang post-correction has been performed). The novel 3D GPU based algorithm resulted significant improvement in the image contrast and spatial resolution in all cases. The reconstructed images showed clear-cut better spatial activity distribution. Significant improvement presents in the signal/noise ratio too both by ~2mm and ~1mm voxel size sampling rate.

NEFROUROLOGY
GENITOURINARY

RENAL GAMMAGRAPHY IN DIAGNOSE FOR COMPLICATIONS IN KIDNEY TRANSPLANTED PATIENT.

Gledys Gómez Sierra. Especialista en 1er grado en Medicina Interna. Diplomado en Medicina Nuclear.
Lic. Lenin Antonio Álvarez. Licenciado en Tecnologías de la Salud, mçMedicina Nuclear y Radiofísica.

CUBA

Abstract:The presented work consists on a revision on the thesis of theRenal Gammagraphy to diagnose the complications that can present a kidney transplanted patient, taking in consideration the experience accumulated by means of the consultation of up date bibliography. In turn we consider the results obtained in a prospective descriptive study carried out in 54 patients of both sexes between 18 and 64 years of age, to those that we realized kidney transplant in the period 1992 in 2014. 9 patients havedeceased and of the alive ones, some presented complications in connection with the transplant, being diagnosed after the revision in the recovered clinical histories rejection in 14 of those cases, as well as 4 cases with diagnostic of sharp Tubular Necrosis they were subjected to a renal gammagraphy study which was very important to obtaining the presented diagnose.

RENAL IMAGING AND TUBULAR FUNCTION QUANTIFICATION USING 99MTC-DMSA SCINTIGRAPHY: A COMPARISON WITH GLOMERULAR FUNCTION IN PATIENTS WITH SICKLE CELL ANEMIA

Daniel Massaro Onusic Sergio Querino Brunetto - PhD, Bárbara Juarez Amorim - MD, PhD Mariana da Cunha Lopes de Lima - MD, PhD Allan de Oliveira Santos - MD, PhD, Elba Cristina Sá de Camargo Etchebehere - MD, PhDSara Teresinha Olalla Saad - MD, PhD Celso Darío Ramos - MD, PhD.

BRAZIL

Nuclear Medicine Division, Department of Radiology and Hematology Division, Department of Internal Medicine, State University of Campinas, Brazil.

OBJECTIVE: Different functional and structural abnormalities of the kidney are common in patients with sickle cell anemia (SCA). Surprisingly, there is no systematic data in the literature reporting the use of 99mTc-dimercaptosuccinic acid (DMSA) renal scintigraphy in SCA. This study aimed to evaluate the utility of DMSA planar and SPECT-CT images and relative renal function quantification in SCA. We also compared tubular and glomerular function in these patients by performing a simultaneous measurement of absolute renal uptake of 99mTc-DMSA (DMSA%) and glomerular filtration rate (GFR).
METHODS: Twenty-six patients (16 female) aged 24-58 years with SCA were studied. Doses of 110-180MBq of 99mTc-DMSA and 10-12MBq of 51Cr-EDTA were simultaneously injected in all patients. Blood samples were taken 2, 3 and 4 hours after injection. Planar and SPECT-CT images were obtained after 3 and 4 hours respectively, using a multislice SPECT-CT camera and relative DMSA quantification was performed. Absolute renal uptake of DMSA (DMSA%) was calculated from SPECT-CT images as a percentage of the injected dose, using with CT-based attenuation correction. Planar and SPECT images were analyzed visually for identification of focal lesions in the renal parenchyma. After 1 week (ensuring the 99mTc radioactive decay) the blood samples were counted using the energy window of 51Cr to determine 51Cr-EDTA based GFR.
RESULTS: Focal lesions were identified in the renal parenchyma of 21/26 patients (81%). In 11/21 of these patients (52%), the renal lesions could only be clearly identified on the SPECT images. Relative renal function tended to be lower on the left than on the right kidney (47.4% vs. 52.6% ±5.2%, p=0.0052). The correlation between DMSA% (37.5% ±2.9%) and GFR (124.7 ±40.9 min) was low (r= 0.204, p= 0.322).
CONCLUSIONS: 99mTc-DMSA scintigraphy identifies focal renal lesions in most patients with SCA, specially using SPECT images, and the left kidney tends to be more affected than the right kidney. The correlation between DMSA% and GFR is low in SCA, suggesting that glomerular dysfunction is not followed by a proportional decrease in proximal tubular function in these patients.

NORMAL CURVE AND EXCRETORY PARAMETERS OF MAG3 IN INFANT POPULATION, PRELIMINARY RESULTS

Funda Üstün.

TURKEY

The purpose of this study was determined dynamic renal scintigraphic parameters of MAG3 under age one year in pediatric population.Material - Method: Data were obtained from retrospective analysis of pediatric patients who referred to dynamic renal scintigraphic imaging with MAG3 and whose images are assessed normally by two experienced experts. The study population consisted of 15 patients, seven of them ≤6 month (4.57 ± 1.4 m) (Group 1) and 8 of them ≥7 month and ≤12 month (9.38 ± 1.41 m) (Group 2). Renal curves and images were analyses visually and quantitatively.Results: In group 1 and 2, blood urea values were 11,98 ± 3,59 and

16,90 ± 6,07, respectivelly. In groups, creatinin values were 0,26 ± 0,04 and 0,20 ± 0,03, respectivelly. All MAG3 renogram parameters and DMSA uptake values are presented in the following table.

	R T_{max}	L T_{max}	R $T_{1/2}$	L $T_{1/2}$	R %	L %	R20 min %	L20 min %	DMS A% R	DMS A%L
Gr1	2,9 ±1,2	2,6 ±0,5	7,5 ±5,5	6,8 ±3,4	48,7 ±3,1	51,3 ±3,1	24,5 ±9,8	28,6 ±8,2	49,2 ±2,6	50,8 ±2,6
Gr2	3,4 ±1	3,5 ±0,8	5,3 ±1,6	5,0 ±1,5	49,7 ±3,5	50,3 ±3,5	19,5 ±4,9	19,6 ±8,1	50,6 ±3,34	49,4 ±3,4

TMax: Right or Left time to peak
T ½: The activity in the kidney fall to 50% of its maximum value 20 Min %: 20 minutes % uptake ratio. Conclusion: Normal ranges of MAG3 parameters for pediatric age groups may assist in the interpretation of dynamic images and facilitates the accurate assessment of patients.

CLINICAL AND SURGICAL VALUE IN DECISION-MAKING OF HEMI-RENAL ROI ANALYSIS IN NUCLEAR-NEFROURTOLOGIC PROCEDURES IN PATIENTS WITH DOUBLE EXCRETORY SYSTEMS

Raúl Carlos Cabrejas, Argentina* Andrea Exeni**; Ma Paula Rigali**; Germán Falke*** * Nuclear Medicine- Sanatorio Mater Dei, CABA, Argentina.

***Pediatric Nephrology Htal Univ Austral, Pilar*
**** Pediatric Urology - Sanatorio Mater Dei, CABA; Htal Univ austral, Pilar Argentina*

ARGENTINA

Objectives: To define the utility of hemi-renal RoI analysis (dynamic curves and relative function) in surgical decision-making.Material and methods: In a period of 2 years, 56 paediatric patients with double excretory systems (DUS) were studied with nuclear medicine procedures; 9 of them had bilateral pathology and 3 were monorenal. Diuretic Renogram (w/wo indirect cystoureterograhy) and Renal Scintigraphy were performed in all 54 the patients. These procedures were performed following institutional guidelines: F+20 Renogram (40 min dynamic study. DTPA-^{99m}Tc -IV; 0,5-1mg/k IV Furosemide at 17-20 min) and Renal scintigraphy (3 SD Static 4-24h delayed images. DMSA-^{99m}Tc –IV). Radioactive doses were determined by EANM dose card. Sixty-three DUS were analysed following SOPs. In the analysis, hemi-renal RoIs were included in addition to the standard processing method. Using Hemi-RoIs in the Renogram, curves of each excretory system were analysed, allowing differentiation of obstruction vs. uroectasia vs. normal dynamics in each system. In Renal scintigraphy, hemi-renal quantitation was calculated, expressing the relative functional contribution of each system to the total renal function. Patients with obstruction and/or severe reflux and functional parenchyma (> 15% relative function) were elective to conservative surgery; whilst nephrectomy (Radical/Hemi-nephrectomy) was performed if non-functional parenchyma was depicted (<15% relative function).
Results: 26 patients (41%) matched the criteria for surgical treatment: Based on hemi-quantitation 20% (#11) had conservative surgery (Uretero-pyeloplastia: 7%; Antireflux surgery: 6%; Ureterocele surgery: 2%); only 6% (#4) underwent Nephrectomy and 17% Hemi-nephrectomy (#6 upper hemi-nephrectomy; #5 lower hemi-nephrectomy). Normal or non-significant functional altered studies, with no recurrence of infection (w/wo chemoprophylaxis) were found in 59% and therefore clinical follow-up was implemented. From these patients, if they recur infected: 2 are elective for Hemi-nephrectomy, 1 for Nefrectomy and 1 conservative surgery (anti-reflux)

Conclusions: The inclusion of hemi-renal RoIs in cases of DUS is of great value to the nephrologist and urologist to determine the treatment to implement. The number of Nephrectomies and Hemi-nephrectomies were reduced in number, being able to limit surgical procedures to conservative ones, when weighty function was achieved in the hemi-quantitative analysis. Hemi-renal processing also allowed performing more Hemi-nephrectomies in relation to Nephrectomies. The implementation of this *Processing Method* improved medical decision-making and aimed it more reliable; reducing the on-set of renal insufficiency and other post-surgical morbidities.

ONCOLOGY
HEMATOLOGY

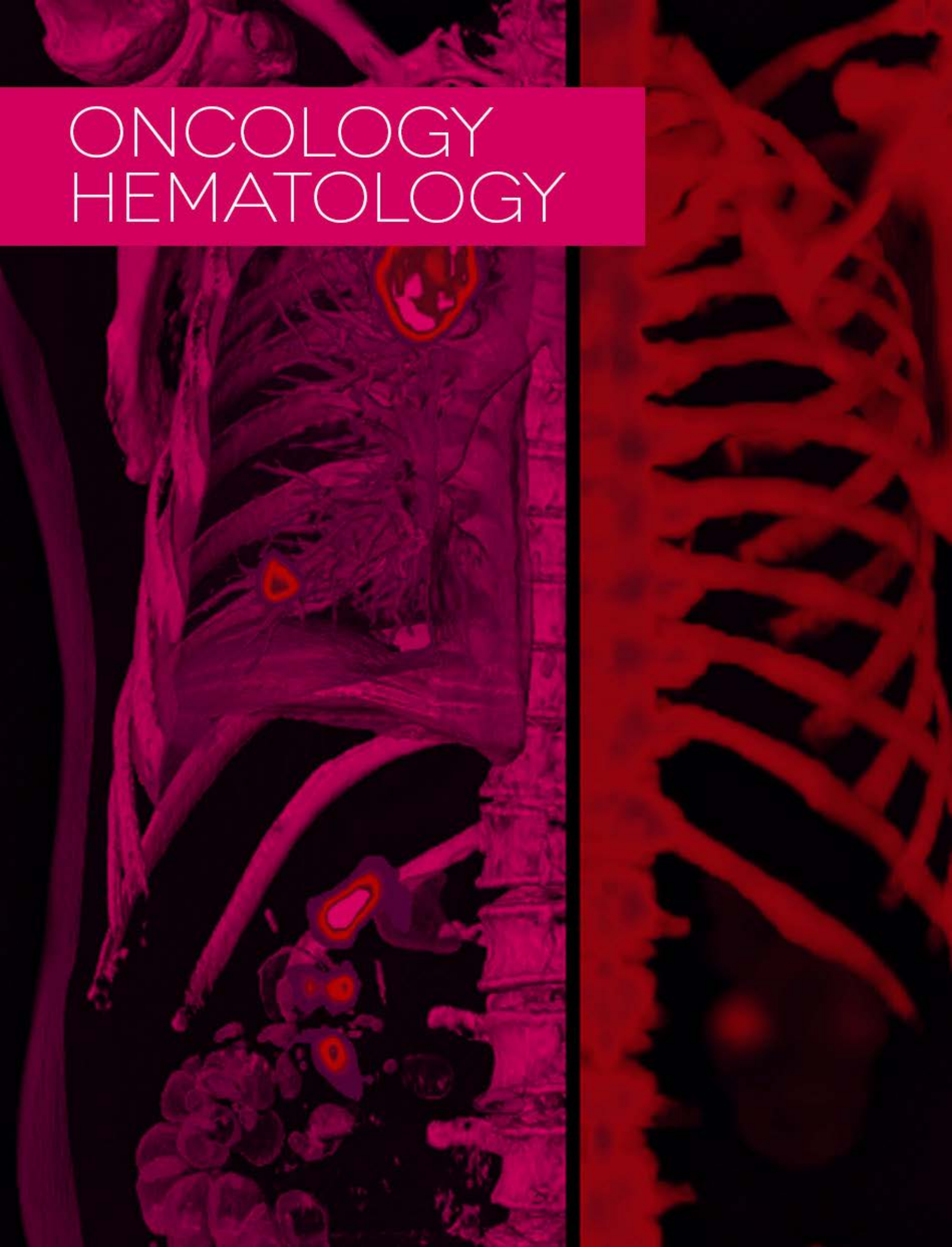

TUMOR KINETIC WITH ^{18}F-FDG PET/CT IN THE PREDICTION OF NEOADJUVANT RESPONSE IN LOCALLY ADVANCED BREAST CANCER

Ana María García Vicente. Nuclear Medicine . University General Hospital. Fernández Calvo G (2), Muñoz Sanchez MM (3), Pruneda González RE.

(2), Cruz Mora MA (4), Jiménez Londoño GA (1), Palomar Muñoz A (1), Soriano Castrejón A (1)

SPAIN

Aim: To explore the relation between tumor kinetic assessed by ^{18}F-FDG PET/CT and final neoadjuvant chemotherapy (NC) response in locally advanced breast tumors. Methods:Prospective study including 144 women with locally advanced breast cancer (multicentre study, FISCAM Grant 2009/40). All patients underwent ^{18}F-FDG PET/CT previous to NC. SUVmax was obtained in the primary tumor in PET-1 (1 hour after FDG administration) and PET-2 (2 hours after the PET-1 acquisition). The percentage variation or retention index (RI), between these values was calculated After NC, residual primary tumor specimen was histopathologically classified according Miller and Payne tumour regression grades (TRG), from G1 to G5 and in response groups as good responders (G4 or G5), partial responders (G2 or G3) and non-responders (G1). Furthermore, residual lesions were classified following a binary assessment as responders (G4 or G5) and non-responders (the rest of cases).The relation between SUV-1, SUV-2 and RI with TRG and response groups was evaluated Results145 tumors were assessed (a patient had bilateral breast lesions). The TRG were: G1 (30), G2 (30), G3 (36), G4 (14) and G5 (35). 49 were classified as good responders, 66 as partial responders and 30 as non-responders.

For the binary assessment, 49 lesions were classified as responders and 96 in non-responders. The mean values ± SD of SUV-1, SUV-2 and RI were: 7.75±5.72, 9.06±7.13 and 14.50%±31.75% respectively. SUV-1 and SUV-2 showed a very good linear dependency relation (R2=0.948).Statistical differences were observed between TRG and SUV values ($p<0.001$). Good responders showed greater values of SUV-1 and SUV-2 compared to the partial or non-responders ($p<0.001$ and $p<0.01$ respectively). For the binary assessment, statistical significant differences of SUV-1 and SUV-2 with respect to responders and non-responders were found ($p<0.001$). SUV-1, SUV-2 and RI of 10.30±6.72, 11.92±8.21 and 18.30±23.47 for responders vs 6.45±4.65, 7.55±6.01 and 12.51±35.27 for non-responders. RI value did not show any significant relation with TRG, response groups or binary assessment ($p>0.05$).Conclusion Baseline tumor metabolism assessing by dual time point FDG PET/CT, was associated with the final histopathologic status after NC, with greater SUVmax values for good responders compared to the less responders cancers. Kinetic pattern assessed by RI did not show any significant relation to response.

HOW DOES PET/CT CHANGE TREATMENT DECISIONS IN PATIENTS WITH LOCALLY ADVANCED CERVICAL CANCER

Bruno Gabriel [1], De Dios Diana [2], González Christian [1], Tinetti Carolina[1], Traverso Sonia[1], Jaimez Fernando[1], Namías Mauro[1], Damiani Fernanda [2], Lay Laura [2], Ostojich Marcela [2], Zeff Natalia [2], Sánchez Ariel[2], Gianni Sergio [2], Parma Patricia[1]

[1] PET/CT Department, Fundación Centro Diagnóstico Nuclear (FCDN), Buenos Aires, Argentina.
[2] Gynecology Department, Instituto Oncológico Ángel H. Roffo (IOAHR), Buenos Aires, Argentina.

ARGENTINA

Introduction Cervical cancer is the first cause of cancer-death among young women in developing countries. The FIGO staging is exclusively clinical; however has a 20% inaccuracy for the initial stages, and up to 67% in the advanced ones, particularly due to the failure for the assessment of nodal status and distant involvement. Because PET/CT has high sensitivity and specificity in the detection of lymph node metastases and hematogenous spread, it could improve the initial assessment of disease and personalize the treatment. ObjectiveTo assess if PET/CT could lead to changes in the treatment planning in locally advanced cervical cancer (LACC).

Material and Method This is an observational, prospective study of the Gynecology Department of the IOAHR and PET/CT Department of FCDN. Between the years of 2009 and 2013, 70 patients with LACC were staged according with the FIGO recommendations. A PET/CT scan was also performed as part of the initial work up. Localization of extrauterine hypermetabolic images were determined as well as classified as pelvic or extrapelvic, and also the extrapelvic ones, in nodal or extranodal distant metastases. Wherever technically feasible, diagnostic confirmation by cytological puncture and/or histology was performed. All patients were considered to be treated with the standard concurrent chemo-radiation therapy to pelvic field plus brachitherapy. In those patients with extrapelvic disease by PET/CT, changes in therapeutics approaches were considered. The assessment included 1- Frequency and localization of the extrauterine hypermetabolic lesions, 2- Distribution of the lesions according with the FIGO staging, 3- Perceptual changes in the

initial therapeutic planning related to the PET/CT findings.

Results_In 51/70 (72,8%) of the patients, 77 extrauterine hypermetabolic lesions were detected: of those, 51 (66%) were pelvic (34 single and 17 combined with other localizations), and 26 (34%) were extrapelvic (16 nodal lumbo-aortic, 1 supraclavicular, 2 mediastinal, 2 inguinal y 5 extranodal). The per stage distribution were: EIIA 3/4 (75%), EIIB 27/39 (69%), EIIIB 19/23 (82, 6%), and EIVB 2/2 (100%). The 26 extrapelvic localizations were found in 19/70 (27.1%) patients, and in all of them the initial proposed therapeutic approach was modified (extended lumbo-aortic, and/or inguinal radiation therapy field, and/or chemotherapy).

Conclusion_The frequency of the extrapelvic nodal and/or extranodal distant metastases involvement in LACC emphasizes the need to use other diagnostic methods not included by the FIGO such as PET/CT. In our series, PET/TC was able to detect about 27% of extrapelvic localizations that led, in all cases to change the original planned therapeutic approach.

DEVELOPMENT OF PREDICTOR SCORE OF EFFECTIVENESS NEOADJUVANT CHEMOTHERAPY IN LOCALLY ADVANCED BREAST CARCINOMA

Katia Hiromoto Koga.

BRAZIL

Institucion: São Paulo State University-Botucatu Medical School Estado: São Paulo,Brasil Coautores: Sonia Marta Moriguchi, Jorge Nahás Neto, Eduardo Tinois da Silva,Napoleão Ramalho Rodrigues

In order to develop a prediction score of neoadjuvant chemotherapy response, we proposed the breast scintigraphy with ^{99m}Tc-sestamibi associated prognostic factors as predictor method. We studied 65 patients diagnosed with ductal carcinoma undergoing breast scintigraphy before neoadjuvant chemotherapy, immunohistochemical panel and surgical specimens. The scintigraphic analysis included the development of uptake index made by counts/pixels in identical region of interest under tumor lesion and the reference region in the contra lateral breast and area calculation. The statistical analysis was performed for the total group of patients and separately for groups of AC(adriamycin and cyclophosphamide) chemotherapy regimen and ACT(adriamycin, cyclophosphamide and taxane). It was made a logistic regression model using variables, age, index, tumor location, immunohistochemical panel and axillary nodes, obtaining values predicted according to the complete pathologic response, ROC curve was drawn up, to get score a higher sensitivity and specificity. The area under the ROC curve was significant for all groups and the score obtained was 0.728, 0.834 and 0.667 for the groups total, AC and ACT, respectively. The sensitivity, specificity, and positive and negative predictive values were 81.6%, 81.2%, 93% and 59% for the total group, 75.8%, 90%, 96.1% and 52.9%, for the AC group and 81.3%, 83.3%, 92.8% and 62.5% for the ACT group. The multifactorial prediction score is an effective method for the prediction of neoadjuvant chemotherapy response, that reflects the biology of the tumor against chemotherapy regimen, early identification of patients who would not benefit from this treatment.

RELATION BETWEEN SCINTIGRAPHIC IMAGING 99MTC EDDA / HYNIC-LYS 3-BOMBESIN AND 99MTC-EDDA/HYNIC-RGD WITH HISTOPATHOLOGICAL DIAGNOSIS OF BREAST TUMORS IN EARLY STAGES. PRELIMINARY COMMUNICATION

Alberto E. Hardy Pérez1,3 Guillermina Ferro Flores2 Claudia Herrera1 Araceli García Flores3. Brenda León Mejía1.

1 Centro Oncológico Estatal-ISSEMyM (COE).
2 Instituto Nacional de Investigaciones Nucleares. 3 Facultad de Medicina UAEMex.

MEXICO

Background Early detection of breast cancer with radiolabeled peptides is subject of current research.

Receptors gastrin releasing peptide (GRP-R) over-expressed in breast cancer cells and metastatic nodules and specifically bind the peptide bombesin. Specific binding of integrins □ angiogenesis (v) □ (3) and □ (v) □ (5) to the cycle-arginine-glycine-AC sequence. aspartic acid (RGD-c) are the foundation to mark bombesin and c-RGD peptides with 99mTc. In previous communication showed uptake of both peptides in mammary tumors auto-detected and corroborated by mammography. The differential uptake in non-cancerous and cancerous tissue is critical for diagnosis, prognosis and treatment of breast cancer in early stages. Objective. Relate levels and

uptake 99mTc-EDDA/HYNIC-Bombesina 99mTc-EDDA/HYNIC-RGD in scintigraphic imaging with histopathology diagnosis of mammary tumors auto-detected and corroborated by mammography in 15 patient's early stages of COE-ISSEMyM. Material and Methods. Translational T1. Two early clinical phase. ROC rating. Opportunity nonrandom, sequential sample, 15 patients signed informed consent. Project approved by Research Ethics Committees: Faculty of Medicine and Cancer Center UAEM ISSEMyM State. Patient dose: 740 MBq or 740 MBq 99mTc-EDDA/HYNIC-Lys3-BN, after 99mTc-EDDA/HYNIC-RGD intravenously.Imaging: supine, hands behind his head.

Country armpits, mammary glands and upper thorax. Anteroposterior static images, SPECT 10 minutes and 10 minutes. Two ROIs were drawn on each breast, one outlining the suspect and peripheral region of the same dimensions. Count rate in each ROI and the ratio of accounts between peripheral ROI (S) / suspicious ROI (L) was calculated Statistical analysis. Mean, SD, Student t confidence intervals and X2 to link accounts with histopathology results.Results: Reasons tissue healthy / injured or cancerous tissue by histopathology indicate greater uptake in injured tissue, statistically significant, with t-test for difference between means, paired groups, 99mTc-EDDA/HYNIC-Lys3-BN p 0.009 and 99mTc-EDDA / HYNIC-RGD p 0.01. Confidence intervals for difference between means: 0.23 to 0.09 and 0.27 to 0.09 respectively, do not include zero, p 0.05 significant difference. Yates X2 without significance in both radiopharmaceuticals. Sensitivity 0.77 and 0.88; specificity; 0.80 and 0.80; 0.87 and 0.88 + VPP, VPP-0.66 and 0.80, respectively BN and RGD. Discussion and Conclusions: The differential visual sharpness between healthy tissue and injured scans on images 99mTc-EDDA/HYNIC-Bombesina 99mTc-EDDA/HYNIC-RGD and significant statistical differences between uptakes of healthy tissue less of the injury tissue, cancer, makes them more useful for diagnosis and prognosis of breast cancer early, and probably to assess therapeutic response. Results guiding scientific imposed obligation to conduct similar studies with larger sample and in different populations.

COMPARISON OF TC-99M V-DMSA SCINTIGRAPHY AND F-18 FDG PET/CT IN BREAST CANCER

Sezen ELHAN VARGÖL ,Eser LAY ERGÜN ,Kadri ALTUNDAĞ ,Taner BABACAN
ERGÜN,Can ATEŞ.

TURKEY

Aim: FDG-PET/CT is well-known for the evaluation of breast cancer. Tc-99m V-DMSA uptake has been shown in many types of cancers. Clinical researches about Tc-99m V-DMSA in breast cancer are limited. The aim of this study is to compare Tc-99m V-DMSA scintigraphy and FDG-PET/CT in breast cancer. Methods: V-DMSA planar-SPECT images versus FDG-PET/CT were compared in 23 breast cancer patients. Qualitative-quantitative evaluation were performed. Uptake activities in tumor sites (VUS-visual uptake score) were classified from 0 to 3 (1-mild,2-medium,3-significant uptake) visually within both of two techniques. For quantitative evaluation SUVmax values of PET/CT and V-DMSA uptake ratio (DUR) were compared. V-DMSA uptake ratio was calculated (DUR=ROItumor/ROIbackgroundX100). Statistically, intraclass corelation coefficient (ICC) was used. Results: No correlation was determined between planar V-DMSA and FDG-PET/CT images. In bone metastases, VUS of V-DMSA and FDG showed statically significant, but low correlation (ICC=0.365). Low number of primary breast lesions(8) were detected, no significant correlation was found. In axillary metastasis; 30,33% of FDG positive foci showed V-DMSA positivity. In other site-lymph nodes, no statically significant correlation was obtained. Among 43 FDG positive lung metastases, only one showed V-DMSA avidity. In liver metastases, 37,5% of FDG positive liver foci were detected by V-DMSA SPECT. Among brain metastases 2 of them showed Tc-99m V-DMSA and one displayed FDG uptake. Additional physiological V-DMSA uptake sites were determined.Conclusion: This study is the first clinical research which compares Tc-99m V-DMSA scintigraphy and FDG-PET/CT in breast carcinoma. For the evaluation of breast cancer metastasis, we advocate to perform FDG-PET/CT. In bone metastasis, V-DMSA has low, but statically significant correlation with FDG-PET/CT. SPECT is important for the differentiation of malignant/physiological/deeply-located V-DMSA uptake. Future research with high number of primary breast lesion is needed in this respect. Keywords: Tc-99m V-DMSA, breast cancer, F-18 FDG PET/CT, V-DMSA SPECT-imaging

THE INVOLVEMENT OF CRANIAL AND PERIPHERAL NERVES AND ROOTS BY NEUROLYMPHOMATOSIS EVIDENCED BY 18F-FDG PET/CT

Ana Carolina Trevisan[1], Belinda Pinto Simões[2], Whemberton Martins Araújo[2], Antonio Carlos Santos[2], Leonardo Alexandre Santos[2], Daniele Kanashiro Sonvenso[2], Felipe Arriva Pitella[2], Emerson Nobuyuki Itikawa[1], Camila Eduarda Polegato Baltazar[2], Lauro Wichert Ana[2].

[1]Faculdade de Engenharia de São Carlos, Pós-graduação Bioengenharia EESC/FMRP/IQSC, Universidade de São Paulo – Brasil.

[2]Faculdade de Medicina de Ribeirão Preto, Universidade de São Paulo – Brasil.

BRAZIL

Aim: We report a case of neurolymphomatosis (NL), which presented with the involvement of cranial and peripheral nerves and roots, and presenting with a remarkable uptake of 18F-FDG in the trigeminal ganglia.

Materials and Methods: A 56-year-old female patient presented with lump in he left breast, hoarseness and nasal obstruction. Treated as sinusitis without mprovements, she identified a nodular lesion in the right scapular region and underwent for the Computed Tomography (CT), we observed other infiltrative mass and through biopsy was diagnosed non-Hodgkin's diffuse large B cells. After chemotherapy, CT showed another persistence of lesions then we ordered other exams like Magnetic Resonance Imaging (MRI) and Positron EmissionTomographhy/ Computed Tomography (PET / CT).

Results: The MRI showed thickening and infiltration in 75% of Peripheral Nerves systems and the PET/CT showed thickening in nerve topographies with hyperfocus along the left cervical plexus, was rounded formation and welldefined on the upper anterior mediastinum and in two focal areas of anomalousradio concentration in bilateral parasellar topography of skull, concluding Neurolymphomatosis.

Conclusions: Although CT and MRI are the best known methods, PET/CT is showing the areas more functionally involved by Neurolymphomatosis. It is allowing greater sensitivity in identifying recurrences and may be essential to diagnose the involvement of the trigeminal nerve and nerve plexus.

IS BONE SCINTIGRAPHY NECESSARY IN PROSTATE CANCER PATIENTS WITH LOW PSA LEVEL?

Antigoni Velidaki, Anna Kolindou, Anastasia Evagellatou, Maria Karkani, Evangelos Dagrakis, John Koutsikos*.

*Nuclear Medicine Dept., Laiko General Hospital of Athens, GREECE * Nuclear Medicine Dept., 401 General Military Hospital of Athens, Greece.*

GREECE

Objectives: Serum Prostate Specific Antigen (PSA) levels correlate with the risk of extra-prostatic disease extension. Bone metastases represent the main metastatic site in about 80% of prostate cancer patients. Despite the fact that bone scintigraphy (BS) is considered the most sensitive modality for the detection and follow up of bone metastases, many studies propose that BS are not necessary in patients who have PSA <20 ng/ml, unless the history or clinical examination suggests bony involvement. The aim of our study was to evaluate the correlation of PSA with bone metastases in patients with prostate cancer.

Materials and method: This retrospective study included 234 prostate cancer patients, referred for BS last 5 years. According to PSA levels patients were divided into 3 groups. Group I included 111 patients with PSA<10 ng/ml, group II 15 patients with PSA>10ng/ml and <20 ng/ml and group III 108 patients with PSA >20 ng/ml. 20 mCi 99mTc-MDP was injected to all patients and whole body acquisition combined with spot images (if necessary) were performed at least 2 hours post injection. Other imaging modalities were performed to establish osseous metastatic disease in equivocal cases.

Results: Overall bone metastases were detected in 129 patients (54%). Group I 39/111 patients (35%), group II 6/15 patients (40%) and group III 84/108 patients (77%).

Conclusion: This study demonstrates that bone scan is mandatory even in patients whose PSA level is less than 10 ng/ml since the incidence (35%) of bone metastases in this population is quit high.

PREDICTIVE VALUE OF DUAL TIME POINT IMAGING DIFFERENTIATION BETWEEN MALIGN AND BENIGN PANCREATIC LESIONS, PRELIMINARY RESULTS

Funda Ustun, Alev Ergulen, Gülay Durmus Altun. Trakya Üniversitesi Tıp Fakültesi Nükleer Tıp A.D.

TURKEY

The aim of the study was to explore the value of dual-time-point 18F-FDG PET/CT in differentiation of malignant from benign pancreatic lesions.

Materials and methods: 18F-FDG PET/CT scans of 45 patients with histologically proven pancreas lesions were retrospectively reviewed. Standardized uptake value (SUV)max was calculated for semi-quantitative assessment. The SUV of the two acquisitions were signed SUV(early) (E-SUV) and SUV(delayed) (D-SUV), respectively. The relationships between E-SUV, D-SUV according to postoperative pathologic diagnosis were analyzed.

Results: A subset of 16 patients was also scanned at 1 h and 2 h following the injection of 18F-FDG. The mean age of the patients in our study was 62 ± 10 years (range 35-80 years; 26 males and 19 females). The mean size of the pancreatic lesions measured at PET on CT images examination was 38 ± 12,8 mm (range 11-77mm). Tumour was located in the head of the pancreas in 20 patients (54%). Of 45 patients, were diagnosed as having a malignant pancreatic tumor, including 17 with positive metastatic liver diseases and with 22 another area of metastasis. The E-SUV of the malignant and benign tumors obtained at early images were 8,25 ± 6,49 and 4,6 ± 1,5, respectively, with this difference statistically significant (p = 0.01). However, late images SUV values' were not significantly different (p>0.5).

Conclusion: Differentiation between malignant tumors and benign lesions remains a major problem in diagnostic imaging. Dual time acquisition may be difficult to perform in routine clinical settings because it is a time consuming procedure. The current data suggest that delayed 18F-FDG-PET/CT scanning at 2 hours not recommend.

VALUE OF SENTINEL LYMPHNODE BIOPSY IN PAPILLARY THYROID CANCER

Raquel Novas Cabrera.

BRAZIL

University of Campinas (UNICAMP)
SÃO PAULO,BRAZIL

OBJECTIVES: Evaluate the performance of sentinel lymph node (SLN) biopsy in detecting occult metastases in papillary thyroid cancer (PTC) and the correlation of occult LN metastases to histology of the primary tumor and patient characteristics.

MATERIALS AND METHODS: Forty-two patients (34 females, mean age 46.9 years 1736) with PTC diagnosed by fine-needle aspiration biopsy and without evidence of loco-regional LN metastases by clinical exam and ultrasound were prospectively enrolled. Patients with prior neck surgery or radiotherapy, cervical lymphadenopathy and pregnancy were excluded. All patients were submitted to SLN lymphoscintigraphy prior to total thyroidectomy. An ultrasound guided peritumoral injection of 7.4 MBq of phytate-^{99m}Tc was performed as either a single injection or two injections (in multifocal diseases). SPECT/CT images of the cervical region were acquired 15 minutes after radiotracer injection and 2 hours prior to surgery. Intra-operatively, a hand-held gamma probe was used to locate the SLN. SLNs were removed along with non-SLNs located in the same neck compartment level. Histopathology of PTC was divided into: aggressive type (solid, tall and oxyphilic cells) and non-aggressive type (papillary, follicular and classic variants). All SLNs and non SLNs were submitted to histopathology analysis immunohistochemistry.

RESULTS: SLNs were located in levels VI in 94.6% of patients, level II in 32.4%, level III in 27.0%, level IV in 18,9%, and one in level VII (2.7%). One single metastatic SLN in level V occurred in one patient (4.3%) with a 3.5 cm multifocal PTC, aggressive variant, extra-thyroid extension, positive surgical margins and vascular invasion with a metastatic. Metastases in the SLN were noted in 14 patients (37.8%) and SLN was false-negative in 3 patients. Histology of SLN and non-SLNs was: aggressive (10/37), positive surgical margins (10/37), and extra-thyroid extension (8/37) and angio vascular invasion (8/37). SLNs contra-lateral to the primary tumor were also noted in 5/37 patients (levels II, III and IV) and none were metastatic. There were significant associations between LN metastases and age (p = 0.024 T-student Test) and tumor size (p = 0.034; T-student Test). No correlations were noted among LN metastases and patient sex, stimulated thyroglobulin levels, tumor angio vascular invasion, extra-thyroid extension, positive surgical margins, aggressive histology and multifocal lesions.

CONCLUSION: SLN biopsy can detect occult metastases in PTC. The risk of a metastatic SLN is increased in larger tumors and in younger patients. This may help guide future patient surveillance and radioiodine therapy doses.

BONE SUPERSCAN AS AN UNCOMMON PRESENTATION OF HISTOLOGICAL PROVEN METASTASIC GASTRIC CANCER.

Birocco, María José; Facello, Adolfo; Flores Turk, M.Guadalupe; Clariá, Marcelo; Massanet, Diego.

ARGENTINA

Instituto Oulton. Córdoba. Argentina.

Bone superscan pattern is uncommon in bone scans and is related to a variety of metabolic bone disorders (hyperparathyroidism, renal osteodystrophy, osteomalacia and others) as good to malignancies, in such case representing widespread diffuse metastatic disease of bone. Intense bone activity and absence or decreased visualization of kidneys in whole body scan can be explained by diffuse bone marrow involvement. This pattern was reported for metastatic prostate, breast, lung, bladder, colon and transitional cell carcinomas, lymphoproliferative diseases and myelofibrosis. Bone metastastatic spread is uncommon in gastric cancer an mainly shows osteolytic appearance, nevertheless superscan pattern was occasionally reported. We present the case of a 72-years old male patient referred from his primary physician for persistent and progressive diffuse bone pain during last three months. He had a history of prostate cancer treated with radical prostatectomy followed by local radiotherapy twelve years before. Additionally, partial gastrectomy was performed 18 months before and a poor differentiated gastric adenocarcinoma, signet ring cell type, pT2 pN0 pMx stage, was found. Physical examination showed an anemic but in good general condition patient, without gastrointestinal or abdominal complaints. Relevant lab showed: hemoglobin 8.7 gr%, hematocrit 27%, serum calcium 8.7 mg/dL, alkaline phosphatase 7 755 IU/L and PSA 0.5 ng/mL. Whole body scan was performed three hours after 740 MBq MDP-Tc99m intravenous administration, using a dual head camera. An intense, diffuse bone uptake was found over axial and proximal appendicular skeleton with poor renal visualization, consistent with superscan pattern. Gastric origin was suggested in nuclear report.

Oncologist performed iliac bone biopsy that showed diffuse metastatic infiltration by signet ring cells of gastric origin. Chemotherapy was started. In conclusion, looking a bone superscan in a male patient, even in presence of prostate cancer history, other clinical facts must be evaluated and uncommon primary pathologies considered.

ADDITIONAL VALUE OF SPECT/CT IN IDENTIFYING SENTINEL LYMPH NODES IN PAPILLARY THYROID CANCER

Raquel de Paula Mendes de Oliveira, Oliveira RPM1; Cabrera RN1, Chone CT2, Zantut-Wittmann D3, Matos P4, Miranda D5, Pereira PSG2, Ferrari RJR1, Santos AO1, Etchebehere ECSC1.

BRAZIL

Sentinel lymph node biopsy (SLNB) is a well-established method for the identification of nodal metastases in various cancers. Its use has been a matter of debate in patients with papillary thyroid cancer (PTC), since the incidence of nodal metastases in PTC can be as high as 80%. The value of SPECT/CT in patients submitted to SLNB for PTC has not yet been evaluated.

OBJECTIVE: To compare planar with SPECT/CT images in SLNB in PTC patients. METHOD: Twenty-five patients (22-75 years old, mean 44.4 years, 20 females) were prospectively enrolled. Patients with Bethesda V or VI nodules underwent preoperative lymphoscintigraphy for identification of the sentinel lymph node (SLN) prior to SLNB. Lymphoscintigraphy was performed by acquiring planar (anterior, posterior and lateral projections) and SPECT/CT images immediately after injection of 3.7 MBq of 99mTc-fitate. The SPECT/CT images were acquired in a 360° arch, 32 views/detector and a 64 x 64 matrix. The CT parameters were as follows: 130 kV; 60 mAs, 3 mm slice thickness. Planar and SPECT/CT images were analysed independently.

RESULTS: SPECT/CT images improved the preoperative evaluation of PTC by changing overall SLN mapping in 21/25 patients (84%). This was due to changes in SLN level in 18/25 patients (72%) and correct differentiation of SLN from radiotracer spilling, drainage pathway or radiotracer skin contamination in 10/25 patients (40%). SPECT/CT also identified additional lymph nodes in 12/25 patients (48%).The planar images contributed to the identification of additional SLNs in 8/25 patients (32%) by either identifying SLNs not identified in SPECT/CT images or showing that doubtful areas in SPECT/CT were indeed SLN. There were 9/107 lymph nodes identified with the use of planar images (8%), seven of which were very close to the injection site.There was no significant difference (p = 0,379; Student´s T Test) in the number of focal regions of LN uptake comparing planar to SPECT/CT images.

CONCLUSION: SLNs were easily identified and with a higher degree of certainty using both planar and SPECT/CT images. Identification of lymph nodes close to the injection site was accomplished effortlessly by planar images in the anterior projection. SPECT/CT allowed precise SLN localization by levels and identification of additional SLNs. SPECT/CT has become a powerful tool for surgeons since they rely on anatomical landmarks to help plan surgery ahead with a potential to decrease surgical time and morbidity. SPECT/CT is an increasingly required technique in the operating room.

RADIOGUIDED OCCULT LESION LOCALIZATION (ROLL) IN REOPERATIVE PROCEDURES OF PATIENTS WITH LOCOREGIONAL METASTASES OF PAPILLARY THYROID CANCER : INITIAL EXPERIENCE FROM A THYROID CANCER CENTER

Ilgin Sahiner Ankara Oncology Hospital.
Gulin Ucmak, Mehmet Ali Gulcelik, Tuba Sengezer, Seyfettin Ilgan.

TURKEY

Aim: Surgery is the preferred modality of treatment in locoregional recurrences of papillary thyroid cancer (PTC) providing improved disease control. However, reoperative surgery in patients with previous neck exploration in either central and/or lateral compartments carries increased risks associated with surgery in addition to diminished operative success. The aim of our study was to determine if radioguided occult lesion localization (ROLL) technique was feasable in terms of surgical success and reduction in complication rates in reoperations of PTC recurrences.

Materials and methods: Eight consecutive patients (6 female, 2 male) who were previously operated for papillary thyroid cancer with cytological proof of locoregional recurrences in the previously operated neck compartments were included in the study. Preoperative mapping and injection of Tc-99m labeled macroaggregated albumin into selected lesions were performed under guidance of ultrasonography (US). Surgical exploration was carried out according to the US map and labeled lesions were localized with a hand-held gamma probe intraoperatively. After the excision of lesions; counts from the background, lesion and postexcisional site were compared to confirm the success of the procedure. All excised specimens were evaluated histopathologically and serum levels of thyrotropin (TSH), thyroglobulin (Tg), anti-Tg antibodies and calcium were recorded for each patient before and (minimum 45 days) after the surgical procedure.

Results: Mean patient age was 40.5 (range: 17-54). Seven of eight patients had previous therapies with radioiodine (cumulative activity range:100-1150mCi, median:300mCi of I-131). The smallest lesion injected was 5x5mm and the largest lesion was 15x13mm in two dimensions. An average of 2.25 injections were performed per patient (range:1-4 injections). A total of 51 suspicious lesions were detected preoperatively, 104 lesions were excised and 54 were histopathologically proven to be infiltrated by PTC. In 2 patients unilateral central compartment exploration, in 1 patient unilateral level IV and bilateral central exploration, in 1 patient bilateral lateral (levels II-IV) and bilateral central exploration, and in the remaining 4 patients 2 different compartmental explorations were performed. Serum Tg levels of all patients displayed reductions on similar pre- and post-operative TSH levels with one patient showing declines both in anti-Tg antibody and in Tg levels. Ductus thoracicus injury occured only in 2 patients without any chyle leak observed in the follow up period.

Conclusion: ROLL technique and lesion mapping under preoperative US guidance is a safe and efficient method in terms of surgical success with reasonable complication rates in reoperations of locoregional PTC recurrences.

ADDITIONAL VALUE OF SPECT-CT IMAGES IN RADIOIODINE SCANNING AT FOLLOW-UP OR POST ABLATION THERAPY IN DIFFERENTIATED THYROID CANCER.

J. Vilar, E. Moreira, V. Depons, R. Hitateguy, A. Battegazzore, A. Sánchez, K. Bayardo, K. Suanes, M. Langhain, R. Ferrando.
Consultorio de Medicina Nuclear “Ferrari-Ferrando-Páez”-Montevideo-Uruguay.

URUGUAY

The protocol for differentiated thyroid cancer includes whole-body scanning with iodine-131 for detecting residual thyroid tissue and distant metastases after thyroidectomy. We evaluated the advantages of SPECT-CT with respect to conventional whole-body images. Two experienced observers interpreted conventional planar images and SPECT-CT independently and differences were resolved by consensus. We evaluated whether the SPECT-CT images provide additional diagnostic information in two categories in terms of new disease locations and false positive recognition. We reviewed 161 patients who underwent radioiodine whole-body scanning and SPECT-CT in the last 5 years at follow-up (n = 67) or post ablation therapy (n = 94). Average age was 53 years (range 15-78 years) in the first group and 47 years (14-84) in the second. Female sex predominated in both groups. In follow-up studies new disease locations were confirmed with SPECT-CT in 8 cases (12%), including lymph nodes (n = 4), bone (n = 2) and lungs. False positive findings were confirmed in 19 studies (30%), including accumulation of radioiodine in digestive tract (n = 13) most of them in the esophagus, followed by head and neck focal uptake (n = 4) in dental processes, salivary glands, respiratory tract (n = 2) and skin contamination (n = 1). New lesions were detected by SPECT-CT in 30 patients (31%) with post ablation studies, corresponding to lymph nodes in 17, bone metastasis in 8 and focal lung in 5. False positives were confirmed in 25 studies (26%), including focal uptake in head and neck

(n = 14), most of them related with dental processes (n = 8), followed by accumulations at the digestive tract (n = 7), skin contamination (n = 3) and thymus (n=1). No additional impact of SPECT-CT was observed in 40 follow-up and 45 post ablation scans in which the procedure was indicated because of previous lymph node involvement or suspected local or regional recurrence on ultrasound. Conclusion: The detailed anatomical information provided by SPECT-CT is able to increase the diagnostic power of the conventional whole-body radioiodine scans in both follow-up and post ablation studies, allowing detection of new lesions and reducing false positive findings. SPECT-CT impact seems to be al least very limited in patients with negative whole-body images.

DIAGNOSIS CHALLENGE OF SUSPECTED LIVER METASTASES IN A PATIENT WITH COLORECTAL CANCER AND CAROLI'S DISEASE

MD Moises Aracena[1], MD Shigeru Kozima[1], MD Ricardo Oddi[2], MD Nebil Larragaña[1],MD Juan Cruz Gallo[1],MD Carlos Ferrarotti[1], MD Danny Mena[1], MD Carlos Ospina[1], MD Maria Bastianello[1], Argenitna.

[1]Imaging Department. Hospital Universitario CEMIC
[2]Surgery Department. Hospital Universitario CEMIC

ARGENTINA

SUMMARY:Caroli's disease is a condition caused by poor absorption of the ductal plate, which leads to saccular dilatation of intrahepatic bile ducts, associated or not with congenital hepatic fibrosis. This illness may develop hepatolithiasis with cholangitis or biliary obstruction, thus appearing clinical suspicion.The diagnosis is imagenologic, observed by tomography or ultrasound which manifests the "central point" sign. Anyhow, the gold standard is the magnetic resonance cholangiopancreatography. The main complication is cholangitis with and without cholangiocarcinoma. The treatment is only possible by lobectomy in patients with limited involvement of the hepatic lobe or liver transplant in cases of diffuse disease.This present case describes a patient diagnosed with Caroli's disease, who presented concomitantly Mucin-secreting adenocarcinoma within the sigma, Dukes C, T4N1 (1/23). It was managed with surgical resection and chemotherapy. Five years later, follow-up tomography presented a suspicious image of liver metastases in VII segment. PET CT was performed with FDG, showing multiple hypodense rounded hypometabolic lesions in the I, IV and VII liver segments. It also showed two hypermetabolic images without clear tomographic translation in III / IV and VII segments with early SUV max 8 and 3.6 and 10.6 and 3.8 late respectively. These findings did not manifest the typical behavior of hypermetabolic colorectal metastases but rather a local inflammatory / infectious process, so liver puncture was performed to confirm the suspicion. The latter was reported as Caroli's disease with extensive chronic inflammatory process associated with residual calculi activity.

CONCLUSION:The purpose of this case report is to review the usefulness of FDG PET CT in the study of metastatic liver lesions of difficult valuation in the context of Caroli's disease and its metabolic and morphological behavior.

THE IMPACT OF STAGING FDG PET/CT IN THE EVALUATION OF BONE MARROW INVOLVEMENT IN PATIENTS WITH HODGKIN LYMPHOMA - A MULTICENTRIC STUDY IN BRAZIL.

Juliano Julio Cerci. Brasil, Elba Etchebehere, Rômulo Hermeto Bueno Do Vale; Allan De Oliveira Santos, Andreia Vicente, Paulo Schiavom Duarte; Marcos Santos Lima; Marcelo Tatit Sapienza, Carlos Chiatoni, Celso Dario Ramos.

BRAZIL

Objectives: To assess the impact of staging FDG PET/CT (PET) in the evaluation of bone marrow involvement in patients with Hodgkin lymphoma (HL) in multiple centres in Brazil.Methods: All patients were submitted to pre-treatment staging with PET; the studies were performed in each participating PET centre. Bone marrow biopsy (BMB) results were compared to staging PET results. PET in bone marrow was classified as completely negative, with mild diffuse uptake (also considered negative), moderate to severe diffuse uptake and presence of focal uptake.

Results: One hundred and seventy seven patients, median age 34.0 years (range16-80) wererecruited. BMB and PET were concordant in 144/177 (81.4%) and discordant in 33/177 (18.6%) patients. Only two patients (1.1%) presented PET-negative and BMB-positive results, while 31 (17.5%) patients presented BMB-negative and PET-positive results. Of the two patients with PET-negative and

BMB-positive results, one had already been classified as stage IV by PET due to other lesions. While FDG PET/CT impact of bone marrow commitment, regarding clinical staging, was seen in 19/177 (10.7%) patients.

Conclusion This large multicentric study shows that FDG-PET might replace BMB in the evaluation of bone marrow commitment in HL.

ADDITIONAL VALUE OF SPECT/CT IN IDENTIFYING SENTINEL LYMPH NODES IN PAPILLARY THYROID CANCER

Raquel de Paula Mendes de Oliveira.

BRAZIL

Sentinel lymph node biopsy (SLNB) is a well-established method for the identification of nodal metastases in various cancers. Its use has been a matter of debate in patients with papillary thyroid cancer (PTC), since the incidence of nodal metastases in PTC can be as high as 80%. The value of SPECT/CT in patients submitted to SLNB for PTC has not yet been evaluated.

OBJECTIVE: To compare planar with SPECT/CT images in SLNB in PTC patients.

METHOD: Twenty-five patients (22-75 years old, mean 44.4 years, 20 females) were prospectively enrolled. Patients with Bethesda V or VI nodules underwent preoperative lymphoscintigraphy for identification of the sentinel lymph node (SLN) prior to SLNB. Lymphoscintigraphy was performed by acquiring planar (anterior, posterior and lateral projections) and SPECT/CT images immediately after injection of 3.7 MBq of ^{99m}Tc-fitate. The SPECT/CT images were acquired in a 360° arch, 32 views/detector and a 64 x 64 matrix. The CT parameters were as follows: 130 kV; 60 mAs, 3 mm slice thickness. Planar and SPECT/CT images were analysed independently.

RESULTS: SPECT/CT images improved the preoperative evaluation of PTC by changing overall SLN mapping in 21/25 patients (84%). This was due to changes in SLN level in 18/25 patients (72%) and correct differentiation of SLN from radiotracer spilling, drainage pathway or radiotracer skin contamination in 10/25 patients (40%). SPECT/CT also identified additional lymph nodes in 12/25 patients (48%).The planar images contributed to the identification of additional SLNs in 8/25 patients (32%) by either identifying SLNs not identified in SPECT/CT images or showing that doubtful areas in SPECT/CT were indeed SLN. There were 9/107 lymph nodes identified with the use of planar images (8%), seven of which were very close to the injection site.There was no significant difference (p = 0,379; Student´s T Test) in the number of focal regions of LN uptake comparing planar to SPECT/CT images.

CONCLUSION: SLNs were easily identified and with a higher degree of certainty using both planar and SPECT/CT images. Identification of lymph nodes close to the injection site was accomplished effortlessly by planar images in the anterior projection. SPECT/CT allowed precise SLN localization by levels and identification of additional SLNs. SPECT/CT has become a powerful tool for surgeons since they rely on anatomical landmarks to help plan surgery ahead with a potential to decrease surgical time and morbidity. SPECT/CT is an increasingly required technique in the operating room.

SARCOIDOSIS AFTER ABIRATERONE THERAPY IN PROSTATE ADENOCARCINOMA: A POTENTIAL CAUSE OF FALSE-POSITIVE ON ^{18}F-FDG PET/CT

Raquel de Paula Mendes de Oliveira.

BRAZIL

INTRODUCTION: The association of sarcoidosis and sarcoid-like reactions and malignancy is controversial, but there is evidence to suggest that such a relationship exists. The sarcoidosis-related cancer includes lymphomas, other hematologic malignancies and solid tumours. Furthermore, some antineoplastic agents appear to contribute to the induction of new-onset sarcoidosis or the exacerbation of pre-existing disease. We here present a case, in which it was hypothesized that sarcoidosis may have been induced by abiraterone, since the drug was introduced 3 months prior to the appearance of the hypermetabolic thoracic lymph nodes.

CASE REPORT: A 74-year-old man with prostate adenocarcinoma metastatic to bones and pelvic lymph nodes underwent serial ^{18}F-FDG PET/CT (FDG-PET/CT) studies during 6 years. The treatment for local disease and bone metastases during this period consisted of orchiectomy, hormonal therapy, chemotherapy, radiotherapy and cryoablation. FDG-PET/CT control studies became negative. New increased PSA levels led to 3 months of abiraterone therapy. The FDG-PET/CT performed at the end of this period (5 months after the previous study) demonstrated enlarged hypermetabolic mediastinal and hilar lymph nodes bilaterally. Since there was a dis-

crepancy between the low levels of PSA and the amount and the very high metabolism of the thoracic lesions, a finding unusual for metastases from prostate cancer, the patient underwent ultrasound-guided endoscopic biopsy. Thoracic lymph node histopathology revealed granulomatous lymphangitis without tumour or infections disease, consistent with a sarcoid-like reaction.After 2.5 months of corticosteroid therapy (prednisone, 40 mg/day), the hypermetabolic pulmonary and mediastinal lymph nodes were no longer detected on a follow-up ^{18}F-FDG PET/CT study, a finding that further supports the diagnosis of sarcoidosis.DISCUSSION: It has been estimated that approximately 4 - 14% of all patients with cancer exhibit evidence of sarcoid-like reactions on histopathology and that the prevalence of suspected sarcoid-like reactions is of 1.1% of cancer patients undergoing ^{18}F-FDG PET/CT examinations. Therefore, this possibility should be taken in consideration amongst those patients, especially those in whom the exam findings are not in accordance to what is expected. CONCLUSION: These findings emphasize the importance of recognizing sarcoidosis/sarcoid-like reaction as a potential cause of false-positive ^{18}F-FDG PET/CT studies, which could potentially lead to inappropriate management decisions in oncologic patients.

SENTINEL LYMPH NODE BIOPSY IN SKIN MELANOMA: ANALYSIS OF PATTERNS OF FIRST-RECURRENCE, DISEASE FREE SURVIVAL, POST-RECURRENCE SURVIVAL AND CLINICAL PATHOLOGIC FACTORS RELATED TO THEM.

Carmen Estebanez Estebanez.

SPAIN

OBJECT: To determine initial relapse patterns, disease free survival (DFS), post-recurrence survival (PRS) and clinical pathologic factors related after sentinel lymph node biopsy (SLNB) in patients with skin melanoma. METHODS: Retrospective study of 402 patients (181 men; mean age 54.5±15.1 y/o; range: 13-89) who underwent lymphatic mapping and SLNB with colloids alone, at our institution, between 1999 and 2012. We used the protocol of our Melanoma Committee for follow up, setting up the end point at March, 2014. Relapse was defined as local if limited to skin or subcutaneous tissue, as lymphatic if situated in lymph nodes of the lymphatic territory or subcutaneous lymph nodes nearest to the tumour, and as remote when outside these territory, distinguishing between skin and lymphatic or visceral disease. In case of simultaneous relapse, the one with the worst prognosis was pondered.Sex, age, tumour site, thickness, mitotic rate, inflammation, ulceration status, Clark level and SLN status were evaluated for their influence on DFS and PRS by log-rank and Cox regression analysis. The study of relation between the different factors and the relapse patterns was carried out with the x^2 test.

RESULTS: Of the SLN-negative patients 40/296 (13.5%) experienced recurrence compared with 57/106 (53.8%) SLN-positive, p<0.001. In only one place 71/97 (73%) patients presented recurrence, 24/97(25%) in two and 2/97 (2%) simultaneously in 3. The pattern was more often local or nodal in patients with SLN- negative (77.5% vs. 43.9% ,p=0.001) , women (72.5% vs. 47.4, p=0.014) and localized in lower extremities (75.9% vs. 50.0, p=0.018). 10-Year DFS was 82.5% for node-negative patients and 40.9% for node-positive patients (p<0.001). On multivariate analysis the strongest prognostic factors for DFS were SLN positivity, Hazard Ratio (HR) of 4.2 (CI 95%: 2.6-6.8), p<0.001 and Breslow thickness ≥2 mm of HR 3.1 (CI 95%: 1.9-5.1), p<0.001.Of the SLN negative patients, 19 /40 (47.5%) died, and 42/57 (73.7%) with SLN positive (p=0.009). On multivariate analysis the strongest prognostic factors for PRS were visceral recurrence, HR of 5.0 (CI 95%: 2.8-9.1), p<0.001, Clark level ≥4 HR 2.2 (CI 95%: 1.2-4,1), p=0.009 and nodal/acral melanoma type, HR 2,2 (CI 95%: 1.2-4,1), p=0.008

CONCLUSIONS: In SLN-negative patients were less recurrences, the more frequently found pattern was local or nodal relapse and DFS was bigger than in SLN-positive. DFS independent predictive factors were SLN positivity and Breslow. After recurrence were more deaths in SLN positive patients. Visceral recurrence, Clark level and nodal/acral type were the only factors related with PRS. To know relapse patterns, DFS and PRS permits us a more individualized surveillance strategy.

NON-SENTINEL LYMPH NODES STATUS IN LYMPHADENECTOMY OF MELANOMA PATIENTS WITH POSITIVE SENTINEL NODE SELECTIVE BIOPSY, CLINICOPATOLOGIC FACTORS RELATED AND THEIR INFLUENCE IN THE RELAPSE AND SURVIVAL.

Carmen Estebanez.

SPAIN

OBJECT: First, analyze the rate of non-sentinel lymph nodes (NSLN) affected in lymphadenectomy related to the number of sentinel lymph node (SLN) positive, the size of the metastases in the SLN and other clinicopatologic factors. Second, verify if the existence of

NSLN-positives influence patients relapse and survival.

MATERIAL AND METHOD: Sentinel node selective biopsy (SLNB) was performed between 1999 and 2012 at a tertiary hospital by a single surgical team on a cohort of 403 melanoma patients stage I and II, that underwent lymphatic mapping with colloids alone. When the result of deferred histopathologic analysis with H&E and IHQ (HMB-45, melan A) of SLN was positive, total lymphadenectomy of lymphatic territories involved was carried out. Sex, age, tumor site, thickness, mitotic rate, inflammation, ulceration, Clark level, number of SLN positive and their tumor size were evaluated for their influence on NSLN status by bivariate and multivariate statistical analyses, and the NSLN status influence on the relapse and survival by Kaplan Meier analysis.

RESULTS: SLN positive were 106/403 patients (26.3%). Lymphadenectomy of lymphatic territories involved was carried out in 98 of these, but in 1 case the result is unknown. The median of lymph nodes extracted was 13.5 (IQR: 9-21) In 21/97 patients (21,6%) were metastatic NSLN (median 1 (IQR: 1-3). When only 1 SLN was affected, 15/85 (17,6%) were NSLN positive and 6/12 (50,0%) (p=0,011) when were more positive nodes in SLNB. When the SLN presented metastases ≤ 2 mm, 10/65 patients (15,4%) were NSLN positive, and when those were > 2 mm, were positive 11/32 (34.4%) (p=0.033). We also found a significantly bigger rate of positive NSLN in melanomas located in extremities (35.7%) to compare with the others sites (10.9%) p=0.003. On multivariate analyses we didn't found any independent predictive factor. When there weren't metastatic NSLN, 37/76 patients relapsed (48,7%) and 14/21 cases (66.7%) when there were positive NSLN, ns. 10-year disease free survival (DFS) was 46.9% in NSLN negative patients vs. 23.9% in those positive. When there weren't metastatic NSLN, 26/76 patients (34.2%) died because of the melanoma and 11/21 cases (52.4%) with positive NSLN, ns**.** 10-year melanoma specific survival (MSS) was 55.9% in NSLN negative patients vs. 24.3 in those positive, ns.

CONCLUSIONS: When there were more than 1 SLN positive and SLN metastases were > 2 mm, there were significantly more NSLN affected .We found differences in percentages of relapses and deaths melanoma related and in 10-year DFS and MSS depending on the existence of NSLN affected, although they weren't statistically significant, probably due to the limited patients number.

THE CLINICAL VALUE OF THE COMBINATION OF ^{18}F-FDG PET/CT AND SERUM TUMOR MARKER TO DETECT RECURRENCE AND METASTASIS OF COLORECTAL CANCERXu

Chun Zhang, Rong Fu Wang.

CHINA

Department of nuclear medicine, Peking University First Hospital, Beijing 100034 China

Objective: To evaluate the diagnosis efficacy of ^{18}F-FDG PET/CT and tumor markers (CEA, CA19-9, CA24-2) in recurrence and matastasis of postoperative colonrectal carcinoma. Methods: 90 patients were enrolled in this study including 56 rectal carcinoma, 34 colon carcinoma. All of the patients tested serum CEA within 2 weeks at the time of underwent PET/CT scan, partly of those patients tested serum CA19-9 and CA24-2. The follow-up time is 0.5 month to 26 months, with the mean follow-up time of 8.25 months. According to the pathology and clinic result of follow-up, calculate the sensitivity, specificity, positive predictive value negative predictive value of ^{18}F-FDG PET/CT and tumor markers, respectively. Result: According to the pathology and the result of clinic follow-up, the sensitivity of 18F-FDG PET/CT CEA CA19-9 CA24-2 were 96.10% 74.03%,31.88%,37.50% , respectively. The specificity of 18F-FDG PET/CT CEA CA19-9 CA24-2 were 76.92% , 46.15% , 72.73%, 63.34%, respectively. The positive predictive value of ^{18}F-FDG PET/CT CEA CA19-9 CA24-2 were 96.01%,89.06%,88.005,85.71% respectively. The negative predictive value of ^{18}F-FDG PET/CT CEA CA19-9 CA24-2 were 76.92%, 23.08%,14.55%,14.89% respectively. The PET/CT Kappa value is 0.7030, the P value of Kappa is 0.0001. CEA with CA19-9,CEA with CA24-2,CA19-9 with CA24-2, CEA with CA19-9 and CA24-2, the series of combination result is that the sensitivity were 26.09% 32.81% , 25.00%, 23.44% , respectively. The specificity were all 72.73%. The positive predictive value were 85.71%, 87.50%, 84.21%, 83.33% respectively. The negative predictive value were 13.56%, 15.69%, 14.29%, 14.04% respectively. Conclusion: The combination of 18F-FDG PET/CT and serum tumor marker to detect recurrence and metastasis of colorectal cancer has an important clinical value.

PORTABLE GAMMACAMERA IN DETECTION OF SENTINEL LYMPH NODE COMPARING WITH FREEHAND SPECT

H. Bowles-Antelo[1]. España, J. Orozco-Cortés[1], C. Rocafuerte-Ávila[1], A. Martínez-Agulló[2], C. De la Fuente[2].

[1]Nuclear Medicine Department. Hospital Clínico Universitario, VALENCIA, SPAIN,[2]Surgery Department. Hospital Clínico Universitario, VALENCIA, SPAIN.

SPAIN

INTRODUCTIONRecently it has been developed freehand SPECT(FSPECT) (declipseSPECT®) for radioguided surgery. It combines gamma probe, infrared detector, tracking targets(patient-probe), optical camera as well as processor. This equipment scan the studied area in the three axis, obtaining 3D reconstruction of the radioactivity in the surgical field, providing additional deep information. We present our experience in sentinel node(SN) detection with FSPECT, comparing with portable gammacamera (PGC, Sentinella ®).

MATERIAL AND METHODS We studied 18 patients, mean age 51(23-73) y/o, 5 malignant melanoma(MM) and 13 breast cancer(BC). The same day of surgery, we detect SN with conventional planar scintigraphy(PS) after administration of 2mCi 99mTc-nanocolloid albumin (MM: subdermal around scar, BC: intratumoral (guided by ultrasound/stereotactic in non-palpable) with periareolar reinjection if necessary). In the operation room, we obtain SN location by FSPECT, PGC and gamma probe, with histopathological study and lymphadenectomy if SN was involved.

RESULTS SN was located in all patients(100%) by PS. During surgery SN was identified by FSPECT in 11/18(61.1 %), by PGC in 15/18(83.3 %) and with both in 16/18(88.8 %). There was some difficulty in BC because SN-injection point proximity, more evident with FSPECT. We obtained coincidence FSPECT-PGC in 12/18(67%) patients: positive SN location(10)-no SN location(2). No coincidence in 6/18(33%): PGC location/FSPECT no location(5), PGC no location/FSPECT location(1). FSPECT provided precise information of SN depth and distance(mm) to the cutaneous border. After SN removal, there was agreement FSPECT-PGC in ex-vivo SN activity and surgical bed verification. It was possible to remove SN in 16/18(88.8 %) and not in 2 BC patients, one was in close proximity with tumor and was removed together with tumor and the other was involved after histopathological study. There were 4/16(25%) involved nodes: 1 MM/3 BC, with more involved nodes in 2/4 after lymphadenectomy.

CONCLUSION We obtained coincidence in SN location results with FSPECT and PGC in 67% of patients, being location possible with both in 88.8%. There was agreement with PS results in 83%(PGC) and 61%(FSPECT). In BC patients, SN-injection point proximity caused difficulties in SN identification, more with FSPECT in our group of study. We obtained important deep information of SN with FSPECT and useful superposition of 3D reconstruction in the surgical bed during surgery, both very useful to facilitate SN access and removal. It would be necessary to study more patients.

METABOLIC CHARACTERIZATION OF CERVICAL CANCER AND LYMPH NODE METASTASIS

Rossana Pruzzo[1]. Chile, Dania Acuña[2], Pedro Torres[2], Nicanor Barrena[2], Yuri Mc Conell[2], Eva Hernández[1], Francisca Redondo[1], Hugo Lavados[1], Horacio Amaral[1].

Nuclear Medicine and PET/CT center[1] and Gineco-oncology Unit[2].

CHILE

Fundación Arturo López Pérez. Santiago, Chile.

Cervical carcinoma is a serious public health problem in Chile, being the 6th cause of death for cancer in women. Cervical carcinoma staging is based on the International Federation of Gynecology and Obstetrics (FIGO) system, a clinical staging system that not include nodal status. However nodal status is a determining factor in therapeutic management.There is increasing evidence that ^{18}FDG PET/CT has a role in primary evaluation of cervical carcinoma, particularly, evaluating lymph node status in which case is more accurate than CT and distant metastatic disease. We evaluated tomographic and metabolic characteristics of cervix carcinoma and its lymphatic metastases.

MATERIALS AND METHODS:Between 2012 and 2013, whole-body ^{18}F-FDG PET/CT was performed in 51 patients with histologically proved and non operated cervical cancer. Ages ranged from 18 to 86 years. 44 of them had squamous cell carcinoma and 7 adenocarcinoma. FIGO system classified 22 patients in stage I, 18 in stage II, 6 in stage III and 3 in stage IV.We examined SUVmax, metabolic volume, primary tumor size and lymphatic metastases size (pelvis and retroperitoneum). Finally we confirmed the lymph node histology in the surgical cases, that didn´t show hypermetabolic adenopathies in PET/CT.7 women underwent diagnostic lumboaortic lymphadenectomy and 4 were treated by radical hysterectomy and pelvic lymphadenectomy. 72 lumboaortic and 107 pelvic lymph nodes were biopsied. RESULTS: In all cases, the primary lesion showed increased ^{18}FDG uptake with an average SUVmax of 18.9 (range from 6.9 to 36.4). The average metabolic volume was 108.5 cc (range from 4.8 to 300 cc) and the primary tumor size was superior to 40 mm in 42 patients.We observed hypermetabolic pelvis lymph nodes in 32 patients. 7 were less than 10 mm in their short axis, 18 between 10 and 15 mm, 2 between 15 and 20 mm and 5 over 20mm. The average SUVmax was 7.8 (range from 2.7 to 29.3).We observed hypermetabolic lumboaortic lymph nodes in 9 patients, all also having hypermetabolic pelvic nodes. The average SUVmax was 6.9 (range from 2.9 to 12.7).Histology of the hypermetabolic adenopathies was not available.In contrast, all patients with negatives lymph nodes in PET/CT were surgically confirmed.In cases of negative lymph nodes, the average SUVmax of primary tumor was 15.4 and metabolic volume 48.4 cc. In positive lymph nodes cases, the results were higher with SUVmax 19.7 and metabolic volume103 cc.

CONCLUSION:^{18}FDG PET/CT showed increased uptake in all cervical carcinoma with higher SUV in squamous ones. In those with higher metabolic volume, increased frequency of secondary pelvic adenopathies was observed. PET/CT had high negative predictive value for lymphatic metastases.

BONE METASTASES IN BREAST CANCER. COMPARISON OF FDG-PET/CT AND BONE SCINTIGRAPHY

Patricia Paredes Rodríguez.

SPAIN

AIMTo compare bone scintigraphy performed with technetium-labeled bisphosphonates and whole-body FDG-PET/CT for the detection of bone metastases in patients with suspected metastatic breast cancer, by retrospective study.Bone scintigraphy is the standard procedure for the detection of bone metastases in breast cancer patients, but FDG-PET/CT provides a specificity advantage over bone scan and higher spatial resolution.

MATERIAL AND METHODSWe reviewed 27 patients with breast cancer , whom were assessed with bone scintigraphy and FDG-PET/CT, within two months.Number of metastatic bone lesions detected with each technique and radiographic characteristics of lesions (lytic, blastic, mixed or no visualization) Both imaging procedures were evaluated by a radiologist and two nuclear medicine physicians.RESULTSConcordant results between bone scintigraphy and FDG-PET/CT 21/27 patients:14/21 PET and scintigraphy positives (9 of them without visualization CT) 7/21 negatives (1 of them with nonspecific findings on CT)
PET detected more lesions than bone scintigraphy, however PET detected fewer bone metastases compared with scintigraphy in patients with osteoblastic disease (without statistical significance by insufficient number of patients)

CONCLUSION FDG-PET/CT is more sensitive for the detection of bone metastases compared with bone scintigraphy. FDG PET is superior to bone scintigraphy in the detection of small metastases, osteolytic metastases, and can identify bone metastases when bone scintigraphy was negative or uncertain.Bone scintigraphy is more available and less expensive, and today is the standard procedure for the detection of bone metastases in breast cancer patients.

FEASIBILITY OF PARAMETRIC IMAGING IN ^{18}F-FDG PET/CT DYNAMIC MULTI-BED SCANNING FOR PULMONARY LESIONS

Rong Fu Wang[1]. China, Qiang Wang [1], Jian Hua Zhang, Yun Zhou [2]

1. Department of Nuclear Medicine, Peking University First Hospital, Xichengqu, West District, Beijing, China
2. Russell H. Morgan, Department of Radiology and Radiological Science, School of Medicine, Johns Hopkins University, Baltimore, USA

UNITED STATES

Objective: Benign and malignant pulmonary lesions are not easy to distinguish in a clinical setting. Our aim was to investigate the feasibility of ki parametric imaging in the diagnosis of pulmonary lesions. Dynamic multi-bed scanning followed by a routine examination was performed on fifty patients who had pulmonary lesions.

Methods: The fifty patients were divided into groups with malignant and benign lesions. The number of cases and lesions in the malignant and benign groups were 6(9) and 9(12), respectively. The left ventricular blood pool was used for an image derived input function. The influx rate constant ki of the pulmonary lesions and parametric images were generated with the Patlak plot method. In our study, the difference between ki , SUV_{max} and the activity curves of ^{18}F-FDG between the malignant and benign lesions were analyzed. At the same time, we investigated the correlation of ki to SUV_{max}.

Results: The results showed that the maximum diameter of the pulmonary lesions was not significantly different between the malignant and benign lesions (P>0.05).The ki and SUV_{max} in malignant lesions were significantly higher than in benign lesions (P<0.05). The ki was highly correlated with SUV_{max} in pulmonary lesions(r=0.821, P<0.01). The malignant lesions showed gradually increasing time activity curves, whereas, benign lesions were gradually decreasing curves. The parametric images of ki were useful to distinguish malignant lesions from normal tissue.

Conclusion: ki parametric imaging in ^{18}F-FDG PET/CT dynamic multi-bed scanning may play a very important role in the diagnosis of pulmonary lesions.

[Keywords] ^{18}F-FDG PET/CT, pulmonary lesions, parametric imaging, tumor.

DIFFERENTIAL DIAGNOSIS OF PULMONARY LESIONS BY PARAMETRIC IMAGING IN 18F-FDG PET/CT DYNAMIC MULTI-BED SCANNING

Rong Fu Wang1, China, Qiang Wang1, Jian Hua Zhang1, Yun Zhou2

1 Department of Nuclear Medicine, Peking University First Hospital, Xichengqu, West District, Beijing, P. R. of China
2 The Russell H.Morgan, Department of Radiology and Radiological Science, Johns Hopkins University, School of Medicine, Baltimore, USA

UNITED STATES

Objective: Benign and malignant pulmonary lesions are not easy to distinguish in a clinical setting. We investigated the feasibility of using parametric imaging of the rate constant Ki to diagnose the nature of pulmonary lesions.

Methods: Dynamic multi-bed scanning followed by a routine examination was performed on 21 patients with pulmonary lesions who were divided into two groups with malignant or benign lesions based on biopsy and follow-up. The number of patients in the malignant and benign groups were 10 with 15 lesions and 11 with 14 lesions, respectively. The left ventricular blood pool was used for an image-derived input function. The influx rate constant Ki of the pulmonary lesions and parametric images was generated with the Patlak plot method, and the inter-group differences for Ki, maximum standardized uptake value (SUVmax), and the time-activity curves (TAC) of fluorine-18-fludeoxyglucose (18F-FDG) were analyzed. At the same time, we investigated the correlation of Ki to SUVmax.

Results: The maximum diameters of the pulmonary lesions were not significantly different between the malignant and benign groups ($p>0.05$). Ki and SUVmax were significantly higher in malignant lesions compared to benign lesions ($p<0.05$). Ki was highly correlated with SUVmax in pulmonary lesions ($r=0.815$, $p<0.01$). The malignant lesions showed gradually increasing TAC, and benign lesions exhibited gradually decreasing curves. The parametric images of Ki were useful to distinguish malignant lesions from normal tissue.

Conclusion: Our results indicate that Ki parametric imaging in 18F-FDG PET/computed tomography (CT) dynamic multi-bed scanning may be useful in the differential diagnosis of pulmonary lesions.]Key words] cancer, diagnosis, 18F-FDG PET/CT, parametric imaging, pulmonary lesions.

COMPLEMENTARY ROLES OF CONCURRENT MULTIMODALITY FDG-PET AND ADVANCED MRI IN PELVIC MALIGNANCIES.

Shanker Raja. Estados Unidos, Abdullah Aldossary, Sharad George, Sergey Rumyantsev. Dept. of Medical Imaging, KFMC Riyadh, KSA.

UNITED STATES

Optimal management of common pelvic malignancies (pelMalig), including colorectal Ca., cervical and uterine cancers etc., necessitates an extensive pre-surgical work up, including lesion histology, grades, local invasion and metastatic spread. However, conventional MRI ((cMRI) -T1W, T2-W etc.) is limited in grade prediction, evaluation of loco-regional and distant metastases, and also post therapeutic evaluation. Though, FDG-PET has a limited role at initial diagnosis, it is recommended for post therapeutic evaluation and in restaging. And more recently, advanced MR (aMR) especially Diffusion Weighted Imaging (DWI) and ADC mapping is being increasingly utilized as a complementary tool to cMRI. We explored the complementary roles of multimodality FDG-PET and multiparametric MRI in the work up of pelvic malignancies.

Methods: On retrospective chart review, we identified 14 pts. with suspected pelMalig (primary and recurrent), and also undergoing concurrent (+/-3 months) aMR and FDG PET. Patient demographics were (male=5, female=9; mean age=50 (range=37-80) yrs. The break of the tumors were – rectal 8 (primary 6, presacral recurrent mass 2), Cervical cancer 3, uterine 2(endometrial Ca. 1, Lymphoma 1), and rectal metastasis to ovary 1. All PET and aMR were acquired with routinely accepted protocols. PET and MR images were qualitatively reviewed by experienced physicians. Quantitative estimates – SUV on FDG-PET and ADC were obtained from represen-

tative ROI's on co-registered PET and multiparametric MRI . Results: All lesions (primary and recurrent) were concordant and positive on PET and MR. For pelvic lymph node involvement 11/14 were positive on MR out of these 6/11 were positive by PET and 5/11were negative, in three pts. both MR and PET were concordantly negative. While MR was suggestive of lympho-vascular space (mesorectal fat, and parametrium) involvement in 7/14 pts., only 1/7 was positive on PET. PET was helpful in confirming suspicious lesions on MR in 2 pts., while MR was helpful in precise localization of hypermetabolic foci noted on PET-CT in 2 pts. PET demonstrated more extensive lymphadenopathy outside the MR field of view in 3 pts. Additional lesions (not determined) were also noted on PET outside the pelvis. Correlation of quantitative estimates of lesional suvMAX and mean ADC revealed a modest negative correlation (higher the SUV lower the ADC), however, not statistically significant.

Conclusion: In our small series concurrent imaging by aMR and PET appears to be complimentary, providing incremental value. Further analysis in a larger series, and in future simultaneous multimodality imaging with integrated PET-MR is warranted.

INTEGRATED MULTIPHASE FDG PET AND ADVANCED MULTIPARAMETRIC MRI IN DIFFERENTIATING SUSPECTED BRAIN TUMOR RECURRENCE FROM POST RADIATION CHANGES, CORRELATION WITH STEREOTACTIC BIOPSY AND FOLLOW-UP.

Raja, Shanker. UNITED STATES. Abdullah A. Alrashed, George, Sharad P, Sven Larson.

UNITED STATES

Objectives : Differentiating brain tumor recurrence (BTR) from post radiation changes (RT) is challenging even by conventional MRI (cMRI i.e. T1, T2 , Flair). And, image guided stereotactic biopsies may be limited by sampling errors. We explored the role of integrating functional data from multiphase PET (mPET), and advanced MRI (aMRI i.e. DWI/PWI/MRS) to differentiate between the two entities. Methods : Retrospective review of all pts with suspected BTR on cMRI from Oct 2012 to date, revealed 14 pts (male=8, female=6; age 5-54, mean age=34) having both mPET and aMRI. mPET (2 or 3 datasets acquired between 30-300 mins post FDG inj) and aMRI were acquired per standard protocols. The visual findings on mPET and aMRI spatially corresponding to suspicious findings on cMRI, were correlated with histopathology and/or follow-up.Results : Of the above 14 pts suspicious for BTR, 12 were based on increasing lesion size (inc_sz) on f/u cMRI, while 2 regressed in size (reg_sz), but had new contrast enhancing lesions. In the 12 pts with inc_sz of lesions: 9 pts were positive (pos) on both mPET and aMRI, 2 pts were negative (neg) on both modalities, 1 pt showed discordant findings between mPET and aMRI. In 2 pts with reg_sz of lesion but new focus of contrast enhancement on cMRI, both mPET and aMRI were pos for BTR. In comparison to histopathology and/or follow-up 13/14 pts were either TP(11) or TN(2) by both mPET and aMRI. The sens., spec., and acc. of mPET and aMRI was 92%, 100%, and 93% respectively.. mPET and aMRI versus follow-up/sterotatic biopsy.

	histo/ follow-up BTR +ve	histo/ follow-up BTR -vre	Total
mPET & aMRI +ve	11	0	11
mPET & aMRI -ve	0	2	2
mPET & aMRI nondiagnostic	1	0	1
Total	12	2	14

Conclusions : Our findings suggest that mPET and aMRI are complementary. Qualitative integration of findings on mPET and aMRI appears promising with improved accuracy in differentiation of BTR from RT, as opposed to cMRI. Further exploration with integration of quantitative parameters derived from multimodality-multiparametric imaging is warranted.

ARE CONCURRENT RETROSPECTIVELY COREGISTERED PET AND MR COMPLEMENTARY OR CONTRARIAN IN THE EVALUATION OF VIABLE OSSEOUS METASTASIS?

Shanker Raja [1,2] . Estados Unidos, Sharad George[1], Nizar Al-Nakshabandi [2], Mohammed Obaid AlHarbi [2], Sergey Rumyantsev[2].

1. Baylor College of Medicine, Houston, TX USA.
2. King Fahad Medical City – Riyadh, Saudi Arabia.

SAUDI ARABIA

Introduction:At initial diagnosis, both PET-CT and MRI are known to be exquisite for the evaluation of osseous metastasis of common malignancies (breast, lung, head and neck, lymphoma etc). Compared to PET, conventional MRI (cMR) is superior in sensitivity at detecting vertebral metastasis pre-therapeutically. However, in the interim and immediate post chemoRT settings, the role of cMR in response to therapy is yet to be defined. We explored the roles of concurrent PET and MRI in the evaluation of viable vertebral metastasis during/post ChemoRT.

Materials and methods: Retrospective review of charts from Aug-2012 to current, revealed 23 pairs of concurrent PET-CT and cMR (acquired +/- three months of each other) in 19 pts (male=10, female=9; mean age=40 (range=3-74) yrs. The histopathology in the 19 pts were, lymphoma 9, head and neck tumors 4, unspecified 2, one each of breast, endometrial Ca., Ewing's sarcoma, and AML. All FDG PET and MRI were acquired per routinely accepted protocols. Concurrent PET, cMR and retrospectively fused PET-MR were reviewed for vertebral involvement, by experienced nuclear medicine physicians and radiologists,. The findings were analyzed in Excel (Microsoft Corp. Redmond, USA).Results:Concordant findings were noted in 14/23 (61%) of concurrent PET-MR pairs; while in 9/23 (39%) both modalities were discordant for viable metastasis. Of the concordant PET-MR pairs both were positive for viable metastasis in 6/14, while both were negative in 8/14. In the discordant group, cMR was either positive (4), suspicious (3), or indeterminate (1) for persistent viable metastasis, while PET was negative on all seven of these scans. Of the remaining 2 PET-MR discordant paired scans, MR was reported as stable disease in both, however, PET correctly identified progressive disease in the first, while it was negative for viable tumor in the second scan.Limitations: Our exploratory analysis is small in number and retrospective. Furthermore, the histology of the tumors are varied. Lastly, cMR scans were initiated due to clinical suspicion and/or suspicious findings on multimodality (PET, CT) image findings during/post therapy, hence the elapsed time (less than 3 months) between the scans, and their relation to therapy is varied.

Conclusion:Despite the limitations of our study, our results suggest that in comparison to PET-CT, interim/immediate post therapy cMR may be limited in its role for evaluating viable vertebral metastasis. A larger prospective study along with advanced MR sequences (DWI, PWI, MRS) is necessary to better define its role.

SENTINEL LYMPH NODE DETECTION IN SAME-DAY VS PRIOR-DAY PREOPERATIVE BREAST LYMPHOSCINTIGRAPHY

Donald R. Neumann.

UNITED STATES

OBJECTIVE: While injections of radiotracer for breast lymphoscintigraphy can be administered on the same day as surgery, alternatively, injections using greater activity may be administered on the day prior to surgery. We evaluated the effectiveness of breast lymphoscintigraphy for sentinel lymph node (SLN) detection in same-day compared to prior-day injections.

MATERIALS AND METHODS: 152 patients with early stage breast cancer (clinical stages I and II) were referred for breast lymphoscintigraphy. Lymphoscintigraphy was performed on the same day as surgery in 70 patients (Same-Day), and on the afternoon of the day before surgery in 82 patients (Prior-Day). Tc-99m filtered sulfur colloid in a total volume of 6.0 mL, split into 3 aliquots, was injected in the retroareolar breast. The mean injection dose was 0.434 mCi (SD=0.068) in the Same-Day group and 3.0 mCi (SD=0.3) in the Prior-Day group. 30 minutes after injection, with a Co-57 flood source behind the patient, planar scintigrams were acquired (256x256 matrix, 5-minutes, 15% energy window centered at 140 keV) in the anterior, anterior oblique and lateral projections. Images were evaluated for the presence of SLNs. As a measure of image contrast, the ratio of maximum pixel value of each SLN to average background (target-to-background) was determined. At surgery, a handheld gamma probe was used to localize and resect radioactive SLNs.

RESULTS: In the Same-Day patients, 4.3% had no radioactive SLNs at surgery, 34.3% had 1 radioactive SLN, 37.1% had 2 radioactive SLNs, and 24.3% had 3 or more radioactive SLNs for a total of 142 radioactive SLNs (mean=2.0). In the Prior-Day patients, 4.9% had no radioactive SLNs at surgery, 20.7% had 1 radioactive SLN, 26.8% had 2 radioactive SLNs, and 47.6% had 3 or more radioactive SLNs for a total of 222 radioactive SLNs (mean=2.7, p=0.008). Of the 67 Same-Day patients with radioactive SLNs at surgery, 30 had at least one SLN detected at imaging (patient-level estimate of sensitivity = 44.8%). Among the 78 Prior-Day patients with radioactive SLNs at surgery, 61 had at least one SLN detected at imaging (patient-level estimate of sensitivity = 78.2%, p<0.001). The mean target-to-background ratio for SLNs in the Prior-Day group (60.2) was significantly greater than in the Same-Day group (24.0, p=0.002).

CONCLUSIONS: Breast lymphoscintigraphy using retroareolar Tc-99m radiocolloid injections performed on the day prior to surgery is more sensitive for the detection of sentinel lymph nodes than lymphoscintigraphy using injections given on the same day of surgery. In addition, more radioactive sentinel lymph nodes were detected at surgery in the Prior-Day group than in the Same-Day group.

PROSPECTIVE EVALUATION OF COMBINED ^{18}F NAF/^{18}F FDG PET/CT VS. WHOLE-BODY MRI IN PATIENTS WITH BREAST AND PROSTATE CANCER

Iagaru Andrei.UNITED STATES, Mosci C, Jamali M, Loening A, Mittra ES, Gambhir SS, Vasanawala SS

UNITED STATES

Introduction: We previously reported the pilot evaluation of separate ^{18}F NaF PET/CT and ^{18}F FDG PET/CT vs. whole-body MRI (WB-MRI), as well as the use of combined ^{18}F NaF/^{18}F FDG PET/CT in cancer patients. Here we prospectively compare the combined ^{18}F NaF/^{18}F FDG PET/CT and WBMRI against ^{99m}Tc-MDP in patients with breast and prostate cancers for the detection of metastatic disease.

Methods: Twenty-four patients referred for ^{99m}Tc-MDP bone scans were prospectively enrolled with IRB approval and informed consent from Nov 2012 to Dec 2013. The cohort included 9 men with prostate cancer and 15 women with breast cancer, 34 – 84 year-old (average 60 ± 14). ^{18}F NaF and ^{18}F FDG were subsequently injected from separate syringes. The PET/CT and MRI were done 1-21 days apart (average 2.2 ± 4.1). MRI protocol consisted of T1, STIR, DWI, and contrast-enhanced imaging. The interval from the bone scan to PET/CT or MRI ranged 1-30 days (average 16 ± 8). Lesions detected with each test were tabulated and the results were compared.

Results: One patient with negative bone scan and PET/CT could not tolerate the WBMRI. Eight patients had no bone metastases identified on any of the three scans. Bone scintigraphy showed osseous metastases in 12 patients, while the combined ^{18}F NaF/^{18}F FDG PET/CT and the WBMRI showed skeletal metastases in 4 more and 3 more, respectively (14 patients total). More numerous bone findings were noted on PET/CT than on WBMRI in 7 patients. Lesions outside the skeleton were identified by PET/CT and WBMRI in 10 patients. In one patient MRI showed brain metastases not noted on PET/CT. In one patient PET/CT showed axillary and internal mammary lymph nodes not described on MRI.

Conclusion: Our prospective trial demonstrates superior evaluation of skeletal disease extent with the combined ^{18}F NaF/^{18}F FDG PET/CT and the WBMRI compared to ^{99m}Tc-MDP scintigraphy. Further, PET/CT and WBMRI detected extra-skeletal disease that may change the management of these patients. A combination of ^{18}F NaF/^{18}F FDG PET and WBMRI may provide the most accurate staging of patients with breast and prostate cancers. Larger cohorts are needed in order to confirm these preliminary findings.

PROGNOSTIC VALUE OF INTERIM PET IN PATIENTS WITH DLBCL TREATED WITH RITUXIMAB BASED REGIMEN AND COMPARISON OF VARIOUS INTERPRETATION CRITERIA- RESULTS OF LONG TERM FOLLOW UP FROM A SINGLE CENTER PROSPECTIVE STUDY.

Manohar Kuruva. India,[1] Bhagwant Rai Mittal,[1] Arun Kumar Reddy[1],Anish Bhattacharya,[1]Pankaj Malhotra,[2] Subhash Varma[2]
manokmc@gmail.com

[1]Dept. of Nuclear Medicine, Post Graduate Institute Of Medical Education and Research, India.
[2]Dept. of Internal Medicine, Post Graduate Institute Of Medical Education and Research, India.

Objective: Role of interim FDG PET/CT in prognosticating patients with lymphoma has been widely evaluated in multiple studies but has not been well established yet. Also, lack of standardized interpretation criteria led to inconsistent results across the studies. In this context this prospective study was carried to evaluated the role of interim FDG PET/CT in prognosticating the patients with DLBCL treated with rituximab based chemotherapy regimen with an emphasis to compare the existing interpretation criteria.Materials and Methods: 47 patients with histologically proven DLBCL were prospectively included in this study. Interim FDG PET/CT was carried out after 4 cycles of standard chemotherapy regimen with R-CHOP. All the patients were followed up for a minimum of 1 year or progression whichever occurs earlier. 2 reviewers independently interpreted all the interim FDG PET/CT scans according to IHP , Gallamini , London criteria and dynamic score and consensus was reached after discussion. Scores of 4 and above were considered as positive for London criteria. Survival curves were generated by the method of Kaplan and Meier curves. Differences between groups were analysed using the log-rank test.

Results: 16 males and 31 female patients were included in the study. Age of the patients ranged from 20-78 years with a median of 54 years. After a median follow up of 38 months (12-60 months) 17/47 (36%) patients had experienced progression and 30/47 (64%) were in durable complete remission. Accuracies of IHP, Gallamini, London criteria and dynamic score were 55.3%, 75%,70.2% and 70.2% in predicting progression. (table 1) Statistically significant differences in progression free survival were observed in between positive and negative groups according to all criteria except for IHP criteria. (table 2).Highest specificity was observed with dynamic score criteria and highest sensitivity was observed with both IHP and London criteria.

Conclusions:In interpreting interim FDG PET/CT in patients with DLBCL Gallamini criteria have highest accuracy and IHP criteria have least accuracy. However Gallamini criteria depend on an absolute SUV cut off value of 3.5 and hence might lack inter centre reproducibility. London criteria (with score of 4 as positive) have comparable accuracy and being more reproducible and relatively simple to interpret can be used in interpreting interim FDG PET/CT in patients with DLBCL. Highest specificity (with low sensitivity) was observed with dynamic score criteria and these criteria can be used when aggressive treatment changes are contemplated based on interim PET scan findings.

COMPARISON OF INTERPRETATION CRITERIA TO INTERPRET END OF THERAPY F-18 FDG PET/CT IN PATIENTS WITH HODGKIN'S LYMPHOMA.

Kuruva Manohar[1] . India, B R Mittal[1] Anish Bhattacharya[1] Pankaj Malhotra[2]

Department of Nuclear Medicine and PET Center[1] and Department of Internal medicine and Hematology[2].

INDIA

Post Graduate Institute of Medical Education and Research, Chandigarh,India.

Background: FDG PET/CT is being increasingly used as a first line investigation to detect residual disease at the end of therapy in patients with HL and aggressive NHL.Various interpretation criteria exist to interpret FDG PET/CT including International Harmonisation Project (IHP) criteria.However very scarce literature exists comparing these criteria. In light of this, this study was carried out to compare the various interpretation criteria in interpretation of end of therapy F-18 FDG PET/CT to detect residual disease in patients with Hodgkin's lymphoma.Materials and methods: Data of 54 patients with histologically proven Hodgkin's lymphoma who underwent F-18 FDG PET/CT to detect residual disease at the end of conventional therapy (ABVD regimen with or without EBRT) were retrospectively analysed. All the scans were independently interpreted by 2 experienced nuclear medicine physicians according to IHP, Gallamani and London criteriae and the consensus was reached after discussion. All the patients were followed up for a minimum period of 18 months or relapse/recurrence whichever occurred earlier. Acuuracies of various criteria were compared using log-rank test (Kaplan Meir curves) and also by Mc Nemar's test. Results: On a median follow up period of 25 months (range 6-39 months) 39 were in complete remission and 15 were diagnosed with residual/recurrent disease. The accuracy for predicting residual disease for IHP criteria, London criteria and Gallamani criteria and was 67%, 76% and 81.5% respectively. Gallamani and London criteria had greater accuracies in predicting residual disease than London criteria (p=0.001). The major difference in accuracy was due to poor positive predictive value of IHP criteria. PPV of both London and Gallamani criteria was high when compared to IHP criteria 55.55% and 66.66% vs 44 % (p=0.001). Majority of the false positive uptake occurred in mediasitnal lymph nodes and cut off SUVmax of 3.5 by Gallamani criteria could reduce false positives in only some fraction of patients suggesting higher cut offs might be required to rule out false positive uptake in mediastinal lymph nodes.NPV was similar for all the criteria. When Kaplan Meier curves were plotted all the criteria could predict Time to second treatment (TTST) with statistical significane, while Gallamani criteria showed highest accuracy. Conclusion: IHP criteria have high NPV in detecting residual disease in patients with HL at the of therapy, however PPV appears low. Usage of Gallamani and London criteria improves specificity without loss of sensitivity to detect residual disease.

SPECT/CT IN SENTINEL LYMPH NODE (SLN) MAPPING IN ENDOMETRIAL CARCINOMA

V. Simonovsky.

ISRAEL

Endometrial cancer is the most common gynecologic malignancy in the western world. The primary treatment is hysterectomy& bilateral salpingo-oophorectomy, while the role of routine lymphadenectomy is controversial. LN dissection can diagnose the patients who will benefit from adjuvant therapy, but on the other hand exposes these patients for side - effects as lymphocyst formation leg lymphedema, possible vascular and nerve damage and prolonged operation.Sentinel LN dissection is a well-accepted practice in the treatment of melanoma and breast cancer, and is gaining ground in vulvar cancer and cervical cancer.The Aim of the current study was

to assess the value of the preoperative lymphoscintigraphy SPECT/CT for SLN mapping in patients with endometrial cancer. Methods: 29 patients with endometrial cancer of various grades were included into the study. All of them underwent preoperative planar and SPECT lymphoscintigraphy combined with low dose CT using hybrid SPECT/CT system (SIEMENS Symbia) 1-2 hours after injection of 7.4 – 11.1MBq Tc99m labeled nanocolloid. The tracer was injected 24 hours before surgery using a spinal needle in the cervix of the patient at the 3 o'clock and 9 o'clock positions, shallow and deep injections by a gyneco-oncologist. In the operating room, at the time of the examination under anesthesia the patients were injected with blue dye (Methylen- blue) using the same technique. The operations were performed either laparoscopic or abdominally. In all cases full pelvic lymph node dissection was performed in addition to SLN dissection. A positive LN was considered one that was detected by blue- dye, or detected as "hot" node by a gamma probe, or both. The SLN were sent separately for pathological examination.

Results: The lymphoscintigraphy with hybrid SPECT/CT system identified and localized correctly SLN in 26 (89.1%) patients with false negative rate 0%. Metastatic lymph disease was found in five patients and in three of them the SLN was the positive one . In three cases SLN were detected only by lymphoscintigraphy.

Conclusion: The major diagnostic value of the method is it's high detection rate and easy intraoperative SLN discrimination.

CASE REPORT: LIVER METASTASES FROM PROSTATIC CARCINOMA.

Cortés-Hernández, Violeta Ofelia[1]. México, Pitalúa-Cortés, Quetzali Gabriela[1]. HernándezÁlvarez, Rocío[1]. Arellano-Hernández, Guillermo[2]. García-Resendez, Arturo Armando[1]. Arguelles-Pérez, David Antonio[1].

1. Nuclear Medicine and Molecular Imaging Department. Instituto Nacional de Cancerología México.
2. Nuclear Medicine Department. Centro Oncológico de Querétaro, México.

MEXICO

Background: Prostate cancer is a major cause of morbidity and mortality worldwide. It remains the second leading cause of cancer deaths of men in Europe and USA. In Mexico it represents the third cause of mortality from cancer. The onset of metastases dramatically changes the prognosis of prostate cancer patients, determining increased morbidity and a drastic fall in survival expectancy. Bone is the most frequent metastatic site with a 98% of the cases, and visceral locations occur in 45% of patients and are also associated to bone metastases. Liver locations of metastases have a frequency of 25% and are more frequent when the primary tumor is > 8 cm of diameter.

Objective: To present a case report of a patient diagnosed with metastatic prostate cancer, for analyzing what are the best studies that help us diagnosing and following this kind of patients. Case report: We collected the clinical information and the results of different imaging modalities to follow up the evolution of the patient. We describe the case of a 59 year male with right upper quadrant abdominal pain and weight loss. He was undergone a prostatic ultrasound in May 2013, that was reported with normal prostate, but liver lesions. So, an 18F-FDG PET/CT was performed, where the patient was diagnosed with metastatic lesions in liver, lungs and bone, but no primary lesion. Finally liver biopsy revealed foci of carcinoma cells in the portal tracts which exhibited positive cytoplasmic staining for prostate-specific antigen, thus confirming the presence of metastatic prostatic adenocarcinoma. A bone scan showed abnormal uptake of 99mTc-MDP by sacrum, ischium and vertebral bodies of L4-L5, and a diffuse uptake in the liver.Discussion and conclusions: Evolution possibilities of prostate cancer are the spread through the lymphatic vessels and frequently to the bones. Liver metastases occurred late in the course of the disease in most patients. The successful management of prostate cancer requires early detection of clinically significant disease in order to select the optimum treatment. Functional imaging provides information on the biologically active volume of cancer. In the current case we focus in radionuclide based imaging techniques using SPECT/CT and PET/CT technologies that were important for selection of the patient´s treatment.

VISUALISATION OF HISTOLOGIC PROVEN BREAST CANCER ON THE MAMMI-PET: A DEDICATED PET FOR HANGING BREAST IMAGING

Suzana Teixeira.

NETHERLANDS

Objective: The MAMMI-PET, a high-resolution full-ring system for dedicated hanging breast imaging was originally developed in the context of a EU-founded project to improve the detection of breast cancer. The aim of the present study was to evaluate the performance of the MAMMI-PET device in patients with at least one histologic confirmed primary breast cancer lesion (or index lesion), scanned in two European centres. All patients were included in the study after being scheduled to receive pre-operative chemotherapy (NAC) or radiotherapy.Material and methods: From March 2011 to March 2014, we included 234 female patients (mean age 52 y, range 24-82y) with histologically confirmed breast cancer. All patients were scanned with the MAMMI-PET (Oncovision, Valencia, Spain) after giving informed consent. Scans were acquired 110 after a dose of a mean dose of 197.12 MBq 18F-FDG. In both centers the acquisitions, the reconstruction of the images and the data collection were performed using similar standardized methods. We tested the relation between visualization of the primary tumor and possible additional lesions on the MAMMI-PET as well as the influence of various variables; including age, weight, breast cancer subtypes and receptor status, breast length, maximal tumor diameter and affected breast quadrants. Results: A total of 236 breasts were imaged and 211 (98.4%) of the index lesions (diameter 5-170 mm, mean 32 mm) were located within the MAMMI-PET scanning range. Of all index lesions within the scanning range 1.4% was not FDG avid on the MAMMI-PET images. Lesions that were FDG-avid were either clearly (86.3%) or moderately (12.3%) visible. The overall MAMMI-PET sensitivity increased from 88.6% to 98.6% after exclusion of lesions outside the scanning range. No significant differences in lesion visibility were found due to breast cancer subtypes or breast quadrant location. Of the 35 index lesions touching the pectoral muscle 62.9% reached into the scanning range. A total of 41 additional FDG-avid lesions were detected, not categorized as an index tumor.Conclusions: The MAMMI-PET missed only a small percentage of malignant lesions located within the scanning range of the device. Lesions near the pectoral muscle were the subgroup less often visualized. No significant influence on the visualization of the FDG avid lesions was seen due to tumor subgroups, hormone receptor status, and breast quadrant location or tumor size.

THE DILEMMA OF ADRENAL HYPERMETABOLISM ON FDG PET/CT SCANS OF VARIOUS CANCER PATIENTS: METASTASIS OR NOT?

Murat Fani BOZKURT. Turquia, MD, FEBNM, Eser LAY ERGÜN, MD.
Hacettepe University Faculty of Medicine Department of Nuclear Medicine, Ankara.

TURKEY

Aim: Depending on the primary malignancy, adrenal gland is a common site for metastases with a varying ratio of %25 to 75%. The most common cancer types in which adrenal metastases are encountered are mainly lung cancer, breast cancer, gastrointestinal cancers, malignant melanoma as well as lymphoma. Bilateral adrenal masses or increased FDG metabolism usually suggest other ethiologies such as primary adrenal hyperplasia and more rare primary adrenal neoplasms, mostly seen in particular syndromes. The aim of this study is to retrospectively review a rather large number of oncologic PET/CT studies to find out the frequency of adrenal hypermetabolism and to make differential diagnosis based on other modalities. Material and Methods: A total of 576 oncologic FDG PET/CT studies in 564 patients in about 3-year-period were included. All patients had confirmed malignancy. PET/CT was performed 1 hour after iv injection of 6 MBq/kg FDG mostly from vertex to upper femoral region and from vertex to feet for malignant melanoma patients. The images were retrospectively reviewed by 2 experienced nuclear medicine physicians and correlated to histopathology, CT and/or MR findings.Both visual and quantitative analysis were used for interpretation.

Results: Among all patients 32/564 (6%) showed adrenal hypermetabolism on FDG PET/CT, where 25/32 (78%) were found to be malignant and 7/32 (22%) benign. Adrenal metastates were unilateral in 22/25 (88%) while bilateral in 3 (12%) patients. Leading cause of adrenal metastates was lung cancer followed by lymphoma, colorectal, breast cancer and miscellanous. All metastatic sites were confirmed by other modalities (2 by histopathology and 23 by CT and/or MRI). Among benign adrenal hypermetabolism, 6/7 (86%) was due to adenoma where 1/7(14%) was lipoma, confirmed by radiology. Adenomas were bilateral in only 1/7 (14%) patient. Mean absolute value of SUVmax of malignant adrenal hypermetabolism was significantly higher than that of benign adrenal FDG uptake ($p<0,05$). Only 3/7 (43%) patients with benign uptake showed higher intensity than liver while all malignant FDG uptake values were higher compared to liver SUVmean.Conclusion: Adrenal FDG hypermetabolism is a dilemma which can refer to both metastasis and benign etiology in oncologic FDG PET/CT imaging. The intensity of uptake compared to liver SUVmean, uni/bilateral pattern and the primary diagnosis of the patient may be the key parameters which lead to correct differential diagnosis, based on confirmation by some other methods.

THE PROGNOSTIC IMPACT OF FDG PET/CT IMAGING IN THE INITIAL WORK-UP OF PATIENTS WITH HIGH RISK DIFFERENTIATED THYROID CARCINOMA

Gulin Ucmak.

TURKEY

Introduction: The aim of this study was to evaluate the impact of FDG PET/CT imaging on prognosis in the initial work-up of patients with high risk differentiated thyroid carcinoma (DTC) in comparison with post-therapy iodine scan findings.Method: Thirty patients with high risk DTC (20 F, 10 M, age:46±17 yr, 24 papillary, 6 non-papillary cancer), who were referred to radioiodine ablation therapy underwent FDG PET/CT as a part of initial work-up. PET/CT was indicated to define disease extent; in 21 patients with serum Thyroglobulin (Tg) levels out of proportion to the identified disease, in 4 patients with unfavorable histopathology (Hurthle cell cancer n:3, tall cell variant n:1), in 4 patients with suspected distant metastasis before thyroidectomy and in 1 patient with rising anti-Tg antibody levels. Patient management was planned based on clinical, laboratory and PET/CT findings. The contribution of PET/CT findings to patient management and clinical outcome was evaluated. Results: PET/CT detected metastatic cervical and/or mediastinal lymph nodes in 14 patients, lung metastasis in 13 patients, bone metastasis in 2 patients and multiple sites of metastasis in 2 patients. In the light of PET/CT findings, 9 patients were referred to surgery for focused neck dissection or completion compartmental neck dissection and/or metastatectomy, 3 patients received external beam radiotherapy for bone metastasis. Then, all patients received I-131 radioiodine therapy with doses of 150-250 mCi. Of these, PET/CT detected non-radioiodine avid lung and mediastinal metastasis in 5 patients. Findings of PET/CT and post-ablation radioiodine whole body scan were comparable in others. PET/CT provided a change in treatment plans for patients who were referred to surgery/radiotherapy (13/30 patients, 42%). In addition, PET/CT defined extra sites of distant metastasis and changed TNM stage in 4 patients (13%). Totally, in 55% of patients with high risk DTC, PET/BT contributed to patient management in the initial work-up. After 36 months of median follow-up, 3 patients had progressive disease, 8 patients had stable disease, 19 patients had clinical/biochemical remission.Conclusion: As a part of initial staging algorithm, FDG PET/CT has an important role on the management of patients with high risk DTC. We consider that, especially in patients with Tg levels out of proportion to the identified disease, PET/CT provides unique opportunity to select patients who has surgically amenable disease and help to increase therapeutic response to further radioiodine therapies which all result in an improvement of progression-free survival.

METABOLIC SUPER SCAN IN ^{18}F-FDG-PET/CT IMAGING OF THREE PATIENTS WITH RELAPSED ONCOLOGIC DISEASE. INTERESTING IMAGES AND LITERATURE REVIEW

Thiago Souza Rocha Alves.

BRAZIL

Objective:Share rare and typical manifestation of metabolic super scan in ^{18}F-FDG-PET/CT imaging Cases:Three cancer patients were evaluated, male, aged between 58 and 70 years. CASE 1: Diagnosis of gastric adenocarcinoma with apparent cure after partial gastrectomy 20 years ago, local recurrence treated one year ago with total gastrectomy, chemotherapy and radiotherapy. Disease progression with vertebral metastases detected by bone scan occurred after 10 months. The restaging with ^{18}F-FDG-PET/CT revealed remarkable hypermetabolism in the bone marrow, liver, peripancreatic and supra diaphragmatic lymph nodes (SUVmax 13.8). CASE 2: Diagnosis of non-Hodgkin lymphoma (NHL) of diffuse B cell in nodule in the lumbar region 13 months ago with disappearance after chemotherapy. Local recurrence occurred after seven months and spread to bones while undergoing treatment with chemotherapy. ^{18}F-FDG-PET/CT showed hypermetabolism in bone marrow diffusely (SUVmax 12.0), cervical and mediastinal lymph nodes and splenomegaly (SUVmax 10.6). CASE 3: Diagnosis of lymphoma in stomach, liver and spleen 20 years ago, underwent splenectomy and chemotherapy with stable disease after 10 years. Twenty days ago was detected recurrent disease in palpable lymph node in the left anterior cervical region. ^{18}F-FDG-PET/CT identified hypermetabolism in cervical, axillary, diaphragmatic, thoracic, abdominal and iliac lymph nodes (SUVmax 10.0), in ileal loops (SUVmax 9.2) in the liver parenchyma (SUVmax 20.0) and multiple areas distributed along the axial skeleton (SUV to 14:6). Antagonistically hypometabolism was observed in the brain, mediastinum, bowel and urinary tract in three cases. Patients died respectively at two, four and one months after PET/CT imaging.Comments:Superscan is a well known phenomenon in bone scan, is characterized by symmetrical bone uptake and increased extremely uniform in contrast to low or absent background radiation, with absence of renal imaging. The super scan in ^{18}F-FDG-PET/CT, or metabolic super scan, is described as image with remarkable metabolism in the bone marrow, very similar to bone scan, associated to diffuse increase in hepatic parenchyma and primary tumor. It is associated with malignant disease with multiple bone metastases, particularly, in patients with prostate, breast, lung and stomach cancer. Antagonistically, there is a decrease or absence of physiological uptake of ^{18}F-FDG in the brain, mediastinum, bowel, urinary tract and skeletal muscles, probably due to the intense uptake of ^{18}F-FDG in bone and liver metastatic lesions. Super scan on ^{18}F-FDG-PET/CT is a rare syndrome with a typical pattern. In the cases presented was related to recurrence and disease progression, even in the presence of therapy and may be a prognostic value.

HOW DOES PET/CT CHANGE TREATMENT DECISIONS IN PATIENTS WITH LOCALLY ADVANCED CERVICAL CANCER

Bruno Gabriel [1]. Argentina, De Dios Diana [2], González Christian [1], Tinetti Carolina[1], Traverso Sonia[1], Jaimez Fernando[1], Namías Mauro[1], Damiani Fernanda [2], Lay Laura [2], Ostojich Marcela [2], Zeff Natalia [2], Sánchez Ariel[2], Gianni Sergio [2], Parma Patricia[1]

[1] PET/CT Department, Fundación Centro Diagnóstico Nuclear (FCDN), Buenos Aires, Argentina.
[2] Gynecology Department, Instituto Oncológico Ángel H. Roffo (IOAHR), Buenos Aires, Argentina.

ARGENTINA

Introduction Cervical cancer is the first cause of cancer-death among young women in developing countries. The FIGO staging is exclusively clinical; however has a 20% inaccuracy for the initial stages, and up to 67% in the advanced ones, particularly due to the failure for the assessment of nodal status and distant involvement. Because PET/CT has high sensitivity and specificity in the detection of lymph node metastases and hematogenous spread, it could improve the initial assessment of disease and personalize the treatment. ObjectiveTo assess if PET/CT could lead to changes in the treatment planning in locally advanced cervical cancer (LACC).Material and Method This is an observational, prospective study of the Gynecology Department of the IOAHR and PET/CT Department of FCDN. Between the years of 2009 and 2013, 70 patients with LACC were staged according with the FIGO recommendations. A PET/CT scan was also performed as part of the initial work up. Localization of extrauterine hypermetabolic images were determined as well as classified as pelvic or extrapelvic, and also the extrapelvic ones, in nodal or extranodal distant metastases. Wherever technically feasible, diagnostic confirmation by cytological puncture and/or histology was performed. All patients were considered to be treated with the standard concurrent chemo-radiation therapy to pelvic field plus brachitherapy. In those patients with extrapelvic disease by PET/CT, changes in therapeutics approaches were considered. The assessment included 1- Frequency and localization of the extrauterine hypermetabolic lesions, 2- Distribution of the lesions according with the FIGO staging, 3- Perceptual changes in the initial therapeutic planning related to the PET/CT findings.

Results: In 51/70 (72,8%) of the patients, 77 extrauterine hypermetabolic lesions were detected: of those, 51 (66%) were pelvic (34 single and 17 combined with other localizations), and 26 (34%) were extrapelvic (16 nodal lumbo-aortic, 1 supraclavicular, 2 mediastinal, 2 inguinal y 5 extranodal). The per stage distribution were: EIIA 3/4 (75%), EIIB 27/39 (69%), EIIIB 19/23 (82, 6%), and EIVB 2/2 (100%). The 26 extrapelvic localizations were found in 19/70 (27.1%) patients, and in all of them the initial proposed therapeutic approach was modified (extended lumbo-aortic, and/or inguinal radiation therapy field, and/or chemotherapy).

Conclusion: The frequency of the extrapelvic nodal and/or extranodal distant metastases involvement in LACC emphasizes the need to use other diagnostic methods not included by the FIGO such as PET/CT. In our series, PET/TC was able to detect about 27% of extrapelvic localizations that led, in all cases to change the original planned therapeutic approach.

STAGING OF LOCALLY ADVANCED BREAST CANCER: THE VALUE OF THE PET/CT IN THE DETECTION OF DISTANT METASTASIS

Gabriel Bruno[1]. Argentina Christian González[1], Carolina Tinetti[1], Sonia Traverso[1], Fernando Jaimez[1], Amilcar Osorio[1], M. Eugenia Azar[2], Cristina Noblía[2], Patricia Parma[1].

[1] PET/CT Department, Fundación Centro Diagnóstico Nuclear (FCDN), Buenos Aires, Argentina.
[2] Mastology Department, Instituto Oncológico Ángel H. Roffo (IOAHR), Buenos Aires, Argentina.

ARGENTINA

Objective: To determine the efficacy of PET/CT in the detection of distant metastasis in patients with breast cancer considered locally advanced and compare the results with the clinical exam and conventional diagnostic methods.Materials and MethodsThis is an observational, prospective study of the Mastology Department of the IOAHR and PET/CT Department of FCDN. Between the years of 2007 and 2013, 60 patients were included with the diagnosis of breast cancer considered as locally advanced according to the initial staging based on clinical exam and conventional diagnostic imaging (radiograph and/or CT thorax, abdominal ultrasound, and bone scan). All patients also underwent whole body 18-FDG-PET/CT utilizing GE Discovery SRE 16 equipment. The results of both diagnostic modalities (conventional and PET/CT) were then compared for efficacy.Results.Distant metastases were diagnosed in 24 of 60 patients (40%); all of these were identified by 18FDG-PET/CT. By contrast, metastases were recognized by conventional diagnostic methods only in 8 of the 24 patients (33.3%), including bone lesions in 5 patients, liver lesions in 3, and pulmonary nodules in 2 of them. In the other 16 out of 24 patients left, distant disease involvement was detected by 18FDG-PET/CT only (66.6%, $p < 0.0001$ z-test), including the internal mammary chains in 4 cases, the mediastinum in 8, the lungs in 3, the liver in 6, and bone in 10 patients. Some of the lesions were confirmed by biopsy, and the follow up was performed with conventional diagnostic methods as well as

PET/CT.

Conclusion. 18FDG-PET/CT resulted in greater efficacy for the detection of distant metastasis in comparison with clinical exam and conventional diagnostic method modifying, in many cases, the therapeutic management. PET/CT should be considered a useful tool for the staging of locally advanced breast cancer.

DETECTION RATE OF RECURRENT MEDULLARY THYROID CARCINOMA USING ^{18}F-FDG PET, CORRELATION WITH CALCITONIN LEVEL

Mollerach A, Hume I, Arma I, Collaud C, Sidelnik M, Biedak P, Paganini L, Russo Picasso F, Cabezon C, Jager V.

ARGENTINA

Hospital Italiano de Buenos Aires. Argentina.

Objective: Serum calcitonin represents the most sensitive tumour marker in the postoperative management of medullary thyroid carcinoma (MTC). We evaluated the detection rate of ^{18}F- FDG-PET in patients with MTC and different calcitonin level.Materials and methods: Between March 2003 and February 2014, 21 ^{18}F-FDG-PET were performed in patients with MTC and elevated calcitonin level, for localization of recurrent disease. Conventional morphologic imaging methods were negative or showed equivocal findings. Detection rate(DR) of ^{18}F-FDG-PET was determined from the number of patients with recurrent MTC detected by ^{18}F-FDG-PET (A) and the number of patients performing ^{18}F-FDG-PET (B), according to the following formula: DR = (A)/(B). Sub-analysis considering serum calcitonin level. Results: 21 ^{18}F-FDG-PET scans were included in this study. All patients were asymptomatic and all had elevated serum calcitonin levels (52 a 8400 pg/ml). There were 9 positive and 12 negative ^{18}F-FDG-PET scans for detection of MTC recurrence. Pooled detection rate of ^{18}F-FDG-PET: 43%. In patients with serum calcitonin levels > 1000 pg/ml, DR: 87.5%; calcitonin levels > 150 pg/ml, DR: 64 %; calcitonin levels < 150 pg/ml, all ^{18}F- FDG-PET were negative.

Conclusions: The results from this cohort of patients suggest that ^{18}F-FDG-PET provides additional information for detecting occult sites of calcitonin production or confirming equivocal findings of other imaging modalities when the calcitonin levels were greater than 1000 pg/ml, with a detection rate of 87.5%. However in patients with lower calcitonin levels, ^{18}F-FDG-PET contribution is questionable and with calcitonin levels < 150 pg/ ml ^{18}F-FDG-PET should not be indicated. Our findings are in agreement with prior published studies.

IMMEDIATE POST OPERATIVE FDG-PET/CT TO EVALUATE SUCCESS OF PERCUTANEOUS ABLATION

Nascimento, BB; Romanato J; Menezes M; Bezerra R; Vicente A; Santos A; Cerri G; Camargo EE; Etchebehere EC.

BRAZIL

Division of Nuclear Medicine and PET/CT, Sírio Libanês Hospital, São Paulo, Brazil

Percutaneous ablative treatments (PA) such as cryoablation or radiofrequency for metastases of solid tumors have increased the possibility of oncological control in non-surgical candidates. After PA it is crucial to evaluate treatment outcome to avoid recurrences. Follow-up studies with CT and MRI are not able to differentiate scar from viable tissue after ablation. AIM: Demonstrate if 18F-FDG PET/CT (FDG PET/CT) performed in the immediate post operative hours after PA (immediate post operative FDG-PET/CT) is able to evaluate the success of PA. MATERIALS AND METHODS: Twenty patients (13 males, mean age 65.8 years), submitted to PA, were retrospectively reviewed. All patients with solid tumors metastases with indication for PA who exhibited focal uptake of 18F-FDG prior to PTA were included. The maximum interval between a baseline FDG PET/CT and the PA were 30 days. Exclusion criteria consisted of patients that had a change in chemotherapeutic regimen or that began chemotherapy during the 6 month follow-up period. An immediate post operative FDG-PET/CT study to evaluate the presence of residual viable lesion was performed between one and 8 hours after PA. The treatment was considered a success (no viable lesion) if no uptake of 18F-FDG was noted after PA on the immediate post operative FDG-PET/CT. Patient follow-up after 6 months was performed by clinical examination and imaging studies (FDG-PET/CT, MRI or contrast-enhanced CT).RESULTS: Twenty-six lesions were submitted to PA with either cryoablation (7/26) or radiofrequency (19/26) with mean lesion size of 2.5 cm. The metastatic lesions locations were liver (13/26), lung (8/26) and other sites in the abdomen (5/26). The immediate post operative FDG-PET/CT was performed between 1 and 8 hours after PA and detected viable tumor with a sensitivity, specificity, accuracy, positive and negative predictive values of 66.7%, 95%, 88.5%, 80% and 90.5%, respectively. False-positive cases consisted of two lung metastases (1.5 and 0.7 cm) of colon cancer submitted to cryoablation. The false-negative case consisted of a 3.0 cm lung metastasis of melanoma also submitted to cryoablation. There was a significant agreement between

the immediate post operative FDG-PET/CT findings and the results on the follow-up study (Kappa = 0.66; p < 0.01).

CONCLUSION: An immediate post operative FDG-PET/CT performed between 1 and 8 hours after PA may reliably evaluate the success of these procedures. This strategy may potentially allow early re-intervention of viable lesions and reduce morbidity. A larger number of patients are necessary to confirm these findings.

SYNTHESIS, RADIOLABELING AND IN VITRO AND IN VIVO CHARACTERIZATION OF A SYNTHETIC PEPTIDE DERIVED FROM THE HER2/NEU SEQUENCE FOR DIAGNOSIS AND TREATMENT OF HER2/NEU POSITIVE BREAST CARCINOMA.

S.M. Okarvi, I. AlJammaz.

SAUDI ARABIA

Cyclotron & Radiopharmaceuticals Dept; King Faisal Specialist Hospital and Research Centre. Riyadh 11211, Saudi Arabia.

Objectives: HER2/neu is a transmembrane glycoprotein with tyrosine kinase activity and extensive homology to the epidermal growth factor receptor. It is overexpressed in several human cancers of epithelial origin, such as breast and ovarian cancer. The low expression of this tumor antigen in normal tissues renders it an attractive molecular target for the diagnosis and targeted therapy of HER2/neu positive tumors. To develop a tumor-antigen based peptide for breast cancer targeting, we prepared and evaluated a synthetic peptide derived from HER2/neu sequence. Methods: DOTA-Glu-Lys-Ile-Phe-Gly-Ser-Leu-Ala-Phe-Leu-NH2 was synthesized by solid-phase peptide synthesis following standard Fmoc/HBTU chemistry. A negatively charged glutamic acid residue was added as a spacer between the chelating group and the targeting peptide and to enhance renal excretion. DOTA was attached to the targeting peptide at the end of solid-phase synthesis by manual conjugation. Labeling of DOTA-HER2/neu with 68Ga and 177Lu radionuclides was achieved in the presence of 2.5 M NaOAc and 0.1 M NH4OAc buffer, respectively. In vitro tumor cell binding was performed on HER2/neu expressing SKBR3 breast cancer cells and in vivo animal biodistribution and biokinetics was carried out in balb/c mice. Results: The identity of the synthetic tumor antigen peptide was confirmed by mass spectrometry and its purity by HPLC analysis. Radio-HPLC analysis showed that HER2/neu peptide labeled efficiently with 68Ga and 177Lu with high labeling efficiency (>98%). The radiopeptide displayed a high chemical resistant to DTPA transchelation and a high metabolic stability in human plasma. 68Ga/177Lu-labeled HER2/neu exhibited high binding affinity to HER2/neu expressing SKBR3 cells (Kd= <20 nM). The radioactivity internalized into breast cancer cells was ~20%. In mice, 68Ga/177Lu-labeled HER2/neu exhibited fast clearance from the blood and excretion mainly by the renal pathway. The uptake in the major organs, such as the lungs, liver, stomach, bone and intestines was low (<5% ID/g). Surprisingly, the uptake in the kidneys was found to be variable between the 68Ga-labeled and 177Lu-labeled HER2/neu peptide (5% ID/g for 68Ga-HER2/neu versus 15% ID/g for 177Lu-HER2/neu).

Conclusions: The development of a dual labeled 68Ga/177Lu-DOTA-HER2/neu peptide (theranostic agent) can be useful for both diagnosis and targeted therapy of HER2/neu positive tumors. A more comprehensive in vitro and in vivo characterization is in progress in order to determine the real potential of this new and attractive class of tumor antigen peptides for targeting of human cancer.

RADIOPHARMACY

PREPARATION AND IN VITRO AND IN VIVO EVALUATION OF A NOVEL PEPTIDE BASED ON TUMORRELATED HUMAN EPITHELIAL MUCIN (MUC1) AS A POTENTIAL BREAST CANCER IMAGING AGENT

S.M. Okarvi, I. AlJammaz. Cyclotron & Radiopharmaceuticals Dept; King Faisal.
Specialist Hospital and Research Centre. Riyadh 11211, Saudi Arabia.

SAUDI ARABIA

Objectives: MUC1 epithelial mucins are produced by both normal and malignant cells.MUC1 is overexpressed by most epithelial cancers and attracting increasing clinical interest as a potential target for imaging and targeted therapy of certain cancers. MUC1 is a classical example of tumor antigen because of its overexpression on almost all human epithelial cancers including >90% of breast and ovarian cancer. Increased expression of the epithelial mucin MUC1 is linked to tumor aggressiveness in human breast cancer. The low expression of this tumor antigen on normal tissues makes MUC1 an attractive target for breast cancer diagnosis and treatment. The goal of the present study was to develop a small synthetic MUC1-derived peptide combined with 4-amino acid, EPPT peptide, derived from tumor-associated ASM2 antibody, for targeting of breast cancer. Methods: Ac-Gly-Gly-Cys-Asp-Glu-Pro-Pro-Thr-Pro-Asp-Thr-Arg-Pro-NH2 was prepared by Fmoc-based solid-phase synthesis and labeled with 99mTc by stannoustartrate ligand exchange approach. In vitro cell-binding was performed on MDA-MB-231 and T47D breast cancer cell lines and in vivo biodistribution was conducted in healthy mice and in vivo tumor targeting in nude mice with MDA-MB-231 xenografts.

Results: The structural identity and purity of the synthetic peptide was confirmed by mass spectrometry and HPLC. The peptide radiolabeled efficiently with 99mTc (>80%) as determined by HPLC. 99mTc-MUC1 showed high affinity binding to MDA-MB-231 and T47D cell lines with Kd values below 10 nM. In normal mice, the radiopeptide displayed efficient clearance from the blood and excreted mainly through the urinary pathway with some elimination by the hepatobiliary system. The concentration of radiopeptide in the lungs, liver, stomach and kidneys was low (<5% ID/g) both at 1 and 4 h p.i. In nude mice with MDA-MB-231 xenografts, 99mTc-MUC1-derived peptide exhibited a good tumor uptake (4.41±1.51% ID/g, 1 h). The uptake in the tumor was always higher than in the blood and muscle resulting in favorable tumor/blood and tumor/muscle ratios.

Conclusions: Our results suggest that the fusion of two tumor targeting peptides appears to hold a great promise in nuclear oncology and this new and emerging approach can be beneficial for rapid and efficient targeting of human cancers.

2PREPARATION OF ^{99M}TC- CLOMIPHENE CITRATE AS A NOVEL AGENT FOR BREAST CANCER IMAGING

Ismail Taha Ibrahim.

EGYPT

Egyptian Atomic Energy Authority

This paper addresses the development of a new radiopharmaceutical for breast cancer imaging. The optimization of the labeling yield of Clomiphene citrate, with ^{99m}Tc is described. ^{99m}Tc- Clomiphene citrate was obtained with a radiochemical yield of 94.4% by adding ^{99m}Tc to 1.5mg Clomiphene citrate in the presence of 10µg SnCl2 at pH 7. Radiochemical purity of the product has been verified by means of paper chromatography and paper electrophoresis after Millipore filtration (0.22 µm). Ehrlich Ascites Carcinoma (EAC) as amodel of breast cancer cells was injected intraperitoneally (I.P) to produce ascites and intramuscularly (I.M) to produce solid tumor in the right thigh. Biodistribution study was carried out by injecting solution of ^{99m}Tc- Clomiphene citrate in normal and tumor bearing mice. The uptake in ascites was over 12.5 % injected dose per gram tissue body weight, at 1hr post injected and above 12% in solid tumor. This data revealed localization of tracer in tumor tissue with high percent sufficient to use ^{99m}Tc- Clomiphene citrate as a promising tool for diagnosis of breast cancer.

EVALUATION OF TWO FORMULATIONS FOR THE PREPARATION OF 99MTC-MIBI USING A BIOLOGICAL DISTRIBUTION IN MICE

Leonardi, Natalia Mónica [1] Calcagno, María de Luján [2]; Zubillaga, Marcela Beatriz [1]

[1] Radioisotopes Laboratory, Physics Department, School of Pharmacy and Biochemistry, University of Buenos Aires, Buenos Aires, Argentina.
[2] Mathematics Cathedra, Physics Department, School of Pharmacy and Biochemistry, University of Buenos Aires, Buenos Aires, Argentina.

ARGENTINA

Objective: Although all the kits for the preparation of 99mTc-methoxyisobutylisonitrile (MIBI) include the same Active Pharmaceutical Ingredient (API), differences on its formulation, could cause a variation in the organ distribution pattern at different times. The aim of this study was to compare myocardial and hepatic uptake of two formulations (with different qualitative and quantitative composition) for the preparation of 99mTc-MIBI in a mice model.

Materials and Methods: We studied two formulations (A and B) with equal amounts of API and stannous chloride but with different cysteine content, and different excipient composition. For each formulation 18 mice were subdivided into 3 groups (n=6 each subgroup) according to timing of euthanasia after 99mTc-MIBI injection. Mice were supplied with mice chow and drinking water ad libitum. Radiolabeling procedure of MIBI was performed according to manufacturer's instructions. Radiochemical purity was performed according USP. Each mouse was intravenous injected with 5,6–21,3 MBq of 99mTc-MIBI. The subgrouped animals were euthanized at either 60, 120 and 180 minutes after radiopharmaceutical injection. Heart and liver were excised, weighed and counted on a gamma counter. Organ uptake was calculated as a percentage of the injected dose per gram of tissue mass (%ID/g) and heart/liver ratios were calculated. Data were analyzed using three-way ANOVA ($p<0.05$).

Results: Myocardial uptake was 16.75±3.07, 15.80±4.30, 14.23±1.22 for formulation A and 16.32±5.87, 22.18±1.92, 19.71±3.63 for formulation B at 60, 120 and 180 minutes respectively. Hepatic uptake was 3.47±0.66, 4.10±1.33, 2.39±0.57 for formulation A and 5.08±0.86, 2.27±0.67, 1.83±0.70 for formulation B at 60, 120 and 180 minutes respectively. No difference in heart uptake was observed as a function of time for both formulations. Hepatic uptake profiles are different for each formulation. While formulation A shows a maximum liver uptake at 120 min, the formulation B shows a constant liver clearance. Heart to liver ratios were 4.98±1.30, 4.28±2.01, 6.23±1.49 for formulation A, and 3.35±1.65, 10.42±3.72, 12.36±5.57 for formulation B at 60, 120 and 180 minutes respectively, showing no differences over time for formulation A, but with statistical increase for the formulation B.

Conclusions: The kinetic profile of the hepatic clearance shows a faster removal from the liver for the formulation B, demonstrating that a difference on the composition and the technological procedures for the formulation of the kits for the preparation of 99mTc-MIBI modifies the liver uptake in mice. Clinical relevance of this finding is under study.

PRODUCTION OF I-124 AT IEN/RIO DE JANEIRO

Ana Maria S. Braghirolli1 Gonçalo R. dos Santos1 , Juliana Batista da Silva2 , William Waissmann3

1 Instituto de Engenharia Nuclear, IEN-CNEN-RJ
2Centro de Desenvolvimento da Tecnologia Nuclear, CDTN-CNEN-BH
3 Fundação Oswaldo Cruz, RJ Escola Nacional de Saúde Pública Sérgio Arouca

BRAZIL

ABSTRACT Iodine-124 is a positron emitter with physical half-life of 4.2 days. Its decay occurs by positron emission (23.3%) and electron capture (76.7%). Their physical and chemical characteristics make it an attractive isotope for medical applications. The development of new imaging techniques, improvements in Positron Emission Tomography (PET), the development of new detectors and computational methods of signal processing, open new perspectives for its application. The increasing use of PET technology in medical oncology, pharmacokinetics and drug metabolism, make the radiopharmaceuticals labeled with 124I a tool of great interest and usefulness. The use of 124I - labeled molecules stands out particularly due to the convenient half-life of 124I. This feature enables diagnostic imaging in PET centers far away from the radionuclides producing center. Within this context, this work presents a method for the production and separation of 124I. In this pioneering method in the country, the natTeO2 targets are irradiated in a charged particles accelerator, with variable energy, the IEN's CV-28 cyclotron. The irradiations are performed with 24 MeV, initial energy, proton beams. The produced 124I was separated from the target material by dry distillation and trapped in a NaOH solution (0.02 M), in an automated system. The thick target yield was 6.81 MBq/μAh, and the synthesis yield was 90%. The 124I obtained was then used in preliminary biodistribution studies. These studies were performed on a microPET, model LabPET 4 of the CDTN, in Swiss type mice. The results of the application of Na124I showed high quality PET imaging of the thyroid, with the maximum uptake at 6 h after injection.

LONGITUDINAL PERFORMANCE EVALUATION OF SNO2-BASED 68GE/ 68GA GENERATORS FOR ECONOMICAL RADIOLABELING OF DOTA/NOTA-PEPTIDE DERIVATIVES

Thomas Ebenhan1,2; Deon Kotze3; Botshelo Mokaleng1; Isabel Schoeman4; Mariza Vorster1; Mike Sathekge1and Jan Rijn Zeevaart4

1 Department of Nuclear Medicine, University of Pretoria and Steve Biko Academic Hospital, Pretoria,South Africa
2 School of Pharmacy, University of KwaZulu Natal, Durban, South Africa

3 Radiochemistry and Radioanalysis, The South African Nuclear Energy Corporation, Pelindaba,Pretoria, South Africa
4 Department of Science and Technology, Preclinical Drug Development Platform, North West University, Potchefstroom, South Africa

SOUTH AFRICA

Objectives: The food and drug association has recently assigned orphan-drug status to GMP kit-produced 68Ga-1,4,7,10-tetraazacyclododecane-N′,N″,N‴,N⁗-tetra-acetic-acidoctreotate (68Ga-DOTA-TATE) as diagnostic agent for neuroendocrine tumors which exemplifies the trust in the manufacture of generator-based radiopharmaceuticals. There is a mounting interest in using radioisotopes such as 68Gallium (68Ga) for peptides labeling, i.e. 68Ga could be a vital alternative to 18F, offering shorter imaging times, no special patient preparation, an on-demand and year-round tracer availability. This would lead to a more cost-efficient, decentralized way of diagnostic imaging, especially in areas without access to a nearby cyclotron. However, very few studies considered the longitudinal verification of the 68Ga, being eluted from the SnO2-based 68Ge/68Ga-generator, therefore we have evaluated the quality of 68Ga-radiolabeling towards different peptides with prolonged generator operation. Methods: 68Ga-eluate quality was compared longitudinally from four individual 68Ge/68Gagenerators (G1-G4) (Type: SnO2-matrix; 1.85GBq-loaded; iThemba LABS). Eluate fractionation (EF) was combined with 68Ga-eluate purification procedures: a) BondElutSCX-based or b) Dowex-resin-SAX-based. Buffered citrate (68Ga-ACD-A) was utilized as reference compound, produced using an aseptic one-vial approach. The following compounds were utilized: 1) DOTA-TATE; 2) 1,4,7-triazacyclononane-1,4,7-triacetic-acid (NOTA)-c(RGDyK), conducting manual- and kit-based production and 3) Ubiquicidin (UBI) fragment NOTA-UBI(29-41). Radiolabeling followed pH-adjustment, high-temperature incubation and final purification from unbound 68Ga with C18-based cartridges. The labeling efficiency (LE) was determined by thin-layer- or high-pressure-liquid-chromatography. The 68Ga-eluate- and peptide samples were assessed using gamma spectrometry and inductively coupled plasma and optical emission spectrometry for metal impurities and 68Ge-detection.Results: A 68Ga-yield of ≥ 90% (r2=0.70-0.98) was achieved over 190, 261, 137 and 172 days, for G1, G2, G3 and G4, respectively. Generator re-elution 3-5 hours after the first elution/day (r2 = 0.89) yielded in 89% (2ndelution/day) and 72% (3 rdelution/day) 68Ga-activity. The 68Ge-levels (0.05–1.5%) in 68Ga-eluate samples ≥ 400 days were minimized significantly by FE (P=0.013). The 68Ga-eluate purification led to (a) 40-44% and (b) to 69-74% 68Ge-reduction (N=4). The LE of NOTA-c(RGDyK) kits (r 2=0.76) and NOTA-UBI29-41(r2=0.88) decreased in-significantly with prolonged generator usage. DOTA-TATE radiolabeling was competitively labeling until 200 days (r2 =0.75) followed by larger LEvariability at 200-325 days (r2=0.12) generator operation. The 68Ge-content was not detectable for all radiopharmaceuticals up to 298-325 days; except 68Ga-citrate showed increasing 68Ge-levels (r2= 0.73) to 0.0375 % at 275 days. The total longitudinal Al(III)-,Cu(II)-, Fe(III)-, Sn(II)- and Zn(II)-contents amounted to ≤19.5 ppm per NOTA/DOTApeptide sample with prolonged generator operation.

Conclusion: Although 68Ga is eluted from a SnO2-based generator with more acidic condition, its longitudinal quality warrants high-yield, high-economical peptide radiolabeling procedures. The robust generator performance facilitates its prolonged operation in a hospital environment and stipulates a cost-efficient approach in radiopharmaceutical production. Keywords: 68Ge/68Ga-generator; NOTA; DOTA; 68Ge-breakthrough; 68Gallium, DOTATATE

CHEMOTHERAPEUTIC TREATMENT HEPATOTOXICITY EVALUATED BY MEANS OF SMALL ANIMAL IMAGING. THE ROLE OF COMMONLY USED RADIOPHARMACEUTICALS IN BACK TRANSLATIONAL RESEARCH

Tesán FC, Martinell Lamas D, Portillo MG, Leonardi N, Giaquinta Romero D, Medina V, Salgueiro MJ, Zubillaga MB.

ARGENTINA

The objective was to determine the usefulness of the hepatobiliary and colloid scintigraphies, employing 99mTc-disida and 99mTc-phytate, respectively, in the evaluation of the hepatotoxicity of two chemotherapeutic treatments assessed in rats. Male Sprague-Dawley rats (n = 12 each group, body weight = 300 g) were administered ip. with doxorubicin 2mg/kg (group G1) or doxorubicin 2mg/kg + histamine 5mg/kg (group G2) within a scheme of six doses along two weeks. Scintigraphy studies were acquired using a small-field-of-view gamma-camera equipped with a high-resolution collimator, before starting the treatment (control), at 1 week and at 2 weeks. Dynamic 99mTc-disida (37 MBq) in ventral position was perfomed (1 frame/3 minutes). Since rats lack gallbladder, regions of interest (ROIs) were drawn just at the beginning of the bile duct in order to capture the time to the maximum 99mTc-disida extraction. Static 99mTc-phytate (37 MBq) biodistribution at 30 minutes post-injection was performed at ventral, right anterior oblique, right lateral views. ROIs were drawn for estimate liver uptake (L) as well as for bone marrow (BM) uptake and the ratio L/BM was calculated. Additionally, whole-body ventral images were acquired. At the end of the protocol, animals were sacrificed and samples of blood were taken for liver biochemistry assay, while liver tissue samples were processed for histopahological studies using Haematoxylin eosin stain. The results showed that hepatotoxicity of doxorubicin was significantly higher when it was administered alone than when it was co-administered with histamine, as previously reported by the authors elsewhere. Liver biochemistry showed no significant changes in treated groups with regard to normal expected values. However, hepatobiliary scintigraphy showed that bile flux was accelerated in G1 with regard G2 (G1 control= 10 min, G1 1-week= 6 min and G1 2-weeks= 5 min; G2 control= 9 min, G2 1-week= 8.7 min and G2 2-weeks= 7 min). Colloid scintigraphy showed an impairment in the scavenger function of the liver since the ratio L/BM of 99mTc-phytate uptake

was diminished in G1 (G1 control L/BM= 0.92, G1 1-week L/BM= 0.85 and G1 2-weeks L/BM= 0.80; G2 control L/BM=0.99, G2 1-week L/BM= 0.99 and G2 2-weeks L/BM= 0.98). Functional imaging showed correlation with histopathological results since the liver of G1 animals showed disorganization and loss of sinusoidal spaces, areas of focal necrosis and decrease of the number of Kupffer cells, while treatments of G2 showed preservation of the liver structure with reduced sinusoidal disarrangement. We conclude that functional imaging in the experimentation with animal models is a useful tool to assess chemotherapy-induced hepatotoxicity. Translations of findings as well as the contribution to the 3R concept are a main goal of small animal imaging in experimentation.

SYNTHESIS AND CHARACTERIZATION OF RGD-MODIFIED LIPOSOMES FOR TARGETING V3 INTEGRIN

Mitsuyoshi Yoshimoto, Takuya Hayakawa, Sadaaki Kimura, Izumi O. Umeda, Hirofumi Fujii.

JAPAN

Division of Functional Imaging, National Cancer Center Hospital East

Objective: Pancreatic cancer is one of the common causes of cancer-related mortality and its 5-year survival rate is very poor. In addition, only 15−20% of tumors are resectable at the time of diagnosis. To overcome pancreatic cancer, we need to develop new therapeutic strategy. v3 integrin is overexpressed in endothelial cells and various tumor cells including pancreatic cancer. We have previously reported that SPECT with 111In-DOTA-c(RGDfK) successfully detected pancreatic cancers in a hamster carcinogenesis model (J. Nucl. Med., 53:765-71, 2012). Therefore, v3 integrin is a possible target for drug development. We synthesized RGD-modified liposomes for imaging and internal radiotherapy. Methods: Liposomes composed of 1,2-distearoyl-sn-glycero-3-phosphocholine (DSPC), cholesterol and N-(carbonyl-methoxypolyethyleneglycol 2000)-1,2-distearoyl-sn-glycero-3-phosphoethanolamine (mPEG-DSPE) were prepared by thin film hydration method. RGD-modified liposomes were synthesized by coupling c(RGDfK)-SH with maleimide-mPEG-DSPE. The amount of RGD-modification was regulated by changing ratios of maleimide-mPEG-DSPE to total mPEG-DSPE (5−50%). As reference liposomes without targeting ability, RKG-modified liposome and unmodified liposome were prepared. Particle size of the liposomes was measured by dynamic light scattering. Binding affinities of RGD-modified liposomes to v3 integrin were assessed as IC50s for 125I-echistatine binding to PANC-1 human pancreatic cancer cells. Biodistribution of the RGD-modified liposomes loaded with 111In was carried out in a PANC-1 xenograft model. Results: Particle size of the RGD-modified liposomes was 103.7±3.9 nm. The RGD-modified liposomes dose-dependently inhibited the binding of 125I-echistatin to PANC-1. The IC50 values were 5–67 μM as phospholipids. In contrast, RKG-modified liposome and unmodified liposome did not inhibit the binding. Biodistribution studies using the liposomes loaded with 111In indicated rapid clearance of the RGD-modified liposome (50%) from blood (0.41% ID/g at 4 h). Significant accumulation of radioactivity in spleen was found with increase in the amount of RGD modification (170.4–403.9% ID/g at 24 h). Unmodified liposome showed the highest tumor uptake (2.80% ID/g) at 24 h, whereas the RGD-modified liposomes showed the lower tumor uptake (1.47–2.25% ID/g). However, tumor to blood (T/B) and muscle (T/M) ratios of the RGD-modified liposome (5.0%) were highest among the liposomes used in this study (3.7 and 8.0, respectively). Conclusions: The RGD-modified liposomes was successfully synthesized and labelled with 111In. The RGD-modified liposomes showed the targeting ability to v3 integrin.

CONTRAST MEDIA-RADIOPHARMACEUTICAL PHARMACOKINETIC INTERACTION IN A BASIC RADIO RENOGRAM

Portillo MG, Tesán FC, Giaquinta Romero D, Costa J, Zubillaga MB, Salgueiro MJ.

ARGENTINA

It has long been known about the existence of drug-drug interactions and the mechanisms involved, affecting the kinetic, the efficacy and the toxicity of conventional medications. On the other hand, it is a common Nuclear Medicine (NM) practice to use some drugs to enhance diagnostic procedures, so-called interventional NM. Nevertheless, in the last years there has been an increasing interest in evaluating and recognizing drug-radiopharmaceutical interactions, and systematically report them. In this sense, the study reports the modification of the results in the radionuclide basic renogram (RBR) in control animals after the administration of iodine contrast media. The context of contrast media administration deals with some common facts at NM departments such us when patients came for health controls during their cancer treatment, or when multimodality imaging is employed (even in small animals). We used 9 healthy Sprague-Dawley rats (average weight 250 mg) to perform RBR with 99mTc-DTPA (37 MBq) under control conditions. Dynamic studies were acquired using a small-field-of-view- gamma-camera equipped with a high-resolution collimator and dedicated software for small animals taking 1 frames/1 second during the first minute and then 1 frames/15 seconds until at least 30 minutes for each study. After 1 week, we repeated the RBR but this time it was perform 1 hour after the intravenous administration of iodine contrast media (1mg/Kg body weight) as Iopamidol (iodine 370 mg/ml). The results showed that RBR under control conditions displayed functional curves with the 3 phases of perfusion-function-elimination within the expected normal patterns. Average Tmax (2.3 min) and T50% (8 min) were obtained as well as right and left relative renal functions within normal range (45-55%). On the contrary, qualitative and

quantitative changes affected functional curves after iodine contrast media administration. Although the 3 phases were visualized changes in the functional phase that prolonged Tmax (8 min) was sometimes recorded and in all cases the elimination phase was significantly prolonged (T50 % > 30 min). In these cases, relative renal function was always observed in the normal range and resumed images showed that elimination of 99mTc-DTPA was being accomplished. In conclusion, iodine media contrast interfered with normal renal function as demonstrated by results obtained in BRR. The consequences and significance of these findings highlights the importance of considering the effect of iodinated contrast media on renal function, derived from their own physicochemical characteristics. The pharmacokinetic interactions with other radiopharmaceuticals which biodistribution depends on renal function should also be studied and enlightened.

SYNTHESIS AND PRECLINICAL EVALUATION OF 68GA-NOTA-UBI 29-41 FOR DIAGNOSIS OF INFECTION BY PET/CT

Mónica Vilche, Ana Laura Reyes, Elena Vasilskis, Javier Giglio, Patricia Oliver, Henia Balter and Henry Engler.

URUGUAY

Uruguayan Centre of Molecular Imaging (CUDIM), Montevideo Uruguay.

UBI 29-41, a cationic peptide (Thr-Gly-Arg-Ala-Lys-Arg-Arg-Met-Gln-Tyr-Asn-Arg-Arg) derived from Ubiquicidin binds to microorganisms. Derivatized with NOTA can be labeled with 68Ga (+, T1/2 68m) allowing PET/CT studies. Preliminary results of the synthesis and characterization of 68Ga-NOTA-UBI 29-41, as well as their biological behavior are presented. Labelling of UBI 29-41 conjugated with NOTA (2-[4,7-bis(carboxymethyl)-1,4,7-triazonan-1-yl]acetic acid) and 68Ga (from a 68Ge/68Ga ITG generator) was optimized at different temperatures (20°C-100°C) and pH (3.5-5.5). Radiochemical purity was determined by RP-HPLC on a C-18 column (4,6 x150 mm x 5µm) (Agilent ZORBAX ECLIPSE PLUS C18) and gradient of A: 0,1% TFA in H2O and B: 0,1% TFA in acetonitrile, from 100% to 40% in 6 minutes and maintaining 40% until 10 minutes, flow 1 mL/min and by ITLC-SG in citric acid 0,1M (Rf 68Ga-NOTA-UBI 29-41: 0,0; Rf 68GaCl3: 0,75-0,85). The stability of 68Ga-NOTA-UBI-29-41 along time was monitored up to 260 min, using the same methods as for quality control. Binding to serum proteins was determined at 30, 60, 90 and 120 minutes. In vitro binding to St. aureus was evaluated with increasing amounts of microorganism (9,14x106 to 1,17x109 cfu in 0,1 mL) incubated 1h at 4°C and further centrifugation. Biological behaviour was evaluated in vivo in Swiss male mice "Mus Musculus" (25-30g) by biodistribution and PET/CT imaging. Three groups of animals were analyzed: a) Mice infected intramuscularly (i.m) with St. Aureus by injection of 0,1mL of 1,2 x109 cfu/mL (left upper thigh muscle), b) Mice with inflammation induced by i.m injection of 0,1 mL of heat shock treated 1,2x109 cfu/mL St. aureus; and c) Healthy mice. Biodistribution was performed at 30, 60 and 120 min post injection of the radiopharmaceutical (n=4 for each condition), whereas imaging acquisitions were performed up to 120 minutes. Radiochemical purity was >90% in the optimized conditions: 90°C for 5 min and pH between 3,5 and 4,0. The radiotracer was stable for more than 3 hours. 68Ga-NOTA-UBI-29-41 show high renal excretion and rapid blood clearance. Binding of 68Ga-NOTA-UBI was higher than 95% for 5x108 cfu St. aureus in 0,1 mL. T/NT reached 5,0 at 60 min and 4,1 at 120 minutes while for the inflamed mice these values were 1,6 and 1,2 respectively. The difference in uptake of the radiopharmaceutical in the infected muscle regarding the inflamed one is based in the fact that the cationic peptide UBI 29-41 preferentially binds to anionic microbial cell membranes at the site of infection. This was evidenced in the PET/CT images. Our findings suggest that the 68Ga-NOTA-UBI might differentiate infection from sterile inflammation having an excellent potential for human use.

Aknowledgements: IAEA, Cátedra de Microbiología, Facultad de Química.

EX-VIVO EVALUATION OF 99MTC LABELED GLUCOSAMINE SULFATE (99MTCGS) IN ARTICULAR CARTILAGE. RELEVANCE FOR OSTEOARTHRITIS IMAGING

Grazyna Sobal, Ernst Johannes Menzel*, Ronald Dorotka§, Helmut Sinzinger, Marcus Hacker
Division of Nuclear Medicine, Department of Biomedical Imaging and Image-guided Therapy, *Institute of Immunology, §Department of Orthopaedic Surgery, Medical University of Vienna, Austria,.

AUSTRIA

Aim: Glucosamine sulfate (GS) is widely used in the treatment of osteoarthritis, but no data concerning the local uptake of GS in articular cartilage exist. For this reason we performed radiolabeling of GS (Rottapharm, Monza, Italy) using 99mTcO4-/tin method and investigated its uptake in articular cartilage.

Methods: Radiolabeling of GS is difficult, because of the small MW of GS (450Da) and of 99mTcO4- for separation after radiolabeling. For uptake studies, articular surgery tissue from patients (n=6, 68-79a) undergoing knee arthroplasty (pieces of ~3mg wet weight), or frozen tissue sections (10µ) for autoradiography (10µCi) were used. The uptake of 99mTcGS was monitored from 0.5 to 72h of incubation to achieve saturation, by quantitation of radioactivity with a Gamma-counter or autoradiography. To mimic in-vivo treatment, tis-

sue pieces were preincubated with cold GS (80µg/ml) for 16 weeks prior to incubation with 99mTcGS. The incubation was performed with tissues with different degree of degeneration. Results: The best radiolabeling results were obtained using 25mg of GS, 120-150 MBq of 99mTc, separation on G10 column, specific activity of 162.2-202.8 mCi/mM, n=4. Results: The uptake was time-dependent and amounted to a maximum of 77.4. -71.7% at 48h versus 72h, at saturation. Saturation was achieved already after 24h of incubation. When the tissue was preincubated with cold GS the additionaly uptake of 99mTcGS was strongly reduced by 52.3-71.8 %, proving the chondrotropic effects of GS during preincubation. The reduction of 99mTcGS uptake was observed also in areas of different grade of degeneration from the same patient by 27.8-35.8%, proving the specificity of uptake. Autoradiographic studies paralleled the uptake in tissue pieces and saturation was achieved at 24h by all patient tissue samples. The non-specific uptake in the presence of 50-fold excess of cold GS was increasing with time up to a maximum of about 10%, at saturation. Conclusion:99mTcGS could be a suitable tracer to quantify degeneration in articular cartilage, because of its high uptake and specificity. It could be a potential candidate for imaging osteoarthritis in cartilage and possibly for monitoring therapeutic effects.

EXPERIENCE WITH TOP-OF-FOIL LOADING [O18]WATER TARGETS ON AN IBA 18 MEV CYCLOTON

L. Silva[a], P.Pace[a], C. Hormigo[a], Y.Litman[a], S. Fila[a], H.Gutierrez[a], Gillermo Arturo Casales[a] Argentina, C. Gonzalez-Lepera[b], R. Srtangis[c]

[a]*Laboratorios BACON SAIC, Buenos Aires, Argentina*
[b] *University of Texas MD Anderson Cancer Center, Houston TX*
[c]*Cyclotope Houston TX, USA*

UNITED STATES

Introduction: Liquid targets using top-of-foil loading concept have been succesfully employed for routine high current production of ^{18}F and ^{13}N at Cyclotope (Houston,TX), over the past ten years[1,2]. These targets are typically filled with 3.5 ml of water, then pressurized with helium gas at 22bar and bombarded with 18 MeV protons (70-100µA). Average calculated saturation yield for production of ^{18}F is ~7.8 GBq/µA (210 mCi/µA) using in-house recycled [^{18}O]-water at approximately 93% enrichment. Reduction of beam power per unit of area is one of the advantages of a tilted entrance-foil geometry Implementation of this target geometry. On the ACSI TR19 cyclotron 25degrees upwards irradiation port, results in an almost horizontal target entrance foil. A 6ml total cavity volume target allows variable liquid fill volumes of 1.2-4.5 ml for beam current operation from 30-120µA, resulting in a very efficient use of the costly ^{18}O-water. In a near horizontal installation as in the mayority of cyclotrons, the fill volume flexibility is drastically reduced, having a minimum fill volume of 3.3 ml. At the requirement of Laboratorios Bacon, Cyclotope modified the target design with a front mounted collimator compatible with the IBA Cyclone 18/9 cyclotron. A second requirement was to reduce the minimum fill volume for horizontally mounted targets to 2.5 ml or less, while maintaining saturation yield performance. To preserve compatibility with existing IBA targets, the target hardware was modified to operate in self-pressurization mode. This paper presents the results obtained with high and low volume Niobium target inserts (6ml and 4 ml) mounted near horizontally on the IBA Cyclone 18/9 cyclotron and operated in self-pressurization mode. We present pressure/current characteristics, target performance (saturation yield, produced activities, maintenance frequency, FDG yields, etc.). Material and Methods: The following targets manufactured by Cyclotope were tested and routinely used for production at Laboratorios Bacon:1-High Volume Target CY2 model (“American Standard”), 6ml Niobium cavity.2-Low Volume Target, CY3a model (“Traful”), 4ml Niobium cavity. 3- Low volume Target, CY3b model (“Ferrum”), 4.1ml Niobium cavity.Results and ConclusionThe advantages of self-pressurization mode (Laboratorios Bacon setup) aremUsing the vapor pressure as a performance parameter, heat removal by boiling/condensation cycle starts at lower temperature (beam current) . While, the advantages of the pre-pressurized targets (Cyclotope setup) are reduced pressure fluctuations, performance is basically unaffected by plumbing dead volume, flexibility to locate instrumentation farther away from radiation field, less dependence on fill volume, potential target leaks can be detected before starting an irradiation. No significant differences were found in target performance when operated in either pressurization mode. The self-pressurizing setup seems to require a sligthly lower fill volume (approximately 5%). The maximum beam current was limited by the foil rupture pressure (~ 40 bar). Safe maximum operating pressure was determined as 30 bar. No foil rupture was experienced during nine months of daily irradiation of these targets in self-pressurizing mode at Laboratorios Bacon. The irradiation parameters and target performance for the different targets are shown in Tables 1 and 2 below. The low volume Traful and Ferrum targets have the best saturation activity vs. fill volume, A(sat)/V, relation. Both targets produce 310±31GBq (8.4±0.8Ci) of high quality fluoride (F-18) in two hours of irradiation at 70 µA. The low volume targets have a low operation pressure (20bar @ 70uA) when compared to the IBA (NIRTA XL) targets. The typical saturation activity for the low volume targets was 592±59GBq (16±1,6Ci) of F-18 at 70 µA, 8.5GBq/µA (228 mCi/µA) using 2,7ml enriched O-18 water (98%+). The maintenance interval (>10mA.h) is very conveniente to reduce personnel radiation dose. No reduction in FDG yields was observed during that operation interval.

TARGET	I(μA)	P(bar)	V(ml)
AMERICAN STANDARD*	90	20	3.8
TRAFUL	70	20	2.7
FERRUM	70	20	2.7
IBA (NIRTA XL)	40	30	2.0

TABLE 1. Targets parameters for self-pressurizing mode on the IBA Cyclone 18/9. Where, I is the beam current, P is the operating pressure, V is the fill volume.

In contrast, operation of the high volume targets in pre-presurization mode at the Cyclotope facility results in a higher maximum beam current limit (135μA) for the same operating pressure (25 bar). Nevertheless, more O-18 water will be required to irradiate at this high current (4.5 ml vs. 3.0 ml). In self-pressurizing mode, a higher filling volume will reduce the expansion volume and, in consequence, the maximum beam current.

TARGET	N. Runs	ASat	ASat/V
GBq(Ci)	1263	694(19)	**209**
TRAFUL	314	592(16)	**218**
FERRUM	10	592(16)	**218**
IBA XL	>1000	310(8,4)	**155**

TABLE 2. Targets performance for self-pressurizing mode on the IBA Cyclone 18/9. O-18 water enrichment 98%+. Where, A_{Sat} is the saturation activity and A_{Sat}/V is the performance parameter.

* Operated in pre-pressurized mode and using recycled O-18 water (~93%).

References

1. S. R. Strangis, and C. Gonzalez Lepera. "Breaking the 1KW Target Barrier for the Routine Production of F18 With O18-Water ..." 2004 Conference on the Application of Accelerators in Research and Industry. October 10 – 15, 2004. Denton, TX.
2. S. R. Strangis and C. Gonzalez Lepera. "Reliable Fluorine-18 [18F-] Production at High Beam Power." 18th International Conference on Cyclotrons and Their Applications. September 30 – October 5, 2008. Catania, Italy.

CLINICAL FDOPA: ITS TIME HAS COME

[1]Silva L.; [1]Litman Y.; [1]Pace P.; [1]Hormigo C.; [1]Sebastián F.; [1]Gutierrez H.; [2]Bastianello M.; [1]Zubata P.; [1]Casale Gillermo Arturo, Argentina.

[1] Laboratorios BACON SAIC
[2] Centro de Educación Médica e Investigaciones Clínicas Norberto Quirno CEMIC

ARGENTINA

It has been demonstrated that [18F] Fluor-L-dopa is a significant specific neurological and tumoral tracer since the first electrophilic synthesis pathway was reported by Dr Jorge Barrio at UCLA(1) in 1979. The electrophilic process, however has limited the use of FDOPA to a few PET services due to its low activity and the gas target complexities. .Several nucleophilic pathways for FDOPA were sought, as was once done with FDG after its successful nucleophilic synthesis in 1986, when it got spread globally (2) Coenen- Hamacher and col. However, until now, all the reported electrophilic syntheses have been complex and low activity was obtained.We have been studying and developing several nucleophilic pathways published by Emer, but although its radiochemical yield at the first step of

labelling was high, the next steps turned out to be difficult to implement, specially the hydrolysis.Lemaire et al. designed a promising nucleophilic process, which may result in obtaining larger amounts of FDOPA so that it can be spread globally, too.The radiochemistry automation experts from Trasis, who in the mid nineties created the famous "Coincidence" module (also called Tracerlab) lately developed a maximal refinement module called "AllinOne". We present our experience with more than 30 production runs for a clinical trial, following the procedure by Lemaire et al. using the AllinOne module from Trasis. Some minor adjustments were made. The product has a radiochemical purity > 99 %, an enantiomeric purity > 97% and complies with the other standard quality control tests. The overall synthesis showed an average uncorrected yield of 30±3%, and a new methodology reaches >40%. This method will be a breakthrough for the clinical use of this radiopharmaceutical, such as the FDG nucleophilic synthesis was in 1986.The existence of a European marketing authorization for this molecule has facilitated its registration by the Argentinean Sanitary Authorities.

USE OF RADIOIODINATED HSP90 TARGETED TO TUMOR CELLS IN MOLECULAR TUMOR IMAGING

Rong Fu Wang, China. Hong Wei Sun.

CHINA

Department of nuclear medicine, Peking University First Hospital, Beijing 100034 China.

Objective: Hsp90 is a highly abundant and ubiquitous molecular chaperone which plays an essential role in many cellular processes including cell cycle control, cell survival, hormone and other signalling pathways. It is important for the cell's response to stress and is a key player in maintaining cellular homeostasis. Hsp90 has become a major therapeutic target for cancer. The overall aim of this study was to establish the method of 131I radiolabel of heat shock protein 90, investigate the labeling conditions. Method: The HSP90 sample provided by the school of life science, Tsinghua University and its purity is 98%, preserved in 25% glycerol. ^{131}I-Hsp90 was radiolabeled by chloramine-T method. Different conditions of reaction time and temperature were tested to get a better radiolabeling yield. Radiolabeling yield and radiochemical purities of 131I- Hsp90 were analyzed by paper chromatography. Results: The labeling efficiencies of 131I-Hsp90 reached 70.9%±4.5% (n = 5), specific activity 30μci/μg and the radiochemical purity exceeded 90% after purification. The best labeled condition is Hsp90 20μg, 131I 2mci, chloramine-T 10μg , react in 50μl Phosphate buffer pH7.5 for 6 min in room temperature(about 22). Conclusion: The Hsp90 can be successfully radiolabeled with 131I using the chloramine-T method.131I- Hsp90 can be used as a potential candidate for visualization of tumor in malignant carcinomas. Further study is going on.
[Key word] 131 I, Hsp90, tumor imaging.

TC^{III}-BASED MIXED COMPLEXES USEFUL IN DESIGN AND THE DEVELOPMENT OF NEW SPECT AGENTS

Nicola Salvarese[1], Laura Meléndez-Alafort[1]. Italia, Nicolò Morellato[2], Alessandro Dolmella[2], Debora Carpanese[1], Antonio Rosato[1], Fiorenzo Refosco[3], Cristina Bolzati[3]

[1]DiSCOG-University of Padua, [2]DSF-University of Padua, [3]IENI-CNR, Padua, Italy.

ITALY

Aim. The trivalent state is one of the most common and stable oxidation states of technetium and rhenium. In spite of this, none of the radiopharmaceuticals currently in clinical use contains the metal in this oxidation state and only a limited number of studies involving the use of M(III)(^{99m}Tc/^{188}Re) are reported. In this study we described a general procedure for the preparation of a new series of six-coordinated mixed ligand [$^{99m}Tc^{III}(PS)_2(L^n)$] compounds, (PS = bis-aryl-alkyl or tris-alkyl-phosphino-thiolate; L^n = dithiocarbamate) that could be used to design a new class of Tc^{III}-imaging agents. Methods. The synthesis of [$^{99m/99}Tc^{III}(PS)_2(L^n)$] complexes, and their in-vitro stability as well as their in-vivo biological assay were investigated. Results. [$^{99m}Tc^{III}(PS)_2(L^n)$] complexes were efficiently prepared, following a one-pot procedure which required the addition of pertechnetate to a reaction vial containing $SnCl_2$ and the selected PS and L^n ligands. Radio-synthesis was performed in aqueous solution and was completed within 30 minutes at 75 °C. The chemical identity of ^{99m}Tc-complexes was determined by HPLC comparison with the corresponding ^{99}Tc-complexes [1]. All complexes are constituted by the presence of the [$^{99m/99}Tc^{III}(PS)_2]^+$ moiety where two phosphino-thiolate ligands are tightly bound to the metal while the remaining two positions are saturated by a dithiocarbamate chelate, also carrying bioactive molecules (e.g. 2-methoxyphenilpiperazine). [$^{99m}Tc^{III}(PS)_2(L^n)$] complexes were inert toward ligand exchange reactions. No significant in-vitro serum protein binding and no notable biotransformation of the native compounds into different species by the in-vitro action of the serum enzymes was observed. Biodistribution of the complexes are characterized by a rapid blood clearance, a high lung, liver and spleen uptakes followed by slow wash-out. Conclusion: [$^{99m}Tc^{III}(PS)_2(L^n)$] compounds were efficiently prepared in nearly physiological conditions by using a one pot pathway of synthesis, which allows to overcome the limitations commonly involved in the synthesis of $^{99m}Tc^{III}$-based radiopharmaceuticals. More-

over, the applied procedure perfectly meets the basic principle of the one pot synthesis and the requirements for Nuclear Medicine practice application.

Complexes were found to be stable in vitro and in vivo, underlining their remarkable thermodynamic stability and kinetic inertness. These results could be conveniently utilized to devise a novel class of $^{99m}Tc^{III}$-based compounds useful in radiopharmaceutical applications. Acknowledgements This research was supported by MIUR (PRIN 20097FJHPZ-004 and FIRB RBAP114AMK "RINAME") and by AIRC (IG-13121).

Salvarese N, et al. Inorg Chem 2013, 52, 6365-6377.

SYNTHESIS AND PRELIMINARY EVALUATION OF A NEW 99MTC LABELED SUBSTANCE P ANALOGUE AS A POTENTIAL TU MOR IMAGING AGENT

Davood Beiki[1]. Iran, Mostafa Erfani[2], Saeed Mozaffari[1], Fariba Johari Daha[2], Farzad Kobarfard[3], Saeed Balalaie[4], Babak Fallahi[1]

[1]Research Center for Nuclear Medicine, Tehran University of Medical Sciences, Tehran, Iran [2]Nuclear Science Research School, Nuclear Science and Technology Research Institute (NSTRI), Atomic Energy Organization of Iran (AEOI), Tehran, Iran
[3]Department of Medicinal Chemistry, School of Pharmacy, Shaheed Beheshti University of Medical Sciences, Tehran, Iran
[4]Peptide Chemistry Research Center, K. N. Toosi University of Technology, Tehran, Iran

IRAN

Objective: Neurokinin 1 receptors (NK_1R) are overexpressed on several types of important human cancer cells. Substance P (SP) is the most specific endogenous ligand known for NK_1Rs. Accordingly, a new SP analogue was synthesized and evaluated for detection of NK_1R positive tumors.Materials and Methods: [6-hydrazinopyridine-3-carboxylic acid (HYNIC)-Tyr^8-$Met(O)^{11}$-SP] was synthesized and radiolabeled with ^{99m}Tc using ethylenediamine-N,N'-diacetic acid (EDDA) and Tricine as coligands. Common physicochemichal properties of radioconjugate were studied and in vitro cell line biological tests were accomplished to determine the receptor mediated characteristics. In vivo biodistribution in normal mice and in tumor bearing nude mice bearing tumor xenografts was also assessed. Results: The cold peptide was prepared in high purity (>99%) and radiolabeled with ^{99m}Tc at high specific activities (84-112GBq/μmol) with an acceptable labeling yield (>95%). The radioconjugate was stable in vitro in the presence of human serum and showed 44% protein binding to human serum albumin. In vitro cell line studies on U373MG cells showed an acceptable uptake up to 4.91 ± 0.22 % with the ratio of 60.21 ± 1.19 % for its specific fraction and increasing specific internalization during 4h. Receptor binding assays on U373MG cells indicated a mean Kd of 2.46 ± 0.43 nM and Bmax of 14325 ± 904 DPM/8×10^5cells 128925 ± 8145 sites/cell. In vivo investigations determined the specific tumor uptake in 3.36 percent of injected dose per gram (%ID/g) for U373MG cells and noticeable accumulations of activity in the intestines and lung. Predominant renal excretion pathway was demonstrated. Conclusions: This new radiolabeled peptide could be a promising radiotracer for detection of NK_1R positive primary or secondary tumors.

RALIOLABELING AND BIODISTRIBUTION OF PAMAM-DENDERIMER COATED SUPERPARAMAGNETIC IRON OXIDE NANOPARTICLES

Mehdi Akhlaghi[1]. Iran, Nazila Gholipour[2], Amin mokhtari Kheirabadi[1], Seyed Hassan Hosseini[3], Amirreza Jalilian[4],Ali khalaj[2] Akhlaghi.mehdi@gmail.com

[1] Research Institute for Nuclear Medicine, Tehran University of Medical Sciences, Tehran, Iran
[2] Faculty of Pharmacy, Tehran University of Medical Sciences, Tehran, Iran.
[3]Polymer Research Laboratory, Department of Chemistry, Sharif University of Technology, Tehran, Iran.
[4]Nuclear Science and Technology Research Institute, Tehran, Iran.

IRAN

Abstract: Superparamagnetic iron oxide nanoparticles (SPIONs) offer great potential applications in a variety of biomedical fields, such as improved MRI diagnostic contrast agents, tumor hyperthermia and as magnetic field-guided carriers for localizing drugs or radioactive therapies. SPIONs are typically embedded in a matrix material for stabilizing and reducing toxicity, which are then functionalized with complexing agents for radiolabeling with radio cations and with functional groups for conjugation with biologically active species. In this study, denderimer coated SPIONs were synthesized in which coating layer plays three roles: Stabilizing coating,

complexing agent, and functional group. SPIONs were synthesized by co-precipitation of $Fe^{+2}$and Fe+3and then their surfaceswere modified by amine groups. Subsequently, PAMAM dendrimer was growing up on the surface of SPIONs by 4 times repetition of Michel reaction on methyl acrylate and followed amidation with ethylendiamine to create NH2 groups as terminal functional groups. The prepared nanoparticles were characterized with FT-IR, XRD, SEM, TEM and VSM. The size of nanoparticles were about 30 nmshowed super paramagnetization profile on the applied external field Denderimer coated SPIONs were directly radiolabeld with Yttrium-90, a pure beta emitter, for radiotherapy purposes and with Indium-111, for diagnostic purposes. The radiolabeling efficiency was checked by two methods: Radio-TLC on whatman 1 Paperusing 1:1 (10%ammonium acetate: methanol) as mobile phase and magnet separation. The radiolabeling efficiency was about 95%. The radiolabeled nanoparticles were purified to radiochemical purity of more than 99% by magnet separation and dispersed in normal saline. Cytotoxicity of nanoparticles and radiolabeled nanoparticles were investigated on Daudi cell line. Radiolabeled nanoparticles were injected intravenously to mice and biodistribution of radionuclide were determined by measuring uptake radioactivity in mice organs or/and by ROI analysis of SPECT images.Key Words: (Superparamagnetic iron oxide nanoparticles, PAMAM denderimer, Radiolabeling).

[^{99M}TC(N)PNP]-MOIETY, A SUITABLE SCAFFOLD FOR THE DEVELOPMENT OF RADIOLABELED PROBES FOR SPECT OF MULTY-DRUG RESISTANCE: CELL STUDIES

Cristina Bolzati[1], Laura Meléndez-Alafort[2]. Italia, Valentina Gandin[3], Nicolò Morellato[3], Nicola Salvarese[2], Eleonora Cella[3], Debora Carpanese[2] Antonio Rosato[2,4], Fiorenzo Refosco[1]

[1] IENI-CNR, Padua, Italy; [2]DiSCOG-University of Padua, Italy; [3] DSF-University of Padua, Italy, [4]IOV Padua, Italy

ITALY

Introduction. ^{99m}Tc(N)-DBODC(PNP5) [DBODC = bis(N -ethoxyethyl)dithiocarbamato; and PNP5 = bis(dimethoxypropylphosphinoethyl)ethoxyethylamine], namely ^{99m}Tc(N)-DBODC(5), is a lipophilic cationic mixed-compound originally investigated as myocardial imaging agent. This compound has been recently identified as a suitable scaffold for the design of new ^{99m}Tc-based agents useful in noninvasive imaging of P-gp and closely related transporter activities [1].
To evaluate the impact of the [^{99m}Tc(N)PNP]-moiety on the tumor cell accumulation and on the MDR recognition different ^{99m}Tc(N)-DBODC(5) like complexes were synthesized varying the substituents on the PNP ligand and their in-vitro biological behaviors on selected human cancer cell lines and in the corresponding sub-lines were investigated.

Method. ^{99m}Tc(N)-DBODC(n) complexes were efficiently prepared as previously described [2], n is: PNP3 bis(dimethoxypropylphosphinoethyl)-methoxyethylamine; PNP7 (bis(dimethoxyethylphosphinoethyl)-ethoxyethylamine); PNP10 (bis(dimethoxyethylphosphinoethyl)-methoxyethylamine). The kinetic of uptake, at 4 and 37 °C, of the ^{99m}Tc(N)-DBODC(n) complexes were evaluated in-vitro in selected cell lines such us MCF7 (human breast cancer) and 2008 (human ovarian cancer), and in the corresponding sub-lines by using ^{99m}Tc-sestamibi and ^{99m}Tc(N)-DBODC(5) as references.
Results. A significant increase of the % of cell accumulation of ^{99m}Tc(N)-DBODC(7) and ^{99m}Tc(N)-DBODC(10) complexes with respect to ^{99m}Tc-sestamibi and ^{99m}Tc(N)DBODC(5) was observed in drug-sensitive cell lines. At steady-state level, this amount was quantified to be two or three times the % of uptake value of the reference compounds.
A reduction of the net cell uptake between drug-sensitive cells and drug-resistant tumor cells was detected ($p < 0.001$ for the ^{99m}Tc-complexes in all cell lines).

Conclusion. Changes of the chemical-physical properties of [^{99m}Tc(N)PNP]-moiety significantly affect the capability of the complexes to cross the plasma membrane increasing their cellular accumulations and their affinity for the MDR transporters. Hence, ^{99m}Tc(N)-DBODC(7) and ^{99m}Tc(N)-DBODC(10) represent good candidates for the in-vivo exploration of P-gp/MRP functions.
This research was supported by MIUR (PRIN 20097FJHPZ-004) and by AIRC (IG-13121)

[1] Bolzati, C. et al J Biol Inorg Chem 2013, 18, 523-538.
[2] Bolzati C, et al Bioconjug Chem 2010, 21:928–939.

TUMOR DOSIMETRY IN 64CUDOTANOC THERAPEUTIC ADMINISTRATION: A CASE REPORT

Enza Capasso.

ITALY

Objective: Copper-64 (t1/2 = 12.7 h, □+=17,4%, E□+=656 keV; □-= 39%, E□-=573 keV) has emerged as an important theranostic agent

(positron-auger emitting radionuclide that has the potential for use in diagnostic imaging and radiotherapy) both as $^{64}CuCl_2$ and ^{64}Cu-compouds. Our aim is to show you our own experience about ^{64}Cu-DOTANOC therapy in one patient. We try to establish tumor absorbed dose and tumor/organs absorbed dose ratio to obtain better radiopharmaceutical performance.

Methods and Materials: One female patient, affected by refractory thyroid cancer, underwent to therapeutic intravenously administration of ^{64}Cu-DOTANOC, previous positive diagnostic findings proof. She subjected to serial positron emission tomography/computed tomography (PET/CT) imaging at 10 minutes, 1 h, 3 h, 18 h, 24 h, 42 h, 49 h and 66 h after administration. During this observation time, since T0 to forty hours after administration, the patient sampled several urinary selections. Then the patient took blood sample at T0, 1d, 3d, 10d, 17d, 24d, 34d and 45 days after administration of radiopharmaceutical. Quantitative PET analysis was performed to determine biodistribution of ^{64}Cu radioactivity and ^{64}Cu radiation dosimetry estimated for target and no target organs. Time-activity concentration was fitted and the area under the curve provided the number of disintegration/cc. The cell number existing in 1 cc was then extimated to obtain the n°disintegration/cell. Urinary and blood tests were finally evaluated.Results: 13% of activity lost via urinary tract in the first hour from administration, the 30% in the first 24 hours instead. Subtract the amount loss in urine, the time/remaining wholebody percentage activity curve followed the same trend of physical decay of ^{64}Cu. In order Kidneys, Gall Bladder and Liver presented the higher radioactivity concentration. The Kidneys are the critical organ for radiation dose. Organs and tumor absorbed doses were expressed as number of disintegrations/cell; right lung metastasis has 16.28 n°dis/cell, kindneys 78.85, bone marrow 10,99 instead. Biochemical evaluatione demonstrated that no hepatic alterations occurred. Reversible renal failure was demonstrated by hematological findings just in the first day after administration. In the complete blood count cells contest, white blood cells only modified, in particular neutrophils changed immediately like renal function parameters. Tumor markers changed late instead, and tissue polypeptide specific antigen and thyreoglobulin simultaneously arose at twenty-forth day after administration.

Conclusions: Dosimetric evaluation suggested that our ^{64}Cu-DOTA-NOC radioactivity biodistribution was in line with the literature. By our knowledege there aren't any studies about tumor dosimetry with ^{64}Cu. In our case report the ^{64}Cu radioactivity in tumor expressed as n°dis/cell is lower than that reported in the in vitro study by Obata et al. (2005). The patient is actually on follow up and the therapy efficacy evaluation is on going.

PRECLINICAL EVALUATION OF A 99MTC-FLUORESCEIN-LIPOSOME COMPLEX FOR SENTINEL LYMPH NODE DETECTION

Cecilia Bentancourt.

URUGUAY

Introduction: Pre-operative lymph node mapping and sentinel lymph node biopsy followed by selective lymphadenectomy determinates higher sensitivity in nodal staging among other benefits like lower surgical morbidity and mortality due to a shorter surgical time, reduced length of hospitalization, lesser complications such as lymphedema and infection, and a shorter recovery time. Objective: To develop a new hybrid radiotracer from a nanoparticle labeled with both ^{99m}Tc and fluorescein.Materials and methods: Liposomes were prepared by "hand shaken" method, obtaining a DTPA-liposomes film by combining phosphatidylcholine, cholesterol and stearylamide-DTPA in a chloroform-methanol solution (2:1) and evaporated until dry at 60°C. The resulting film was then hydrated with a solution of fluorescein, DMSO and bidistilled water, acquiring multilayered vesicles which were extruded by polycarbonate membranes to obtain mono-layer liposomes. These were later coordinated to ^{99m}Tc, and tested by thin layer chromatography and molecular exclusion chromatography. In vitro stability was evaluated challenging the ^{99m}Tc-liposome-fluorescein complex to cysteine solutions in different concentrations (0.1, 1.0 and 10mM) at 1 and 3 hours, at 37°C. For preclinical evaluation we used C57 black mice, which were injected subcutaneously with the complex in a posterior paw. Immediately thereafter, mice were anesthetized for the acquisition of a lymphoscintigraphy performing dynamic images at 1 second per frame during 15 minutes and a 300 seconds static image 20 minutes after the injection. They were later sacrificed to dissect the injected limb in search for the popliteal lymph node. Results: Labeling efficiency was higher than 90%. In molecular exclusion chromatography, marked liposomes were eluted at 3-3.5 ml, and free fluorescein at the 11th ml. Labeled liposomes featured radiochemical purity higher than 75% even at the higher cysteine concentration (10mM), after 3 hours of incubation. Scintigraphic images showed radiotracer uptake in the popliteal node of the injected extremity. When dissecting the injected posterior limb, yellow staining was evident in the popliteal node, in accordance with the scintigraphic findings.Conclusions: ^{99m}Tc-liposome-fluorescein is a promising hybrid radiotracer for the detection of sentinel lymph node, although further evaluation would be needed.

THIRTEEN YEARS OF CYCLOTRON RADIONUCLIDE PRODUCTION AT UNAM PET CENTER

A. Zarate-Morales. México, A. Flores-Moreno, M.A. Avila-Rodriguez.

MEXICO

Unidad PET, Facultad de Medicina, Universidad Nacional Autónoma de México, 04510, D.F. México

The Positron Emission Tomography (PET) Center of National Autonomous University of Mexico (UNAM) is a core facility offering state-of-the-art molecular imaging studies and a broad palette of radionuclides and radiopharmaceuticals for clinical and research applications. It was the first PET Center in Mexico and nowadays it continues at the forefront in PET technology in the country.The facility is located in the University´s Campus and belongs to the Medicine School. Major equipment and operation areas includes an accelerator laboratory for radionuclide production, a fully equipped laboratory for radiopharmaceutical production, a preclinical imaging laboratory for small animals and a PET/CT scanner.In 2001 a self-shielded CTI RDS-111 proton-only 11 MeV cyclotron with targetry for production of sequence CNOF (^{11}C, ^{13}N, ^{15}O, and ^{18}F) radionuclides was installed. The cyclotron had two beam lines (BL) with capacity to accommodate up to 8 targets in each BL (Figure 1, left), and a maximum beam current of 40μA in single-mode bombardent.Due to the increased demand of PET radiopharmaceuticals in Mexico City, in 2007 one of the BL´s was upgraded to a high power configuration. The main features of the upgrade included a new ion source that increased beam current from 40 to 60μA, a new four-position target carrousel capable to handle 60μA of beam current, high power gridded targets designed to be operated under high pressure conditions (>1000 psi), target body of refractory material (Ta) for the production of ^{18}F. With this upgrade we practically double the yield of ^{18}F with the same time of bombardment.The growing capacity to produce cyclotron radionuclides for PET applications was further enhanced with the upgrade of BL2 in 2011 to the same Eclipse HP configuration, but including the option for the irradiation to solid targets for the production of metallic radioisotopes (Figure 1, right).

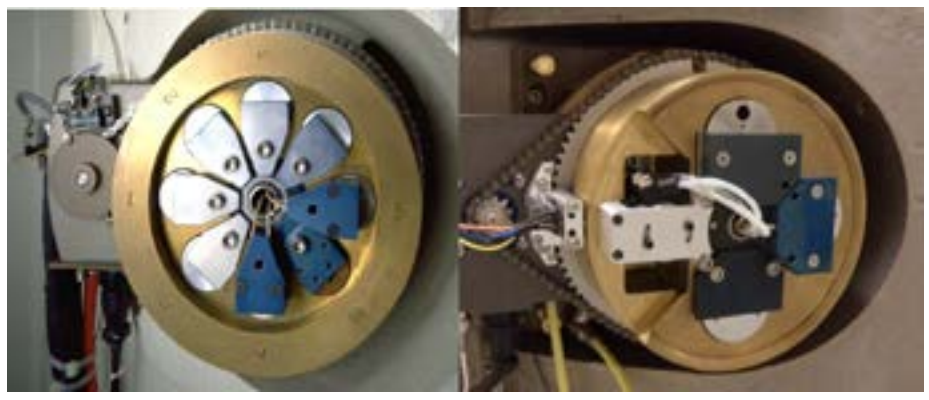

Figure 1: Configuration of the carrucels for the CTI-RDS 111 and Siemens-Eclipse HP with the option for solid targets irradiation.

Currently, our Eclipse HP cyclotron includes the high yield production of ^{11}C, ^{13}N and ^{18}F for nucleophilic and electrophilic substitution reactions (Table 1), and limited quantities of copper ($^{61,64}Cu$) and gallium ($^{66,68}Ga$) isotopes for research and preclinical applications.

Table 1: Production yields of ^{11}C, ^{13}N and ^{18}F.

Radionuclide	Production yield
11C	1900 mCi (60μA, 40 min)
13N	200 mCi (60μA, 10 min)
18F-	2300 mCi (60μA, 60 min)
18F2 (double-shoot)	452 mCi (30μA, 40 min)

Over 1,200 of cyclotron production-runs were performed during 2013 yielding over 13,000 uni-doses of PET-radiopharmaceuticals for clinical and research applications.
Acknowledgments: We acknowledge financial support of CONACYT Grant 179218.

UPTAKE EVALUATION OF A NEW LIPOSOMAL 99MTC-SESTAMIBI FORMULATION. IN VIVO AND IN VITRO ASSAYS

Fiorella Carla Tesan. Argentina, Portillo MG, Giaquinta Romero D, Martinell Lamas D, Martinez Sarrasague M, Cimato A, Medina V, Salgueiro MJ, Zubillaga MB.

ARGENTINA

^{99m}Tc-sestamibi is a routinely used radiopharmaceutical predominantly for evaluation of myocardial perfusion. Its use in oncology is also known. Nanoparticles have been postulated as drug delivery systems that could improve tumor targeting by the enhanced permeability and retention effect. Since liposomes are one of the most commonly used nanosystems for drug delivery and some formula-

tions are already commercially available, the objective of this work was to evaluate in vitro and in vivo uptake of a new ^{99m}Tc-sestamibi liposomal formulation.Materials and Methods: Sestamibi was radiolabeled according to the manufacturer instructions. Briefly, 60mCi of a pertechnetate solution eluted from a ^{99}Mo–^{99m}Tc generator were aseptically added to the 0.5mg freeze-dried sestamibi kit. Saline solution was added to the preparation reaching an activity concentration of 20mCi/mL. Finally, vial was heated for 10min at 100ºC and then left at room temperature for 15min until thermal equilibrium. Phosphatidilcoline liposomes were formed by the lipid-film hydration method with ^{99m}Tc-sestamibi solution and sonicated for 30min for particle size reduction. Total lipid concentration was 1mg/mL. Entrapment efficiency was calculated by a exclusion chromatography with Sephadex G-25. For in vitro assays a human melanoma cell line (1205-LU) was cultured in 6 well plates and incubated for 30, 60 and 90 min with either ^{99m}Tc-sestamibi or liposomal ^{99m}Tc-sestamibi. Cellular uptake percentage was calculated and normalized by cell number. In vivo assays were performed in normal Sprague Dawley rats (250-270g). Animals were administered intravenously with either ^{99m}Tc-sestamibi or liposomal ^{99m}Tc-sestamibi previously intraperitoneally anesthesized (ketamine/xilazine). Biodistribution was evaluated by gamma camera images acquired at 30, 60 and 90 min post radiopharmaceutical injection.

Results: radiochemical purity of ^{99m}Tc-sestamibi resulted 96% and the entrapment efficiency was 66%. In vitro assays showed a similar uptake kinetic profile for both formulations with increasing % uptake as a function of time. However at 60 min a slight difference was observed for the %uptake/10^6cells (2,59 ± 0,07 and 2,95±0,04 for ^{99m}Tc-sestamibi and liposomal ^{99m}Tc-sestamibi respectively).

In vivo imaging analysis showed a similar biodistribution at all time points evaluated for both formulations. Both radiopharmaceuticals accumulated predominantly in the heart, liver, gastrointestinal tract and kidneys while bladder accumulation means there is renal elimination. However a minor increased liver uptake was observed for liposomal ^{99m}Tc-sestamibi as expected for particulate radiopharmaceuticals biodistribution.

Conclusions: liposomal entrapment of ^{99m}Tc-sestamibi could be an interesting strategy to enhance tumor targeting due to improvement in radiopharmaceutical delivery. Further research is needed to evaluate its biodistribution in tumor bearing animals.

ADVERSE REACTIONS IN BRAZILIAN NUCLEAR MEDICINE SERVICES

Catanoso, Marcela F.; Barboza, Marycel F.; Nogueira, Solange A.; Wagner, Jairo and Funari, Marcelo B. G.

BRAZIL

Hospital Israelita Albert Einstein. Departamento de Medicina Nuclear.
São Paulo – Brazil

Adverse reaction is an unexpected clinical manifestation after any pharmaceutical administration. The incidence of radiopharmaceuticals reactions is very low, particularly in comparison with reactions to radiographic contrast media or other drugs. Most of the reactions were attributed to the emotional state of the patient but a pharmacologic effect of the drug cannot be excluded. The Brazilian Health Authorities (ANVISA), in the RDC- published in June recommended to investigate any adverse event in the nuclear medicine routine, like as a serious neurological or cardiovascular disorders or misadministration, and implement prevented and corrected actions. The aim of this study is to verify, since January-2012 to May- , the incidence of radiopharmaceutical adverse reaction or mistakes in patient doses administration at the nuclear medicine department. The reported data were separated in two groups: symptoms and the impossibility to perform the SPECT or PET scan procedure after the dose administration. During the mentioned period were performed 21,129 exams and reported 47 incidences (0.25%). The related cases referred to symptom during the exam and 22 cases related to non-complete procedure after tracer injection. In this study we concluded that the incidence was low but is necessary to verify if adverse reaction is related to the radiopharmaceutical or result of another symptomatic patient reaction or technical problems. In cases of recall or misadministration, it is recommended to take corrective measures to prevent those events.

EVALUATION OF RADIOCHEMICAL PURITY OF 99MTC-SESTAMIBI (99MTC-MIBI)

Catanoso, Marcela F.; Lima, Sildomar C.; Barboza, Marycel F.; Nogueira, Solange A.; Wagner, Jairo and Funari, Marcelo B. G.

BRAZIL

Hospital Israelita Albert Einstein. Departamento de Medicina Nuclear.
São Paulo – Brazil

Technetium-99m-sestamibi (99mTc-MIBI) is an agent widely used in nuclear medicine imaging. The drug is a coordination complex of the radioisotope Tc- 99m with the ligand MIBI (methoxy-isobutyl-isonitrile). 99mTc-sestamibi is a lipophilic cation which, when injected intravenously into a patient, distributes proportionally to the myocardial blood flow. As other 99mTc-labelled compounds, 99mTcO4, and reduced-hydrolyzed-99mTc (99mTcO2) or any other 99mTc complexes species may be present in the preparation. Alternative methods for 99mTc-MIBI have been proposed and they are not practical for the clinical setting. The aim of this work was to evaluate and validate the radiochemical purity of 99mTc-MIBI by chromatographic methods, as well the Rf value in different solvents, to introduce in routine at the hospital radiopharmacy, in accordance to the health authorities (RDC-38), before the dose administration in patients. 99mTc-MIBI was prepared from a commercial kit following manufacturer's instructions, by adding about 11,100MBq / 3-5mL freshly eluted from a 99Mo/99mTc generator (IPEN-Tec), heated hermetically at 100oC for 10 minutes and cooled to room temperature. The 99mTc must be recently eluted (<2hours) and the content of 99Mo and the aluminum determined before labeling process, as well the pH and the radiochemical yield. After cooling, the product was submitted to radiochemical purity tests. Three different chromatographic systems assays were performed: solvent extraction (chloroform:0.9%NaCl), paper chromatography and solid phase extraction (Sep-Pak C18), at 30; 120 and 240 minutes, after the addition of 99mTc. The radiochemical purity of 99mTcO4 eluted in 677 generators in 2012 and in 574 generator in 2013, were (99.32±0.36)% and (99.12±0.35)%, respectively.

The radiochemical yield of 99mTc-MIBI by chromatography paper were (98.7±0.98)%, solid phase extraction (98.85±0.72)% and solvent extraction (98.75±0.45)%, at 30 minutes after labeling, respectively. The radiochemical purity were higher than 90% at 2 and 4 hours after labeling, in the same chromatographic systems with pH = 6.0 in all samples. The solid phase extraction method was adopted before dose administration in the routine at the nuclear medicine service of HIAE and during 2012 and 2013; more than 1,000 "kits" were analyzed, with high level of radiochemical purity, confirmed by the clinical application. It was demonstrated the efficiency of these method in the control test of 99mTc-MIBI, defining as an ideal and single assay, using one chemical solvent in the routine process, compared to the paper chromatography system. Related to solvent extraction, acute exposures to chloroform have been reported, considering this method no appropriate in routine. The results obtained in this study: Rf range, pH, labeling efficiency and quickness for its execution, are consistent to adapted in the hospital radiopharmacy, in accordance to the rules of ANVISA (RDC-38), before the dose administration in patients.

NOVEL RADIOTRACERS IMAGING TUBERCULOSIS – A PRECLINICAL APPROACH USING ANTIMICROBIAL PEPTIDES

Thomas Ebenhan1,2, Jan Rijn Zeevaart3 Jacobus Venter4, Thavendran Govender5, Hendrik G. Kruger3 and Mike M.Sathekge1

1 Department of Nuclear Medicine, University of Pretoria and Steve Biko Academic Hospital, Pretoria, South Africa
2 School of Pharmacy, University of KwaZulu Natal, Durban, South Africa
3 Departments of Science and Technology, Preclinical Drug Development Platform, North West University, Potchefstroom, South Africa
4 Medical Research Council of South Africa, Pretoria, South Africa
5 Catalysis and Peptide Research Unit, University of KwaZulu Natal, Durban, South Africa

SOUTH AFRICA

Objectives: Tuberculosis (TB) is known for its high prevalence in South Africa, especially in HIV/TB co-infected population. Antimicrobial peptide's (AMP) cationic domains bind to negatively charged molecules of the bacterial cell wall such as lipoarabinomannan in Mycobacterium tuberculosis (M.tb) and causes membrane alterations. Therefore, we aim to synthesize and radiolabel tuberculostatic compounds to be used as diagnostic TB-imaging agents. Peptides can be conjugated to macrocycle molecules which will allow complexation of metal radioisotopes such as Gallium-68 (68Ga), ideally maintaining the peptide's property as targeting vector. Clinical PET studies with 18F-FDG and 68Ga-citrate allowed sensitive detection of pulmonary lesions in TB-compromised patients; however both tracers couldn't distinguish the infection from inflammation [1]. In preclinical studies an infection-selective imaging agent (68Ga-NOTA-UBI) was achieved [2]. AMP-derivatives were not exploited for non-invasive M.tb detection, thus 68Ga-NOTA-UBI-PET is envisaged to (1) monitor muscular M.tb-infection in guinea pigs and rabbits as "proof of target" procedure and (2) detect advanced-state intra- and extra-pulmonary TB-lesions following acute airway infection with M.tb. in guinea pigs. Methods: (1) Animals received 1x108 M.tb bacilli intramuscular and 1x108 Staphylococcus aureus (SA) cocci subcutaneous 60 hours before PET/CT. (2) Guinea pigs were nebulized with 1x106 M.tb bacilli, TB-infection was verified by tuberculin skin test for imaging studies following at week 5 (18F-FDG) and 4, 6 (68Ga-NOTA-UBI). 68Ga was obtained from 68Ge/68Ga-generator to radiolabel NOTA-UBI and citrate as described [2, 3]; 18F-FDG was utilised as reference. All animals underwent PET/CT (immediate (im) or 20 min and 60 min p.i.). Maximum standardised uptake values were normalising against healthy muscle tissue (Tb/M) or background (Tb/B). Results: (1) Guinea pigs showed avid 68Ga-NOTA-UBI accumulation, targeting M.tb (Fig.1C) (SUVmax 4.88; Tb/M 3.90(60min)) and SA (SUVmax 3.29; Tb/M 2.79(60min)). (2) Guinea pigs revealed multiple whole-body TB-lesions with 18F-FDG-PET following airway M.tb-infection (Tb/B 1.55 – 4.53), however, no notable accumulation was found with 68Ga-NOTA-UBI in the pulmonary or extrapulmonary nodules (Fig.1A,B). Both, 68Ga-citrate (Tb/M 1.45(20min), 2.24(60min)) and 68Ga-NOTA-UBI (Tb/M 2.58(im), 3.64(60min)) were accumulating less intensively in M.tb-infected thigh

muscles of rabbits compared to guinea pigs. SA-infection was visualised by 68Ga-NOTA-UBI (Tb/M 2.15(im), 2.72(60min)), only faint uptake occurred utilizing 68Ga-citrate. All relevant infections were verified post-mortem with immunohistological and biochemical methods.

Conclusion: 68Ga-NOTA-UBI-PET detects acute thigh infection of M.tb in rabbits but cannot visualise advanced TB-lesions in a guinea pig infection model. This may indicates that NOTA-UBI isn't targeting phagocyted M.tb bacilli in vivo. The later findings are subject to ongoing research and may warrant drug efficacy studies for new TB-drugs. References:

[1] M. Sathekge, Semin Nucl Med 2013, 43, 349.
[2] T. Ebenhan, J Nucl Med 2014, 55, 308.
[3] M. Vorster, Hell J Nucl Med 2013, 16, 193.

Supplementary data: if figures are allowed to be part of the abstracts.

QUALIFICATION OF IN-HOUSE PREPARED 68GA-NOTA-RGD KIT IN MICE AND MONKEYS FOR SUBSEQUENT MOLECULAR IMAGING OF V3 INTEGRIN EXPRESSION IN CANCER PATIENTS

Thomas Ebenhan1,2, Isabel Schoeman3, Niel Roussow4, Anne Grobler3, Biljana Marjanovic-Painter5, Judith Wagener5, Hendrik G. Kruger2, Mike M. Sathekge1 and Jan Rijn Zeevaart3

1 Department of Nuclear Medicine, University of Pretoria and Steve Biko Academic Hospital, Pretoria, South Africa
2 School of Pharmacy, University of KwaZulu Natal, Durban, South Africa
3 Department of Science and Technology, Preclinical Drug Development Platform, North West University, Potchefstroom, South Africa
4 iThemba LABS, Faure, Cape Town, South Africa
5 Radiochemistry, The South African Nuclear Energy Corporation, Pelindaba, Pretoria, South Africa

SOUTH AFRICA

Objectives: Non-invasive imaging is a powerful tool for early diagnosis and monitoring of various disease processes. Nowadays, receptor-specific radiopharmaceuticals play an innovative role in Theranostics. Particularly South Africa awaited a non-invasive highly specific lung cancer probe,such as 68Ga-NOTA-RGD, that accumulates in 3 integrin-expressing cells which can be visualized using PET/CT and differentiates pathology of a Single Pulmonary Nodule (SPN). This approach will give an advantage to discern malignant lesions from other pulmonary infection or inflammation occurring in patients with HIV/AIDS and co-infection with tuberculosis. NOTA-Bz-SCNc(RGDyK) kits were donated by Seoul National University but despite the fact these kits showed great results using a TiO2-based 68Ge/68Ga generator (t1/2 of 68Ge and 68Ga are 270.8 days and 67.6 min, respectively) they could not accommodate the higher acidic condition of the SnO2-based 68Ge/68Ga-generator manufactured under cGMP conditions at iThemba LABS, Cape Town.Therefore, the qualification of an adapted in-house NOTA-RGD kit production, that would enable efficient high-yield production of clinical 68Ga-NOTA-RGD, was envisaged.Methods:The original kits were freeze-dried. Kit mass integrity was determined by comparing labeling efficiencies of 10, 30 and 60 µg of RGD per kit and manual labeling. 68Ga-eluates were buffered with 2.5M sodium acetate and exploited C18 cartridge purification of the crude 68Ga-NOTA-RGD mixture. Kit shelf-life was assessed up to 200 days. Quality control measures included standard ITLC/HPLC analysis. The radiolabeled in-house kits were qualified by ex vivo biodistribution in balb/C mice A549-tumour bearing xenografts and by in vivo biodistribution in healthy vervet monkeys with 68Ga-NOTA-RGD-PET/CT (Siemens Biograph).Results:Kits showed significantly higher radiolabeling efficiency (LE) ($P \leq 0.081$) over manual radiolabeling. HPLC analysis showed 96-99% radiochemical purity, a linear decrease (r2= 0.892, N=19) was Sudafrica observed for the kit integrity indicating > 75% LE and > 50% LE radiolabeling occurred within 75 d and 150 d, respectively. Vervet monkeys showed fast clearance of blood-bound activity(pharmacological half-life ca. 5.8 min, elimination rate of 9.1 %ID/h) and predominately renal excretion (SUVKidneys 1.94 - 3.54; urinal activity recovery of 54 ± 4 %ID at 120 min). Heart, liver and spleen showed notable early-on uptake (SUV 1.01-1.24) (Fig.1). Increased 68Ga-NOTA-RGD accumulation was evident in A-549 tumour xenografts with maximum tumour/muscle-andtumor/lung-ratios of 6.1 and of 5.1, respectively.Conclusion:Cold kit formulation radiolabeling and purification methods were established successfully and SOP's for subsequent clinical use created. 68Ga-NOTA-RGD kits met criteria to be qualified for further clinical research in lung cancer patients compromised by HIV and/or TB-infections. Results from vervet monkeys warrant dosimetry calculations translational to humans.Keywords: integrin 3-integrin expression, 68Ge/68Ga generator, 68Ga-NOTA-RGD, vervet monkeys, PET/CT.Supplementary data: if figure are accepted to be part of the abstract.

LONGITUDINAL PERFORMANCE EVALUATION OF SNO2-BASED 68GE/68GA GENERATORS FOR ECONOMICAL RADIO-LALONGITUDINAL PERFORMANCE EVALUATION OF SNO2-BASED 68GE/68GA GENERATORS FOR ECONOMICAL RADIOLA-BELING OF DOTA/NOTA-PEPTIDE DERIVATIVES

Thomas Ebenhan1,2; Deon Kotze3; Botshelo Mokaleng1; Isabel Schoeman4; Mariza Vorster1; Mike Sathekge1 and Jan Rijn Zeevaart4

1 Department of Nuclear Medicine, University of Pretoria and Steve Biko Academic Hospital, Pretoria, South Africa
2 School of Pharmacy, University of KwaZulu Natal, Durban, South Africa
3 Radiochemistry and Radioanalysis, The South African Nuclear Energy Corporation, Pelindaba, Pretoria, South Africa
4 Department of Science and Technology, Preclinical Drug Development Platform, North West University, Potchefstroom, South Africa

.

SOUTH AFRICA

Objectives: The food and drug association has recently assigned orphan-drug status to GMP kit-produced 68Ga-1,4,7,10-tetraazacyclo-dodecane-N',N'',N''',N''''-tetra-acetic-acidoctreotate (68Ga-DOTA-TATE) as diagnostic agent for neuroendocrine tumors which exemplifies the trust in the manufacture of generator-based radiopharmaceuticals. There is a mounting interest in using radioisotopes such as 68Gallium (68Ga) for peptides labeling, i.e. 68Ga could be a vital alternative to 18F, offering shorter imaging times, no special patient preparation, an on-demand and year-round tracer availability. This would lead to a more cost-efficient, decentralized way of diagnostic imaging, especially in areas without access to a nearby cyclotron. However, very few studies considered the longitudinal verification of the 68Ga, being eluted from the SnO2-based 68Ge/68Ga-generator, therefore we have evaluated the quality of 68Ga-radiolabeling towards different peptides with prolonged generator operation. Methods: 68Ga-eluate quality was compared longitudinally from four individual 68Ge 68Gagenerators (G1-G4) (Type: SnO2-matrix; 1.85GBq-loaded; iThemba LABS). Eluate fractionation (EF) was combined with 68Ga-eluate purification procedures: a) BondElut-SCX-based or b) Dowex-resin-SAX-based. Buffered citrate (68Ga-ACD-A) was utilized as reference compound, produced using an aseptic one-vial approach. The following compounds were utilized: 1) DOTA-TATE; 2) 1,4,7-triazacyclononane-1,4,7-triacetic-acid (NOTA)-c(RGDyK), conducting manual- and kit-based production and 3) Ubiquicidin (UBI) fragment NOTA-UBI(29-41). Radiolabeling followed pH-adjustment, high-temperature incubation and final purification from unbound 68Ga with C18-based cartridges. The labeling efficiency (LE) was determined by thin-layer- or high-pressure-liquid-chromatography. The Sudafrica 68Ga-eluate- and peptide samples were assessed using gamma spectrometry and inductively coupled plasma and optical emission spectrometry for metal impurities and 68Ge-detection.
Results: A 68Ga-yield of ≥ 90% (r2=0.70-0.98) was achieved over 190, 261, 137 and 172 days, for G1, G2, G3 and G4, respectively. Generator re-elution 3-5 hours after the first elution/day (r2= 0.89) yielded in 89% (2ndelution/day) and 72% (3rdelution/day) 68Ga-activity. The 68Ge-levels (0.05–1.5%) in 68Ga-eluate samples ≥ 400 days were minimized significantly by FE (P=0.013). The 68Ga-eluate purification led to (a) 40-44% and (b) to 69-74% 68Ge-reduction (N=4). The LE of NOTA-c(RGDyK) kits (r2=0.76) and NOTA-UBI29-41 (r2=0.88) decreased in-significantly with prolonged generator usage. DOTA-TATE radiolabeling was competitively labeling until 200 days (r2=0.75) followed by larger LEvariability at 200-325 days (r2 =0.12) generator operation. The 68Ge-content was not detectable for all radiopharmaceuticals up to 298-325 days; except 68Ga-citrate showed increasing 68Ge-levels (r2= 0.73) to 0.0375 % at 275 days. The total longitudinal Al(III)-, Cu(II)-, Fe(III)-, Sn(II)- and Zn(II)-contents amounted to ≤19.5 ppm per NOTA/DOTApeptide sample with prolonged generator operation.

Conclusion: Although 68Ga is eluted from a SnO2-based generator with more acidic condition, its longitudinal quality warrants high-yield, high-economical peptide radiolabeling procedures. The robust generator performance facilitates its prolonged operation in a hospital environment and stipulates a cost-efficient approach in radiopharmaceutical production.Keywords: 68Ge/68Ga-generator; NOTA; DOTA; 68Ge-breakthrough; 68Gallium, DOTATATE.

CHEMICAL SYNTHESIS AND EVALUATION OF A 68GA/177LU-LABELED UNIVERSAL BOMBESIN PEPTIDE LIGAND FOR TARGETING OF BOMBESIN RECEPTOR-POSITIVE TUMORS

S.M. Okarvi, I. AlJammaz.

SAUDI ARABIA

Cyclotron & Radiopharmaceuticals Dept; King Faisal Specialist Hospital and Research Centre. Riyadh 11211, Saudi Arabia.

Objectives: Bombesin (BN) peptide receptors are of great clinical interest in nuclear oncology because of the overexpression of their receptors on various important human cancers such as breast and prostate cancer. The high expression of receptors in cancer cells together with low receptor density in normal human tissues making these receptors potential molecular targets with radiolabeled BN

peptide analogs. This study was undertaken to design and develop a BN peptide based on the universal BN sequence (capable of targeting all four BN receptor subtypes) thus having wide receptor affinity, and labeled it with both diagnostic (68Ga) and therapeutic radionuclide (177Lu) to formulate a potential theranostic agent for targeting BN receptor-positive tumors. Methods: DOTA-Glu-Gln-Trp-Ala-Val-•Ala-His-Phe-Nle-NH2 was prepared by solid-phase peptide synthesis following Fmoc/HBTU methodology. Radiolabeling with Ga-68 and Lu-177 was performed by using 2.5 M NaOAc and 0.1 M NH4OAc buffer, respectively. In vitro cell-binding was conducted on BN receptor-positive T47-D breast cancer cell line. In vivo biodistribution and biokinetics was performed on Balb/c mice.

Results and discussion: The structure and purity of the DOTA-coupled BN peptide was confirmed by mass spectrometry and HPLC analysis. HPLC analysis revealed that the BN analog radiolabeled efficiently with both radionuclides with high labeling efficiency (~98%). In vitro cell-binding assay indicated the high affinity and specificity of the radiolabeled peptide towards T47-D human breast cancer cells (Kd = 5 nM) and also significant internalization (~19%) into the breast cancer cells. In mice, 68Ga/177Lu-labeled BN peptide displayed a fast clearance from the blood and excretion mostly by the renal route, with some elimination through the hepatobiliary system. The uptake in the major organs (i.e., lungs, stomach, liver, intestines kidneys, etc.) was low (<3% ID/g). Conclusions: This initial study towards the development of a potent and broad affinity BN-like peptide suggest that the peptide under investigation possesses certain favorable properties that need further evaluation in order to determine the real usefulness of this receptor binding peptide for targeting tumors expressing BN receptor types.This initial study of the development of a breast cancer imaging peptide radiopharmaceutical indicated that the hybrid peptide possesses certain favorable properties and deserves further evaluation to determine the real potential of this new and interesting class of peptides for tumor imaging.

Bombesin (BN) peptide based on the universal sequence is conjugated with a well-known and extensively characterized antineoplastic agent, MTX, which is chemically suitable for conjugation to peptides.

PREPARATION AND IN VITRO AND IN VIVO EVALUATION OF A NOVEL PEPTIDE BASED ON TUMOR-RELATED HUMAN EPITHELIAL MUCIN (MUC1) AS A POTENTIAL BREAST CANCER IMAGING AGENT

S.M. Okarvi, I. AlJammaz.

SAUDI ARABIA

Cyclotron & Radiopharmaceuticals Dept; King Faisal Specialist Hospital and Research Centre. Riyadh 11211, Saudi Arabia.

Objectives: MUC1 epithelial mucins are produced by both normal and malignant cells. MUC1 is overexpressed by most epithelial cancers and attracting increasing clinical interest as a potential target for imaging and targeted therapy of certain cancers. MUC1 is a classical example of tumor antigen because of its overexpression on almost all human epithelial cancers including >90% of breast and ovarian cancer. Increased expression of the epithelial mucin MUC1 is linked to tumor aggressiveness in human breast cancer. The low expression of this tumor antigen on normal tissues makes MUC1 an attractive target for breast cancer diagnosis and treatment. The goal of the present study was to develop a small synthetic MUC1-derived peptide combined with 4-amino acid, EPPT peptide, derived from tumor-associated ASM2 antibody, for targeting of breast cancer. Methods: Ac-Gly-Gly-Cys-Asp-Glu-Pro-Pro-Thr-Pro-Asp-Thr-Arg-Pro-NH2 was prepared by Fmoc-based solid-phase synthesis and labeled with 99mTc by stannous-tartrate ligand exchange approach. In vitro cell-binding was performed on MDA-MB-231 and T47D breast cancer cell lines and in vivo biodistribution was conducted in healthy mice and in vivo tumor targeting in nude mice with MDA-MB-231 xenografts.

Results: The structural identity and purity of the synthetic peptide was confirmed by mass spectrometry and HPLC. The peptide radiolabeled efficiently with 99mTc (>80%) as determined by HPLC. 99mTc-MUC1 showed high affinity binding to MDA-MB-231 and T47D cell lines with Kd values below 10 nM. In normal mice, the radiopeptide displayed efficient clearance from the blood and excreted mainly through the urinary pathway with some elimination by the hepatobiliary system. The concentration of radiopeptide in the lungs, liver, stomach and kidneys was low (<5% ID/g) both at 1 and 4 h p.i. In nude mice with MDA-MB-231 xenografts, 99mTc-MUC1-derived peptide exhibited a good tumor uptake (4.41±1.51% ID/g, 1 h). The uptake in the tumor was always higher than in the blood and muscle resulting in favorable tumor/blood and tumor/muscle ratios.

Conclusions: Our results suggest that the fusion of two tumor targeting peptides appears to hold a great promise in nuclear oncology and this new and emerging approach can be beneficial for rapid and efficient targeting of human cancers.

NEW TARGET-SPECIFIC RADIOPHARMACEUTICALS FOR PANCREATIC CARCINOMA DETECTION

Laura Meléndez-Alafort1, Gaia Zuccolotto2, Giulio Fracasso3, Cristina Bolzati4, Nicola Salvarese1, Clara Santos-Cuevas5, Marco Colombatti3, Antonio Rosato1, 6.

1 DiSCOG-University of Padua, Italy.
2 DIMED-University of Padua, Italy.
3 Department of Pathology and Diagnostics, University of Verona, Italy.
4 CNR-IENI of Padua, Italy.
5 ININ, México.
6 Veneto institute of Oncology, Italy.

ITALY

IntroductionPancreas carcinoma is responsible for more than 30% of tumor-related because is notoriously difficult to diagnose in its early stages. Thus, new diagnostic approaches are imperatively needed. Monoclonal antibodies (mAb) have been effectively applied clinically in tumor diagnosis. Recently, Prostate Stem Cell Antigen (PSCA) and Mesothelin have emerged for their high expression and wide distribution in pancreatic cancer, but not in normal pancreas.

ObjectiveThis research aims to image pancreatic cancer through the development of new target-specific radiopharmaceuticals based on mAb directed to PSCA and Mesothelin antigens, which are heavily overexpressed in this tumor histotype. MethodsAnti-PSCA and anti-Mesothelin mAbs were fluorophore-labeled (FL) to assess their binding properties on Ag+/- tumor cells. The in vivo capability of either mAbs to identify the corresponding antigen on tumor cell surface was evaluated injecting mice with tumor cells harboring or not the antigen. Mice received FL-mAbs and were optically imaged at different time points. 99mTc-labeled immunoconjugates were obtained by reduction of MAbs with 2-ME and incubation with 99mTcO4- in presence of a weak competition ligand using different formulations. Stability tests of radioimmunoconjugates (RIC) were performed after dilution in human serum, phosphate buffer, cysteine and saline solutions.ResultsThe FL anti-PSCA mAb intensively stained T3M4 pancreatic tumor cells stably transfected with the PSCA antigen; similarly, FL anti-Mesothelin mAb was able to identify 293 cell transfectants at high expression of Mesothelin. Moreover, mice imaging showed that both mAbs tended to accumulate at either tumor sites during the first 24h post-injection; thereafter, the non-specific signal detectable in Ag-negative tumors progressively reduced, while the intensity of signals on Ag-positive masses constantly increased up to days 5-7. The highest labeling efficiency (LE) was obtained when 200 µg of reduced mAb were incubated with 200 µl of 99mTc-pertechnetate solution, 2.5 nmol of HEDP and 4.4 nmol of SnCl2. RIC were obtained with a LE of 98%, and proved to be very stable after dilution on all the solution tested. ConclusionWe have demonstrated that both Anti-PSCA and anti-Mesothelin mAbs were able to detect efficiently pancreas carcinoma cells in vitro and in vivo. Both mAbs were radiolabeled using 99mTc with a reproducible technique. The RIC obtained showed high radiochemical efficiency and stability. Therefore we conclude that both mAbs are suitable for the development of new target-specific radiopharmaceuticals for pancreas carcinoma.

Acknowledgement
This research was supported by the Italian Association for Cancer Research (AIRC, IG 13121 to A.R.)

MUSCULOSKELETAL

BONE SCINTILOGRAPHY WITH SPECT-CT: BETTER CLINIC RESOLUTION

Allan Vieira Barlete Hospital Pró-Cardíaco

Rio de Janeiro, Brasil Jader Cunha de Azevedo, Mariana Ferreira Veras, Maria Fernanda Rezende, Bernardo Sanches Lopes Vianna, Tatiane Vieira Santos, William Kleyton de Mello Aguiar, Nilton Lavatori Correa, Gustavo Borges Barbirato, Alan Cotrado, Christiane C. Wiefels, André Volschan, Cláudio Tinoco Mesquita.

BRAZIL

INTRODUCTION: A bone scan is a test of high sensitivity, but has relatively low specificity, often requiring additional studies with other imaging methods. SPECT added to the X-ray computed tomography (Single Photon Emission Computed Tomography and Computed Tomography, SPECT-CT) combines the functional information with one from a low-dose CT anatomical images. Some studies suggest that the addition of techniques increases the clinical impact of the exam and speeds up the therapeutic decision making. OBJECTIVE: The aim of this study is to evaluate the role of bone scintigraphy with SPECT-CT in clinical practice, especially because of it´s hability to be conclusive without requiring additional investigations.

MATERIALS AND METHODS: Seventy consecutive patients from January to December 2013 that performed bone scintigraphy with SPECT-CT in our institution were chosen. Scintigraphy of the whole body, lateral skull and SPECT CT (low-dose CT) of the chest and abdomen were performed 3 hours after intravenous administration of 925 Mbq 99mTc-MDP in equipment Symbia T2 Siemens. The cases were grouped according to clinical indications, scintigraphic findings, incremental value of CT image and the need for investigations by methods additional image.

RESULTS: Of the 70 patients, the majority were male (41), mean age 55 +/- 25 years. The most frequent clinical indications were: evaluation in cancer patients (43 cases); reviews of orthopedic complaints (13 cases); suspected infection (10 cases); suspected metabolic disease (4 patients). The SPECT-CT was useful in the evaluation of 59 of the 70 patients (84%). Of the 70 examinations, it has been necessary to request additional imaging exams to complement the diagnosis in 19 cases (27%): 12 cases were cancer, 5 cases were infectious disease,1 case was metabolic suspicious and 1 case was orthopedic disease. In 14 cases (74%) further investigation with anatomical methods was necessary: 3 cases (16%) with MRI and 2 cases (10%) with scintigraphy with labeled leukocyte/marrow. Among oncological patients, in 19 cases were identified low probability/absence of bone metastases. The higher incidence of bone metastatic sites were in thoracic spine, ribs, pelvis, lumbar and sacral spine and femur.

CONCLUSION: Bone scintigraphy with SPECT-CT is extremely useful in clinical practice, especially because of it's greater resoluteness therefore significantly reduces the need for additional investigations.

EARLY DETECTION OF OSTEOARTHRITIS USING 99MTC RADIOLABELED CHONDROTIN SULFATE

ESobal, G, Pagitz, M, Velusamy, K, Kosik,S,* Menzel EJ§, Sinzinger, H, Hacker M. Division of Nuclear Medicine, Department of Biomedical Imaging and Image-guided Therapy, §Institute of Immunology, Medical University of Vienna, *Veterinary Medical University of Vienna, Austria.*

AUSTRIA

Aim: As there is no specific radiotracer for imaging osteoarthritis (OA) available we present 99mTc labeled chondroitin sulfate (99mTcCS) as a potential tracer for this issue. Methods: Radiolabeling of CS (Chondrosulf, IBSA, Italy) was done using TcO4- (120-150 MBq) / tin method. We performed comparative ex-vivo uptake studies in postsurgical cartilage tissues from humans suffering from OA, undergoing knee arthroplasty (n=4) and OA dogs (n=6). From athroplasty patients we selected tissues with lower degeneration grade II and higher degeneration grade III, defined via a radiological and/or histological score and performed 99mTcCS uptake studies in tissue pieces (3-5 mg wet weight). In parallel isolated chondrocytes (0.5x106 cells /tube) and autoradiography in frozen tissue sections (10 µ) from each patient were used for this aim. We compared these uptake results in grade II and III tissues. In OA dogs we compared uptake in grade I and grade II of contralateral joints or with joints of control dogs. The examination was performed in carpal, elbow and tarsal joints by monitoring the uptake at 2, 4, 6 and 24 hours using a planar gamma camera (Diacam, MiE GmbH). For whole body scintigraphy animals were under general anaesthesia, for planar under sedation only. Results: In tissue pieces from patients we observed a much higher maximal uptake at saturation (24 h) in grade III as compared to grade II (up to 50,1 % vs. up to 34.0%). In isolated chondrocytes from these patients the corresponding uptake amounted to maximal 18.5% vs. 10.5 %. Autoradiographic maximal uptake amounted to 55.3 % vs. 30.1%. In dogs median target (joint) to background (mid antebrachium) ratio in OA joints after 4, 6, and 24 hours was 2.2, 2.7, and 2.9, respectively and 1.4, 1.4, and 1.6, respectively in controls. We observed the same uptake pattern as in humans correlating with the grade of degeneration. In contralateral tarsal joints we found a significantly ($p \leq 0.05$) higher uptake in grade II versus grade I joints (15-20%), while no uptake was observed in control joints. In contralateral elbow joints the respective uptake values differed by 20-25%, while control joints showed 0-5% uptake. Conclusion: 99mTcCS seems to be a valuable specific radiotracer to image OA. It allows to differentiate between OA grades (I-III) and could be used to diagnose early OA. This could be particularly important for treatment of OA before an irreversible joint damage takes pla ce.

SOFT TISSUE LESIONS WITH FDGPET/CT – A PROSPECTIVE TRIAL

Aline Lopes Garcia Leal University of Campinas - Division Nuclear Medicine Coautores: Maurício Etchebehere, Allan Santos, Gustavo Kalaf, Elisa Pacheco,Eliane Amstalden, Sérgio Gapski, Celso Ramos, Carlos Hanasilo, Edwaldo Camargo, Elba Etchebehere.

BRAZIL

MRI cannot differentiate benign from malignant solid soft tissue limb lesions (SSTLL), leading to unplanned resections of malignancies, thus increasing risk of local recurrence. PURPOSE: Evaluate if FDGPET/CT can differentiate benign from malignant SSTLL. MATERIALS AND METHODS: Seventy patients with SSTLL underwent MRI and FDGPET/CT, followed by biopsy and surgery. RESULTS: Histopathology revealed 29 (41.4%) malignant SSTL. SUVmax was significantly different in these groups ($p < 0.001$). SUVmax cutoff of 3.0 differentiated malignant from benign SSTLL with 93.1% sensitivity, 80.0% specificity, 77.1% PPV, 94.1% NPV and 85.5% accuracy. CONCLUSION: FDGPET/CT accurately differentiates benign from malignant SSTLL, and its use in the diagnostic algorithm of SSTLL may avoid unplanned resections and unnecessary biopsies.

UTILITY OF SPECT/CT IN THE DIAGNOSIS APPROACH OF THE LUMBAR PAIN IN PATIENTS WITH FAILED BACK SURGERY SYNDROME

Luz Kelly Anzola Fuentes1, MD. Ana María Quintero2, MD. José Mario Mosquera3, MD.

COLOMBIA

General Objective: To evaluate how much contributes SPECT/CT in the diagnosis approach of Failed Back Surgery Syndrome (FBSS) in the lumbar spine.Materials and Methods: A historical study was conducted on a sample of 45 patients with low back pain after spinal fusion surgery, who underwent between May 2010 and June 2014 to CT and SPECT/CT of the lumbar spine. In our analysis the findings were classified as: instrumented segment: a) screws: loosening, broken, badly positioned, micromotion. b) adjacent segment: vertebral body, facet joints, spinous process, sacroiliac joint c) other segments. Results: The findings were described in terms of prevalence, comparing CT vs SPECT/CT. In the instrumented segment: loose screws CT (32%) - SPECT/CT (32%), broken screws CT (1.7%) - SPECT/CT (1.7%), malpositioned screw CT (8.6%) - SPECT/CT (0%), micromotion CT (0%) - SPECT/CT (22.4%), facet joints CT (62.5%) - SPECT/CT (37.5%). In the adjacent segment: facet joints CT (58.7%) - SPECT/CT (25.4%), sacroiliitis CT (2,2%) - SPECT/CT (6.6%). Other segments in whole body bone scan image (44%). Conclusions: SPECT/CT is a diagnostic tool that should be considered in the study of low back pain in patients with Failed Back Surgery Syndrome. Only SPECT/CT could identify micromovement screws, which represented 22.4% of the sample abnormal screws; could identify facets anatomically abnormal but with an inflammatory process added, decreasing its prevalence in the instrumented segment from 62.5% in the CT to 37.5% in the SPECT/CT and in the adjacent segment from 58.7% in the CT to 25.4% in the SPECT/CT; Additionally could identify other inflammatory sites in anatomical structures as the sacroiliac joints and thanks to the ability to view the entire body, could also evaluate other anatomical structures affected. This leads us to propose that the SPECT/CT increases diagnostic accuracy that can potentially increase the success rate of treatment, avoiding unnecessary surgical procedures and reviews, and provide valuable information about segments distant to the adjacent segment and about musculoskeletal structures that may be causing the back pain.
Keywords: SPECT/CT, Failed Back Surgery Syndrome, Postoperative Lumbar Pain, Spinal Fusion, Osteoarthritis Facet, Pseudoarthrosis Graft.

EXTRAOSSEOUS CONCENTRATION AND UPTAKE ON THE SCINTIGRAPHY WITH DIPHOSPHONATES. RECENT EXPERIENCE IN OUR INSTITUTE

Miguel Papadakis.

MEXICO

OBJECTIVE. One purpose of this study was to define the frequency of extraosseous concentration and uptake sites in patients who underwent a bone scan with technetium - diphosphonates (99m Tc – MDP and 99m Tc – HDP). Having a SPECT/CT hybrid team at the National Institute of Respiratory Diseases (INER - Mexico), another purpose was to evaluate the usefulness of such hybrid images obtained in cases of doubt or to better location accuracy of the detected lesion.

MATERIALS AND METHODS - Prospective, we evaluated 154 patients who were performed bone scintigraphy at INER from January to April 2014 (four months). Their age range was from 2 years to 89 years (mean 61.1 years). In addition to whole body scanning, 47

of the 154 (30.5%) patients underwent study complementary with SPECT/CT. The main reasons for the referral patients to study were 52 lung cancer (33.7%), 28 prostate cancer (18.1%), 20 breast cancer (13%) and other various diagnoses.

RESULTS - Of 154 patients (81 women = 52.6% and 73 men = 47.4%), 13 patients (8.5% of the sample) showed extraosseous uptake, of which 10 were women and 3 men. There were 4 women with concentration in breast, 2 patients with a concentration in lungs (one lung cancer and the other by severe pulmonary alveolar microlithiasis), 2 in liver (one of them by hemangioma), 2 with calcification in soft tissues of buttock and thigh, 1 in myocardium, 1 in spleen, 1 in cutaneous leg ulcers. Nine patients (almost 6% of the sample) with alterations to the elimination of the radiotracer, such as retention pyelic or calyceal or ureteral dilatation were also detected. Anyway there were very interesting cases.

CONCLUSIONS The frequency of uptake and extraosseous concentration of diphosphonates on the bone scans that we obtained, indicates us the importance of intentionally seek such finds and report them to interpret these studies, in addition to the discoveries focused on the skeleton. In the bone scintigraphy, SPECT/CT is a useful tool that allows us to elucidate when there is doubt in the planar images if the uptake is in bone or not (e.g. the bladder can mask a bone lesion in the pubic symphysis) and provides the precise location of the abnormality.

FIRST EVALUATION OF A TIME-OF-FLIGHT WHOLE-BODY PET/MRI SCANNER IN ONCOLOGY PATIENTS: COMPARISON WITH PET/CT

Iagaru Andrei. Estados Unidos, Jamali M, Minamimoto R, Mittra ES, Gold GE, Vasanwala S, Gambhir SS, Zaharchuk G.

UNITED STATES

Purpose: The recent introduction of hybrid PET/MRI scanners in clinical practice showed promising initial results for several clinical scenarios. However, the first generation of combined PET/MRI lack time-of-flight (TOF) technology. Here we report the results of the first patients to be scanned on a completely novel integrated PET/MRI scanner with TOF capabilities. Methods: We analyzed data from patients who underwent a clinically indicated ^{18}F FDG PET/CT, who then received a subsequent PET/MRI. Maximum standardized uptake values (SUV_{max}) were measured from ^{18}F FDG PET/MRI and ^{18}F FDG PET/CT for lesions, cerebellum, salivary glands, lungs, aortic arch, liver, spleen, skeletal muscle, and fat. Two experienced radiologists reviewed the MR data for image quality.

Results: Sixteen patients (8 men, 8 women, mean [±standard deviation] age of 68±9 years [range: 48-82 years]) with a total of 33 discrete lesions met the inclusion criteria. PET/CT images were acquired at a mean (±standard deviation) of 74±14 minutes (range: 52 - 98 minutes) after injection of 10±1 mCi (range: 6 – 12 mCi) of ^{18}F FDG. PET/MRI scans started at 169±36 minutes (range: 125 – 286 minutes) after the ^{18}F FDG injection. All lesions identified on PET from PET/CT were also seen on PET from PET/MRI. The mean SUV_{max} values were higher on PET/CT than on PET/MRI for all lesions. No degradation of MR image quality was observed.

	PET (PET/CT)	PET (PET/MRI)	P value
Lesions (n=33) SUVmax	6.16	7.38	0.0001
Cerebellum SUVmax	11.30	9.69	0.0001
Salivary gland SUVmax	2.47	2.53	0.4652
Aortic arch SUVmax	2.05	1.14	0.0001
Lung SUVmax	0.57	0.38	0.0001
Liver SUVmax	3.39	2.46	0.0001
Spleen SUVmax	2.52	2.25	0.0285
Gluteal muscle SUVmax	1.07	1.22	0.0658
Gluteal fat SUVmax	0.26	0.23	0.4041

Conclusion: Despite the lower residual activity due to the delay of at least 2 hours post-injection for all PET/MRI scans, image quality was excellent due to the combination of TOF and high sensitivity detectors, with no lesions missed on ^{18}F-FDG PET from PET/MRI. The TOF PET system is capable of excellent performance during simultaneous PET/MRI, without compromising MR image quality.

RADIATION EXPOSURE TO THUMB OF NUCLEAR MEDICINE PHYSICIAN DURING INJECTIONS IN CONVENTIONAL NUCLEAR MEDICINE PROCEDURES

Vishal Agarwal.

INDIA

In a busy nuclear medicine department like ours, substantial number of injections are given (depending on the number of cases) and if there are not enough nuclear medicine physicians available to distribute this radiation exposure, then whatever little exposure he/she may receive, has to be validated. Though it's a standard practice to inject using the lead syringe shield (to use shield to reduce the radiation exposure), to inject into the already secured line by vein-flan or butterfly; in place of direct i.v (to reduce time taken for inj.) and to maintain as much distance as possible.When we use the lead shield, by the very virtue of its design, it does give protection to the fingers which are rolled around the cylindrical part of the lead to hold to syringe-shield containing the syringe but when we press the piston to push the contents of the syringe, there is no protection to the isolated unprotected thumb during that procedure. So, we tried to estimate the radiation exposure to the 'thumb' during the injection. We estimated the average time taken to push the piston during injection to the patient and it came out to be approximate 3 seconds. It means, whatever the amount of activity is being injected to the patient, it gives exposure to the unprotected thumb for that much period. Secondly, it was not possible to directly measure the radiation exposure during the injection period because it was cumbersome to put the dosimeter between the thumb and the piston and then push. Even if we tried in some cases, it significantly increased the time taken for injection. Thirdly, the radiation exposure from each injection was too low for the threshold of the dosimeter to give us some measurable reading.

So, we tried to circumvent this uneasiness by putting the dosimeter directly in front of the piston of the loaded syringe with the average amount of activity used during that month, with syringe shield in-situ; separately on the table, for the calculated total time taken for all the injections (total no. of cases x 3 sec) and calculated the reading. This exercise gave us the radiation exposure reading of 3μsv to the unprotected thumb in one month, which can be extrapolated to the annual radiation exposure of around 36μsv; which is way below the recommended international guidelines for annual radiation exposure to the extremities. So, there is no need to panic but this study does give us some data for the thumb.

RADIATION DOSE MANAGEMENT OF ^{18}FDG (F-18) FOR OCCUPATIONAL WORKERS AND COMFORTERS

Shaukat Khanum Memorial Cancer Hospital & Research Center, Lahore, Pakistan
Shahid Younas[1]. Paquistan, Ahmed Yar[1], Ehsan Qadir[1], Ismaeel[2], Ameer Hamza[2]
[1.] *Shaukat Khanum Memorial Cancer Hospital & Research Center, Lahore, Pakistan.*
[2.] *Department of Physics, Government College for Science, Lahore, Pakistan.*

PAKISTAN

Objective: The control mechanism of radiation has always been challenging since its inception from Roentgen's mysterious rays. The study reflects our aptitude to manage radiation doses to our workers and comforters when dealing with ^{18}FDG under ALARA principle. Material and Method: Pakistan's first PET CT suite with on-site cyclotron was designed under the guidelines of AAPM Task Group Report # 108 in 2009. Concrete, Perspex and lead were used as shielding materials to justify cost and space availability. The controlled areas were designed for permissible dose limit of ≤ 2 μSv/ hr. The members involve with direct contact with ^{18}FDG are given Thermolumiscence dosimeters to record their monthly whole body and extremities doses.

Results and Discussions: Once operational the maximum prevailing exposure is ≤ 10 μSv/ hr in FDG Synthesis unit at 5 Ci. The prevailing exposure in the PET CT Console and injection room is ≤ 2 μSv/ hr, Pre-scanning room ≤ 5 μSv/ hr, post scanning room ≤ 0.2 μSv/ hr; cyclotron vault surrounding is ≤ 0.1 μSv/ hr. Nursing staff, injecting and dispensing ^{18}FDG is rotated once in a week to inject ten patients per day / week using lead shielding to cover syringe, lead bricks and movable trolley. This made us to bear ≤ 0.75 mSv/ month (≤ 27 mSv/ month) dose for nursing staff. Patients are continuously watched by technologists by CCTV and two-way communication. Technologists guide the patient by making announcement to follow RED color line to reach to PET CT and Green line to reach post-scanning room. This short interaction reduces the technologist's dose ≤ 0.6 mSv/ month (≤ 17 mSv/ month). Three radio-chemists produce up to 5 Ci radioactive ^{18}FDG on daily basis in automated shielded synthesis unit. The average radiation dose for each

radio-chemist is ≤ 0.7 mSv/ month. Medical Physicists and cyclotron engineers receive ≤ 0.5 mSv/ month (≤ 10 mSv/ month). The comforters receive ≤ 1.5 mSv / scan recorded by EPD. Each patient is released when the radiation exposure is reduced to ≤ 20 μSv/ hr @ 1 meter. Patient is instructed to avoid children and pregnant women for next five hours.

Conclusion: In the last five years, 2009 to 2013, 10,000 patients scanned with average 330 MBq injected dose. The maximum average dose received was 4 mSv/ year for some members of nursing staff and radio-chemists whereas the least average dose 1 mSv/year was for technologists whereas rest of the staff received doses ≤ 1 mSv/ year.

PERFORMANCE EVALUATION OF PRE-CLINICAL MICRO-SPECT USING ^{99M}TC

Ahmad Yar. Paquistan, MS, Hans Lundqvist,PhD, Pasha Razifer,PhD, Shahid Younas, MS , Tazeen Saeed Bukhari, Meng.

PAKISTAN

Department of Biomedical Radiation Sciences, Uppsala University Sweden
Shaukat Khanum Memorial Cancer Hospital and Research Center Lahore Pakistan

Objective The intention of this work was to investigate the physical performance of small animal micro-SPECT imaging system in order to calculate spatial resolution and effect of scattering. Material and Methods: The current study was performed using axial and transversal phantoms at various energy window settings. Two narrow, thin plastic tubes with an inner diameter of 0.8mm and 0.28mm were filled with different radioactivity concentrations 105 & 27 MBq and 435 & 20 MBq of ^{99m}Tc respectively. The axial phantom, shaped in a horizontal rectangular waveform, was filled with activity for both spatial resolution and scattering (flood source). Then, it was placed in the field of view of the camera to focus the axial resolution at three different points (20mm apart) along the axis of rotation. Similarly, an experiment with the transversal phantom, shaped in a vertical rectangular waveform, was also carried out. The focus here was to estimate the spatial resolution and scattering at different distances on and off from the axis of rotation. The obtained data from both the experiments was reconstructed according to the standard procedure. Data obtained from the perpendicular slices was plotted and fitted to single and double Gaussian functions.

Results and Discussion: The spatial resolution was measured as a full width half maximum. These assessments were developed in an adequate way to deliver the highest calculated spatial resolution (1.00 mm) at the center for the two tubing sizes and the phantoms (axial and transversal). This is actually double the maximum built-in spatial resolution (0.5 mm) of the camera for pinhole collimators. In addition, the percentage of scattering was observed which had an error of +/- 20% around the object, (flood source) of dimensions 100x60x40 mm, with both the phantoms.

Conclusion: To conclude, the spatial resolution can be further improved by reducing the scattering effects with the help of more sophisticated Gaussian model which can handle the lower and higher gamma radiations simultaneously and can easily differentiate between the background and the actual signal peaks. Key words: SPECT, spatial resolution, scattering, axial phantom, transversal phantom.

BONE SUPERSCAN AS AN UNCOMMON PRESENTATION OF HISTOLOGICAL PROVEN METASTASIC GASTRIC CANCER

BIROCCO, María José; FACELLO, Adolfo, Argentina; FLORES TURK, M.Guadalupe; CLARIÁ, Marcelo; MASSANET, Diego. Instituto Oulton. Córdoba. ARGENTINA.

ARGENTINA

Bone superscan pattern is uncommon in bone scans and is related to a variety of metabolic bone disorders (hyperparathyroidism, renal osteodystrophy, osteomalacia and others) as good to malignancies, in such case representing widespread diffuse metastatic disease of bone. Intense bone activity and absence or decreased visualization of kidneys in whole body scan can be explained by diffuse bone marrow involvement. This pattern was reported for metastatic prostate, breast, lung, bladder, colon and transitional cell carcinomas, lymphoproliferative diseases and myelofibrosis. Bone metastastatic spread is uncommon in gastric cancer an mainly shows osteolytic appearance, nevertheless superscan pattern was occasionally reported. We present the case of a 72-years old male patient referred from his primary physician for persistent and progressive diffuse bone pain during last three months. He had a history of prostate cancer treated with radical prostatectomy followed by local radiotherapy twelve years before. Additionally, partial gastrectomy was performed 18 months before and a poor differentiated gastric adenocarcinoma, signet ring cell type, pT2 pN0 pMx stage, was found. Physical examination showed an anemic but in good general condition patient, without gastrointestinal or abdominal complaints. Relevant lab showed: hemoglobin 8.7 gr%, hematocrit 27%, serum calcium 8.7 mg/dL, alkaline phosphatase 7 755 IU/L and PSA 0.5 ng/mL. Whole body scan was performed three hours after 740 MBq MDP-Tc99m intravenous administration, using

a dual head camera. An intense, diffuse bone uptake was found over axial and proximal appendicular skeleton with poor renal visualization, consistent with superscan pattern. Gastric origin was suggested in nuclear report. Oncologist performed iliac bone biopsy that showed diffuse metastatic infiltration by signet ring cells of gastric origin. Chemotherapy was started. In conclusion, looking a bone superscan in a male patient, even in presence of prostate cancer history, other clinical facts must be evaluated and uncommon primary pathologies considered.

RUGGER JERSEY SPINE SIGN DETECTED ON ^{18}F-FLUORIDE PET/CT

Nascimento Beatriz Birelli, Brasil [1], Ribeiro MP [1], Amorim BJ[1], Santos AO [1], Mosci C [1], Lima MCL [1], Lima BS [2], Casarim ALM [3], Tincani A [3], Ramos CD [1], Etchebehere M [2], Etchebehere E[1].

Division of Nuclear Medicine [1] of the Department of Radiology and Departments of Orthopedics and Traumatology [2] and of Head and Neck Surgery [3], Campinas State University (UNICAMP), Campinas, BRAZIL.

BRAZIL

INTRODUCTION: The Rugger-jersey Spine Sign is a radiologic mark described when there is increased density of the vertebral body end plates at multiple levels with a lucent center, producing an effect of alternating dense-lucent-dense appearance, similar to the transverse bands of a rugby jersey. This pattern is typically seen in patients with hyperparathyroidism. We report a case in which this sign was noted on a ^{18}F-fluoride PET/CT study, correctly diagnosing hyperparathyroidism and in addition, detecting the primary lesion.

MATERIALS AND METHODS: A 34-year old male patient with a history of spontaneous fracture of the left humerus, suspicious of fibrous dysplasia underwent bone scintigraphy with ^{99m}Tc-MDP. The images demonstrated regions of marked diffusely heterogeneous increased radiotracer uptake in the proximal third of the left humerus, right ulna, anterior portion of the 5th ribs bilaterally and right femur. In addition, increased linear tracer uptake in the cortical portion of both humeri and femur was noted. Bone scan findings were inconclusive.The patient was submitted to a ^{18}F-fluoride PET/CT study that revealed multiple focal osteolytic lesions increased tracer uptake, low attenuation (similar to blood/fibrous tissue) and a thin, expanded cortex. These lesions were noted in the 5th ribs bilaterally, the left scapula, humeri bilaterally, right olecranon, pelvic bones, right femur, left patella and right distal fibula. A diffuse tracer activity in the vertebral spine, similar to the rugger Jersey spine sign, was noted and interestingly was only faintly seen in the CT portion of the scan. Additionally, a nodule in the right parathyroid region was noted. These findings were consistent with hyperparathyroidism with multiple brown tumors and possibly a parathyroid adenoma.Follow-up studies revealed serum PTH levels of 364 IU/L (normal: 15 - 65 IU/L), calcium levels of 14,6mg/dL (normal: 8,8-10mg/dL) and nodule in the right inferior parathyroid gland on the parathyroid SPECT/CT ^{99m}Tc-sestamibi scintigraphy The patient was submitted to surgical excision of the right inferior parathyroid gland and histopathology revealed parathyroid adenoma.

CONCLUSION: This is the first report of the rugger Jersey spine sign with ^{18}F-Fluoride PET/CT. This sign was helpful to lead to the correct diagnosis of hyperparathyroidism, which in turn lead to the judgment that the other lesions were brown tumors and a possible primary parathyroid adenoma. ^{18}F-Fluoride PET/CT should be considered in cases of bone disorders because it is a more sensitive and specific with a shortened exam time compared with ^{99m}Tc-MDP bone scintigraphy.

STAGING OF PYOMYOSITIS BY 18F-FDG PET/CT - A CASE REPORT

Nascimento BB, Etchebehere ECSC. Brasil, Santos AO, Amorim BJ, Mosci C, Lima MCL, Souza TF, Souza LG, Brenelli S, Auletta LL, Ramos CD.

Division of Nuclear Medicine of the Department of Radiology and Department of Internal Medicine, Campinas State University (UNICAMP), Campinas, BRAZIL.

BRAZIL

BRIEF DESCRIPTION OF THE PURPOSE OF THE STUDY: Pyomyositis is defined as an acute intramuscular bacterial infection secondary to hematogenous spread of a microorganism. This report shows the use of ^{18}F-FDG PET/CT to evaluate the extension of the disease. CLINICAL HISTORY: We report a case of a 67 year-old, male patient, without comorbidities, which presented with weakness, weight loss, swelling, pain and increased temperature of the right thigh. Laboratory exams revealed anemia associated with increased leucocyte counts and erythrocyte sedimentation rate. MRI was suggestive of pyomyositis. ^{18}F-FDG PET/CT, performed for staging purposes, demonstrated intense radiotracer uptake in all the muscle groups of the right thigh with regions within the muscles with no uptake (suggestive of necrosis); right lung base pulmonary consolidation (consistent with primary focus of infection); focal liver

uptake without anatomical changes (possible infectious dissemination); hypermetabolic right external iliac and inguinal lymph nodes and bone marrow and spleen increased uptake (consistent with reactive sites). The patient was submitted to surgical resection and the fluid culture was positive for streptococcus pneumoniae. Antibiotic therapy was directed to the isolated agent. The patient had improvement of the clinical symptoms and laboratory data. DIAGNOSIS: Pyomyositis. BRIEF DISCUSSION OF THE CASE: This is the first case to describe the value of ^{18}F-FDG PET/CT for staging patients with pyomyositis.

BONE SCINTIGRAPHY IN THE ASSESSMENT OF SKELETAL BRUCELLOSIS AND Q FEVER.

Javier Vilar Gonzalez. Uruguay, R. Hitateguy, V. Depons, E. Moreira, A. Battegazzore, K. Bayardo, A. Silveira, R, Ferrando.

URUGUAY

Consultorio de Medicina Nuclear "Ferrari-Ferrando-Páez"-Montevideo-Uruguay

Brucellosis and Q fever are relevant zoonosis in Uruguay because they are considered occupational diseases for the lifestock sector. The diagnostic value of bone scintigraphy for the detection of osteoarticular involvement was evaluated retrospectively in 63 patients (brucellosis 53, Q fever 10) with humoral confirmation and osteoarticular symptoms sent to our nuclear medicine clinic in the last 5 years. Whole body planar and sectorial images were complemented with SPECT-CT depending on the topography of the findings. The mean age was 40 years (range 19-61years) for brucellosis and 34 years (28-62) for Q fever. Male gender prevailed with 87% and 60% of the cases respectively. Twenty three patients with brucellosis (43%) presented anomalies, affecting musculoskeletal joints in 14 (60%). Osteoarticular lesions prevailed in the spine (30%) most of them involving the low lumbar segment (L4-L5), followed by knees (29%), shoulders (17%), tarsals (13%) and other locations (10%) as sacroiliac joints, hips and elbows. Bone lesions were more common in ribs (50%) and lumbar spine (30%). SPECT-CT images allowed differential diagnosis with osteoarthritis. Patients with Q fever showed abnormalities in 50% without articular predominance. There was slight majority of the findings at the level of shoulders and knees. Thirty three follow-up studies were performed in 15 patients with brucellosis. Disease progression was found in 9 studies, improvement in 6 and 18 remained unchanged. Five patients with Q fever underwent follow-up scintigraphic studies. Only one showed changes (progression). We conclude that bone scintigraphy is a useful tool for the detection and follow-up of skeletal involvement in patients with brucellosis an Q fever referred with osteoarticular symptoms. SPECT-CT has added value particularly in the spine and sacroiliac joints.

THE PHYSICAL DETECTION PERFORMANCE OF EUROPROBE II FOR A LOW ENERGY SOURCE (99MTECHNETIUM): AN EXPERIMENTAL STUDY

Emerson Nobuyuki Itikawa, Leonardo A Santos, Joseane F Souza, Sandro S Shakushiya, Camila E.

BRAZIL

AIMS: To evaluate the physical detection parameters of a gamma probe including the angular, spatial and energy resolutions, side and back shielding and the final sensitivity according to international standards of quality control for non-imaging probes. The objective here is to assure its usefulness in sentinel lymph node localization in patients with melanoma and breast cancer patient

METHODS: We used the CZT probe detector EUROPROBE II ® (Eurorad, Italy) for low energy isotope (20 ~ 170 keV) in this study. The tests were performed using low activity 99m- Tc radiation sources (12 MBq upper) and also, acrylic devices for point sources and scatter medium simulators were developed to run the tests. Count acquisition was performed by using the time integration mode, which is displayed in the equipment. Probe performances (shielding; angular, spatial and energy resolution) were evaluated using a collimator, a device that increases the lateral shielding and decreases the sensitive area of the detector tip. RESULTS: For the angular resolution test, the probeshowed 31.4 and 31.6-FWHM(°) for 3 and 30 centimeters-distance, respectively. In the spatial resolution, the probe was able to identify two closely but separated sources of radiation, through a acrylic scatter medium of 10 mm.

The energy resolution test demonstrated a 20.5-FWHM(%) and proved to correctly discriminate the photopeak of 99m-Tc (140-keV). The probe showed good intrinsic sensitivity of 510 counts per second per unit of activity (cps/MBq), according to the manufacturer guidelines. The side and back shielding test showed that the probe tip was efficient to stop photons that came from spurious or background radiation. We observed similar performance in the tests when using the collimator. The reduction of the sensitive area by the collimator improved the distinction of both point sources in the spatial resolution test, and decreased the FWHM values in the angular resolution test.

CONCLUSIONS: The EUROPROBE II ® gamma probe showed performance according to the international standards for non-imaging intraoperative probes, either with or without the use of the collimator.

COMPARISON BETWEEN 18F-FDG PET/CT AND 18F-FLUORIDE PET/CT IN A PATIENT WITH EQUIVOCAL BONE SCAN

Ana Emília Teixeira Brito, Nathália Novaes Cosenza; Paulo Henrique Silva Monteiro.

BRAZIL

Introduction Breast cancer is a very common cancer worldwide and one of the most frequent sites of metastases is the skeleton. The conventional ways to stage patients are CT and bone scan with 99mTc-MDP. 18F-FDG-PET/CT, however, is reported to be more sensitive and specific in detecting hematogenic metastases than conventional imaging.18F-Fluoride is used as a bone radiotracer for PET/CT studies, showing higher sensitivity for bone metastases diagnosis than bone scan with 99mTc-MDP for both blastic and lytic bone lesions. Case report Female patient, 66 y.o., on follow-up after breast cancer therapy for 6 years, when lymph node involvement was detected while the patient was, at that moment, under no oncological treatment. A bone scintigraphy revealed new focal areas of uptake in the right parietal bone, proximal third of right clavicle and posterior portion of right ninth costal arch, considered to be probably due to post-traumatic bone remodeling or metastatic disease. The patient had a five-months prior cranium CT that didn´t show any bone lesions. 18F-Fluoride PET/CT scan showed bone metastasis in an osteolytic lesion on right parietal bone (SUV=36,5) and osteoblastic lesions on proximal third of right clavicle (SUV=22,8) and posterior portion of right ninth costal arch (SUV=7,6). To complete restaging, 18F-FDG-PET/CT scan was performed and didn't show any area of increased uptake even on the anatomical bone lesions detected by CT.Discussion Some reports have proposed that 18F-FDG-PET/CT would have equal or superior sensitivity than bone scintigraphy for bone metastases detection, especially in case of lytic lesions. It has been suggested that 18F-FDG-PET/CT could even replace bone scan in staging or restaging of some oncological patients for bone metastases detection.This case shows an example where 18F-FDG-PET/CT missed both osteoblastic and osteolytic metastases that were detected and reported as equivocal in 99mTc-MDP scan and characterized as bone metastases in 18F-fluoride PET/CT.

ConclusionThis report suggests that 18F-Fluoride PET/CT probably still has a role in patients with breast cancer and equivocal bone findings even in 18F-FDG-PET/CT era.

SPECT-CT BONE SCINTIGRAPHY FOR DIAGNOSIS AND DIFFERENTIAL DIAGNOSIS OF TUMOR-INDUCED BONE DISEASE

B.Robev, S.Sergieva,M.Dimcheva
Sofia Cancer Center
Sofia, Bulgaria.

BULGARIA

INTRODUCTION: Whole body bone scintigraphy (WBBS) is the most sensitive but low specific method for early detection of secondary skeletal lesions. The combined application of baseline WBBS, followed by more specific techniques such as SPECT-CT fusion is an advanced approach for diagnosis, differential diagnosis and staging of osseous metastases. PURPOSE: To evaluate the role of SPECT-CT bone scintigraphy for diagnosis, differential diagnosis and follow-up of patients with tumor-induced bone disease.

PATIENTS & METHODS: This study included 89 pts with various types of tumors. For some of the cases WBBS was carry out to follow-up pts with breast and prostatic cancer after complex therapy including radiotherapy, biphosphonate infusions and chormonal therapy as follows: naromat® /Letrozol nucleus® in postmenopausal women and LHRH with/without Tamoxifen in premenopausal women and Bicusan® with/without LHRH in patients with breast and prostate cancer. Other pts were directed to the nuclear medicine department due to some subjective complaints or because of abnormal laboratory indices. METHODS: All pts underwent routine WBBS with 99mTc-MDP as well as target SPECT-CT imaging. The field of target SPECT-CT images correlated with areas of uncertain abnormal tracer uptake visualized on the WBBS. SPECT-CT camera (Symbia T2, Siemens) was used. Low-dose CT scanning (130 kV; 20 mA, 5-mm reconstruction) was performed.

RESULTS & DISCUSSION After retrospectively review of WBBS and SPECT-CT fused images 141 bone lesions in 89 pts were analyzed. The skeletal findings were classified as definitely benign, indeterminate or definitely malignant. · 47 (33%) of all lesions in 36 pts could be correlated with benign degenerative findings on SPECT-CT images. · 41 (28,1%) single osseous metastatic spots (up to 3 foci) were scanned in 31 pts. · 13 (10%) lesions caused by direct infiltration of bone structures was observed in 6 pts as a result of proximity to the neoplastic recurrent localized in the surrounding soft tissues. · 21 (15%) lesions with prevailing "cold" osteolytic component were observed in 8 pts with renal, NSCLC, endometrial, colorectal, urinary bladder cancer. They were not visualized clearly on the WBBC. · 17 (12%) "mixed-type" lesions - osteolytic and osteosclerotic were obtained in 6 cases with breast and prostatic cancer after complex treatment.

Two pts were with 2 (1.9%) single extraosseous lesions: with myositis ossificans and
with soft tissue calcifoid metastasis. CONCLUSION: **1.** The most important clinical application of bone SPECT-CT imaging is differ-

ential diagnosis between degenerative and metastatic foci with abnormal tracer uptake and similar scintigraphic appearance on the WBBS. **2.** CT is a valuable method for characterizing osteolytic, sclerotic and mixed lesions, their consolidation or calcium accumulation. It has direct relation to the therapeutic approach of tumor-induced bone disease by determining the necessity of prescribing diphosphonate medication, chormonal therapy or metabolic radiotherapy.

THREE PHASE BONE SCAN INTERPRETATION BASED UPON VASCULAR ENDITHELIAL RESPONSE

Kush Kumar, MD.

UNITED STATES

Objetives: A new mothed of interpretation of TPBS scan based upon the normal physiological vascular endothelial related response is proposed ti improve the specificity of TPBS. Methods: Fifty cases of TPBS were evaluated. Thirteen studies were normal. In remaining 37 positive studies, 20 showed localized or focal vascular endothelial independent response and 17 showed generalized or large vascular endothelial dependent response. One patient with septic arthroplasty of th knee joint with endothelial dysfuction showed localized response. Two cases were of CRPS/RSD. Micro bacterial or histological confirmation of infection was obtained in 9 cases and in rest of the 6 cases fidings were reported as consistent with infection. Two cases were of cellulitits and responsed well to antibiotic therapy. Rest 4 patients were having diabetic neuropathic foot with chronic ulcers and were treated accordingly. Additionally, 20 published cases in the literature of osteomyelitis were also analyzed.

Results: The data clearly indicated that all the cases of bone infection (osteomyelitis/arthritis/cellulitis) showed generalized vascular endothelial dependent flow and pool response pattern, except one with vascular endothelium dysfunction. All the cases of CRPS/RSD also showed generalized similar pattern, though in depends upon the stage of the disease. Infection could be ruled out in absence of generalized vascular endothelial dependent flow and pool response. All published cases of osteomyelitis in the literature showed positive vascular endothelial dependent pattern.

Conclusions: Visual or quantitative segmental evaluation of the three phase scan based upon the normal physiological reaction to the etiology of the disease process i.e. the vascular endothelial response (vascular endothelium dependent response; large/ generalized response or vascular endothelium independent response; limited/ limited/ focal response) is a helpful method in narrowing the different permutations and combination of clinical scenario and pathologies.

UTILITY OF SPECT BONE WITH 99mTc-MDP IN THE DIAGNOSIS OF JAW CONDYLAR HYPERPLASIA: OUR EXPERIENCE

Rubén Rojas, Luis Monteverde, Carlos Estrada.

PERU

Nuclear Medicine Service.

P.N.P. National Hospital "Luis Saenz N.". Lima-Peru.

Objectives: The mandibular condylar hyperplasia (HCM) is a rare disease that is expressed by excessive bone growth that results in facial asymmetry, deformity and malocclusion, and pain and dysfunction. The purpose of this study is to share our experience in the use of SPECT in detecting this condition for the proper surgical treatment of patients. Material and methods: We carried out the review and follow-up of 31 cases with facial asymmetry probably condylar hyperplasia to which bone scintigraphy was performed 3 hours after injection of 740 MBq of 99mTc-MDP planar and SPECT acquiring views of skull. Gamma camera Philips BrightView dual-head, LEHR collimation, 140 Kev peak and window width 20% was used. Of the 29 patients, 16 were women (55.2%). The ages range from 13-31 years (19.9 ± 3.2). The images were evaluated and the activity was quantified both condyles. Results: Significant increase in quantification was observed in 15/29 (52%) of SPECT, 10 in the right condyle, with IC 55.5 - 67.7% (60.0 ± 3.2), and 5 in left condyle, with IC 58.0 - 64.3% (60.7 ± 1.9). HCM was confirmed by pathological examination, and were in active phase (difference between upper quantification condyles al10%) in 14 of them (9 rights and 5 lefts), performing orthognathic surgery and subsequent control. The other case was an osteochondroma with a value of 66% in the right condyle, performing one condylectomy.

Conclusions: The utility of SPECT bone in cases of mandibular condylar hyperplasia suspicion is proven to help improve the diagnosis of the disease in the active phase and permitting appropriate surgical management of cases.

SPECT-CT ASSESSMENT OF LUMBOSACRAL TRANSITIONAL VERTEBRAE

Verónica Depons, felipe Brazão Carvalhaes; Fernando Alves Moreira.

BRAZIL

Introduction: Lumbosacral transitional vertebrae (LSTV) are common congenital anomalies of the lumbosacral segment present in 3%–21% of humans. The transitional vertebra may have different morphology ranging from broadened elongated transverse processes, often unilateral, to complete fusion to the sacrum. Inaccurate identification of LSTV may lead to surgical and procedural errors and poor correlation with clinical symptoms. The relationship between low back pain and LSTV (Bertolotti syndrome) has been debated but pain may arise from varying levels and L5 sacralization can contribute to the development of orthopedic diseases. The Castellvi classification system describes four types of LSTV with increasing levels fusion (IJIV) and unilateral (a) or bilateral (b) dysplastic transverse processes. LSTV are difficult to recognize in SPECT images and currently CT is the best imaging technique for characterization of this entity. Objective: To describe SPECTJCT findings in a retrospective cohort of patients with LSTV. Methodology: The study population included 50 consecutive patients (27 female), with a mean age of 23 years (range 8J49), who underwent SPECTJCT imaging in our Clinic in which a LSTV was identified. Low back pain was present in all but two patients. Patients older than 50 years were excluded.

Results: CT images identified 18 type Ia LSTV, 4 type Ib, 12 IIa, 7 IIb, 1 IIIa, 7 IIIb, and 1 type IV with SPECT showing associated increased uptake in 42 patients. SPECT images were negative in 8 cases. Four of them had type IIIB LSTV, in which increased uptake is less likely because of bilateral complete fusion. The other 4 cases were type I LSTV. The remaining type III LSTV had only mild uptake at the level of the vertebral body transition. All type II LSTV and the only patient with type IV had more intense lateralized incresed uptake associated with incomplete fusion. Moderately increased sacroiliac joint uptake was present in 9 patients and facet joint uptake in 3. Associated anatomical anomalies included incomplete vertebral fusion in 3 patients and disc herniation in 2.

Conclusion: Hybrid imaging with SPECTJCT provides a new scenario for the characterization of LSTV. Specific morphological features can be recognized while the presence of stress in the lumbosacral transition or neoarticulation can be detected, as well as associated reactions in facet and sacroiliac joints. Bertolotti syndrome should always be considered in radionuclide studies assessing low back pain, particularly in young patients.

PHYSICS INSTRUMENTATION

OPTIMAL IMAGING CONDITIONS FOR SIMULTANEOUS DUAL ISOTOPES MYOCARDIAL PERFUSION IMAGING USING SEMICONDUCTOR SPECT

Makiko Kurihara Sakakibara Heart institute Fuchu-shi,Tokyo, Japan Coautores: Yasuhiro Suzuki,Nobuo Iguchi,Tetsuya Sumiyoshi.

JAPAN

Background and Objectives: Imaging using simultaneous dual isotopes (SDI) of 99mTc and 123I has been considered difficult because their energy windows are close to each other. However, with the commercial availability of semiconductor SPECT characterized by high energy resolution, it will be possible to realize 99mTc and 123I SDI imaging. The purpose of this study was to investigate the optimal imaging conditions for SDI in the clinical setting. Materials and Methods: Twenty-four patients who underwent imaging using the semiconductor SPECT (D-SPECT, Spectrum Dynamics Medical) were studied. Firstly, 370 MBq of 99mTc was injected intravenously one hour prior to the first scanning. Then, 111 MBq of 123I was injected 20 minutes prior to the second scanning. We compared 99mTc imaging data of QPS (extent values) and QGS (EDV, ESV, and EF) under three imaging conditions: 1. only 99mTc (Tc); 2. 99mTc and 123I (Dual); and 3. 99mTc and 123I with scatter correction (Dual-scatter). In addition, we evaluated the decrease in cavity to myocardium count ratio due to scatter correction.Results: QGS values did not differ significantly among the three conditions (EDV: p=0.09, ESV: p=0.39, EF: p=0.54). QPS values did not differ significantly between Tc and Dual (p=0.11), but were significant different between Tc and Dual-scatter (p=0.01). The mean decreases in cavity to myocardium count ratio due to scatter correction were 57.77% for 99mTc and 50.24% for 123I.

Conclusion: The present study indicates that 99mTc and 123I SDI imaging can be used clinically. However, we found that obtaining counts approximately two times higher for 123I and 99mTc would be preferable when conducting SDI with scatter correction. Furthermore, QPS image of 99mTc may be modified by scatter correction, which should be taken into consideration when interpreting the images.

"FAT-WATER-SHIFT" ARTIFACTS ON μMAPS OF HEAD BED POSITION IN WHOLE BODY PET/MR SCANS

Daisuke Shimao, Fukushima Medical University, Fukushima, Japan
Coautores: Takamitsu Hara, Shiro Ishii, Fumio Shishido, Seiichi Takenoshita.

JAPAN

Objective: Magnetic resonance (MR)-based attenuation correction (MRAC) in hybrid positron emission tomography/MR systems is still a challenging technique for clinical use. "Fat-water shift" is one of the artifacts seen with MRAC, resulting from the misclassification of fat and water. It is considered more likely to occur in slim patients and children than in normal patients. However, we have experienced "Fat-water shift" artifact in head bed position among many non-slim patients. The objective of this study was to assess the frequency of this artifact in Japanese adult oncological patients in relation to body mass index (BMI). Materials and methods: We retrospectively reviewed segmented attenuation maps (μMaps) using Dixon imaging of 241 oncological patients (134 men, 107 women) who underwent whole-body PET/MR. Mean age was 59.9 years (range, 21–87 years). Mean BMI for all patients was 23.4 kg/m2 (range, 12.1–39.7 kg/m2). The number of imperfect cases including head bed position among automatically processed μMaps due to "fat-water-shift" was counted, and classified into the following two categories: "only head bed position" and "head bed position with other bed positions". Relationships between the frequency of the artifact and BMI were then investigated. Results: Imperfect μMaps were seen in 73 of 241 patients (30.3%). The number of imperfect cases including head bed position was 29 among those 73 imperfect cases. The breakdown of that and BMI was as follows: 16 cases of "only head bed position" (mean BMI, 24.0 kg/m2 ; range, 18.6–30.3 kg/m2) and 13 cases of "head bed position with other bed positions" (mean BMI, 17.7 kg/m2 ; range, 12.1–20.2 kg/m2). Conclusion: "Fat-water-shift" artifacts in "head bed position with other bed position" were likely to occur in patients with low BMI. On the other hand, the artifact in "only head bed position" arose independently of MBI. Imperfect μMaps in head bed position arose in approximately 12% of Japanese adult oncological patients, which cannot be ignored. Measures must be taken to address this issue, as standardized uptake values are directly affected by μMaps.

SIMULATION OF Electromagnetic Field EFFECT over a human's BRAIN

R. Rojas and J. A. Calderón.

MEXICO

Objective. Matter radiation interaction appears in different situations like: medical radiology or electric high tension systems. The electromagnetic radiation can injure people. Make a prediction about the effects of radiation over the organic tissue require the Maxwell's equations solution [1]. Many investigators works in numerical solutions in 2D with organic pixeled phantoms, but there are designed with simple geometrical structures, and when somebody proposed a 3D model, just take a 2D slice, because they spend less

memory. Our objective is, make an electromagnetic field effect simulation, over a realistic pixeled phantom human's brain. Materials and methods. To design a pixeled anatomical phantoms from Magnetic Resonance Imaging [2], we take a stack of slices from organ, and using a computational packet we obtain a 3D image (Figure 1). This anatomical model, have electric and magnetic properties in function of frequency [3]. The simulation solve the Maxwell's equations to obtain the electric and magnetic fields and the induced current density, produced over a pixeled model.Results. We apply this methodology to a subway's catenary (Figure 2), there transport 600A of electrical current, with 750V of voltage, we propose a distance between catenary and driver just of 50cm. Figure 3, shows the magnetic flux density field (in Tesla) simulated in slices and in stream lines. Figure 4, shows a graphic of induced current density, distance was measured since the catenary position to the brain, there starts at 50cm and ending at 62cm.

Conclusions. The effect of current in catenary over subway's driver is a very low induced current, because the magnetic field is weak and decay with distance, then the injured brain possibility is very little. Another expected result, is that the spurious currents, are more intense when the frequency are increasing.

EFFECTIVE RADIATION DOSES IN SPECT/CT PROCEDURES

M.Dimcheva, S.Sergieva, A.Jovanovska.

BULGARIA

Department of Nuclear Medicine, Sofia Cancer Center, Sofia, Bulgaria.

Objective:
The effective dose associated with a diagnostic SPECT/CT procedure is the sum of the effective dose due to the nuclear component and the effective dose due to the CT component. The aim of the study was to assess the radiation burden on patients from low-dose CT in SPECT/CT studies. Material: Data from 140 scans of various nuclear medicine procedures with 131I or 99mTc-labelled radiopharmaceuticals, comprising 100 patients, were presented in this study. Acquisition of patient examinations on the SPECT/CT Symbia T2, Siemens were performed. For each patient the low –dose CT scan were performed using a tube current modulation system, Care Dose 4D. Results: The contribution of total e ective radiation dose from SPECT component were calculated using the activity of the injected radiopharmaceutical(MBq) and the effective dose (mSv) tables published by the conversion factors listed in the International Commission on Radiological Protection (ICRP) Publication 53 and 80. The effective dose (mSv) due to CT was calculated as the product of Dose Length Product (DLP) and a correction factor depending on the region of investigation, using standard guidelines. Conclusion: The increases in effective doses from SPECT/CT study is considered clinically acceptable in view of the diagnostic benefits of the CT. It does not increase the radiation burden on patients significantly. The main radiation burden is related to the applied radiopharmaceuticals. When SPECT-CT is being performed, all measures should be taken to reduce both the radiopharmaceutical dose and the CT effective dose following the principle of As low As Reasonably Achievable (ALARA).

USEFULNESS OF SCATTER CORRECTION IN 99MTC AND 123I SIMULTANEOUS DUAL ISOTOPE (SDI) IMAGING USING THE SEMICONDUCTOR SPECT

Yasuhiro Suzuki.

JAPAN

Background and Objectives: Semiconductor SPECT utilizes a novel high-speed gamma camera with semiconductor detectors and this technology has been shown to provide high-energy resolution. Semiconductor SPECT will therefore allow 99mTc and 123I SDI dual isotope imaging. However the usefulness of scatter correction remains unclear. The purpose of this study was to evaluate the SPECT images of 99mTc and 123I SDI with and without scatter correction.

Materials and Methods: The semiconductor SPECT (D-SPECT, Spectrum Dynamics Medical) was used in this study. 99mTc and 123I (0.15 MBq/ml for each) were infused into the left ventricular myocardium of a heart liver phantom (Kyoto Kagaku). Additionally, only 99mTc (0.15 MBq/ml) was infused into the small part of the left ventricular myocardium of a phantom of cardiac defect (capacity of 4 ml). Acquisition time was set at 10 min. The hybrid method between the TEW method and scatter modeling was used for scatter correction. The Change by QPS 2012 was used for quantitative analysis.

Result: For the energy-spectrum analysis, adequate separation between 99mTc and 123I was observed. For the analysis of SPECT image, 123I image of the defect phantom showed a clear defect area. Furthermore, 123I image depicted the defect much more clearly when scatter correction was used. As for the quantitative analysis of Change by QPS 2012, the dissociation between 99mTc and 123I was 9% without scatter correction and 11% with scatter correction.

Conclusion: It may be possible to perform simultaneous dual isotope of 123I and 99mTc using semiconductor SPECT. However scatter correction is essential to improve the image quality.

COMPARING FILTERED BACK PROJECTION AND ORDERED-SUBSETS EXPECTATION MAXIMIZATION FOR THYROID VOLUME ESTIMATION IN ^{131}I SPECT: VERIFICATION BY PHANTOM AND CLINICAL STUDY

Alev Ergulen. Trakya University.

TURKEY

The measurement of the thyroid volume is one of the cornerstones of the calculation of individualized radioiodine therapy dosages. The functioning volume of the thyroid will generally be different from the anatomical volume; this can only be determined by radionuclide imaging technique. SPECT systems are ideal for volumetric quantification of thyroid gland. Firstly, we apply the optimization process to the basic parameters of SPECT imaging and reconstruction in thyroid gland, and then secondly compare the results of reconstructions in human's.

Methods: The phantom studies were performed by using known volume filled with three different activities of ^{131}I. SPECT imaging was performed using a dual-headed gamma camera with a full 360° and over anterior 180°. FBP and OSEM are the reconstruction algorithms in this study. Area of the organ on transaxial slices was calculated at different thresholds (The threshold has two values (34/20 and 40/100).) and the sum was multiplied by slice thickness to get the volume. Thyroid volume was also calculated by this method in 23 patients (4 men, 19 women; mean age 46±13 year).

Results: There was a significant difference in the thyroid values obtained from 180 and 360 degrees SPECT at 40/100 threshold in the iterative reconstruction ($p < 0.001$). The agreement between SPECT-FBP and SPECT-OSEM with 34/20 threshold and USG volume measurements were found to be good. In human study, regression equations were formed with the thyroid volume obtained from SPECT and the volumes acquired with USG were compatible with those from SPECT-OSEM and SPECT-FBP.

Conclusion: The knowledge of the volume of an organ constitutes an important first step in the quantification of radioactivity within an organ. In our study, thyroid volume obtained by both FBP and OSEM SPECT values is compatible with the values by USG. The obtained formulas can be used.

OPTIMIZATION AND ANALYSIS OF THE MANAGEMENT AND QUANTIFICATION OF SOLID RADIOACTIVE WASTE GENERATED IN A NUCLEAR MEDICINE SERVICE

Pena, G.P.[1]; Santos, J.S.[2]; Gonzalez, J.A.[2]; Passaro, B.M.[2]; Lopes, A.B.[2]; Buchpiguel, C.A.[2]; Guimarães, M.I.C.C.[2]
[1]Pontifícia Universidade Católica de São Paulo (PUC SP), Brasil. [2]Centro de Medicina Nuclear do Instituto de Radiologia do Hospital das Clínicas da Faculdade de Medicina da Universidade de São Paulo (CMN InRad HCFMUSP), Brasil.

BRAZIL

Objectives: To analyze, quantify and qualify the amount of radioactive waste generated by a nuclear medicine center, in order to optimize the management of that waste.

Methods: A retrospective analysis was made of the records of storage and disposal of radioactive waste from January 2008 to December 2012 in the Nuclear Medicine Center of InRad HCFMUSP. The data were tabulated and presented using descriptive statistics.

Results: The greatest quantity of radioactive waste produced was of Tc-99m (Technetium-99m), representing 75%. In terms of mass, this corresponds to approximately 781 kg (~1721 lb). Other nuclides used in the clinic of this study generated the following quantities of waste: 186 kg (~410 lb) of Cr-51, 52 kg (~115 lb) of I-131 and 20 kg (~44 lb) of Ga-67. An average of about 1 kg (~2.2 lb) of radioactive waste per day was generated in the studied period. It was observed that approximately 90% of the solid waste was compactable (gauze, gloves and others) and the remaining 10% were of non-compactable waste, such as needles and others.

Conclusions: The majority of procedures performed for diagnostic purposes in the Nuclear Medicine Center of InRad HCFMUSP uses radiopharmaceuticals labeled with Tc-99m. Thus, the greater quantity of radioactive waste generated of this radionuclide was expected. Among the years there has been a significant variation in the amount of waste, which is directly connected with the quantity of exams performed. An analysis of the values can help in identifying and optimizing all operations improving the process as a whole to minimize the generation of radioactive waste. In order to have a secure storage of the data of solid radioactive waste generated a software is being developed.

EVALUATION OF EFFECTIVE DOSE ASSOCIATED WITH LOW DOSE PROTOCOLS IN WHOLE-BODY DUAL-MODALITY ^{18}F-FDG PET/CT EXAMINATIONS

Wirote Changmuang, Krisanat Chuamsaamarkkee, Kanokon Poonak, Sasithorn Amnuaywattakorn, Saowanee Wipuchwongsakorn
Department of Nuclear Medicine, Faculty of Medicine Ramathibodi hospital, Mahidol University, Bangkok.

THAILAND

Objective: We have started routinely service of PET/CT imaging since 2011. The radioactive-sugar imaging from this dual-modality system has widely accepted role in clinical oncology however it is also associated with an increasing in the radiation dose received by the patient. This study aims to retrospectively calculate patient effective dose from whole body PET/CT scanning with the low-dose protocol on the PHILIPS GEMINI TF PET/CT scanner.

Materials and Methods: Whole body ^{18}F-FDG PET/CT imaging of 360 patients (161 males, 199 females) acquired during June 2011 to December 2013 at Ramathibodi hospital were reviewed. The radiation dose associated with a CT was calculated according to the CT dose-length product. The PET effective dose was estimated based on assumptions of the injected ^{18}F-FDG activity using ICRP publication 106. The estimated doses were also modified with the weight of each patient. The total effective dose was computed by summation of the CT and the PET component.Results: The patient's age ranged from 13 to 85 years (12 children, 348 adults). The mean of CT dose-length product was 313.41±25.83 mGy.cm and it individual depended on the scan length of patient. The CT contribution to the total effective dose was 5.64±0.46 mSv with the CT protocol setting of 120 kVp and tube current-exposure time 50 mAs. For the PET component, the mean administered activity of ^{18}F-FDG was 203.87±17.22 MBq. Correspondingly, the total effective dose found to be 4.80±1.13 mSv when scaling with patient weight. Hence, the mean total effective dose of dual-modality PET/CT was 10.44±1.13 mSv. Additionally, the range of the total effective doses was also reported according to the age and gender of patient. The total effective dose ranges were estimated as follows: children male: 9.81 to 11.99 mSv and children female: 7.61 to 14.21 mSv, adult male: 9.19 to 11.24 mSv and 9.52 to 11.80 mSv for adult female.

Conclusion: The effective dose from the PHILIPS GEMINI TF PET/CT studies with low dose protocols was found to be lower than the previously reported in the literatures. This resulted from the sensitivity gain technology which has allowed less activity of radiotracer and also the reducing of X-ray radiation dose from CT components.

QUANTITATIVE ANALYSIS OF ICTAL SPECT IMAGES IN FRONTAL LOBE EPILEPSY: AN ASSESSMENT OF THE UNIFORM ATTENUATION CORRECTION EFFECTS THROUGH SPM

Leonardo Alexandre Santos Institucion: Ribeirão Preto School of Medicine USP/RPCoautores: E. N. Itikawa, A. C. Trevisan, M. Kato, F. A. Pitella, A. P. P.Martins, H. T. Amaral-Silva, T. R. Velasco, V. Alexandre Jr., C. E. P. Baltazar, D. K. Sonvenso, A. C. Sakamoto, L. Wichert-Ana.

BRAZIL

AIM: The Attenuation Correction (AC) of gamma photons poses a clinical problem in the evaluation of ictal SPECT in Frontal Lobe Epilepsy. The main issue is that mesially located seizure focus may be underestimated. This study aimed to evaluate the impact of the AC on brain SPECT images in patients with Frontal Lobe Epilepsy (FLE). MATERIALS AND METHOD: The ictal SPECT of 10 patients diagnosed with FLE were analyzed using SPM. The brain SPECT of 12 healthy subjects were used as a control group. All SPECT images were divided in two groups: a group containing SPECT images corrected for theattenuation effects of gamma-ray photons (AC), by Chang's Method (0.12/cm), and another group without the AC (nAC). The Statistical Parametric Mapping (SPM) was used to compare the signal changes of the AC and nAC images. To the hypothesis test to this study (Two sample, t-test), two comparison models were specified: single patient (nAC) versus control group average (nAC) and single patient (AC) versus control group average (AC). Each patient was compared with the average image of the control group due to variations of epileptogenic zones locations among the ten patients. The threshold p-value used was to values $p<0.001$, with $Z>3.08$, and cluster size value $k=20$. From each selected cluster we analyzed the cluster size, pick value, and the corrected p-value for each inference evel. All these clusters were evidenced in a MRI standard template for better view of the results.

RESULTS: We found differences between the averaged signals of each comparison performedon both sets of images of interest, AC and nAC. Those clusters than survived the multiple comparisons test were considered. They showed that by applying the AC, the epileptogenic orpropagation zones located mesially in the brain were better evidenced, either visually or quantitatively. Otherwise, the nonlinear weight in the SPECT image used by Chang's Methoddecreased the visualization of the seizure activated regions located in the peripheral or lateralized areas of the brain.

CONCLUSIONS: We concluded that the uniform Attenuation Correction method applied in brain SPECT images is an effective tool in the investigation of FLE cases. The AC contributed tothe exhibition of epileptogenic and propagation zones located mesially within the brain.However, the non AC images should also be clinically used once activated areas in theperipheral or lateralized brain regions may be underestimated with the AC techniques.

PROPOUSAL OF TWO COUNT RATE SATURATION CORRECTION METHOD FOR WHOLE BODY STUDIES.

J.P. Castillo1,*, L.A. Torres1, M.A. Coca1

1 Departamento de Investigaciones Clínicas, Centro de Isótopos (CENTIS)

CUBA

Purpose: To develop two dead time correction methods for whole body (WB) scintigraphy, which are intended to improve accuracy of activity quantification during post therapeutic dosimetry.
Materials and methods: Both methods use reference sources (point like and linear) that are hold to the surface of the detector. Each acquired WB is characterized by the presence of a line patter formed by the reference source, which is parallel to the moving direction of the table (y). Counts from the line patter (N_(y,L) "or " N_(y,P)) are used to calculate a dead time correction curve by mean of the following equations:

$$F_{y,L} = \frac{N_{0,L}}{N_{y,L}} \qquad F_{y,P} = \frac{1}{H} \sum_{j=y-x_0}^{j=y+H-x_0-1} \frac{N_{y,P} v_d}{C_P}$$

These equations contemplate translation speed (v_d), detector size (H) and counts without dead time losses (N_(0,L) and C_P). Every consideration made to obtain the equations was experimentally evaluated before assessing the correction methods.
Two whole body images of 99mTc point like sources (2-40 mCi) located along the table were obtained to verify the proposed correction methods. Each source activity was calculated using the corrected WB and compared to values from activimeter. Furthermore, count rate saturation correction method proposed by Hobbs et al. in 2010 was used as reference during the evaluation. All images were acquired in a Nucline SPIRIT DH-V (MEDISO) gamma camera with low energy high resolution collimator.Results: During the performance evaluation of the gamma camera at high count rate, artefacts created by mispositioned counts were detected. Moreover, it was observed a variation of the dead time value in presence of focalized activity, which impact to the saturation correction factor was below 5%. Correction method based on point like reference source exhibited an average relative difference of 5% for sources over 8 mCi. Similar result was obtained with Hobbs et al. correction method. Method based on linear reference source was easier to implement, but less accurate (8%). Average relative difference without performing any dead time correction method was 16.5% Conclusions: Both saturation correction methods improved activity quantification at high count rates. However, only correction method based on point like reference source was as accurate as method proposed by Hobbs et al.

THE PHYSICAL DETECTION PERFORMANCE OF EUROPROBE II FOR A LOW ENERGY SOURCE (99MTECHNETIUM): AN EXPERIMENTAL STUDY

Emerson Nobuyuki Itikawa, Ribeirão Preto School of Medicine. Leonardo A Santos, Joseane F Souza, Sandro S Shakushiya, Camila EP Baltazar, Carlos A V Junior, Daniele K Sonvenso, Ana C Trevisan, Felipe A Pitella, Mery Kato, Lauro W Ana.

BRAZIL

AIMS: To evaluate the physical detection parameters of a gamma probe including the angular, spatial and energy resolutions, side and back shielding and the final sensitivity according to international standards of quality control for non-imaging probes. The objective here is to assure ts usefulness in sentinel lymph node lcalization in patients with melanoma and breast cancer patients. METHODS: We used the CZT probe detector EUROPROBE II ® (Eurorad, Italy) for low energy isotope (20 ~ 170 keV) in this study. The tests were performed using low activity 99mTcradiation sources (12 MBq upper) and also, acrylic devices for point sources and scatter medium simulators were developed to run the tests. Count acquisition was performed by using the time integration mode, which is displayed in the equipment. Probe performances (shielding;angular, spatial and energy resolution) were evaluated using a collimator, a device that increases the lateral shielding and decreases the sensitive area of the detector tip.RESULTS: For the angular resolution test, the probeshowed 31.4 and 31.6-FWHM(°) for 3 and 30 centimeters-distance, respectively. In the spatial resolution, the probe was able to identify two closely but separated sources of radiation, through a acrylic scatter medium of 10 mm. The energy resolution test demonstrated a 20.5-FWHM(%) and proved to correctly discriminate the photopeak of 99m-Tc (140-keV). The probe showed good intrinsic sensitivity of 510 counts per second per unit of activity (cps/MBq), according to the manufacturer guidelines. The side and back shielding test showed that the probe tip was efficient to stop photons that came from spurious or background radiation. We observed similar performance in the tests when using the collimator. The reduction of the sensitive area by the collimator improved the distinction of both point sources in the spatial resolution test, and decreased the FWHM values in the angular resolution test. CONCLUSIONS: The EUROPROBE II ® gamma probe showed performance according to the international standards for non-imaging intraoperative probes, either with or without the use of the collimator.

EVALUATION OF THE ACCURACY OF THE SUV AND CT NUMBER OF THE BIOGRAPH MCT SCANNER

H. Alva Sánchez, Unidad de Imagen Molecular PET/CT, INNN, A. Reynoso-Mejía, I. Díaz-Meneses, A. Manzo-Sánchez, I.Cruz-Ventura, N.E. Kerik-Rotenberg.

MEXICO

Background: The standard uptake value (SUV) is a measure to quantify radiopharmaceutical uptake in positron emission tomography (PET) scans in user-defined regions of interest. Its use and implementation during image analysis is relatively simple, but its magnitude may be influenced by physical factors: annihilation photon attenuation, more important for larger patients, and by the partial volume effect, important in small objects.

Objective: The aim of this work was to evaluate the accuracy of SUV quantification and CT number determination by a hybrid PET/CT scanner due to physical factors and reconstruction parameters. Materials and methods: We evaluated both the CT number (in Hounsfield units) and SUV determination in a Siemens Biograph mCT with time-of-flight (TOF) capabilities. SUV evaluation was performed with cylindrical phantoms of volumes ranging from 10 ml to 10 liters, filled with 18F-FDG solution with known activity concentrations ~37 MBq/litre (1.0 mCi/litre). Mean and maximum SUV were determined by delimiting spherical volumes of interest (0.8 of phantom internal diameter). Images were reconstructed using 5 different reconstruction protocols. SUV quantification was also assessed in attenuation-corrected images using CT scans acquired with 80, 100, 120 and 140 kV. In addition, the SUV determination was performed at different iodine-based contrast medium concentrations. Finally, SUV was determined in three regions of a brain PET/CT scan (cerebral cortex, cerebellum and white matter) using 8 different reconstruction protocols.

Results: Up to 21% and 50% variations in the mean SUV and SUVmax, respectively, were observed for the different phantom sizes. The lowest mean SUV (0.79) was obtained for the 10 ml cylinder reconstructed with the Brain PET iterative protocol without TOF, while the highest SUV (1.14) was for the 10 liter phantom reconstructed with filtered-back projection. The highest SUVmax was obtained for the 10 litre phantom with the iterative+TOF protocol. Although CT numbers of a phantom containing contrast medium change in 50% when using different kV, the attenuation corrected PET scans show a small variation in SUV (2.7%). Small variations (3%) in mean SUV values were observed in identical volumes-of interest when varying the reconstruction algorithm only.

Conclusions: For objects with dimensions below approximately two times the scanner spatial resolution (4 mm FWHM) SUV is underestimated for approximately 12.4% while for large objects the SUV can be somewhat overestimated (11% for the 10 litre phantom). Even though the CT number in contrast-enhanced scans is largely affected by the kilovoltage, attenuation-corrected PET scans are reconstructed with small SUV deviations. For reproducible results, both PET and CT (especially kV and contrast media concentration) acquisition parameters should be kept the same in particular during follow-up PET/CT scans.

MOLECULAR IMAGING

N-STAGING 64CUCL2 PET/CT IN PATIENTS WITH PROSTATE CANCER

Enza Capasso Institucion: U.O.C. Med. Nucleare ASL Cagliari.

ITALY

Purpose: The use of 64copper-based positron emission tomography-computed tomography (PET/CT) tracers in cancer studies is increasing. Nevertheless few data are available on radiotracers labeled with copper-64 use in cancer patients. Our purpose is to validate $^{64}CuCl_2$ use in the initial staging imaging of localized prostate cancer (PC).Methods: Six patients affected by localized perypheral prostatic cancer (histological examination: small gland adenocarcinoma) has been enrolled. Three were no-treated patients and the other three were treated with bicalutamide monotherapy, (1 of them had radical prostatectomy and lymphadenectomy too). No patients had External Beam Radiotherapy yet. All underwent to multiparametric prostate MRI and intravenously administration of 185 MBq of $^{64}CuCl_2$. All of them subjected to whole-body PET/CT scans at 10 minutes and 1 h after administration (two patients also a 24h scan). All patients had given written informed consent before administration of radiopharmaceutical. Visual Image Analysis PET/CT images were analyzed. Results: $^{64}CuCl_2$ had a significative concentration in liver and renal cortical just after 10 minutes after administration.

No ureteral and bladder uptake of radiopharmaceutical had seen in all analyzed scans. Lesions discovered on the fused PET/CT had to be a clearly detectable, thank to the absence of urinary excretion. $^{64}CuCl_2$ uptake was higher in tumor gland of naif patients than in patient under bicalutamide therapy. In two patient with suspected lymphadenopathy at MRI (> 10 mm diameter) we had no $^{64}CuCl_2$ uptake. In other two patients we had positive findings at PET/CT scan (one of them had < 10 mm diameter lymphadenopathy).

Conclusions: Our data suggest that it is possible $^{64}CuCl_2$ use in prostate cancer for a correct N staging PET/CT instead of 11C-Choline or 18F-Choline, due to its feasibility half life. $^{64}CuCl_2$ enables to detect lesions suspicious for prostate cancer with high contrast as early as 1h post injection with high detection rates even at low PSA levels. Due to ^{64}Cu decay characteristic, the prostatic tumor uptake represents an alternative therapy modality, so performed a basal PET/CT with copper-64 chloride becomes important for the best management of PC patients.

UNEXPECTED METASTASES OF MELANOMA. DETECTION BY PET CT 18F-FDG

Patricia Paredes Rodriguez,Hospital Sanitas La Moraleja, Madrid, España.
Coautores: Jose Manuel Castro Beiras, Angel Crespo Diez.

SPAIN

Purpose: Positron emission tomography (PET) using ^{18}F-fluorodeoxyglucose can detect early or small metastatic deposits of melanoma and guide subsequent correlative anatomical imaging and treatment. The aim of this study is to assess the value of PET in demonstrating previous unsuspected metastatic disease and difficult to detect with other procedures.Methods 18 PET CT studies performed on patients with melanoma were reviewed. Images were independently evaluated by a nuclear medicine specialist and a radiologist, and later write the report together.The findings of PET CT were compared with results of previous PET/CT, CT, MRI, anatomopathology, clinical history, depending on the case.

Results Location of primary lesion: 4 scalp 8 limbs4 thorax 2 unknown In 10 patients PET revealed pathological high metabolic activity:2 patients disseminated metastases in brain, lung, spine, adrenal, all of them were unsuspected except the one in brain, which had been detected by MRI.5 patients had hyper metabolic activity in regional lymph nodes. 1 patient with two unexpected lesions one in the brain and other in muscle in the thigh (that were confirmed histologically), furthermore the primary lesion could be identified in a subcutaneous nodule in supraclavicular region.1 patient lesion in the brain 1 patient with lesion in orbital internal rectum muscle, SUV max6.3, that was reported by RM as probable metastatic lesión , hepatic lesions, and lung nodules suggestive of metastases. In the other 8 patients PET CT was negative. PET CT demonstrated unsuspected lesions by other examinations or clinical signs in 4 patients. These were later confirmed by histological study.

Conclusion FDG PET CT is an useful technique to asses the extension of disease in melanoma It is frequent to find unexpected metastases, that are difficult to diagnose by other techniques (for example the lesion in muscle of leg that was later confirmed histologically)

CLINICAL IMPACT OF FDG PET-CT PERFORMED FOR NON-MEDICARE ELIGIBLE INDICATIONS: AUSTRALIAN EXPERIENCE

P Lin, E Stoakes, A Scott, S Sam.

AUSTRALIA

Department of Nuclear Medicine and PET, Liverpool Hospital, Sydney, Australia

Background: The prospective PET data collection for Medicare funding in Australia between 2003-2005 showed impact on staging and restaging in 64% of patients. Liverpool Hospital was one of the eight hospitals in Australia that participated in that process. The Medicare funded items remained restricted with no new items added since, and the only funded therapy monitoring items are for lymphoma, and head and neck cancer.. Objective: This study aims to prospectively investigate the clinical Impact of FDG PET-CT performed for non-Medicare eligible indications at Liverpool Hospital.

Materials and Methods: Eighty-six patients underwent unfunded whole body FDG PET-CT scans from December 2013 to March 2014, after appropriate vetting of referrals by Nuclear Medicine specialists. The referring doctors were provided with survey forms (pre- and post-PET) for indications, perceived evidence based on literature, impact on staging/restaging, and management impact, with an overall response rate of 62%. The staging and management impact information for the remainder of patients were obtained from clinic and multidisciplinary meeting letters.

Results: Tumour subgroups included; lung (16%), unknown primary (9%), colon (9%), anus (7%), breast (7%), gastric (6%), hepato-biliary (6%), haematological (5%), mesothelioma (5%), pancreas (5%), renal-bladder (5%), germ cell (3%), oesophagus (3%), other oncology (7%) and non-oncological (7%). Indications included; diagnosis = 20, staging = 27 and restaging/recurrence = 39 (which included 15 for treatment monitoring and 4 for radiotherapy planning).PET led to change in diagnosis or staging/restaging status in 40% of patients (34/86 patients): 20% in diagnosis group, 63% in staging group and 44% in restaging/recurrence group.The management impact was considered high (change in treatment modality or intent) in 37 patients (44%) and moderate (change in planned procedures, dose of therapy or mode of delivery) in 18 patients (20%).

Conclusions: Medicare unfunded FDG PET-CT performed in appropriately selected patients can lead to change in diagnosis or staging/restaging status in 40% of patients, and with moderate to high management impact in 64% of patients.

THE UTILITY OF 18F-FDG PET/CT IN PATIENTS WITH MELANOMA.

Rodríguez Cabrera Sergio Adán1, Fernández Soto José Rodrigo1, Rivera Bravo Belén1, Jiménez Arenas Daniela Janet1, Altamirano Ley Javier1, Martínez Martínez Ricardo1.

PET/CT Cyclotron Unit, Faculty of Medicine, National Autonomous University of Mexico, Mexico City.

MEXICO

Objective: The melanoma is a tumor that often spread in early stages. Since the PET/CT is a technique that allows to evaluate the hypermetabolism of primary and metastatic tumor in the whole body, it is important to determine if the ^{18}F-FDG PET/CT has a key role in the workup, management and follow up for patients with diagnosis of melanoma.

Materials and methods: We examine 67 ^{18}F-FDG PET/CT reports from patients with diagnosis of melanoma, and evaluate them according to the findings and the implications in the management of patients. Results: The sensibility of ^{18}F-FDG PET/CT for detection of metastatic melanoma was 97%, and the specificity was 90%. The most frequent site of metastatic melanoma detected on PET/CT was lymph nodes (63%), followed by lungs (43%) and subcutaneous tissue (30%). The result of PET/CT caused a change in management on 93% of patients. 94% of those reported as negative for malignant disease didn't receive adjuvant therapy.

Conclusions: The ^{18}F-FDG PET/CT is an important tool to stage patients with diagnosis of melanoma, as well as to determine the response to treatment, and monitor the patients that don't have evidence of remaining disease. The most important role for PET/CT in patients with diagnosis of melanoma seems to be the recognition of metastatic lesions in a comprehensive detection test, and so determine the best management for each patient. Keywords: melanoma, positron emission tomography/computed tomography (PET/CT), fludeoxyglucose (FDG), metastatic lesion, SUVmax.

THE FDG NEGATIVE PULMONARY NODULE: SPECTRUM OF DISEASE

Dr. Senpei Jin ,Institucion: Monash Health
Melbourne,Victoria ,Australia.

AUSTRALIA

PURPOSE: To present a review of radiological and histological findings of 30 FDG-PET negative pulmonary nodules with neoplastic and non-neoplastic etiologies.

CONTENT ORGANIZATION: Lung nodules are a frequently encountered entity in imaging and require further work up to determine significance. FDG PET/CT has become the mainstay in non-invasive evaluation of pulmonary nodules for suspected malignancy. When a nodule is intensely FDG avid, it is considered malignant until proven otherwise. It may be tempting to regard the FDG non-avid nodule as indolent, however substantial literature exists on malignant but FDG non-avid nodules.This pictorial review will highlight the imaging characteristics and/or temporal evolution, as well as proven pathological findings of 30 FDG non-avid pulmonary nodules. These will include both neoplastic and non-neoplastic causes. Neoplastic etiologies include non-small cell lung cancer (squamous cell carcinoma and adenocarcinoma), neuroendocrine tumours (well-differentiated carcinoid and poorly-differentiated carcinoma) and metastases. The non-neoplastic causes include metaplastic and dysplastic changes, pneumoconiosis, hamartoma, fibrovascular change, lipoid pneumonia and chronic inflammation. Along with histology we will also review radiological findings, looking at structural features which may assist the reader when faced with a “cold” nodule. Structural characteristics of neoplastic and non-neoplastic nodules will be compared. As PET/CT utilisation increases rapidly throughout the world, it is essential for all readers to be aware of the spectrum and thereby the implications of a FDG negative pulmonary nodule. This is especially important because FDG is not a tumour marker, and functional molecular imaging with FDG cannot be considered simply in a dichotomous manner. Information from structural imaging/temporal change plays a crucial role in deciding whether to proceed to invasive intervention.

SUMMARY: This exhibit will provide a comprehensive review of the FDG negative lung nodule. It is designed to allow readers to gain a better understanding of possible neoplastic and non-neoplastic etiologies, and present certain features which readers may need to be cautious of.

68Ga-DOTATATE-PET/CT OUTPERFORMS 99mTc-HYNC-OCTREOTIDE AND WHOLE-BODY MRI FOR DETECTION OF NEUROENDOCRINE TUMORS – A PROSPECTIVE TRIAL

Etchebehere E1, Santos A1, Bezerra R2, Gumz B3, Vicente A1, Hoff PM 3, Corradi G2, Ichiki W1, Almeida Filho G1, Cantoni S2, Camargo EE1, Costa FP3.

Division of Nuclear Medicine and PET/CT 1, Division of Radiology 2 and Oncology Center 3 , Sirio Libanes Hospital; São Paulo, Brazil.

BRAZIL

The incidence and prevalence of NETs has been rapidly rising and therapy with radiolabeled-somatostatin analogues is increasing. Thus, there is a need for more sensitive imaging methods for staging and therapy planning. Given the different metabolic imaging methods, various tracers and emerging anatomic modalities to evaluate NET patients, a better understanding of the performance of each method is warranted, especially to establish the most appropriate patient work-up.

OBJECTIVES: Compare NET lesion detectability between state-of-the-art modalities: 68Ga-DOTATATE-PET/CT, 99mTc-HYNIC-ocreotide SPECT/CT (SSRS-SPECT/CT) and whole-body diffusion-weighted MRI (WbDMRI).

METHODS: Nineteen consecutive patients (ages 34 to 77 years, mean 54.3 ± 10.4 years, 9 females) were submitted to SSRS-SPECT/CT, 68Ga-DOTATATE-PET/CT and WbDMRI. The three imaging modalities were acquired with a maximum interval of 3 months between them and were blindly analyzed by separate teams. 68Ga-DOTATATE-PET/CTs images from head to feet were acquired forty-five minutes after injection of 185 MBq. SSRS SPECT/CT planar whole body and SPECT/CT images of the thorax, abdomen and pelvis were performed at 4 and 24 hours after injection of 185 MBq of 99mTc-HYNC-octreotide. All CT images were acquired with 130 kV, 15 mAs, 0.8 s and 2 mm slice thickness. WbDMRI images were obtained in the coronal plane using a body coil with a 1.5-T whole-body imager (Signa-HDx, GE Medical Systems, USA). The standard method of reference for evaluation of the performance of images was undertaken by the following criteria: consensus among investigators at the end of the study, clinical and imaging follow-up and biopsy of suspicious lesions.

RESULTS: McNemar´s test was applied to evaluate lesion detectability of 68Ga-DOTATATE-PET/CT in comparison to SSRS-SPECT/CT and WbDMRI: a significant difference in detectability was noted for overall solid organs (p= 0.0253 and p= 0.383, respectively), pan-

creas (p = 0.0082 and p = 0.0455, respectively), gastrointestinal tract (p = 0.0082 and p = 0.0253), thoracic lymph nodes (p = 0.0253 and p = 0.0455) and bones (p = 0.0082 and p = 0.0143). Two unknown primary lesions were identified solely by 68Ga-DOTATATE-PET/CT, one in the duodenum and the other in the pancreas. 68Ga-DOTATATE-PET/CT, SSRS-SPECT/CT and WbDMRI demonstrated respectively sensitivities of 0.96, 0.60, 0.72; specificities of 0.97, 0.99, 1.00; PPV of 0.94, 0.96, 1.00; NPV of 0.98, 0.83, 0.88 and accuracies of 0.97, 0.86 and 0.91.

CONCLUSION: 68Ga-PET/CT is clearly more sensitive for detection of well-differentiated NET lesions. Staging of NET patients should be performed with 68Ga-PET/CT and follow-up studies with WbDMRI. SSRS SPECT/CT should be used when 68Ga-PET/CT is not availa

THE PREDICTIVE ROLE OF METABOLIC TUMOR VOLUME ON PRETRAETMENT FDG PET/CT IN DLBCL.

Tamás Györke MD, PhD: Tamás Györke [1,2]; Dávid Molnár [3]; Ildikó Garai [1]; Zoltán Tóth [1]; Botond Timár [4]; Norbert Zsótér [5]; László Papp [5]; Judit Demeter [6]; Lajos Gergely [7]; Tamás Masszi [8]; Ágota Szepesi [4]

HUNGARY

Objective: The aim of this retrospective study was to determine whether whole-body metabolic tumor volume (MTV) and total lesion glycolysis (TLG) measured on pretreatment 18F-FDG PET/CT (PET) can predict prognosis is patients with diffuse large B-cell lymphoma (DLBCL). Materials and methods: 48 patients with newly diagnosed DLBCL underwent PET before standard R-CHOP (rituximab, cyclophosphamide, doxorubicin, vincristine, prednisolone) treatment. Tumors were automatically segmetned by a gradient-maximizing region growing algorithm included in the InterView Fusion software package (Mediso Ltd, Hungary). MTV and TLG were measured inside of the segmented Volume of Interests. Receiver operating characteristic (ROC) analysis was performed to determine optimal cut-off values. Estimates of event-free survival (EFS) in high and low MTV/TLG groups were calculated according to the Kaplan-Meier method and compared with the log-rank test. Results: During a median follow-up of 43.5 months 9 patients (19%) showed study event (incomplete response to primary treatment or relapse). ROC analysis yielded optimal cut-off values for MTV of 235 cm3 and for TLG of 1632. The 3-year EFS for high and low MTV groups were 63 and 96%, respectively (p=0.002). There was no statistically significant difference between the EFS of high and low TLG groups (p=0.08). Conclusions: The MTV measured on pretraetment PET have high potential for predicting outcomes of DLBCL patients treated with standard immuno-chemotherapy.

IMMEDIATE POST OPERATIVE FDG-PET/CT TO EVALUATE SUCCESS OF PERCUTANEOUS ABLATION

Nascimento, BB; Romanato J; Menezes M; Bezerra R; Vicente A; Santos A; Cerri G; Camargo EE; Etchebehere EC. Division of Nuclear Medicine and PET/CT, Sírio Libanês Hospital, São Paulo, Brazil.

BRAZIL

Percutaneous ablative treatments (PA) such as cryoablation or radiofrequency for metastases of solid tumors have increased the possibility of oncological control in non-surgical candidates. After PA it is crucial to evaluate treatment outcome to avoid recurrences. Follow-up studies with CT and MRI are not able to differentiate scar from viable tissue after ablation. AIM: Demonstrate if 18F-FDG PET/CT (FDG PET/CT) performed in the immediate post operative hours after PA (immediate post operative FDG-PET/CT) is able to evaluate the success of PA.

MATERIALS AND METHODS: Twenty patients (13 males, mean age 65.8 years), submitted to PA, were retrospectively reviewed. All patients with solid tumors metastases with indication for PA who exhibited focal uptake of 18F-FDG prior to PTA were included. The maximum interval between a baseline FDG PET/CT and the PA were 30 days. Exclusion criteria consisted of patients that had a change in chemotherapeutic regimen or that began chemotherapy during the 6 month follow-up period. An immediate post operative FDG-PET/CT study to evaluate the presence of residual viable lesion was performed between one and 8 hours after PA. The treatment was considered a success (no viable lesion) if no uptake of 18F-FDG was noted after PA on the immediate post operative FDG-PET/CT. Patient follow-up after 6 months was performed by clinical examination and imaging studies (FDG-PET/CT, MRI or contrast-enhanced CT). RESULTS: Twenty-six lesions were submitted to PA with either cryoablation (7/26) or radiofrequency (19/26) with mean lesion size of 2.5 cm. The metastatic lesions locations were liver (13/26), lung (8/26) and other sites in the abdomen (5/26). The immediate post operative FDG-PET/CT was performed between 1 and 8 hours after PA and detected viable tumor with a sensitivity, specificity, accuracy, positive and negative predictive values of 66.7%, 95%, 88.5%, 80% and 90.5%, respectively. False-positive cases consisted of two lung metastases (1.5 and 0.7 cm) of colon cancer submitted to cryoablation. The false-negative case consisted of a 3.0 cm lung metastasis of melanoma also submitted to cryoablation. There was a significant agreement between the immediate post operative FDG-PET/CT findings and the results on the follow-up study (Kappa = 0.66; $p < 0.01$).

CONCLUSION: An immediate post operative FDG-PET/CT performed between 1 and 8 hours after PA may reliably evaluate the success of these procedures. This strategy may potentially allow early re-intervention of viable lesions and reduce morbidity. A larger number of patients are necessary to confirm these findings.

PET/CT IMAGING OF NEUROENDOCRINE TUMORS WITH 68GALLIUM-LABELED SOMATOSTATIN ANALOGUES: OUR INSTITUTIONAL EXPERIENCE IN A UNIVERSITY HOSPITAL.

Pilar Orellana B.,Rodrigo Pinilla S., Rodrigo Jaimovich F.

CHILE

IntroductionNeuroendocrine tumors (NETs) are uncommon, with an annual incidence of 2-3 cases per 100,000, occur most frequently in the gastrointestinal tract, characterized by overexpression of somatostatin receptors (SSTRs). Functional imaging plays a crucial role in management of NETs. The introduction PET/CT with 68Gallium (68Ga)-labeledsomatostatin analogues has shown excellent results for imaging of NETs and better results than conventional SSTR scintigraphy. We describe our experience with the use of this technique in our Institution. Methods A retrospective review of Ga68 DOTATATE PET/CT performed between 2009 and 2013 was done, analyzing demographic data, study indications and findings. PET/CT results were correlated with histology, surgery, clinical and laboratory data. A dose of 100 MBq of Ga-68 DOTATATE was administrated in all patients and images were acquired at least 40 min after injection. Siemens Biograph True Point 64 PET-CT was used, performing contrast enhanced diagnostic CT 3/3 mm with arterial and venous phases, and 3 min/bed PET images acquired from vertex to mid-thigh. ResultsA total of 195 studies, corresponding to 143 patients were reviewed. The average age of patients was 52.3 years (SD: 15.93), 76 women and 66 men. Thirty two studies were performed in patients undergoing Peptide Radionuclide Receptor Therapy (PRRT).Among the total studies, 116 were performed in patients with carcinoid, 56 with pancreatic NETs and 24 due to other NETs and/or diagnosis. NETs in carcinoid group were located in: stomach (21), duodenum (11), small bowel (52), appendicular (6), colon (15). 48 studies were done in patients with pancreatic NETs. Other locations were: left maxilla (1), parotid (1), bronchopulmonary (2), soft tissue (1) and thymus (1). Other diagnosis were: medullary thyroid carcinoma (11), pheochromocytoma (5), ectopic ACTH syndrome (3), and in 16 cases suspicious NET.138 out of 195 studies (71%) were abnormal. According to indications 21 studies were done for diagnosis (68% abnormal), 84 cases for staging of a known NET (82% abnormal), 64 for therapy control (67% abnormal) and 27 for re-staging (73% abnormal). Malignant abnormal SSTR overexpression was found mainly in the liver (48); lymph nodes (52), pancreas (27), small bowel (22), bone (18), and soft tissue (13). Other locations were colon (6), thyroid (3), pericardium (1), lung (1), stomach (1) and perigastric mass (1). Some benign lesions also showed increased tracer uptake, like bone hemangioma, adrenal adenoma, and inflammatory processes.

Conclusions 68Ga-labeled somatostatin analogue PET/CT is the most sensitive imaging tool for NETs. It can change many aspects of management of such tumors, including selection and follow up for PRRT. On the current scenario, 68Ga-labeled somatostatin analogue PET/CT should be the first-line imaging for NETs evaluation.

DETECTION OF UNKNOWN PRIMARY TUMOR IN PATIENTS WITH METASTATIC LESIONS USING FDG-PET IMAGING: COMPARED WITH THE RESULTS OF CT IMAGING

Tatsuya Yoneyama,Department of Radiology, Toyama University
Coautores: Yuuichi Kamisaki, Kyou Noguchi.

JAPAN

Objective: We investigated the results of FDG-PET imaging whichwere performed to detect unknown primary tumor in patients with metastatic lesions.Methods: We retrospectively investigated 49 patients who haddiagnosed to have metastatic lesions confirmed by histopathologicalfindings or strongly suspected by image diagnosis and had underwent FDG-PET imaging to detect unknown primary tumor.FDG-PET images were interpreted by visual inspection and semi-quantitative analysis (standardized uptake value, SUV). We also retrospectively evaluated the results of other diagnosticmodalities (such as CT, MRI, US, upper gastrointestinal endoscopy, colonoscopy, broncoscopy, etc.), and especially compared the results between FDG-PET and CT imaging. Results: In 30/49 patients (61.2%), primary tumors detected by various diagnostic modalities were histopathologically confirmed orstrongly suspected by image diagnosis. In 19/49 (38.8%) patients, FDG-PET imaging could detect primary tumors (head and neck 1,lung 7, breast 1, stomach 1, pancreas 1, colon 2, rectum 3,uterus 1, prostate 2). In 15/46 patients (32.6%) who were evaluated by both FDG-PET and CT imaging, CT imaging could detect primary tumors (head and neck 1, lung 6, stomach 1, pancreas 1, colon 1, appendix 1,rectum 2, prostate 2). FDG-PET positive and CT negative primarytumors were found in 5 patients (lung 2, colon 1, rectum 1, uterus 1). FDG-PET negative and CT positive primary tumors were found in 2 patients (lung 1, appendix 1). Both FDG-PET and CT negativeprimary tumors were found in 9 patients (lung 2, breast 1, esophagus 1, stomach 4, colon 1). Small primary lesions of breast, lung and appendiceal cancer could not be detected by FDG-PET imaging. In4/5 patients with gastric cancer, FDG-PET and CT imaging could not detect primary tumor site. Primary tumor was not detected in 19/49 patients (38.8%), who were diagnosed as occult primary tumor. Conclusions: FDG-PET imaging might not have high ability to detect unknown primary tumor site, however FDG-PET imaging could be slightly superior to CT imaging. We suggest that it would be difficultfor FDG-PET imaging to detect a small primary lesion and primary tumor site of gastric cancer.

LOCALLY ADVANCED CERVIX CANCER: USING PET/CT FOR EARLY DETECTION OF DISTANT SPREAD

M Morkel, J Warwick, A Ellmann.
Division of Nuclear Medicine, Tygerberg Hospital, Stellenbosch University and
Tygerberg Hospital, Cape Town, South Africa.

SOUTH AFRICA

Cervical cancer is the second most common cancer among women in South Africa and in most of the developing world. A large percentage of these women present with locally advanced Stage IIIb disease. FIGO (International Federation of Gynaecology and Obstetrics) staging is currently being used as a clinical staging tool, however it has many shortcomings, one of which is that lymph node status (especially para-aortic) does not get taken into account. It is known that metabolic changes occur before changes are seen on anatomical imaging and it is therefore possible to detect metastases earlier with the help of FDG PET/CT. Methods: 55 patients with stage IIIB cervical cancer based on conventional imaging were included in this prospective study. A wholebody FDG PET/CT was performed before initiation of treatment and results interpreted byexperienced nuclear medicine physicians and radiologists. We determined the percentage of patients in whom PET/CT changed the stage and/or altered management of the patient.Results: In 11/55 (20%) of patients nodal or distant metastases were found. Pathological FDG uptake in common iliac or para-aortic lymph nodes were seen in 8/55 (15%) patients. One patient with possible bladder infiltration was also seen. 4/55 (7%) of patients had suspicious lesions, however these could not be proven to be malignant. In 15% of our patients it led to extension of the radiation field. In another 20% palliative care was initiated, which was more cost-effective, and prevented unnecessary toxic treatment.

Discussion: The treatment of choice for locally advanced cervix cancer is aggressive chemoradiation with curative intent. This offers a moderate rate of cure but is associated with high patient morbidity and economic cost. Most of our patients require prolonged admissions to hospital in order to receive this treatment. Due to economic constraints this also means that the patients are usually separated from their families and support structures during this time. If patients are understaged, aggressive chemoradiation is unlikely to provide any added benefit, while patients experience severe morbidity and spend valuable time away from their families. Limited financial resources are also not wellutilised. Early detection of distant spread allows more accurate staging of these patients before chemo-radiation and prevents unnecessary treatment of patients in whom palliative care is expected to result in better quality of life, and be more cost-effective. Conclusion: We have shown that a significant proportion of patients (35%) were not only upstaged, but treatment plans were also changed due to additional findings on the PET/CT that were missed by conventional imaging alone.

CONGENITAL HYPERINSULINISM: THE FIRST CASE DIAGNOSED BY 18F DOPA PET TC IN ARGENTINA

MD Maria Bastianello 1. Argentina, MD Danny Mena 1, MD Carlos Ferrarotti 1, MD Juan Cruz Gallo 1, MD Nebil Larrañaga 1, MD Horacio Bignon 1,3, Hugo Corradini 1, Ph Amalia Perez 2, Ph Alejandro Valda 1 MD Ana Tangari Saredo3 1 Hospital Universitario CEMIC. Buenos Aires. Argentina2Escuela de Ciencia y Tecnología. Universidad Nacional de San Martín3 Sanatorio Güemes.

ARGENTINA

Congenital hyperinsulinism (CHI) results from an inappropriate insulin secretion by pancreatic - cells leading to hypoglycemia. Diagnosis of CHI is based on elevated plasma insulin and suppressed OH-butyrate during The hypoglycemia and/or increase of plasma glucose after the injection of glucagon. Some patients normalize glucose level under medical treatment, others require pancreas resection. The pattern of histopathological lesions can be diffuse or focal, which are differentiated by ^{18}F DOPA PET-CT. When it is focal CHI, limited resection is curative, whereas diffuse involvement frequently requires extensive pancreatectomy, which implies higher risk of long standing diabetes mellitus.

Objective: To present a patient with CHI, who as a result of a PET scan with ^{18}F DOPA underwent a curative partial pancreatectomy. Case report: A 5-day-old girl was admitted in the Neonatology Unit with a history of seizures associated to low blood glucose (24 mg/dl) during the first day of life. Parents were not related. Born at term after an uneventful pregnancy . (Apgar:9/10). At birth, weight, length and head circumference were normal, as well as post natal weight gain. No dysmorphic features were noticed. Glucose infusion rate required to maintain normal blood glucose was three times the usual requirement.Laboratory during hypoglycemia: Glucose 36 mg/dl, Insulin 11.2 uUI/l (NV‹1) GH 33ng/ml (NV›20), Cortisol 32 ug/dl (NV›18), Ammonia 56 uMol /l (64-107), -hydroxybutyrate:0.07mmol/l (NV: 0.03 to0.35 in normoglycemia), urinary ketone bodies were negative. Free fatty acids: 0.25 mmol/l (NV0.1-0.9 in normoglycemia). Due to unresponsiveness to medical maximum doses of Diazoxide and octreotide, a 18F-DOPA PET imaging was performed. A focal uptake at the tail of pancreas (SUV Max 3.3) was seen in PET TC. The rest of the pancreas showed normal uptake (SUV Max 1.8). A little non specific distortion in the morphology of the tail of the pancreas was seen on the CT Scan showing enhacement in PET Scan A paternally inherited heterozygous ABCC8 mutation (p.R598X; c.1792C>T) was identified in the patient, consistent with focal hyperinsulinism diagnosis. Laparoscopic proceeded with a frozen biopsy showed, one located node in the tail of the

pancreas . It was decided to perform a body and tail pancreatectomy with conservation of the spleen.Post-operative blood glucosa was normal. Conclusions: ^{18}F -DOPA PET CT enables identification and subsequent limited resection of an abnormal pancreas, preserving normal tissue and thus avoiding diabetes in this patient.

WHOLE BODY FDG-PET/CT IMAGING IN A PREGNANT WOMAN – IS IT SAFE?

J Welch1, P U1, S Berlangieri1, ST Lee1, K Pathmaraj1. Australia, A Scott1

1 Centre for PET, Austin Health, Victoria, Australia

AUSTRALIA

Background: Due to the radioactive nature of Nuclear Medicine imaging, it is usual practice to avoid it in pregnant patients. However, pregnancy need not be considered an absolute contradiction for nuclear medicine procedures, provided there are clinical justifications. We recently received requests for whole body PET/CT scans to be performed in two pregnant women with malignant disease for staging. After careful consideration, the decision was made that there was sufficient medical justification to proceed with the PET/CT studies, assuming that there were no significant detrimental effects on the foetus. Aim: To prepare a PET/CT protocol for pregnant patients that will deliver the lowest possible radiation exposure to the foetus whilst providing a diagnostic quality image. In addition, to calculate the radiation exposure to the foetus so that potential adverse effects to the foetus can be taken into consideration. Methods: For both patients, the following factors were considered: would the PET/CT scan provide the required information, alternative tests available, gestational age of the foetus, estimated radiation exposure and potential radiation risks to the foetus. In both instances, consensus was reached that PET/CT scan was the best modality to stage their disease. The Radiation Safety Officer calculated the estimated absorbed dose to the patient and foetus based on an altered PET/CT protocol that involved a low dose CT and administration of 100MBq of ^{18}F-FDG. Results: The estimated absorbed dose to the fetus was calculated as 6.58mGy when utilizing the altered PET/CT protocol. According to the IRCP84 publication, this translates to a 0.3-0.4% chance of the child developing cancer from this procedure and "malformations due to radiation probably do not occur at fetal doses less than 100–200 mGy".Conclusion: In both instances where the FDG-PET/CT scan was performed, the benefits of staging with PET/CT outweighed the risks of fetal radiation exposure and the scan findings provided information to the referring oncologists which significantly impacted on the patient's subsequent management.

INVASIVE DUCTAL BREAST CANCER STAGE MAY BE PREDICTED BY SUVmax ON 18F-FDG-PET/CT

Elba Etchebehere.

BRAZIL

^{18}F-FDG PET/CT (FDG-PET/CT) has become an integral part of primary staging of invasive ductal carcinoma of the breast (IDCB). Although quantification (SUVmax) is widely used to evaluate response to therapy, its use for patient staging is still a matter of debate. Objective: Evaluate if the SUVmax of the primary tumor and nodal metastases can predict patient stage and histopathological findings.Methods: Ninety-one women ages 53.1 ± 13.95 years, with locally advanced IDCB underwent FDG-PET/CT for primary staging. All patients underwent an FDG-PET/CT study for initial staging and the SUXmax of the primary tumor and nodal metastases was obtained. Post-operative histopathology findings confirmed the final stage. All equivocal lesions suspicious for metastases were confirmed with biopsy. To compare the primary tumor SUVmax and nodal SUVmax with more than two categorical variables the ANOVA was used; with one or two categories, the parametric Student's t-test was applied. The Spearman correlation coefficient was used to compare the primary tumor SUVmax to numerical variables. To compare two dependent categorical variables with more than two categories the nonparametric McNemar Bowker test was used; with one or two categories the McNemar test was used. Results: Univariate and multivariate analyses showed a significant correlation of primary tumor SUVmax with clinical stage ($p<0.0002$) and histological findings: nuclear grade ($p<0.0001$), negative PR ($p<0.0005$), negative ER ($p<0.0009$), triple negative ($p<0.0013$), Ki-67 ($p<0.0003$) and tumor size ($p<0.0002$). The higher the primary tumor SUVmax, the greater the final patient clinical stage. Lymph node SUVmax was significantly lower for clinical stages N0/N1 than N2/N3 ($p<0.0001$).

Conclusion: The SUVmax of the primary tumor has a strong relationship with tumor aggressiveness. Tumor SUVmax is useful to predict the final clinical stage of patients with invasive ductal breast cancer, which can very helpful while reading and interpreting FDG-PET/CT studies. In addition, the axillary lymph node SUVmax has a strong correlation with post-surgical nodal status, which may help plan surgical treatment of these patients.

PERFORMANCE OF SPECT/CT FOR 99MTCBESILESOMAB-LABELED LEUKOCYTE IMAGING

Bernardo Sanches Lopes Vianna.

BRAZIL

Background: This retrospective study evaluated the effect of the of SPECT/CT imaging on the diagnostic accuracy of ^{99m}Tc-Besilesomab-labeled leukocyte scintigraphy.

Methods: Labeled leukocyte scans of 47 patients performed between March 2013 and June 2014 were reviewed. All patients underwent whole-body planar and SPECT/CT imaging with ^{99m}Tc-Besilesomab-labeled leukocytes. The technique used was: whole body and SPECT / CT of all areas of interest 3-6 hours after leucocyte-labeling in vivo. When necessary an additional acquisition was performed 24 hours after the initial injection. We analyzed the clinical and Scintigraphic findings. We also done telephone follow-up with referring physicians. The equipment used was Symbia T2, Siemens.

Results: The mean age was 65.4 ± 19 years, 28 (59.6%) women. Of these, 24 (51%) were inpatients. Clinical indications for the exam were: 14 patients of fever of unknown origin, 13 patients with suspected osteomyelitis, 6 patients with abdominal conditions, 4 patients in the search for the etiology of sepsis, 3 patients with suspected prostatitis, 3 patients with suspected encephalitis, 2 patients with suspected endocarditis and 2 patients with suspected mediastinitis. Scintigraphic findings were positive in 23 of 47 cases (49%). Of the 23 patients who tested positive for infectious focus takes most, 14 cases, were in use of antibiotics at the time of scintigraphy. There were 9 deaths in the sample, and the test was positive in 6 of these. There were 8 surgeries guided by scintigraphy findings. In case in spite of normal findings surgery was undertaken and aseptic loosening of hip prostheses were confirmed. There was a change in medical management of 29 of 47 patients (62%) after performing scintigraphy. Conclusions: Hybrid SPECT/CT ^{99m}Tc-Besilesomab-labeled leukocyte scintigraphy is very useful in patients with suspected infection. In spite of the use of antibiotics we observed a good diagnostic accuracy.

INTERACTION OF "NATURAL THERAPIES" IN ONCOLOGIC PET-CT, MICRONIZED ZEOLITE INTERFERENCE WITH GA68-DOTATATE DISTRIBUTION

Rodrigo Jaimovich.

CHILE

An increasing number of oncologic patients that are on traditional therapies such as chemotherapy or radiotherapy, often are using other therapies known as "natural" or "complementary". Patients take these natural therapies with the belief that it will not interfere with the traditional ones, improving their confidence on the healing process. Micronized Zeolite is one of the so called "natural therapies", as it is a mineral compound obtained from volcanic ash, and is mainly described as a useful element to remove the heavy metals and toxins from the body due to its chelative properties.

These Micronized Zeolites have been recommended as a useful supplement to integrate into oncological treatment programs. We present a patient that came to our center for a Ga68-DOTATATE PET-CT for a neuroendocrine tumor staging. After the usual 100 MBq injection of the tracer and a 60 min time lapse, we acquired vertex to upper thigh images, and noticed an abnormal distribution of the tracer, seeing cardiovascular pool and no somastatin receptor uptake on pituitary, thyroid, liver, spleen or adrenal glands that are normally seen on Ga68-DOTATATE scans. Suspecting a labeling issue, we asked our suppliers to send a new dose from another batch and rescheduled the patient for the next day, obtaining exactly the same abnormal distribution. The quality control from both doses showed a very high radiochemical purity, with no abnormalities. Upon a new interrogation, the patient told us he was taking 8 pills of Micronized Zeolites daily for the last two weeks, so we decided to suspend this treatment for one month and then repeat the PET-CT, that finally showed the typical biodistribution of Ga68-DOTATATE. The main component of Micronized Zeolites are Clinoptilolite: $(Na, K, Ca)_6(Si, Al)_{36}O_{72}$-$20H_2O$ and Heulandite: $CaAl_2Si_7O_{18}$, that act mainly as catalysts, ion-exchangers and adsorbents. These properties have made them useful as detoxifiers of heavy metals, including radioactive ones, and also a as buffer in order to balance the system pH. We were able to submit a sample of this Micronized Zeolite to our radiopharmaceutical supplier, who then performed an in vitro assay that demonstrated a 40% binding of the Ga68-DOTATATE to the zeolites.

This experience shows the need to take in consideration all the possible interactions from the so called complementary or natural therapies in our clinical setting, due to the possibility of abnormal distribution such as our patient's case, or even as a potential interference with traditional therapies.

FIRST USE OF SN117M-DOTA-ANNEXIN AS A NOVEL VULNERABLE PLAQUE TRACER IN HUMANS

Rodrigo Jaimovich.

CHILE

Background: Cardiovascular Atherosclerotic Disease (CAD) is one of the most important and common causes of death and disability, especially when it is associated with the rupture of unstable or vulnerable atherosclerotic plaques. Annexin-V, found on the inner cell membrane, specifically binds to phosphatidylserine (PS). When cells undergo apoptosis, the PS is exposed for binding. The targeting molecule developed for vulnerable plaque (VP) imaging and therapy is [tin-117m]-DOTA-annexin (TA). Due to its nuclear and physical properties (t½ 14days, emission of an imaging photon as well as therapeutic conversion electrons), Sn-117m labelled Annexin-V could be particularly useful for the non-invasive imaging and treatment of CAD. We report the first human use of TA for imaging.Methodology: All studied patients had carotid artery stenosis (CAS), and were candidates for carotid endarterectomy (CEA). The first part of the trial involved 6 patients and the second part 9 patients. For the first part of the study a dose of 500 μCi (18MBq) cGMP TA was used to determine dosimetry and biodistribution. The second part of the trial was performed with 3 mCi (111 MBq) of the tracer (determined by the first part's organ toxicity results) in order to enable a better image quality. All patients were followed with scintigraphic images up to 14 days after the injection. Blood and urine samples were collected to establish blood clearance and urinary excretion. Complete haematological, renal, biochemical and liver parameters were measured in blood weekly until 4 weeks after injection. All patients underwent endarterectomy and both groups had optical, autoradiography and histology data from excised carotid plaque tissue.

Results: Tracer activity in blood cleared after 24 hours. Urine tracer excretion at day 7 was less than 5% of total urinary activity. Scintigraphic images showed mild bone marrow uptake, moderate spleen uptake and high initial uptake in liver and kidneys. Kidney activity decreased after one week and disappeared at 2 weeks. There was no change in uptake pattern in bone marrow, liver and spleen during the two-week period of observation. In three patients bowel activity was seen in the delayed images. No significant clinical changes or blood test abnormalities were detected. Imaging of atherosclerotic plaques was not achieved at these doses, although tissue analysis confirmed the presence of the tracer on all inflammatory plaques. TA uptake was seen in one patient with an abdominal aortic aneurysm (see Figure) and other with a previous surgical procedure at the lumbar spine.

Conclusion: A novel anti-inflammatory tracer, specifically targeting vulnerable/unstable atherosclerotic plaque, is presented. Biological safety and imaging capability is demonstrated. These preliminary results showed selective uptake of TA in cardiovascular VP and other inflammation sites.

RISK CLASSIFICATION ATTENDING TO MOLECULAR SUBTYPES OF BREAST CANCER: DOES ANY RELATION WITH 18F-FDG PET/CT EXIST?

Ana María García Vicente.

SPAIN

Aim: To determine whether metabolic features of breast tumors assessing by ^{18}F-FDG PET/CT differ from risk classification attending to molecular subtypes.Methods:144 women diagnosed of locally advanced breast cancer were prospectively evaluated. One patient had bilateral breast lesions. PET/CT was requested in the initial staging previous neoadjuvant treatment (multicentre study, FISCAM grant).All the patients underwent an ^{18}F-FDG PET/CT with a dual-time-point acquisition. Both examinations were evaluated qualitatively and semiquantitatively with calculation of SUVmax values in PET-1 (SUV-1) and in PET-2 (SUV-2) and the percentage variation of the standard uptake values or retention index (RI) between PET-1 and PET-2 in the breast tumor.The biological prognostic parameters, such as the hormon receptor status, HER-2 expression, proliferation rate (Ki-67) and grading were determined from tissue of the primary tumour. Tumor subtypes were classified, following the recommendations of the 12th International Breast Conference, by immunohistochemical surrogates as luminal A, luminal B-HER2(-), luminal B-HER2(+), HER2(+) or basal. Furthermore, patients were classified as follows: low risk (luminal A), intermediate risk [luminal B-HER2(-) or luminal B-HER2(+)] and high risk [(HER2(+) or basal]. Metabolic semiquantitative parameters with molecular subtypes and risk classification were correlated by means of pairwise comparisons with Bonferroni method.

Results:Tumors were classified as luminal A (15), luminal B-HER2(-) (46),luminal B-HER2(+) (26),HER2(+) (18) and basal (31). Attending to the risk groups, tumors were classified as low (16), intermediate (78) and high risk (51).Statistical differences were found between the SUV-1 and SUV-2 and the different subtypes with greater SUV values in HER2(+) and basal tumours. No statistical differences were found with respect to the RI (p=0.98).We found significant differences between low and high risk categories ($p < 0.0013$ in both SUV cases) and 2-3 ($p < 0.036$ in both SUV cases). The median values±SD of SUV-1 vs SUV-2 were of 4.58±4.18 vs 5.23±4.80; 7.13±5.12

vs 8.13±6.48 and 9.70±6.38 vs 11.58±7.87 for risk categories low, intermediate and high respectively.

Conclusion: Glycolytic tumour characteristics assessed by ^{18}F-FDG PET/CT showed a significant correlation with risk classification based on the molecular phenotypes, with greater SUV values in more biologically aggressive breast tumors. Our results support a relation between molecular and glycolytic phenotypes.

RADIATION DOSE AND PHARMACOKINETIC ANALYSIS OF MOLECULAR PROBE 131I-RRL TARGETING TUMOR ANGIOGENESIS

Rong Fu Wang 1*. China, Qian Zhao 1,2 Lei Yin 1, Ping Yan 1

1.Department of nuclear medicine, Peking University First Hospital, Beijing 100034 China
2.Department of nuclear medicine, General Hospital of Ningxia Medical University, Yinchuan 750004 China.

CHINA

Objective The 131I-tRRL small peptide probe has been identified as a robust tumor molecular radiopharmaceutical that specifically binding to tumor derived endothelial cells in our `previous study. In this study we estimated the radiation absorbed doses of ^{131}I-RRL as a novel peptide probe on tumor angiogenesis molecular imaging in humans and its pharmacokinetic.

Methods ^{131}I-RRL was injected into mice via lateral tail vein. Biodistribution and in vivo imaging were performed periodically. Radiation dosimetry in humans was calculated according to the organ distribution in mice and the standard MIRD method using radioactivity-time curves for humans. Another group of mouse was used in SPECT imaging study. Rabbits were used in pharmacokinetics research.

Results The effective dose for the adult male was estimated to be 0.0293 mSv/MBq. SPECT protocols showed clear images of tumors. Pharmacokinetic analysis showed a quick absorption and a relatively slow distribution of ^{131}I-RRL.

Conclusion Administration of ^{131}I-RRL leads to a reasonable radiation dose burden and safety for human use. A better pharmacokinetic characteristic was shown. All these results reveal the potential use of ^{131}I-RRL as a radiopharmaceutical in treating malignancies.
[Key words] ^{131}I-RRL, Molecular probe, Radiation absorbed doses, SPECT imaging, Pharmacokinetic

CLINICAL UTILITY [68GA] LABELED PSMA, IN CARCINOMA PROSTATE

Dr K.G.Kallur. India, Dr Prashanth, Dr Rajkumar, Dr Nagaraj, Dr Shivakumar Swamy, Dr Indiresh Desai, Dr Sathish, Dr Sridhar , Dr Ajaikumar.

INDIA

Purpose of the study: The aim of the study was to investigate PSMA clinical utility in all clinical scenarios such as initial diagnosis, staging, restaging, radiotherapy planning, and identifying castrate resistance. Also, in follow up of Carcinoma Prostate to evaluate response to hormonal therapies, chemotherapies or combination therapies.

Positron Emission Tomography (PET) with choline tracers is used widely for the diagnosis of prostate cancer (PC). Prostate-specific membrane antigen (PSMA) is a cell surface protein with high expression in prostate carcinoma cells. Recently, procedures have been developed to label PSMA ligands with 68Ga, Zr89,99mTc and 123/124/131-I. Our initial experience with Glu-NH-CO-NH-Lys-(Ahx)-[68Ga (HBED-CC)](68Ga-PSMA) suggests that this novel tracer can detect prostate cancer and metastases with high contrast.Materials and methods: A total of 478 Ga68 PSMA tests were performed in various clinical scenarios, out of which C11- Choline and Ga68 PSMA were both performed on a small percentage of patients. The comparison was evident that Ga68 PSMA revealed better information and better images. Data was analyzed with respect to upfront staging, restaging, radiotherapy planning, response evaluation for varieties of therapeutic options and castrate resistance.Summary and conclusion of study : Ga68 PSMA is beneficial in staging , early detection of recurrent Prostate Cancer , Radiotherapy planning and response evaluation for various therapeutic modalities.

Choline metabolism is not increased in a considerable number of cases during recurrences and makes it challenging for early detection. Currently there is no reliable radiological test which can identify prostate cancer recurrence at low PSA levels . Patients may benefit immensely with therapeutic options, when diagnosed early with Ga68 PSMA.

EVALUATION OF A NEW 99MTC-BOMBESIN ANALOG IN DIFFERENTIATION OF MALIGNANT FROM BENIGN BREAST TUMORS

Davood Beiki1. Iran, Babak Fallahi1, Fatemeh Karami1, Ahmad Kaviani2, Iraj Harirchi2, Ramesh Omranipour2, Mostafa Erfani3, Saeed Farzanefar1, Armaghan Fard-Esfahani1, Alireza Emami-Ardekani1, Mohsen Saghari1, Mohammad Eftekhari.

1 Research Center for Nuclear Medicine, Tehran University of Medical Sciences, Tehran, Iran
2 Department of Surgery, Imam Khomeini Hospital Complex, Tehran University of Medical Sciences, Tehran, Iran
3 Nuclear Science and Technology Research Institute, Atomic Energy Organization of Iran (AEOI), Tehran, Iran

IRAN

Objective: The gastrin releasing peptide receptor (GRPR) is overexpressed in a variety of common human tumors. Radiolabeled bombesin analogues have exhibited high binding affinity for these receptors. The aim of this study was to assess the value of a new ^{99m}Tc -bombesin analog in the differentiation of malignant from benign breast tumors.Materials and Methods: ^{99m}Tc-bombesin scans were performed in 17 patients with breast tumor. Post-injection of 20 mCi ^{99m}Tc-bombesin, planar dynamic images of chest were acquired. SPECT/CT images of the chest were also obtained. Subsequently, whole-body planar scans were carried out by one- and four hours of radiotracer injection. Definite diagnosis was based on excisional biopsy and histopathological examination.

Results: Thirteen patients demonstrated breast carcinoma and 8 patients were diagnosed as benign lesions. 11 out of 13 patients with breast carcinoma showed radiotracer uptake in the breast lesion. Nine out of 13 patients with breast carcinoma showed axillary lymph node involvement from which only two revealed radiotracer accumulation in the axillary lesion. All patients with benign lesions revealed negative scan. Delayed planar whole body images showed no additional diagnostic information in comparison to one-hour images. The sensitivity, specificity, PPV and NPV of 99mTc-bombesin scan were 84.6%, 100%, 100% and 80%, respectively.

Conclusions: Our data suggest that ^{99m}Tc-bombesin SPECT imaging could be useful in detection of primary breast cancer.

18 FES PET/CT IMAGING IN PATIENTS WITH RECURRENT BREAST CANCER: INITIAL EXPERIENCE IN THE NATIONAL INSTITUTE OF CANCEROLOGY OF MEXICO.

Violeta Ofelia Cortes Hernández Md.

MEXICO

Breast Cancer constitutes a major public health issue globally with over 1 million new cases diagnosed annually, resulting in over 400,000 annual deaths.Approximately 75% of breast tumors express estrogen receptor at diagnosis. The level of estrogen receptor expression in breast cancer has important prognostic information and helps to predict the possibility of response to the therapy. ER expression is routinely measured in clinical practice by in vitro assay of biosy material. 18F-FES PET-CT is a molecular imaging modality can be used to assess regional in vivo ER expression and can overcome the sampling errors that arise from disease heterogeneity (2, 3).

During metastatic disease, evaluation of estrogen receptor (ER) status is important to determinate changes in receptor expression, this is relevant because the discordant ER expression between primary tumor and metastatic lesions occurs in 18-55% and 36% of the patients present a loss of ER expression in distant metastases, which is a predictor of poor response to anti-hormonal therapy. Objective:The aim of this study is to show the primary experience of the usage of 18 F-FES PET during the evaluation of patients with suspected breast cancer recurrence, as well as the importance of the results obtained with this molecular imaging modality in the therapy decision of the patients.

Results:Six patients with suspected breast cancer recurrence were evaluated with 18F-FDG and 18 FES-PET CT imaging. 18 FES PET was negative in two patients and in the remaining patients (4 patients) estradiol molecular imaging provides additional information and as a result, the therapeutic choice was affected. Discussion:18 F-FES PET/CT estradiol is a method to obtain molecular information about ER expression. This molecular imaging tecnique can provide additional information in patients with estrogen receptor positive breast cancer in cases where conventional imaging is not conclusive. There has been shown that this modality can detect ER positive lesion with high specificity. The use of 18 FES-PET could lead to change in management in 48% of the patients.

Conclusion: With this initial experience with 18 FES-PET/CT imaging diagnosis, we conclude that it is an important tool to evaluate the extension of the disease specially in patients with luminal molecular subtypes of breast cancer with suspected recurrence and with negative conventional imaging studies. The use of this imaging modality can affect the therapeutic decision and improve the understanding of the disease.

18F-FLUOROTYMIDINE PET/CT SUVMAX LEVEL DETERMINATION IN CNS TUMORS

Jose R. Fernandez Soto, México.

Fernández Soto José Rodrigo, Rodríguez Cabrera Sergio Adán, Rivera Bravo Belén, Gama Moreno Manlio Gerardo, Torres Flores Yuririan, Altamirano Ley Javier.

Unidad PET/CT Ciclotrón UNAM. Edificio de investigación PB Facultad de Medicina, Ciudad Universitaria, C.P. 04510, México, D.F.

MEXICO

Introduction: central nervous system tumors in adults represent less than 2% of all neoplasms; in children are in second place. ^{18}F-Fluorotymidine correlates with tymidinekinasa1 activity, enzyme expressed during DNA synthesis (G1 and S phases of cellular cycle). The ^{18}F-FLT PET/CT is an ideal method for the evaluation of these tumors.Objective: Determine the SUVmax level to differentiate malign from benign lesions, the target/background ratio, and the SUVmax level of physiologic concentration of the radiotracer in bone marrow.

Material and methods: 78 ^{18}F-FLT PET/CT studies were analyzed retrospectively, realized in 2 years in the PET/CT Ciclotrón Unit of the Medicine Faculty, UNAM, in patients with diagnosis of SNC tumors.

Results: ^{18}F-FLT PET/CT lesions with SUVmax greater than 1.14 (±0.70), and target/background ratio greater than 3.6 (±2.24), were positive for cellular proliferation activity, regardless the tumor grade. The SUVmax average of bone marrow concentration was 3.2 (±0.48).

Conclusions: to determine the SUVmax level of ^{18}F-FLT to differentiate malign from benign lesions in SNC, gives information about the tumoral grade. Being a not invasive method that correlates with the cellular proliferation activity, allows the evaluation of the extension of the disease, outcome predictor, and to evaluate the response to treatment. SUVmax greater than 3.2 (±0.48) in bone marrow can be considered pathologic.

USEFULNESS OF 68GALIUM-DOTATATE PET/CT IN THE EVALUATION OF NEUROENDOCRINE TUMORS. INITIAL EXPERIENCE IN MEXICO.

Dra. Ileana Lourdes Tovar Calderón*. México, Dra. Belén Rivera Bravo*, Dr. Manlio Gerardo Gama Moreno*, Dr. Javier Altamirano Ley*.

*Unidad PET/CT Ciclotrón UNAM. Edificio de investigación PB Facultad de Medicina, Ciudad Universitaria, C.P. 04510, México, D.F.

MEXICO

Introduction: neuroendocrine tumors (NET) overexpress somatostatin receptors (SR) in their cellular surface. The expression of this SR is determined by the histologic type and cellular proliferation grade of the tumor. The anatomic methods of imaging are not enough for detection of this pathology. ^{68}Galium-DOTATATE PET/CT can be an appropriate molecular imaging method for the evaluation of the SR expression of NET.Objective: describe the frequency and characteristics of NET in PET/CT assessing the usefulness of the radiotracer ^{68}Ga-DOTATATE.Material and methods: a descriptive, retrospective design was made in PET/CT Cyclotron Unit, Faculty of Medicine of the UNAM. 32 patients with confirmed NET by histopathology and evaluated by ^{68}Ga-DOTATATE PET/CT were included.

Results: 20 patients were female, 12 male, average age 44 years. The SUVmax for the positive studies was 20.73 (IC 95%: 1.00; 71.18), the average for physiologic SUVmax was 4.34 (IC 95%: 1.48; 6.80). ^{68}Ga-DOTATATE PET/CT was compared with the histopathology report giving an index of agreement (Kappa) of 0.737 (73.7%) (95% CI: 45.7, 1.01).

The predictive ability of ^{68}Ga-DOTATATE PET/CT was estimated reporting a sensitivity of 81.48%, specificity of 60%, positive predictive value of 91.67% and negative predictive value of 37.5% for evaluation of NET. Conclusion: ^{68}Ga-DOTATATE PET/CT is a precise method for the evaluation of NET, by staging, re-staging and follow up of patients with this pathology.

TGF-ß1 AND IL_1 BETA INDUCES IL-6 AND IL-8 RELEASE IN COLON CANCER CELLS (LOVO) THROUGH ERK1/2, P38, JNK AND NF-KB PATHWAYS: THE ROLE OF DEXAMETASONE TREATMENT

Abdelhabib Semlali1. Arabia, Omair Al- Shahrani1, Maha Arafah2, Abdulrahman M Aljebreen2, Othman alharbi2, Majid A Almadi2, Nahla Ali Azzam2, Mahmoud Rouabhia3 and Mohammed Al-Anazi1.

1Genome Research Chair, Department of Biochemistry, College of Science King Saud University, Riyadh, Kingdom of Saudi Arabia
2College of Medecin, King Saud University, Riyadh, Kingdom of Saudi Arabia
3Groupe de Recherche en Écologie Buccale, Département de stomatologie, Faculté de Médecine Dentaire, Université Laval, Québec, Québec, Canada.

CANADA

Animal models and epidemiological study suggest that a continuous inflammatory condition predisposes to colorectal cancer (CRC), but the roles of different elements participating in inflammatory responses have been little investigated in relation to CRC. Human colon epithelial cells as Lovo contribute to colorectal cancer inflammation by secreting cytokines, chemokines, and growth factors, including interleukin (IL-6), (IL-8), (IL-1 beta) and so on, and transforming growth factor (TGF-ß1), all of which are elevated in colorectal cancer disease . In this study, we examine the signaling pathways leading to TGFb1 induced IL-6 and IL-8 in epithelial colorectal cells (Lovo). Material and methods: In Vivo, the cytokines inflammatory expression levels were evaluated by real time PCR and by Immunohistochemistry from 40 colorectal cancer tissues compared to 40 colon normal tissues. In vitro, the Lovo cells were stimulated with 5 ng/ml of the TGF-ß1 in the presence or absence of signaling inhibitors. IL-6 and IL-8 protein expression were measured by ELISA, mRNA expression by real-time PCR and the phosphorylation pathways by BREET. Results: IL-6, IL-8 and IL-17 expression were strongly expressed in colon cancer compared to normal tissues and TGF-ß1 increased IL-6 and IL-8 production in colon cancer cells; however, the Inhibition of ERK1/2,p38, JNK MAP kinase and NF-kB reduced TGF-ß1 induced IL-6 and IL-8 in Lovo cell . Using dexametasone treatment we demonstrated that dexametasone reduces the inflammation caused by TGF-ß1, but have a major drawback; dexametasone treatment increase the colon cancer cell proliferation. We conclude that the ERK1/2, p38, JNK and NF-kB pathways were the predominant TGF-ß1 signaling pathway involved in colon cancer inflammaton, and the Smad pathway is altered in colon cancer. Understanding the mechanism of aberrant pro-inflammatory cytokine production in colon cancer is will allow the development of alternative ways to control colon cancer inflammation.

ROSAI DORFMAN DISEASE AND PET 18F-FDG FINDINGS

MD Danny Mena 1. Argentina, MD Maria Bastianello 1, MD Juliana Alderete1, MD Alberto Parra1, MD Carlos Ferrarotti 1, MD Juan Cruz Gallo 1, MD Nebil Larrañaga 1, MD Diego Rosso2 .

1 Hospital Universitario CEMIC. Buenos Aires, Argentina
2 Hospital de Clínicas "José de San Martin". Buenos Aires, Argentina.

ARGENTINA

Objetives:Rosai Dorfman`s disease is also known as sinus histiocytosis with massive lymphadenopathy. It is characterized by nonspecific clinical symptoms with fever, pharyngitis, malaise, weight loss and bilateral painless cervical lymphadenopathy; though axillary, inguinal, para-aortic and mediastinal nodes can be affected too. Sometimes extranodal involvement (43%) can be found, being the skin and renal parenchyma the most common locations. The diagnosis is confirmed by histopathological findings. There are no imaging studies that can identify the extent of extra nodal involement. There is no standard treatment. It is usually self-limited, however the presence of extranodal involvement determines a fatal resolution. Thus, the contribution of 18F-FDG PET is detecting lesions that can provide a diagnostic aid in identifying patients at increased risk versus those with high probability of spontaneous resolution. Methods:15 years old patient that 3 years before the Rosai Dorfman`s disease was diagnosed. He started with cervical node involvement and progressed one year later to abdominal, pelvic and inguinal nodes and extra nodal compromise in renal parenchyma. He was treated with steroids and chemotherapy. PET-CT 18F-FDG was required to evaluate other sites of involvement. For the PET-CT study the patient underwent fasting 6 hours, and was injected with 6.75 mCi of F18-FDG intravenously. PET images acquisition was performed at 87 minutes post injection, from the skull base to the feet. The examination was executed on a Philips Gemini True Flight with TOF (Time of Flight) and LYSO crystals.

Results:The 18F-FDG PET-CT showed multiple hypermetabolic masses in bilateral cervical region, upper and infraclavicular gaps, axillary, mediastinal, retroperitoneal, iliac chain and both inguinal regions, SUV MAX 12 (7.6 to 12); and extranodal compromise in occipital soft tissue SUV MAX 4.5.Conclusion:The findings of 18F-FDG are not specific for Rosai Dorfman`s disease. However it provides an important contribution in assessing the extent of disease, the response to the treatment, and the guidance for biopsy in unconclusive pathological cases.

68Ga-DOTATATE-PET/CT OUTPERFORMS 99mTc-HYNC-OCTREOTIDE AND WHOLE-BODY MRI FOR DETECTION OF NEURO-ENDOCRINE TUMORS – A PROSPECTIVE TRIAL

Etchebehere E1, Santos A1, Bezerra R2, Gumz B3, Vicente A1, Hoff PM 3, Corradi G2, Ichiki W1, Almeida Filho G1, Cantoni S2, Camargo EE1, Costa FP3.

Division of Nuclear Medicine and PET/CT 1
Division of Radiology 2 and
Oncology Center 3 Sirio Libanes Hospital; São Paulo, Brazil.

BRAZIL

The incidence and prevalence of NETs has been rapidly rising and therapy with radiolabeled-somatostatin analogues is increasing. Thus, there is a need for more sensitive imaging methods for staging and therapy planning. Given the different metabolic imaging methods, various tracers and emerging anatomic modalities to evaluate NET patients, a better understanding of the performance of each method is warranted, especially to establish the most appropriate patient work-up.OBJECTIVES: Compare NET lesion detectability between state-of-the-art modalities: 68Ga-DOTATATE-PET/CT, 99mTc-HYNIC-ocreotide SPECT/CT (SSRS-SPECT/CT) and whole-body diffusion-weighted MRI (WbDMRI). METHODS: Nineteen consecutive patients (ages 34 to 77 years, mean 54.3 ± 10.4 years, 9 females) were submitted to SSRS-SPECT/CT, 68Ga-DOTATATE-PET/CT and WbDMRI. The three imaging modalities were acquired with a maximum interval of 3 months between them and were blindly analyzed by separate teams. 68Ga-DOTATATE-PET/CTs images from head to feet were acquired forty-five minutes after injection of 185 MBq. SSRS SPECT/CT planar whole body and SPECT/CT images of the thorax, abdomen and pelvis were performed at 4 and 24 hours after injection of 185 MBq of 99mTc-HYNC-octreotide. All CT images were acquired with 130 kV, 15 mAs, 0.8 s and 2 mm slice thickness. WbDMRI images were obtained in the coronal plane using a body coil with a 1.5-T whole-body imager (Signa-HDx, GE Medical Systems, USA). The standard method of reference for evaluation of the performance of images was undertaken by the following criteria: consensus among investigators at the end of the study, clinical and imaging follow-up and biopsy of suspicious lesions. RESULTS: McNemar´s test was applied to evaluate lesion detectability of 68Ga-DOTATATE-PET/CT in comparison to SSRS-SPECT/CT and WbDMRI: a significant difference in detectability was noted for overall solid organs (p= 0.0253 and p= 0.383, respectively), pancreas (p = 0.0082 and p = 0.0455, respectively), gastrointestinal tract (p = 0.0082 and p = 0.0253), thoracic lymph nodes (p = 0.0253 and p = 0.0455) and bones (p = 0.0082 and p = 0.0143). Two unknown primary lesions were identified solely by 68Ga-DOTATATE-PET/CT, one in the duodenum and the other in the pancreas. 68Ga-DOTATATE-PET/CT, SSRS-SPECT/CT and WbDMRI demonstrated respectively sensitivities of 0.96, 0.60, 0.72; specificities of 0.97, 0.99, 1.00; PPV of 0.94, 0.96, 1.00; NPV of 0.98, 0.83, 0.88 and accuracies of 0.97, 0.86 and 0.91. Conclusion: 68Ga-PET/CT is clearly more sensitive for detection of well-differentiated NET lesions. Staging of NET patients should be performed with 68Ga-PET/CT and follow-up studies with WbDMRI. SSRS SPECT/CT should be used when 68Ga-PET/CT is not available.

ANALYSIS OF PET-CT STUDIES PERFORMED WITH 18F-CHOLINE

** Gonzalez J., **Fernández R. ** Carmona J., * Humeres P., * Bazaes R., **Cuevas D. González P.** Department of Imaging and Nuclear Medicine Santa Maria Clinic . ** University Hospital of Chile.

CHILE

Introduction: At the present time the PET-CT with 18F-choline is within the group of exams proposed for re-staging and treatment planning for suspected recurrence of prostate cancer.Objectives: To characterize patients with PET-CT study using 18F-choline in Department of Nuclear Medicine Santa Maria Clinic and correlate the results with clinical and imaging data and post-study therapy. Methods: We reviewed retrospectively 20 cases of PET-CT 18F-choline between July 2013 - May 2014. We analyzed their initial diagnosis, prostate specific antigen (PSA), results of other imaging studies and post-examination therapy. PET-CT 18F-choline: Philips Gemini TF, hybrid technology, with time of flight. Studies were acquired according to protocol, early images at 5 minutes after injection of the tracer and late images at 60 minutes from the skull base to the middle third of femoral diaphysis. Computed tomography with contrast medium was performed in late study.

Results: All male patients (n = 20), average age 63±8 years old. Average dose of 18F-choline administered 9.6 ± 2.4 mCi.The initial treatment of the patients was radical surgery in 80%. All had histological confirmation, in 15 cases the Gleason score was obtained being 6 to 15% and 7 in 50% of cases.95% of the patients were referred for re-staging with biochemical recurrence and one case was preoperative. PSA levels were 2.2 ± averaged 3.9 ng / dl. (Figure 1).Three patients (15%) had positive PET-CT study with average PSA 10.6 ± 4.1 ng/dl; of these 2 cases had radical surgery with lymphadenectomy and one received radiotherapy in prostate and pelvic lymphnodes.The PET-CT scan was negative in 85% of patients, average PSA of 1.2 ± 2.3 ng/dl. Posterior to the study 59% had local radiotherapy. In 15 of 20 patients, bone scan was performed for staging and/or monitoring, this was negative in all cases. In 4 cases MRI was performed in pelvis which was 100% concordant with PET-CT study.Conclusion: PET-CT with 18F-choline was positive in 15% of patients showing local and distant involvement. We confirmed the significant association between a positive study and a level of PSA.

CARDIOVASCULAR

QUANTIFICATION OF LEFT VENTRICULAR FUNCTION DURING REST AND PHARMACOLOGICAL STRESS BY CARDIAC CT AND SCINTIGRAPHY: CORRELATION BETWEEN DIFFERENT METHODS

Wilter Dos Santos Ker, Daniel Neves, Christiane Wiefels, Sandra Marina Ribeiro de Miranda, Suzane Garcia Ferreira, Eduardo Castelo Branco, Thalita Gonçalves do Nascimento Camilo, Laura Vignoli Oliveira, Alair Augusto Sarmet Damas, Cláudio Tinoco Mesquita, Marcelo Souto Nacif.

BRAZIL

Objective: To identify the methods that best correlate the functional assessment at rest and pharmacological stress for myocardial scintigraphy (SPECT) and 64-slice CT.

Material and Methods: The Germano (G) and Emory methods (E) were studied by SPECT and simplified (QS) and modified (QM) Quinones methods by 64-slice CT (CT). For statistical evaluation we used Pearson correlation, the Bland-Altmann and t-test. The criterion for significance was P <0.05.

Results: The ejection fraction (EF) at rest by SPECT_G was 65 ± 15% and SPECT_E was 71 ± 13%. Using TC_QS the EF was 58 ± 16% and 55 ± 14% by TC_QM. The SPECT_G and SPECT_M has a moderate positive correlation with TC_QS and TC_QM (r> 0.55, p <0.001, for all). The EF between SPECT_G vs TC_QM were not significantly different at rest (p = 0.08). Using dipyridamole stress no EF measurement was different from each other when comparing SPECT vs TC (p> 0.05, for all) and the best correlation was between SPECT_G vs TC_QS (r = 0.76, p <0.001).

Conclusion: Our study showed that SPECT_Germano and TC_Quinones has the best correlation for stress and rest quantification by SPECT and 64-slice CT. Other methods will be better evaluated.

AN ADULT CASE STUDY WITH CORONARY ARTERY ANOMALIES

Ma. Amparo Pineda Tovar1, Alberto Ortega Ramirez1, Ramiro Nava Peña2.
1 Nuclear Medicine department, 2 Cardiology Hospital, National Medical Center. IMSS.

MEXICO

Anomalies of coronary artery are anomalous origination of a coronary artery from the opposite sinus and are associated with adverse cardiac events, typically in young individuals, it is reported that affect about 1% of the population. Anomalous Right Coronary Artery (RCA) appears in adults and suggests less risk than those of the Left Main Coronary Artery or Left Anterior descending coronary Artery.

The presence of an anatomical variant coronary pattern may have clinical consequences, like volume overload, aortic root distortion, bacterial endocarditis, and usually ischemia. This is a case study where initially ischemia was suspected. Three different methods of cardiac imaging identified in detail the coronary anomalies Method A 68 years old patient was referred for a SPECT-gated myocardial perfusion test with 99mTc- tetrofosmin and a stress test. The images were acquired with a gamma camera after de injection of 10 mCi (stress) and 20 mCi (Rest) of 99mTc-tetrofosmin. Tomographic images were reconstructed using Emory Tool Box. Stress Test Bruce protocol was suspended at minute three of first stage because the patient referred general state attack, nausea, diaphoresis, and numbness. The patient reached 90% of Maximum Specific Cardiac Frequency and 3 METS with high blood pressure response.

Results The scintigraphic image showed Lower Moderate Ischemia (fig. 1). The gated image showed good LV walls mobility, with LV eject fraction (LVEF) 78%, volume at end-diastole of 63 ml, volume at the end of systole of 13 ml, systolic volume, 50 ml showing left ventricular hypertrophy. Angiographic image (Fig. 2) showed bifurcated main trunk, left descendent artery with slow flow and circumflex artery is ectasic and not dominant, all without angiographic lesions. There is a fistula from distal RCA to pulmonary trunk artery. Ventriculography showed LV non-dilated with normal mobility, LVEF 65%, without mitral insufficiency. Cardiac angiotomography image (fig.3) showed dominant RCA with minimal diffuse atherosclerotic disease (25 %). The images showed in detail an anatomical variant in which the artery of the sinoatrial node is born from the distal segment of RCA with sinusoidal path.

Conclusion Coronary artery anomalies are a confusing topic in cardiology. In this case, scintigraphic imaging was conclusive for Lower Moderate Ischemia, but coronary angiography showed an image like distal RCA fistula. Later with cardiac angiotomographic, images showed in detail the anatomical variant in which the artery of the sinoatrial node is born from the distal RCA, with sinusoidal path.

CHARACTERIZATION OF ELECTROMECHANICAL COUPLING IN RIGHT BUNDLE BRANCH BLOCK THROUGH GATED-SPECT PHASE ANALYSIS.

Federico Ferrando. Departamento de Cardiología, Facultad de Medicina Montevideo, Uruguay.

URUGUAY

Introduction: Left ventricular mechanical dyssynchrony (LVMD) is commonly associated with left bundle branch block. However, some evidences suggest that other intraventricular conduction disturbances are also associated with LVMD of uncertain mechanisms. Recently, gated-SPECT phase analysis has been validated as a noninvasive and reproducible method to characterize electromechanical coupling through detection of site of onset of mechanical contraction and evaluation of LVMD phenomenon. Objective: To describe LV site of onset of mechanical contraction in patients with right bundle branch block (RBBB).

Materials and methods: We studied patients with RBBB with or without left anterior fascicular block (LAFB) by gated-SPECT 99mTc-MIBI and phase analysis at rest. Patients with extensive myocardial infarction were excluded. QRS duration, summed rest score (SRS), end-diastolic LV volume (EDV) and rest LV ejection fraction (LVEF) were documented. Using V-sync Emory Cardiac Toolbox we obtained phase standard deviation (PSD) and phase bandwidth (PBW) at rest, comparing these with a control population previously reported (Chen J, 2005). Values were presented as mean $\pm$ standard error of the mean. Segments of onset of LV contraction were recorded freezing video images in digital polar map at 90 - 150° phase onset of LV systole. Results: We included 23 patients, 15 men (65.2%), ranged from 50 to 94 years (69.8 $\pm$ 2.2 years). Mean QRS duration was 145.5 $\pm$ 4.5 ms in patients with LAFB and 139.4 $\pm$ 2.3 ms in patients without LAFB. There were no statistically differences in SRS, EDV and LVEF between these groups. Both RBBB groups exhibited significant LVMD according to phase analysis parameters ($P < 0.05$). Patients without LAFB tended to show increased values of LVMD parameters (PSD: 29.1 $\pm$ 3.7 degrees in patients with LAFB, 34.7 $\pm$ 3.1 degrees in patients without LAFB; PBW: 81.3 $\pm$ 13.0 degrees in patients with LAFB, 92.1 $\pm$ 15.0 degrees in patients without LAFB). The onset of LV contraction was distributed in three main LV regions: apical and septal (R1), mid and basal inferior (R2) and mid and basal anterolateral (R3). Most frequent site was R1 in both groups (62.5% vs. 73%), and differences in spatial distribution were mainly detected in R2 (37.5% vs. 7.0%) and R3 (0% vs. 20%).

Conclusions: Through gated-SPECT phase analysis, we demonstrated that patients with RBBB and no myocardial scar exhibited significant LVMD. Association of RBBB with LAFB could modify the site of onset of mechanical contraction. This innovative technique offers additional information about electromechanical coupling process in different ventricular conduction disturbances.

HEART RATE RESPONSE DURING DIPYRIDAMOLE INFUSION IS ASSOCIATED WITH CARDIAC EVENTS IN PATIENTS WITH NORMAL PERFUSION SPECT

Cecilia Bentancourt Institucion: Spanish Association Hospital Coautores: Mario Beretta, Miguel Kapitan, Nicolas Niell, Fernando Mut.

URUGUAY

Objective. Dysfunction of the autonomic system predicts cardiovascular risk and sudden death, especially in patients with type 2 diabetes, regardless of the presence of ischemic heart disease. Cardiac autonomic dysfunction is also a powerful predictor of risk for mortality after myocardial infarction in the general population. As heart rate response (HRR) to vasodilator stress can be a marker of HR variability reflecting the integrity of the autonomic system, we intended to define the prognostic value of HRR during dipyridamole test in a population of patients with suspected coronary artery disease but with normal SPECT myocardial perfusion imaging (MPI). Methods. A total of 845 patients were retrospective analyzed, in whom MPI SPECT imaging was performed in a two-day protocol. Pharmacologic stress included infusion of 0,56 mg/kg of dipyridamole over 4 min followed by IV injection of 99mTc-MIBI, which was repeated at rest. Gated acquisition was only performed at rest. HRR was calculated as the maximum percent HR change from baseline. Patients in the lower quartile of HRR were compared to those in the other quartiles regarding nonfatal MI or cardiac death at 5 years of follow-up. Results. A total of 237 patients (28%) had normal perfusion SPECT MPI (123 women, age 65±11 years), of which 60 (25.3%) had HRR<15% (lower quartile) compared to 177 with HRR≥15%. In the first group, 25 events were identified vs. 33 in the second group (41.7% vs. 18.6%, p<0.001). Diabetes was significantly associated with cardiac events (p=0.037), but was not a predictor of HRR. Rest left ventricular ejection fraction (LVEF) and stress-induced ST depression ≥1 mm were not independently associated with event rate nor were predictors of HRR. Interestingly, the presence of diabetes was not more common in patients with attenuated HRR using a cutoff at the lower quartile.

Conclusions. HRR provides significant prognostic information in patients with normal MPI with dipyridamole, and this variable seems to be even more powerful than ST changes or rest LVEF. Thus, a normal MPI result should be interpreted cautiously when associated with abnormal HRR with dipyridamole. Further work that assesses these results in diabetes patients with abnormal SPECT or known coronary artery disease is warranted.

ALTERNATIVE SEMIQUANTITATIVE EVALUATION FOR HEPATOPULMONARY SYNDROME WITH TC-99M MAA SCINTIGRAPHY

Yuh-Feng Wang, MD, PhD.
Institucion: Buddhist Dalin Tzuchi General Hospital. Tzyy-Ling Chuang, MD., Mei-Hai Chuang, PharmD, PhD.

TAIWAN

Objective: To establish alternative semiquantitative method of Tc-99m macroaggregated albumin (Tc-99m MAA) scan to diagnose hepatopulmonary syndrome with significant right-to-left shunt. Materials and Methods: Tc-99m MAA scan was performed in a patient of hepatopulmonary syndrome (HPS) diagnosed by contrast-enhanced cardiac echo. Another five normal subjects also received Tc-99m MAA scan and one of them receive contrast-enhanced cardiac echo which was normal. Another normal control received repeated scan due to injection loss. We calculated shunt index using several semiquantitative equations according to the literatures and our Chuang's method.Results: Chuang's method had significant difference between the patient and the normal subjects while other semiquantitative methods according to the literatures did not distinguish the two categories.Conclusions: Chuang's method of semiquantitative equation is simpler and may be helpful in the diagnosis of hepatopulmonary syndrome using Tc-99m MAA scan.

IMPACT OF MYOCARDIAL FIBROSIS IN CARDIAC SYNCHRONISM USING GSPECT

Christian Wiefels Reis.

BRAZIL

Objective: Evaluate the impact of fibrosis in contractile synchronism in patients with gated SPECT. Methodology: Sixteen myocardial perfusion imaging exams with Tc-99m sestamibi were analyzed in a university hospital: five normal exams (Group 1 - control), six with ischemic areas (Group 2 - reversible defects) and five with fibrosis (Group 3 - fixed defects). t-test compared the mean results between groups.

Results: Significant differences in the SD parameters and bandwidth in the resting phase were seen between Group 3 compared to Group 1 and between Group 2 and 3. There were no significant differences between group 1 and 2.

Conclusion: Myocardial fibrosis is a significant factor in determining contractile dyssynchrony.

SPECT AND 64-SLICE CT IN THE DETECTION OF MYOCARDIAL ISCHEMIA: A SINGLE STEP PROTOCOL USING DIPYRIDAMOLE IN THE CT SCAN ROOM

Wilter Dos Santos Ker.

BRAZIL

Objective: To evaluate the diagnostic ability of computed tomography (CT) in detecting significant perfusion defects identified by myocardial scintigraphy (SPECT).Material and Methods: This prospective study was approved by the ethics committee including all patients who complied with the inclusion and exclusion criteria and signed the informed consent term above this protocol. The injection of ^{99m}Tc-sestamibi during dipyridamole stress was performed in the CT room 40 ± 25 seconds before the acquisition of myocardial perfusion by CT. Multivariate logistic regression analysis was performed and the criterion for significance was $P < 0.05$. Results: Mean age was 57 ± 10.4 years, 64% were women. CT identified 92% of territories with perfusion defects detected by SPECT in segmental analysis ($p < 0.001$) and 100% of patients with perfusion defect analysis per patient ($p < 0.001$).

Anatomical assessment of CT angiography added in differentiating perfusion defects by significant stenosis (> 70%) of those related to the myocardial bridge. Segmental perfusion defects (8%) not detect by CT may be related to microcirculation or SPECT false positive results.

Conclusion: CT has good ability in detecting perfusion defects identified by SPECT, and can also provide important information about coronary anatomy.

EVALUATION OF ACUTE CHEST PAIN WITH RADIONUCLIDE MYOCARDIAL PERFUSION IN THE EMERGENCY ROOM

Gustavo Borges Barbirato. Brasil, Flávia Freitas Martins, Roberta Vasconcellos Ribeiro, Mariana Oliveira da Silva, Evandro Tinoco Mesquita, André Volschan, Jader de Azevedo Cunha, Nilton Lavatori Correa, Claudio Tinoco Mesquita.

BRAZIL

Studies Center Pró-Cardíaco Hospital (Cepro), Rio de Janeiro, RJ – Brazil

Background: The myocardial perfusion imaging obtained during episode of chest pain has been used as a diagnostic tool in decision making in the emergency department.Objective: To evaluate the accuracy of scintigraphy in patients with chest pain to rule out or confirm Acute Myocardial Infarction (AMI).

Methods: The charts of 25 patients admitted with chest pain or even six hours after the end of symptoms, electrocardiogram (ECG) nondiagnostic, who underwent measurement of troponins and scintigraphy at rest on the device IQ SPECT with attenuation correction were analyzed. Patients with previous myocardial infarction were not excluded. Troponin was measured at baseline and after six hours.

Results: Resting perfusion image was abnormal in 2 patients with AMI. The other 6 patients with abnormal perfusion had negative troponins (<0.16 pg/mL). There was no patient with normal imaging and positive troponin. Disease prevalence was 9%. The sensitivity of the resting images during chest pain to diagnose AMI was 100% and specificity was 70%. The negative predictive value was 100%.

Conclusion: In patients with chest pain and nondiagnostic ECG who present in the emergency department, the myocardial perfusion scintigraphy in early home had a high sensitivity and a good negative to the diagnosis of AMI predictive value. The use of this technique can also assist in screening patients in the emergency, reducing the length of hospital stay the same, as well as avoid unnecessary hospitalizations and optimize hospital costs.

RELATIONSHIP BETWEEN CORONARY COMPUTED TOMOGRAPHIC ANGIOGRAPHY AND MYOCARDIAL PERFUSION SCINTIGRAPHY WITH ATTENUATION CORRECTION AND IQ-SPECT IN EVALUATION OF HEART DISEASE

Allan Vieira Barlete.

BRAZIL

INTRODUCTION: Coronary computed tomographic angiography (Angio CT) has demonstrated high accuracy for detection of coronary stenosis. Although this technique is promising for the diagnostic of coronary artery disease (CAD), its correlation with the functional manifestation of the disease isn´t well established. Myocardial perfusion scintigraphy (MPS) associated with attenuation correction Computed Tomography (CT) - hybrid method - and converging collimator (IQ-SPECT) proposes a better functional assessment of CAD. This protocol reduces the dose of radiation administrated in patient and the period of time the patient remains in gama-camera, but no studies have evaluated its efficacy in the assessment of CAD. OBJECTIVE: The aim of this study is to understand if the presence of CAD and the degree of coronary obstruction assessed by Angio CT are associated with altered with attenuation correction and IQ-SPECT.

MATERIALS AND METHODS: This retrospective and observational study included 55 consecutive patients with known or suspected CAD diagnosed in MPS tests and Angio CT. We compared the presence of perfusion defects found out in MPS with the presence of CAD and degree of luminal obstruction found out in Angio CT. For statistical analysis Student's t test and chi-square test and significance criteria was set at 5% were used as reference.

RESULTS: Mean age was 55 ± 10.5 years, with 43 men (78.2%). The analysis of variables was performed per patient (n = 55) and coronary territory of irrigation (n = 165). 65% of patients with CAD found out in Angio CT showed altered SPECT (p = 0.005). In the analysis by territory, 14% of territories were considered normal or with no significant CAD when analysed in Angio CT, but when analysed in scintigraphy, there was abnormal findings. In those patients who showed moderate CAD in coronary territories in angio CT findings, 40% of the coronary territories showed the same finding in MPS and in those patients who was demonstrated several CAD, 75% of the coronary territories demonstrate a correspondent finding in MPS (p=0,05). The sensitivity of the MPS to detect CAD was 0.35, specificity of 0.88, PPV = 0.63 and NPV = 0.69.

CONCLUSIONS: The MPS with attenuation correction and IQ-SPECT shows high specificity for detection of CAD when compared to coronary Angio CT.

PATIENTS WITH SEVERE AORTIC STENOSIS HAVE COMPROMISED CARDIAC SYMPATHETIC INNERVATION AND CARDIAC SYMPATHETIC TONE PERFORMED BY MYOCARDIAL SCINTIGRAPHY WITH MIBG LABELED WITH IODINE-123

Allan Vieira Barlete.

BRAZIL

INTRODUCTION: The image of the cardiac adrenergic neurotransmission performed by myocardial scintigraphy with ^{123}I-MIBG (metaiodobenzylguanidine radiolabeled with iodine-123) is a noninvasive tool to assess cardiac sympathetic innervation and sympathetic activity in various heart diseases. The aortic valve stenosis (AS) is a serious health problem that impact on quality of life and survival of patients. In the literature there are few studies that evaluated cardiac sympathetic activity in this group of patients and none of them assessed the cardiac sympathetic activity using images and quantitative methods. OBJECTIVE: Evaluation of the pattern of cardiac sympathetic innervation and cardiac sympathetic tone in patients with severe AS with valve replacement and high surgical risk performing myocardial scintigraphy with ^{123}I-MIBG.

MATERIALS AND METHODS: Myocardial scintigraphy with ^{123}I MIBG was performed in patients with severe AS for analysis of cardiac sympathetic innervation. After intravenous administration of a dose of 185 MBq to 370 MBq (5 to 10 mCi) ^{123}I-MIBG, planar and tomographic images of the thorax in 20 minutes and 4 hours were acquired in SPECT-CT equipment Symbia T2 Siemens. A semiquantitative measure of myocardial uptake of ^{123}I-MIBG was obtained by calculating the ratio between the average activity per pixel in the heart area compared to superior mediastino (Co/Me), and the values were considered normal ratio Co/Me 20 minutes and 4 hours ≥ 1.80 and rate of clearance (washout) 27%.

RESULTS: Eight patients were evaluated between December 2010 and February 2014, six women and two men, mean age 79 ± 11.8 years. The mean ratio Co/Me 20 minutes was 1.59 ± 0.23. The mean ratio Co/Me 4 hours was 1.35 ± 0.19 and the mean rate of clearance (washout) was equal to 56 ± 0.15%.

CONCLUSIONS: Patients with AS have severe impairment of cardiac sympathetic innervation and increased cardiac sympathetic tone, and myocardial scintigraphy with ^{123}I-MIBG can measure directly, with high diagnostic accuracy changes in heart´s neurohumoral sympathetic control, caused by left ventricular overload promoted by the left aortic stenosis.

MYOCARDIAL SCINTIGRAPHY WITH MIBG LABELED WITH IODINE-123 IN THE EVALUATION OF PATIENTS SUBMITTED TO TAVI

Allan Vieira Barlete.

BRAZIL

INTRODUCTION: The aortic valve stenosis (AS) is a serious health problem that impact on quality of life and patients survival. Surgical valve replacement is a class I indication in patients with severe AS and with symptoms, however, not all patients can undergo aortic valve replacement due to high operative risk. As alternative, the transcatheter aortic valve implantation (TAVI) was criated. Despite of a promising result, it´s still a new and relevant procedure with important complications.

OBJECTIVE: The aim of this work is to observe the impact of TAVI in patients with severe AS at high risk for conventional surgery on cardiac sympathetic innervation and cardiac sympathetic tone by performing myocardial scintigraphy with ^{123}I-MIBG before and after the procedure.

MATERIALS AND METHODS: An observational longitudinal study, prospective, non-randomized, non-blind. Five patients with severe aortic stenosis, defined by one and two dimensional echocardiography and referred for TAVI due to the high risk of surgical valve replacement, were studied between 2010 december and 2014 february. Myocardial scintigraphic images were conducted before and after the procedure for comparison purposes. A semiquantitative measure of myocardial uptake of ^{123}I-MIBG was obtained by calculating the ratio between the average activity per pixel in the heart area compared to superior mediastino (Co/Me), and the values were considered normal ratio Co/Me 20 minutes and 4 hours ≥ 1.80 and rate of clearance (washout) 27%.RESULTS: Patients completed the images before the TAVI and one week after TAVI. Three women and two men, with a mean age of 77 ± 17 years were analyzed. The average of the heart/mediastinum (Co/Me) after 20 minutes was 1.47 (normal ≥ 1.80) and the Co/Me after 4 hours on examinations performed before TAVI was 1.23 and the rate of clearance (washout) was equal to 49% (normal 27%). Performing the Wilcoxon paired comparing the pre and post-implant found a statistically significant difference for the Co/Me 4 hours (1.23 vs 1.29, P = 0.042).

CONCLUSIONS: TAVI modifies the functional status of the cardiac adrenergic system. There was a statistically significant increase in heart/mediastinum 4 hours after implantation of TAVI. Patients with severe aortic stenosis at high risk for valve surgery with indication for TAVI have severe functional impairment of cardiac adrenergic innervation and increased cardiac sympathetic tone.

DOES THE THALLIUM DEFECT PATTERN IN MYOCARDIAL PERFUSION SCINTIGRAPHY DEPICT THE LEVEL OF STENOSES IN SINGLE VESSEL CAD INVOLVING THE LEFT ANTERIOR DESCENDING ARTERY?

Vishal Agarwal.

INDIA

Background: Coronary artery disease has shown massive progression in the last few decades. Apart from the urgent intervention required in the patients who luckily report in the 'golden hour', emphasis is being paid on the preventive measures, as well as on sensitive and easily available screening tests. Apart from being invasive, coronary angiography does not show the real effect of the stenoses on the myocardial blood flow. However, the myocardial perfusion scintigraphy shows the real ischemic burden on the myocardium. To correlate this reversible defect pattern and deduce some relationship with the level of stenoses, if possible; can be of good guidance to the clinicians, at least in single vessel disease patients.

Methods: We carried out this study in 326 patients out of 1200 patients, in the study period of 7 months, who had SVD involving the left anterior descending based on recent CAG done in the same hospital. Of these, 154 patients had proximal stenoses (proximal to and including first major septal branch - as per SYNTAX scoring for coronary stenoses), 68 patients had mid stenoses (after S1 origin to ½ of distance up to apex) and 104 had distal stenoses (terminal portion of LAD). The MPI was done with dual isotope protocol in our department by injecting 3 mCi of Thallium-201 at rest and 20 mCi of 99m-Tc-Sestamibi at peak exercise.

Results: Five patterns of reversible perfusion defects were identified: type I (apex, anterior wall and septum), type II (apex and septum), type III (antero-septal wall), type IV (apex and anterior wall) and type V (apex).

Conclusions: On correlating with the CAG findings available, proximal stenoses was most commonly related to type I, II and III (in 138 of 154), mid stenoses with type IV (in 54 of 68) whereas distal stenoses was related with type V (in 90 of 104). In the next phase of our study, we aim to validate our findings by reverse matching i.e the thallium reversible defect patterns to the CAG findings; and once this relationship gets established in the 'validation population', hopefully this recognition will be useful for identifying patients with angina who are likely to have proximal LAD stenoses.

QUANTITATIVE MYOCARDIAL BLOOD FLOW WITH (13)N AMMONIA PET/CT USING REGADENOSON AS STRESS PHARMACOLOGICAL AGENT

Dr K.G.Kallur. India, Dr Prashanth, Dr Rajkumar.

INDIA

Abstract: Regadenoson is a selective widely used A2A adenosine receptor agonist for pharmacologic myocardial perfusion imaging. However, clinical data of regadenoson with quantitative PET myocardial perfusion and (13) N ammonia remain very limited. We measured myocardial blood flow (MBF) with (13) N-ammonia and PET/CT at rest and during regadenoson induced hyperemia in patients with known coronary artery disease (CAD). Comparison was done with conventional angiographic findings.Methods : Regional MBF was measured in absolute units with (13)N-ammonia and non intravenous contrast-enhanced PET/CT at rest and during hyperemia (regadenoson iv. 0.4 mg bolus) in a total of 20 patients (15 males and 5 females mean age 55±10 years old) who had undergone conventional coronary angiogram. MBF was determined for each of the 3 major coronary territories. Results: Resting MBF was around 0.8±0.2 in all vascular territories in our patient population. During stress MBF was around 2.6±0.3 in normal vascular territories. MBF was around 1.6±0.23 in territories with significant CAD. Conclusions: Our study suggests that regadenoson can be used safely to quantitatively assess MBF with (13)N-ammonia in patients with CAD and it seems to correlate with the extension and severity of CAD. It is much easier to do the test compared to Adenosine.

ASSOCIATION OF ISCHEMIC HEART DISEASE ASSESSED BY CARDIAC PERFUSION SCAN WITH OSTEOPOROSIS AND VITAMIN D DEFICIENCY

Sina Izadyar.

IRAN

ABSTRACTI: ntroduction: Because of the increasing trends of both coronary diseases and vitamin D deficiency and also due to recent evidences on association between these two phenomena, it is vital to clear association of coronary disease with vitamin D deficiency and osteoporosis. The aim of the present study was to assess this relationship by a functional method using cardiac perfusion scanning.Methods: In this cross-sectional study, 204 consecutive patients aged > 50 years candidate for cardiac perfusion scan were included. Blood sample was extracted to measure the level of serum 25-OH vitamin D using a special kit (IDS kit). The patients were

assessed by perfusion scan using ADAC instrument. After a month of perfusion scanning, subjects underwent bone densitometry by DEXA method.Results: In overall, normal bone density, osteopenia, and osteoporosis was found in 11.8%, 46.6%, and 41.7%, respectively.The mean level of serum vitamin D was 22.7 ng/ml that 25% of patients had adequate level of vitamin D, 50% had inadequate level of vitamin D, and 24% of them suffered vitamin D deficiency. There was no significant difference in serum level of vitamin D between patients with normal perfusion scan and those with abnormal scan result (22 ± 17 ng/ml versus 25 ± 16 ng/ml, p = 0.29).In multivariate logistic regression model and with the presence of potential confounders including gender and body mass index, perfusion scan was not associated with osteoporosis status. Conclusion: Coronary atherosclerosis may not be associated with the severity of osteoporosis or level of vitamin D adequacy. Keywords: coronary artery disease, osteoporosis, vitamin D

INTRODUCTION: Association between low bone density and coronary artery disease remained challenging. According to some recent evidences, not only osteoporotic patients face with the bone fracture, but also may be exposed to increased risk for brain stroke, cognitive disorders, arterial atherosclerosis, and even cardiac-related death in both men and women [1-5]. However, the explaining reasons for this relationship remain unknown. Due to some common risk factors for both atherosclerosis and osteoporosis such as cigarette smoking, systemic inflammatory conditions, or postmenopausal status, common pathophysiological pathways for these two clinical conditions is expectable [6-9]. For instance, postmenopausal osteoporotic women significantly face with higher risk for coronary artery disease compared with other age subgroups of women [10-12].

One of the main causes of osteoporosis is vitamin D deficiency frequently due to inadequate sun exposure, low dietary intake, low physical activity, or air pollution [11,12]. It has been well shown that vitamin D deficiency can have deleterious effects on cardiovascular system [13-15]. Vitamin D receptors are widely distributed in different tissues including smooth muscles of vessels, endothelium, and also cardiomyocytes. In vivo study could reveal that 25-hydroxy vitamin D can directly inhibit expression of genes related to smooth muscle proliferation and cardiomyocytes as well as inhibit secretion of cytokines from lymphocytes [16-18]. Also, some experimental studies on animal models could show that the lack of vitamin D receptors activators can result in hypertension, and left ventricular hypertrophy [19]. Moreover, vitamin D deficiency may be accompanied with the increased level of parathyroid hormone led to insulin resistance that is a major cause of diabetes mellitus, activation of inflammatory processes as well as to coronary atherosclerosis [20-23]. Because of increasing trend of vitamin D deficiency and also osteoporosis, it is vital to clear association between coronary disease and vitamin D deficiency. The aim of the present study was to assess this relationship by a functional method using cardiac scanning. In previous studies, this association assessed using anatomical methods such as coronary angiography, measuring coronary calcification, and also CT angiography. However, in the present study, functional method of cardiac scan was employed to assess cardiac functionphysiologically, not alone anatomically. METHODS Study population:In this cross-sectional study, the consecutive patients aged higher than 50 years suspected to ischemic heart disease and candidate for cardiac perfusion scan at two Imam Khomeini and Shariatihospital between September 2012 and October 2013 were included into the study. The main exclusion criteria were history of fracture or prosthesis of the neck of femur, history of fracture or surgery on vertebralcolumn, any deformity that inhibited performing bone densitometry, the previous history of the use of corticosteroids (at least 15 mg for 3 months within two recent years), antiepileptic drugs, or levothyroxine.

Study measurements:After explaining different steps of the study to patients and obtaining written consent forms, baseline information including demographics, medical history and medications were collected by interviewing or by reviewing the recorded files. Blood sample was extracted to measure the level of serum 25-OHvitamin D using a special kit (IDS kit). Vitamin D deficiency was defined as serum 25-OH vitamin D level < 10 ng/ml. The patients were then assessed by perfusion scan using ADAC instrument to assess presence and extension of cardiac ischemia. Within a month of perfusion scanning, subjects underwent bone densitometry by DEXA method and using HOLOGIC or LEXXOS tool at femoral bone and lumbar vertebrae and thus the status of bone density was classified according to T score as normal, osteoporotic, and osteopenia. Osteoporosis was defined as T score less than 2.5 standard deviation of normal sex and age-matched population.Statistical analysis: For the statistical analysis, the statistical software SPSS version 17 for windows (SPSS Inc., Chicago, IL) was used. Results were presented as mean ± standard deviation (SD) for quantitative variables and were summarized by frequency (percentage) for categorical variables. The variables with significant Kolmogorov-Smirnov test skewness were corrected using data transformation. Categorical variables (ischemia, osteoporosis, vitamin D deficiency) were compared using chi-square test. Binary logistic regression was employed to generate the odds ratios. Continuous variables were compared using t test or one way ANOVA. Multivariate regression analyses were also employed to study the correlation of osteoporosis, gender, obesity (i.e. body mass index > 30), vitamin D deficiency and ischemia. P values of 0.05 or less were considered statistically significant.

RESULTS: Totally, 204 patients (131 women and 73 men with the mean age 59 ± 7 years ranged 50 to 80 years) were assessed. Regarding cardiovascular risk profile, 22.1% were diabetic, 34.8% were hyperlipidemic, 28.4% were hypertensive, and 14.2% were smoker. Family history of coronary disease was revealed in 22.5% and 30% were obese. In cardiac perfusion scanning, 141 (97 women and 44 men) diagnosed as normal, 16 (11 women and 5 men) as mild ischemia, 29 as moderate ischemia (14 women and 15 men), and 18 (9 women and 9 men) as severe ischemia. In total, perfusion defect was more prevalent in men compared with women (p = 0.031). Also, fixed perfusion defect was found more in men than in women (13.7% vs. 5.3%, p = 0.038). The mean level of serum vitamin D was 22.7 ± 16.7 ng/ml ranged 3.3 to 129 ng/ml. in this regard, 25% of patients had adequate level of vitamin D, 50% had inadequate level of vitamin D, and 24% of them suffered vitamin D deficiency (30 women and 19 men). Adequate, inadequate, and deficient level of vitamin D was observed in 22.9%, 54.2%, and 22% of women and 26%, 43.8%, and 30.1% of men with no significant difference (p = 0.40). With respect to the findings of bone densitometry in right femur, 32.8% had normal bone density, 51.2% were osteopenic, and

15.9% were osteoporotic. By measuring bone density in left femur, normal bone density, osteopenia, and osteoporosis was revealed in 31.4%, 52.2%, and 16.2%, respectively. Also, based on T score measurement on lumbar L2-L4 level, normal bone density, osteopenia, and osteoporosis was revealed in 27.5%, 34.3%, and 38.2%, respectively. In overall, normal bone density, osteopenia, and osteoporosis was found in 11.8%, 46.6%, and 41.7%, respectively. The overall prevalence of osteoporosis was significantly higher in women than in men (50.4% versus 26.0%, p = 0.003). The vitamin D values were skewed hence normally distributed log transformed data were used in statistical analyses. There was no significant difference in serum level of vitamin D between patients with normal perfusion scan and those with abnormal scan result (22 ± 17 ng/ml versus 25 ± 16 ng/ml, p = 0.29). In this context, the prevalence of osteoporosis in those women with normal and abnormal perfusion scan was 49% and 56.0% respectively (p = 0.33) and in men with normal and abnormal perfusion scan was 29.0% and 20.0%, respectively (p = 0.30). There was however a significant difference in the mean bone density score at lumbar spine between patients with normal and abnormal perfusion scan (0.86 ± 0.18 g/cm^2 versus 0.93 ± 0.19 g/cm^2, p = 0.023), but this difference was not observed in the mean bone density score at right and left femurs. In multivariate logistic regression model and with the presence of potential confounders including gender and body mass index, perfusion scan was not associated with osteoporosis status. DISCUSSION: In initial studies on association between cardiovascular disorders and bone density, this association had been suggested in women. On the other hand, both phenomenon of coronary atherosclerosis and osteoporosis are potentially dependent to age increasing. On the other hand, by adjusting age as an independent factor, relationship between atherosclerosis and osteoporosis converted to an insignificant relation. For instance, Gulacan and colleagues [2] showed association between the presence of coronary artery disease based on angiography reports and osteoporosis in women, but by adjustment for age variable, this association was not confirmed. Bakhivera et al. [24] also showed no independent association between atherosclerosis and osteoporosis in lumbar vertebrae and hip bone. Kammerer et al. [25] also showed that the obtained association between atherosclerosis and osteoporosis could be strongly dependent to patients' age. In Kim et al [26] study, although univariate analysis between coronary calcium score and T score was significant, this significance was not show in multivariate regression modeling. In most studies, vitamin D deficiency introduced as a well-known risk factor for coronary artery disease, especially when accompanied with other coronary risk factors. Non-significant association between these two parameters may be due to the variations in the definition of cutoff points for normal and abnormal level of vitamin D. In some studies and using the definition by the institute of medicine (IOM) [27], the level of vitamin D > 20 ng/ml was considered as adequate level; while guideline of the international society of endocrinology has recommended the cutoff > 30 ng/ml as the adequate level for this vitamin [28]. In addition, there is no a definitive cutoff point for serum level of vitamin D for differentiating high risk patients for coronary disease from normal coronary condition. As the main limitations of the present study was that the level of vitamin D has been shown to be varied in different seasons and months that is the highest in August and the lowest in February [29,30]. Because our study was designed as a cross-sectional survey, the potential seasonal effect may be ignored. Also, this association can be affected by patients' physical functioning and also by heart failure functional class that were not considered in the present study. So, some patients with normal perfusion scan may be in increased risk for coronary disease (such as the patients with transient left ventricular hypertrophy). Also, in a number of patients with multi-vessel disease, myocardial perfusion impairment may not be detected. These evidences may explain observed paradoxical findings on relationship between coronary atherosclerosis and presence of osteoporosis.In conclusion, we could not show demonstrate association between coronary disease assessed by perfusion scan study and osteoporosis or vitamin D deficiency. Because of this association can be potentially affected by some strong confounders such as age, seasonal changes, dietary patterns, or other coronary risk factors, performing further studies considering adjustment for these confounders is recommended.

REFERENCES1. B. Sinnott I. Syed A. Sevrukov E. Barengolts: Coronary calcification and osteoporosis in men and postmenopausal women are independent process associated with aging. Calcified Tissue International (2006)78:195-2022. GulacanOzgunTekinErsoyKekilli and et al: Evaluation of cardiovascular risk factors and bone mineral density in postmenopausal women undergoing coronary angiography. International Journal of Cardiology 131(2008) 66-69 3. Halk AE Pols HA van Hemret AM Hfman A Witteman JC (2000) Progression of aortic calcification is associated with metacarpal bone loss during menopause : a population longitudinal study. ArteriosclerThrombVascBiol 20:1926-19314. Kiel DP Kauppila LI Cupples LA Hannan MT ODonnell CJ Wilson PW (2001) Bone loss and the progression of abdominal aortic calcification over a 25 year period: the Framingham Heart Study. Calsif Tissue Int 68:271-2765. Tanko LB Bagger YZ ChiristiansenC(2003) Low bone mineral density in the hip as a marker of advanced atherosclerosis in elderly women. CalsifTissueInt 73:15-206. Schulz E Arfai K Liu X Sayre J GilsanzV(2004) Aortic calcification and the risk of osteoporosis and fractures. J ClinEndocrinolnMetab 89:4246-42537. Uyama O Yoshimoto Y Yamamoto Y Kawai A (1997) Bone changes and carotid atherosclerosis in postmenopausal women. Stroke 28: 1730-17328. Browner WS Seeley DG Vogt TM Cummings SR (1991) None-trauma mortality in elderly women with low bone mineral density. Study of Osteoporotic Fractures Research Group. Lancet 338:355-3589. von der Recke P Hansen MA Hassager C (1999) Theassocion between low bone mass at menopause and cardiovascular mortality. Am J Med 106: 273-27810. Kado DM Browner WS Black well T Gore R Cummings SR(2000) Rate of bone loss is associated with mortality in older women: a prospective study. J Bone Miner Res 15:1974-198011.Trivedi DP Khaw KT (2001) Bone mineral density at the hip predicts mortality in elderly men. Osteoporosis Int 12:259-26512.Center JR Nguyen TV Schneider DSambrook PN Eisman JA (1999) Mortality after all major types of osteroporotic fracture in men and women: an observational study. Luncet 353: 878-882 13. Aaron M. Form Joseph A. Hyder and et al: Mayo Clin Proc. June 2007; 82(6): 679-685.14.Yan-Chiou Ku Mu-En Liu Ta-Yuan Liu and et al. Relationship between vitamin D deficiency and cardiovascular disease. Word journal of cardiology.2013Sep26;5(9):337-34615. Thomas. Wang Mivhael J. Pencina Sarah L. Booth and et al. Vitamin D deficiency and risk of cardiovascular disease. Circulation 2008; 503-51116. HaraldDobing Stefan Pilz Hubert Scharnagl and et al. Independent association of low serum 25(OH) vitamin D and 125(OH)2 levels with all-cause and cardiovascular mortality. Arch Inren Med/ vol 168 (NO. 12) June 23 200811.Jeffrey L. AndersonHeidi TMay

Benjamin D. Horne and et al. Relation of Vitamin D Deficiency to Cardiovascular Risk Factors Disease Status and Incident Events in a General Healthcare Population.amjcard.2010.05.027 18.Ian H. de Boer Bryan Kestenbaum Abigail B. Shoben. 25-Hydroxyvitamin D Levels Inversely Associate with Risk for Developing Coronary Artery Calcification.J Am SocNephrol 20: 1805–1812 200919. Nibbelink KATishkoff DX Hershey SD and et al. (2007) 1 25 (OH)2 vitamin D actions on cell proliferation sizegene expression and receptor localization in the HL-1 cardiac myocyte. J Steroid BiochemMolBiol 103:533-537 20.Tishkoff DX Nibbelink KA Holmberg KH and et al.(2008) Functional Vit D recerptor in the t-tubules of cardiac myocates. Endocrinology 149:558-56421. Bodyak N Ayus JCAchinger S Shivalingappa V and et al. (2007) Activated Vit D attenuates left ventricular abnormalities induced by dietary sodium in Dahl salt-sensitive animals. ProcNatlAcadSci USA 104:16810-1681522. Xiang W Kong J Chen S and et al.(2005) role of the systemic and cardiac rennin-angiotensin systems. Am J PhysiolEndocrinolMetab 288: 125-13223.Wu J Garami M Cheng T Gardner DG (1996) 125 (OH)2 Vit D and retinoic acid antagonize endothelin-stimulated hypertrophy of neonatal rat cardiac myocytes. J Clin Invest 97:1577-1588.24. Ludmila N. Bakhireva, MD, MPH, Elizabeth L and etal.Differences in association of bone mineral density withcoronary artery calcification in men and women: theRancho Bernardo Study.MenopauseVol. 12, No. 6, pp. 691-698 25.C. M. Kammerer,A. A. Dualan and etal. Bone Mineral Density, Carotid Artery Intimal Medial Thickness, and the Vitamin D Receptor BsmI Polymorphism in Mexican American Women.Calcified Tissue InternationalOctober 2004, Volume 75, Issue 4, pp 292-29826. Kwang-Il Kim • Jung-Won Suh • Su-Yeon Choi and et al.Is reduced bone mineral density independently associated with coronary artery calcification in subjects older than 50 years.oJ Bone Miner Metab (2011) 29:369–37627. Pamela A. Marcovitz Hillary H. Tran and et al. Usefulness of bone mineral density to predict significant coronary artery disease. Am J Cardiol 2005; 96: 1059-1063 28. Jeffrey L. Anderson Heidi T May Benjamin D. Horne and et al. Relation of Vitamin D Deficiency to Cardiovascular Risk Factors Disease Status and Incident Events in a General Healthcare Population.amjcard.2010.05.027 29. Thomas. Wang Mivhael J. Pencina Sarah L. Booth and et al. Vitamin D deficiency and risk of cardiovascular disease. Circulation 2008; 503-51130. Yan-Chiou KuMu-En Liu Ta-Yuan Liu and et al. Relationship between vitamin D deficiency and cardiovascular disease. Word journal of cardiology.2013Sep26;5(9):337-346.

RELATIONSHIP BETWEEN MYOCARDIAL PERFUSION INDICES AND MECHANICAL DYSSYNCHRONY BASED ON GATED SPECT PHASE ANALYSES IN PATIENTS WITH CORONARY ARTERY DISEASE AND HEART FAILURE

Babak Fallahi[1]. Iran, Afsaneh Khorrami[2], Hasan Firoozabadi[2], Fereidoon Rastgoo[2], Davood Beiki[1], Nahid Yaghoobi[2], Hadi Malek[2], Ahmad Bitarafan[2], Armaghan Fard-Esfahani[1], Mohammad Eftekhari[1]

[1]Research Center for Nuclear Medicine, Tehran University of Medical Sciences, Tehran, Iran
[2]Department of Nuclear Medicine, Shaheed Rajaei Heart Center, Tehran, Iran

IRAN

Objective: Cardiac resynchronization therapy (CRT), in addition to optimal medical therapy, is an approved treatment for patients with coronary artery disease (CAD) and advanced heart failure (HF). Electrical dyssynchrony as determined by QRS duration is currently applied to select the patients for CRT; however, it may not necessarily represent mechanical dyssynchrony and therefore may not necessarily represent patient response to CRT. Some other factors may be related to the dyssynchrony of the left ventricle. The current study is designed to evaluate the relationship between mechanical dyssynchrony and some other factors such as CAD risk factors and myocardial perfusion indices.

Materials and Methods: One-hundred and three patients with angiographically proven CAD and heart failure entered in the study. Gated myocardial perfusion imaging (MPI) using Tc-99m MIBI and quantitative perfusion, function and phase analyses was carried out for each patient. Phase standard deviation (PSD), phase histogram bandwidth (PHB), left ventricular ejection fraction (LVEF), summed rest/stress perfusion scores (SRS/SSS) and summed difference perfusion score (SDS) were calculated according to quantitative perfusion SPECT (QPS) and quantitative gated SPECT (QGS) software.

Results: Both parameters of phase analyses, i.e. PSD and PHB showed significant correlations with SSS ($r=0.61$, $p<0.001$, $r=0.64$, $p<0.001$, respectively). There are also significant correlations of PSD and PHB with SRS ($r=0.56$, $p<0.001$ & $r=0.58$, $p<0.001$, respectively) but not with SDS ($p=0.635$, $p=0.563$). Among different factors such as QRS duration, LVEF <35% vs. 35-45%, SSS, SRS, territory of coronary stenosis and the risk factors of CAD such as diabetes mellitus, hypertension and obesity , the only independent factors affecting the severity of mechanical dyssynchrony were EF, SSS and SRS.

Conclusions: MPI with perfusion, function and phase analyses can be used to select the best candidates for CRT in CAD patients with heart failure. The patients with EF<35% and those with EF of about 35-45% concomitant with SRS>20, regardless of CAD territory, QRS duration, and CAD risk factors, are associated with more severe dyssynchrony and thus may be good candidates for CRT.

TOTAL PERFUSION DEFECT IN CAD PATIENTS USING PET/CT

Erick Alexanderson Rosas. México, Antonio Jordán Ríos, Elisa Magaña Bailón, Sergio Maury Ordaz, Alejandro F. Barrero Mier, Myriam Monserrat Martínez Aguilar, Luis Eduardo Juárez Orozco, Andrea Monroy -Gonzalez, Ana Gabriela Ayala Germán, Luis José Cásares, Aloha Meave González.

MEXICO

Aim: Correlate the degree of coronary stenosis and Total Perfusion Defect (TPD) using ^{13}N-ammonia PET/CT. Methods: 68 patients underwent a PET/CT study. Perfusion defects were evaluated through TPD with CSI-QPS Perfusion defects were evaluated through TPD with CSI-QPS software. We classified CT findings, documented as follows: no coronary obstruction lesions, non-significant atherosclerosis and significant stenosis. Results: Of 68 patients, 50% had no evidence of coronary lesion, 25% had non-significant stenosis atherosclerosis and 25% had significant stenosis. Abnormal TPD (>5%) was found in 21 patients, with abnormal CT. (p=0.036). Conclusion: PET/CT is a useful method for diagnosis and management of patients with suspected CAD. Abnormal TPD correlates with significant stenosis and may be useful to predict functional impact using quantitative analysis.

DIASTOLIC DYSFUNCTION IN ONCOLOGIC PATIENTS

Erick Alexanderson-Rosas. México, Antonio Jordán-Ríos, Sergio Maury-Ordaz, Elisa Magaña-Bailón, Mariano Oropeza –Aguilar, , Luis Eduardo Juárez-Orozco, Myriam Monserrat-Martínez Aguilar, Sebastián Álvarez, Carlos Valdivia, Salvador Hernández, Lucely Cetina.

MEXICO

The aim of this study is to evaluate diastolic function through Radioisotopic ventriculography (RV) in patients receiving chemotherapy. Methods: 30 patients with cervical cancer were included. They underwent RV before cisplatinum-vinorelbine-nimotuzumab administration. After 12 months follow-up and 3 cycles another RV was performed. Peak filling rate (PFR) and Time to peak filling (TTPF) were obtained. Results: Mean PFR was 3.15±0.72 and after treatment 3.07±0.75 (p=0.682), whereas mean TTPF was 139.14±24.7, after treatment 146.64±28.1 (p=0.38). Mean LVEF was 63.8%±6.7, versus 60.1%±9.0 (p=0.95) Differences were neither relevant nor statistically significant. Conclusion: Chemotherapy applied in this study seems to be safe in a 12 months period administration. RV is a useful method for screening and follow-up of cardiac function.

HEART RATE RESPONSE DURING DIPYRIDAMOLE INFUSION IS ASSOCIATED WITH CARDIAC EVENTS IN PATIENTS WITH NORMAL PERFUSION SPECT

Cecilia Bentancourt.

URUGUAY

Objective. Dysfunction of the autonomic system predicts cardiovascular risk and sudden death, especially in patients with type 2 diabetes, regardless of the presence of ischemic heart disease. Cardiac autonomic dysfunction is also a powerful predictor of risk for mortality after myocardial infarction in the general population. As heart rate response (HRR) to vasodilator stress can be a marker of HR variability reflecting the integrity of the autonomic system, we intended to define the prognostic value of HRR during dipyridamole test in a population of patients with suspected coronary artery disease but with normal SPECT myocardial perfusion imaging (MPI).

Methods. A total of 845 patients were retrospective analyzed, in whom MPI SPECT imaging was performed in a two-day protocol. Pharmacologic stress included infusion of 0,56 mg/kg of dipyridamole over 4 min followed by IV injection of 99mTc-MIBI, which was repeated at rest. Gated acquisition was only performed at rest. HRR was calculated as the maximum percent HR change from baseline. Patients in the lower quartile of HRR were compared to those in the other quartiles regarding nonfatal MI or cardiac death at 5 years of follow-up. Results. A total of 237 patients (28%) had normal perfusion SPECT MPI (123 women, age 65±11 years), of which 60 (25.3%) had HRR<15% (lower quartile) compared to 177 with HRR≥15%. In the first group, 25 events were identified vs. 33 in the second group (41.7% vs. 18.6%, p<0.001). Diabetes was significantly associated with cardiac events (p=0.037), but was not a predictor of HRR. Rest left ventricular ejection fraction (LVEF) and stress-induced ST depression ≥1 mm were not independently associated with event rate nor were predictors of HRR. Interestingly, the presence of diabetes was not more common in patients with attenuated HRR using a cutoff at the lower quartile. Conclusions. HRR provides significant prognostic information in patients with normal MPI with dipyridamole, and this variable seems to be even more powerful than ST changes or rest LVEF. Thus, a normal MPI result should be interpreted cautiously when associated with abnormal HRR with dipyridamole. Further work that assesses these results in diabetes patients with abnormal SPECT or known coronary artery disease is warranted.

SIGNIFICANCE OF POST-STRESS DECREASE IN EJECTION FRACTION AT HIGH RANGE VALUES IN PATIENTS WITH NORMAL AND ISCHEMIC PERFUSION RESULTS IN GATED SPECT STUDIES

Miguel Kapitan.

URUGUAY

Objective. Myocardial stunning, defined as a transient post-ischemic ventricular dysfunction, has added prognostic value in gated SPECT studies. In general, myocardial stunning is reflected by a decrease of at least 10% in post-stress left ventricular ejection fraction (LVEF) compared to rest, with absolute values below normal limits or at least at the lower portion of the normal range. However, the clinical significance of a post-stress drop in LVEF preserving above-normal absolute values, a relatively common finding in routine nuclear cardiology practice, is not well established. Our objective was to define the prognostic power of post-stress LVEF decrease at high range values in patients with normal and ischemic perfusion gated SPECT results. Methods. A total of 96 patients submitted for two-day protocol gated SPECT myocardial perfusion imaging and with a post-stress decrease in LVEF ≥10% compared to rest (ΔLVEF), all with absolute values between 65% and 85% were analyzed. Patients were classified as ischemic or non-ischemic based on the automatic-generated summed difference perfusion score (SDS>3 and SDS≤3 respectively), which was manually corrected as necessary. Follow-up was obtained for 17.6±7.3 months, with any cardiac event as endpoint. Results. In the population analyzed, stress test was exercise in 56 cases and dipyridamole in 38. Ischemic (n=34) and non-ischemic (n=62) patients meeting the criteria of lower post-stress LVEF with at least 65% value were similar for demographic and clinical variables. ΔLVEF was 13.2±3% for the ischemic group and 13.1±3.2% for non-ischemic patients (p=0.86), while event rate was 20.6% and 3.2%, respectively (p<0.005). However, in the ischemic group there was a weak correlation between summed difference score (SDS) and ΔLVEF (r=0.3, p=0.07). Conclusions. Ischemia is a strong predictor of cardiac events, but a drop in post-stress LVEF at high range values does not seem to add prognostic significance. Furthermore, the lack of significant association of ΔLVEF at high values with the presence and magnitude of ischemia suggests stunning is not the cause of the finding. Regional wall motion analysis, which was not done in this study, could provide additional information on whether this phenomenon reflects true myocardial stunning.

END STAGE RENAL DISEASE AND MYOCARDIAL PERFUSIÓN TEST. ASSESING RESULTS OF A COHORT CANDIDATES TO KIDNEY OR SIMULTANEOUS KIDNEYPANCREAS TRANSPLANT

Kapitan, Miguel, Uruguay.

URUGUAY

Introduction. Cardiovascular disease is a leading cause of morbidity and mortality among patients(pts) with end-stage renal disease (ESRD) before and after transplantation. Noninvasive stress testing may be considered in kidney (KT) or simultaneous pancreas-kidney(SPKT) transplantation candidates regardless of functional status . Myocardial perfusion using SPECT is a useful screening test for the evaluation of cardiovascular risk in pts undergoing KT or SKPT with high diagnostic accuracy.Objectivs. Analize myocardial SPECT (MPI) results in pts with ESRD candidates for KT or SKPT.

Methods. We evaluated 94 pts with ERSD in a period of 3 years (2011-2013),candidates for KT or SKPT, referred to the Center to evaluate myocardial ischemia.We stratified the pts into 2 groups: Group 1: 72 patients for KT and Group 2: 22 for SKPT. In Group 1: 42 males, mean age 55.9 years, mean body mass index (BMI) 27.7, risk factors (RF): 79 % Hypertension (HT),37 % Type II diabetes (Db), 42 % dyslipidimia (Dlp),15% had demonstrated CAD (previous myocardial infarction, cardiac revascularization), 77 % hemodialisys (HD) , mean duration in dialysis 4.3 years,10 % referred chest pain or angina. Group 2: all patients had type I diabetes about 21 yrs evolution, 9 males, mean age 34.4 years, BMI 20.3. RF: 77 % HT, 9% Dlp, none evidenced CAD, 77 % in hemodyalisis, mean duration 3.6 y, 1 pt referred angina. Most patients in both groups underwent dypiridamole stress test in 2 days protocol. At MPI we considered stress, differential, rest scores to quantify perfusion defects (SSS, SDS, SRS) in order to stratify pts in low, moderate or high risk of CV events, left ventricular ejection fraction (LVEF) at rest and post stress. Statistics: Comparison in and between groups were performed using Chi2, Fischer and t Test. Probability value was considered significant if p ≤0.005.

Results: Group 1: was older than group 2 (p 0.001). BMI showed be higher than in group 2 (p 0.001). 22 patients (30%) showed low differential scores (ischemic defects, SDS ≤ 4), 6 pts (8.3 %) moderate – high (SDS ≥ 5) and 6 pts (8.3 %) fixed perfusion defects (p =0.003) compared con pre MPI test. The mean rest LVEF 56.8 %, mean stress LVEF 56.0% and it was slightly higher than group 2 (p = 0.065).Group 2: 2 pts (9%) showed low risk differential scores (SDS ≤ 4), and 1 patient (4.5%) high (SDS ≥7). No one has fixed defects. MPI did not mark differences (p = 0.23).The mean LVEF was 51 % post stress and rest. Conclusions: KT candidates are significatively older and showed more ischemic in burden in MPI than pts candidates for SKPT. LVEF was lower in SKPT candidates, probably cause of longstanding diabetes.

FUNCTIONAL AND ANATOMIC CORRELATION BETWEEN HIGH RISK GATED MYOCARDIAL PERFUSION STUDIES AND CORONARY ANGIOGRAPHY.

Nicolas Niell.

URUGUAY

Objective. The correlation between high risk functional patterns in myocardial perfusion studies (MPS) and anatomic lesions in coronary epicardial vessels is well established. However, there have not been studies validating those findings in our country. Despite the utility of invasive physiologic parameters for myocardial perfusion evaluation such as intravascular Doppler and fractional flow reserve, in clinical practice noninvasive techniques are extremely useful for therapeutic decision making and patient management. Our objective was to determine the correlation between topography and severity of ischemia and other high risk parameters in MPS and the angiographic anatomic findings in patients referred for evaluation of known or suspected coronary artery disease.

Methods. Clinical records of 171 patients with MPS showing extensive/severe reversible perfusion defects with or without additional high risk signs such as post-stress left ventricular ejection fraction (LVEF) decrease were retrospectively analyzed. MPS were obtained using gated SPECT modality after injection of ^{99m}Tc-MIBI at rest and after physical or pharmacologic stress using a two-day protocol. The results were classified as high risk when extensive and severe reversible defects were detected in one or more vascular territories, associated or not with a post-stress drop in LVEF ≥10% compared to rest. Comparison was made between topography of ischemia and coronary anatomy by angiography using Sperman Rho correlation.

Results. A total of 110 patients were studied with dipyridamole (59 men, 67±10 years) and 61 with exercise test (44 men, 61±11 years). In both populations, a significant correlation was found between the location of ischemia and the stenotic vessels. Global concordance between MPS and angiography for the identification of culprit lesions was 0.56 ($p<0.001$), with PPV of 80% for ADA, 74% for RCA and 94% for Cx. In addition to ischemia, post-stress drop in LVEF was identified in 83 cases, with severe stenotic lesions found in almost 99% of these patients, being the proximal ADA the most frequently affected vessel (83%).

Conclusions. Good correlation exists between high risk functional findings in MPS and coronary angiography regarding the presence of epicardial lesions and the identification of culprit vessel. A drop in post-stress LVEF is a strong predictor of severe epicardial lesions, especially affecting the proximal ADA.

ENDOCRINOLOGY

RELATIONSHIP BETWEEN THE ULTRASONOGRAPHYC, CYTOLOGY, HISTOLOGICAL AND LABORATORY FINDINGS WITH SCINTIGRAPHY PROTOCOL OF TWO PHASES TC99M/TC99M SESTAMIBI IN THE EVALUATION OF THYROID NODULES IN THE NUCLEAR MEDICINE SERVICE OF CARLOS ALBERTO SEGUÍN ESCOBEDO HOSPITAL (HNCASE), 2010-2012

Carlos Arturo Cárdenas Abarca. Cecilia Rossana Aguilar Ramirez.

PERU

Objective: The objective is to establish the relationship between of the laboratory, ultrasound, cytological and histological findings with the findings of the scintigraphy Tc99m/Tc99m Sestamibi in the assessment of thyroid nodules in the Service of Nuclear Medicine of the HNCASE, Perú, 2010-2012.Materials and Methods: Were reviewed and compared the medical records of 53 patients operated for thyroid nodules that had thyroid function tests, thyroid ultrasound (TIRADS classification and flow Doppler), results of fine needle aspiration biopsy (Bethesda classification system), histopathologic findings and thyroid scintigraphy with protocol of two phases Tc99m/Tc99m Sestamibi, with the statistical tests. The patterns of high probability of malignancy is those with acaptación or low uptake in the first stage and uptake in the second, low probability patterns are defined as low uptake or uptake in both phases. Results: Were patterns of high probability of malignancy in 21 patients (39.62%) and of low probability in 32 patients (60.38%). In subclinical hyperthyroidism were predominate patterns of low probability (75% versus 25%), while in euthyroid or subclinical hypothyroidism were presented with close to parity (50%) percentages with a slight predominance of low probability (p=0.66). In nodules between 5 and 9 mm of size, predominated patterns of low probability (80% versus 20%), in lesions > or = 1 cm were almost similar rates between patterns of high and low probability (p=0.35). Predominated patterns of high probability in nodules with central and peripheral flow (100%) or central flow (60%), versus peripheral or low flow patterns only 21.74% and 14.29% respectively (p <0.05). Predominated the patterns of high probability in solid nodules (45.45%) or mixed (41.67%), versus only 12.50% in cystic (p> 0.05). Predominated the patterns of high probability in TIRADS 4 (76.92%) and TIRADS 5 (75%). (p<0.05) Predominated patterns of high probability in Bethesda VI group (85.71%), while there was more benign pattern in the Bethesda II (80.77%) (p<0.01). Were more suspicious patterns of malignancy in papillary carcinoma (81.25% vs 18.75%), follicular carcinoma (100%), Hurthle adenoma (100%); in benign lesions such as adenomatous nodules, follicular adenoma Hashimoto thyroiditis and the pattern of low suspicion of malignancy ranged from 100%, 77.78% and 50% respectively (p<0.01). The sensitivity of gammagraphy was 83.3%, specificity was 82.9%, the positive predictive value was 71.4% and negative predictive value was 90.6%.

Conclusion:The thyroid scintigraphy with protocol of two phases Tc 99m/Tc99m Sestamibi is a useful study for diagnosis of malignant in thyroid nodules of solid density, over 1 cm of size, for her high negative value predictive.

IDENTIFICATION AND CHARACTERISTICS OF BROWN ADIPOSE TISSUE IDENTIFIED IN PARATHYROID STUDIES WITH 99MTC-MIBI.

Miguel Kapitan. Spanish Association Hospital.

URUGUAY

Objective. Brown adipose tissue (BAT) is a relatively common finding in FDG-PET studies, sometimes leading to false positive results. Uptake of various other tracers in BAT (including 99mTc-MIBI) has been occasionally reported as well, but the issue has not been extensively described in the literature. Focal uptake of 99mTc-MIBI in the thorax on planar or SPECT images, which potentially could have been misinterpreted as ectopic parathyroid tissue, was demonstrated on SPECT/CT as corresponding to BAT uptake. Our objective was to define the characteristics of BAT observed in routine parathyroid studies performed in two institutions using exactly the same technology and imaging protocols. Methods. Images from consecutive patients referred for investigation of hyperparathyroidism in these institutions between 2008 and 2014 were analyzed. The protocol included the IV administration of 20 mCi of 99mTc-MIBI, with planar images obtained at 15min and 2h 30min after injection. SPECT was also performed, but generally using only one acquisition at a variable time between early and late planar imaging. BAT was considered present according to the judgment of two experienced nuclear medicine physicians when there was typical symmetric uptake in the cervical, supraclavicular, interscapular, and/or paravertebral regions. Equivocal findings or lack of consensus between the two observers was considered negative for BAT. Target-to-background activity (uptake index) was measured using ROIs drawn over BAT, myocardium (as a reference organ) and mediastinum, both on early and late planar images. Results. From a total of 574 patients, BAT was clearly identified in 9 (1.6%, 6 women, ages 35±19 years, BMI<25). Studies were performed during the winter season in 6 of these patients. Uptake index for BAT (average±1DS) was 2.45±0.33 in the early images and 3.20±0.52 in late images, while for the myocardium it was 2.02±0.22 and 2.29±0.33 respectively. Exact definition of BAT distribution was better achieved with SPECT, especially in the thorax; however, no temporal behavior of uptake could be analyzed due to a single SPECT acquisition included in the protocol.

Conclusions. BAT is not commonly observed in 99mTc-MIBI parathyroid scintigraphy, although when present, uptake is intense (even more than the myocardium) and persistent over time. As has also been described for PET-FDG, with MIBI BAT is predominantly seen in young female subjects with low BMI, and is more often associated with low outdoor temperature (winter season). Awareness and recognition of this pattern on parathyroid scintigraphy could potentially avoid false positive reports.

RESPIRATORY

DIAGNOSIS OF PULMONARY EMBOLISM (PE): CLINICAL IMPACT OF THE NEW VQ SPECT IMAGING

Kevin Xu 1, Sai Han1,2, Gillian Ainslie-McLaren2, Alison Bolster2, David Colville1,2, F W Poon 2,3 and JB Neilly1,2,4

(1) General Medicine
(2) Nuclear Medicine
(3) Radiology
(4) Respiratory Medicine, Glasgow Royal Infirmary, Glasgow.

SCOTLAND

Objectives:
The National Institute of Clinical Excellence (NICE) Guideline 2012 has recommended Ventilation-Perfusion VQ SPECT scan as an alternative to CTPA in assessing suspected PE. Glasgow Royal Infirmary upgraded to VQ SPECT from conventional VQ planar imaging in 2013 and this is the first 3-month service audit on its clinical impact.

Methods:
The results of VQ SPECT, other imaging, and clinical outcome were retrieved from electronic clinical/radiology records and retrospectively reviewed. All patients who had a VQ SPECT scan during 31/07/2013 – 31/10/2013 were included. Final clinical diagnosis or confirmatory CTPA results were considered as gold standard. Mean follow up was 170 days (range 124-217).

Results:
71 consecutive patients had a VQ SPECT scan during the study period. 66/71 patients (54 Female, 12 Male, Mean Age 55y range 17–93) with available outcome data were included. 58/66 patients were for suspected acute PE including 14 patients who were pregnant/postpartum and 15 patients with unsuitable/failed CTPA. 8/66 patients were for suspected thromboembolic pulmonary hypertension. VQ SPECT provided a definite diagnosis in 61/66 patients (92%) – PE positive in 11/66 (17%) and PE negative in 50/66 (76%). Definite VQ reports were in total agreement with the final diagnosis/treatment. 5/66 patients (8%) had indeterminate scans- 2 of them had final diagnosis of PE and 3 had no PE. There were no false negative noted.

Conclusion:
This audit proves the benefit of the upgraded VQ SPECT imaging in the management of suspected PE providing a definite diagnosis in 92% of patients with few indeterminate results.

PEDIATRICS

PET-CT IN PEDIATRIC POPULATION. EXPERIENCE IN A UNIVERSITY HOSPITAL.

Giancarlo Marcenaro Poloni. Pontificia Universidad Católica de Chile. Pilar Orellana, Rodrigo Jaimovich, Juan Carlos Quintana, María Angélica Wietstruck, Francisco Barriga, Cristián García.

CHILE

INTRODUCTION: The role of positron emission tomography with computed tomography (PET/CT) is well established in adult oncology, cardiology and neurology. In pediatric population, PET/CT is a rapidly growing area of imaging and research in children care. In pediatric cancers it has a very important role in diagnosis, staging, therapy evaluation and follow-up, especially in lymphomas. In our country the experience using this technique is limited due to high cost and low availability. GOAL: Show our experience in the use of PET/CT in pediatric population.

METHODS: We retrospectively reviewed the clinical data of pediatric patients sent to our Unit for PET/CT imaging between November 2008 and May 2014. Studies were performed according to a standardized pediatric protocol.Anesthesia or sedation was used when required.

RESULTS: 211 studies were performed in 115 patients; 46 female and 69 male, between 7 months and 20 years old. The studies were done mainly in oncological patients (177 studies), followed by neurological indications (28 studies) and miscellaneous (6 studies). F18-FDG was used in 203 studies and Ga68 DOTATATE in the remaining eight. In the oncological group, 113 studies were requested in children with Hodgkin's Lymphoma (HL), 24 studies in patients with non-Hodgkin Lymphoma (NHL) and in 40 patients with other malignant neoplasms. The number of studies per patient in this group was one study in 41 patients, 2 studies in 13 patients, 3 studies in 14, 4 studies in 2, 5 studies in 8, 6 studies in one and seven studies in 2 children. Considering only the studies performed in patients with lymphoma, the indications for the PET/CT were as follow: staging (31 studies, 30 with abnormal findings), intra-therapy monitoring (30 studies, 23 with some degree of hypermetabolism), end of therapy (28 studies), follow-up (44 studies, 33 without hypermetabolic foci) and relapse (4 studies). Abnormal findings on staging PET/CT was useful as baseline study and also to help determine therapy. Intra-therapy and end of therapy studies without complete resolution helped decide whether therapy should be prolonged or changed. Normal follow-up studies were considered an excellent prognostic element, but did not warrant absence of recurrence.

CONCLUSIONS: In our pediatric population the most frequent use of PET/CT was in oncology, mainly in lymphoma assessment, proving to be a valuable tool for clinical decision making. As 10% of the pediatric oncology patients had more than three studies during this period, the indication and acquisition protocol of PET/CT must be standardized in order to minimize radiation exposure.

THE ROLE OF MYOCARDIAL PERFUSION SCINTIGRAPHY TO EVALUATE OUTCOME OF CHILDREN VICTIM OF SEVERE SCORPIONIC ACCIDENTS - CASE REPORTS

Cosenza, NN.

BRAZIL

INTRODUCTION

The incidence of scorpionic accidents has been increasing yearly, carrying a potential of severe complications, especially in children. The poison has high concentrations of catecholamines which increase blood pressure and venous return causing hemodynamic overload. Myocardial ischemia may also occur and may be caused by: hemodynamic overload; hyperstimulation of alpha-adrenergic receptors causing coronaries microvascular constriction; and a direct toxin effect on myocardial fibers. Myocardial perfusion scintigraphy (MPS) has been shown to demonstrate ischemia in these children. However, perfusion alterations may persist for longer than normally reported in the literature.

OBJECTIVE

To report the different outcomes of children victims of severe scorpionism accident demonstrated by myocardial perfusion scintigraphy.

CASE REPORTS

Two children victim of a severe scorpionism accident (one female, one male, 2 years of age), were admitted after the event (8 hours and 24 hours, respectively) due to symptoms. Both children presented with innumerable vomiting episodes, breathing discomfort, tachycardia, sweating and dehydration. Laboratory tests showed increased serum levels of myocardial muscle creatine kinase, troponin and amylase. Anti-scorpion serum was immediately administered. In addition, the female patient´s electrocardiogram demonstrated sinusal tachycardia and ST segment depression in the lateral wall of the left ventricle.

The female patient´s echocardiogram, performed 2 days after the accident, showed hypokinesia in the apical and septal walls and a 57% left ventricular ejection fraction (LVEF). Her rest MPS with ^{99m}Tc-sestamibi demonstrated marked hypoperfusion of the septal

wall. Two months later, another echocardiogram demonstrated normal findings and a LVEF of 65%. However, a MPS performed after 6 months showed only mild improvement of the perfusion of the septal wall.

On the other hand, the male patient´s echocardiogram showed, two days after the accident, moderate systolic dysfunction, LV dilation, moderate mitral insufficiency, septal wall dyskinesia and LVEF of 46%. The rest MPS demonstrated marked hypoperfusion in the anterior and septal walls. However, his echocardiogram and MPS performed two months after the accident normalized.

CONCLUSIONS

Myocardial perfusion scintigraphy in children victims of severe scorpionism accidents has high sensitivity to detect vascular abnormalities and may contribute to the prognostic evaluation of these patients. Despite the current knowledge that these defects may normalize after 2 months, we demonstrated that this is not always the case, even when the echocardiogram is normal.

DOSIMETRY OF 99MTC-DMSA IN CHILDREN

Christiane Wiefels Reis.

BRAZIL

Objective: Calculate the mean dose of ^{99m}Tc-DMSA used in renal scintigraphy in children in a university hospital in Brazil.

Methods: 26 consecutives pediatrics renal scintigraphy with ^{99m}Tc-DMSA between July/12 and October/13 were analyzed. The activity administered was calculated according to weight and body surface area (BSA).

Results: mean dose injected: 3,4 ± 2,27 mCi; mean BSA : 0,74 ± 0,40 m^2 ; mean activity/BSA: 4,89 ± 2,9 mCi/m^2 . The quality of the images was the same independently of the dose.

Conclusion: There is a need to improve pediatric dose adjustments because 51% of the doses exceeded the maximum recommended in European guidelines. The minimum dose of 1,57 mCi/m^2 can achieve good quality exams.

GASTROINTESTINAL

GASTRIC ACCOMMODATION IN PATIENTS WITH FUNCTIONAL DYSPEPSIA

Dr.Mojtaba Ansari Jafari Institucion: Shahid Beheshti University of Medical Sciences. Dr.Zahra Azizmohammadi ; Dr.Hamid Javadi ; Dr.Majid Asadi.

IRAN

Background: Impaired gastric accommodation has been as one the main symptoms in patients with functional dyspepsia. The aim of present study was to assess symptoms of functional dyspepsia and gastric accommodation using SPECT imaging.

Method and materials: Number of 24 patients with functional dyspepsia and 50 healthy volunteers as control group was selected in this study. All cases were administrated intravenously with 5 mCi99mTc-pertechtenate then served with a low fat meal. Finally, SPECT scanning was performed 20 minutes and 120 minutes after the serving meal for all cases.

Results: Based on the scintigraphic data of our study, gastric volumes have been significantly increased after eating the food in both patients and control group. We also found that while there was no significant difference in patients and control group with respect to fasting gastric volumes but postprandial gastric volume of patients has been reduced significantly in comparison to healthy individuals.

Conclusion: Measuring gastric volume using SPECT can be a valuable method in detection of functional dyspepsia and differentiation of it with other organic disorders.

VALIDATING THE USE OF CORN OIL AS A CHOLECYSTOKINETIC FOR HEPATIC-BILIARY SCINTIGRAPHY AND AS USED TO DETERMINE PERCENTAGE OF GALLBLADDER FLUID EXPELLED

E. Ávila R1 MD, G. Villalobos B.1MD, G Rea F.2MD, L.A. Aceves L. 2 MD.

[1]Medicina Nuclear. [2]Cirugía y Gastroenterología del Centro Médico Dalinde. México. D.F.

MEXICO

INTRODUCTION
Diagnosis for Chronic Colecystitis (CC), Biliary Tract Dyskinesia (BTD) and Oddi Sphinter Dyskinesia (OSD) requires evaluation of the motor function of the gallbladder (GB) and determining the percentage expelled from the gallbladder. The use of hepatic-biliary scintigraphy as a diagnostic method to evaluate these parameters will normally render more precise results. The procedure involves administering a cholecystokinetic that assesses gallbladder motor function. A range of cholecystokinetics are employed, such as those found in foods that are rich in fats, supplementary foods analogous to cholecystokinetics (i.e. Sincalide, Kinevac), with a recent proposal for the use of corn oil to be added to the list. OBJECTIVE To evaluate the use of corn oil ingested with chocolate milkshake as a cholecystokinetic in order to assess motor function and amount of fluid ejected from the gallbladder.

METHOD
Hepatic-biliary scintigraphies were performed on 558 patients who reported acute or chronic pain in right hypochondrium and/or abdomen, in some cases also nausea and vomiting. Studies included 425 females and 133 males with ages ranging between 11 and 79 and were carried out using 4mCi 99mTc-MEBROFENIN activity, (148MBq); the procedure was employed during 60 minute periods which rendered 60 images (64 x 64) lasting 1 minute each. The cholecystokinetic (70 ml of corn oil mixed with 250 ml chocolate milkshake) was administered orally 10 minutes prior to the completion of each 60 minute period, immediately followed by a complementary , 30 minute study where 30 images (64 x 64) were obtained in 60 seconds. Through this second study the percentage of gallbladder fluid expelled is determined using the equipment's built-in Gallbladder Expulsion Portion program. All studies were performed under a Milenium model GE* gamma camera, whose equipment contained a processing program standardized by the manufacturer.

RESULTS
A total of 1116 studies were carried out with these 558 patients (558 stimulated over 60 mins. and then over 30 min. periods). Response to gallbladder function upon stimulation was detected in 494/558 cases, that of the 64 non-responsive patients considered undefined with a 0% value. Gallbladder expulsion percentages for the entire group studied ranged from 0% to 100%. In 55 of these cases, this value varied from 33% to 100% and was considered normal. Gallbladder function alterations were detected in 503 of the patients: OSD in 2 cases, with BDT or CC in 501 cases; of these, 66 presented OSD as well. Cystic and/or choledocal dilation was reported in 50 patients, while dyskinesia or sphinter hypertonia (Oddi) was observed in 57 subjects, duodenogastric reflux in 3, hepatic sufficiency and cholesthasis in 2 of the cases. Gallbladder was ectopic in 5 patients and hardened gallbladder was found in two. Close correlations were found between the scintigraphic results and surgical and hitopathological reports. The single side-effect to the cholecystokinetic was nausea, which appeared in only 2.3% (13/558) of the patients studied.

DISCUSSION
The range of 35% to 100% gallbladder fluid expulsion considered normal and found in 55 of the cases studied here coincides with a large number of other reported cases where cholecystokinetics have been used. In the cases presented, the age range is ample when compared with similar study series. Patients included in this study were referred to us by emergency services, with 503 of such cases reporting gallbladdere function alterations as well as fluid expulsion in close correlation with their respective histopathological records. The ingestion of corn oil combined with a basic chocolate milkshake serves as a cholecystokinetic that is accessible, at a low cost, and that does not affect patients negatively in any way except for the minimal side-effects of nausea that the formula may cause in very limited cases, as has been previously reported by a number of authors.

CONCLUSION
Corn oil, when mixed with chocolate milkshake, acts as a highly effctive, low cost, accessible and well tolerated cholecystokinetic. If this formula were to be standardized, it would serve as an alternative to nuclear medicine, particularly in those countries where Sincalide (Kinevac), a high-cost pharmaceutical, is unavailable. Based on results of the cases studied here, corn oil used in combination with a standard chocolate milkshake can definitely be recommended as a cholecystokinetic useful in determining gallbladder fluid expulsion percentages in studies performed on patients with a probable diagnosis of CC, BTD and OSD.

GASTRIC EMPTYING AND OROCECAL TRANSIT TIMES MEASURED THROUGH H2 BREATH TEST AND RADIONUCLIDES IN SUBJECTS WITH AND WITHOUT IRRITABLE BOWEL SYNDROME

Massardo T, Zhindon JP, Fernández R, Landskron G, Muñoz P, Gonzalez J, Otárola S, Beltran CJ, Madrid AM. Nuclear Medicine and Gastroenterology Sections. Medicine Department University of Chile Clinical Hospital.

CHILE

INTRODUCTION:
Irritable Bowel Syndrome (IBS) is highly prevalent in our media, mainly in females with diverse symptoms. It could be associated with abnormal intestinal transit times and with altered gastric emptying (GE). Our goal was to evaluate orocecal transit time (OCTT) with lactulose H2 breath test and radionuclide test correlating with GE in patients with and without IBS.

METHOD:
Ambulatory patients from gastroenterology section of our hospital, ranging from 22 to 71 years old, 83% females were recruited prospectively. Group A: 10 IBS patients according to Rome III criteria (3 constipated, 2 diarrhea, 3 mixed and 1 indeterminate). Group B: 7 patients without IBS, including 1 female with chronic constipation. There were no significant differences in age, sex or body mass index between groups. Technique: After 8 h of fasting and no interfering medications, 2 mCi of liquid 99mTc-colloid sulfur mixed with 25 mg of lactulose (H2 breath test), were administered per os. Abdominal gamma camera imaging (anterior and posterior views) and serial breath samples every 10 min until 180 min, were obtained. Analysis: a) Pearson correlation test of decay corrected radionuclide geometric mean data and H2 measurements b) comparison between subgroups using unpaired student t test were performed.

RESULTS:
Presence of radioactivity was observed in the caecum between 43 and 113 min in all and 16/17 presented 50% in colon, between 73 and 138 min. The chronic constipated female presented a delayed global transit. Predominantly linear GE half life time (T/2) was observed. There was no difference between groups in all analyzed parameters. Correlations were as follows [95% Confidence interval]

CONCLUSIONS:
OCTT presented a significant positive correlation by using H2 breath test and radionuclide method in patients with and without IBS. GE was similar in both groups. GE measured with colloid sulfur was also well correlated with both OCTT techniques, but slightly better with radionuclide. OCTT using radiolabeled colloids was an easy technique to be implemented and interpreted. OAIC Grant 530/12

INFECTION
INFLAMMATORY

F-18 FDG PET/CT STUDIES IN PATIENTS WITH TUBERCULOSIS

Annare Ellmann[1]. South Africa, S Griffith-Richards[2], SF Malherbe[3], K Ronacher-Mansvelt[3], C Barry[4], G Walzl[3], JM Warwick[1]
[1]Nuclear Medicine, [2]Radiodiagnosis, [3]TB Research Centre, Stellenbosch University and Tygerberg Hospital, South Africa; [4]NIAID, USA.

UNITED STATES

Tuberculosis is a serious health problem in South Africa, often complicated by HIV/AIDS co-infection. FDG uptake in active TB is often said to complicate the interpretation of FDG studies in oncology patients. We report on findings of FDG PET/CT studies in a group of HIV negative patients with active pulmonary TB. Methods:HIV negative patients clinically presenting with active pulmonary tuberculosis were referred for FDG PET/CT studies. Studies were performed from skull base to mid thigh 60 minutes after the administration of F-18 FDG.Results:We recruited 101 patients (64 male, 37 female; age range 17-66 years, mean age 34 years) for the study. All patients showed avid FDG uptake in TB lung lesions (SUV_{max} 1.33-15.1), with 79% of patients having multiple sites of disease in both lungs. Although 19 patients had unilateral disease, only 12 patients had a normal lung with no FDG uptake or CT changes. A significant number of patients had FDG uptake in lymph nodes (LN), both intra- and extrapulmonary, with pulmonary LN uptake in 72% of the cases. Extrapulmonary activity was noted in 37 cases (37%), with LN uptake in 37% of these. The significance of this extrapulmonary LN uptake is unclear. One case each had extrapulmonary TB and a malignant rib lesion. Discussion:This study is the first to document the whole body FDG PET/CT scan appearance of patients presenting with pulmonary TB in a large group of HIV negative patients. The study confirmed avid FDG uptake in TB lung lesions in all patients. The frequent finding of avid FDG uptake in lymph nodes was surprising.Significant extrapulmonary TB was an infrequent finding in this high risk patient group, suggesting that the suggested increased risk of false positive oncology studies due to extrapulmonary TB in HIV negative patients in South Africa may be overestimated.

INCIDENTAL FINDING OF DIFFUSE ARTERITIS IN 18F-FDG-PET/CT FOR STAGING A COLON ADENOCARCINOMA CANCER. CASE REPORT AND LITERATURE REVIEW

Thiago S.A. Rocha.

BRAZIL

Objective: To report a case of fortuitous diagnosis of arteritis with ^{18}F-FDG-PET/CT for staging a colon cancerClinical history:Female, 87 years old, complaining of chronic constipation and diffuse abdominal pain lasting two months. Guided colonoscopy biopsy identified adenocarcinoma in transverse colon and sigmoid. The staging with ^{18}F-FDG-PET/CT showed hypermetabolic areas in the colon, with a maximum SUV of 9.4, without metastatic sites. It showed diffuse thickening across the whole aorta, subclavian, vertebral, internal and common iliac arteries, with a maximum SUV of 7.5, suggesting diffuse arteritis. Patient refused surgical treatment of carcinoma. She was treated with simple analgesics with complete improvement of symptoms, indicating non malignant etiology of the pain. A directed interview identified history of a temporal arteritis from 11 months ago, whose symptoms were headache, dizziness and vomiting. It was treated with steroid cycles and the symptom ceased.Comments: Vasculitis is an inflammation that affects small and large vessels. May be it is secondary to infections, neoplasia or autoimmune diseases. Histology is considered the gold standard for diagnosis however, it is highly invasive. ^{18}F-FDG-PET/CT is added like a functional method for scanning and to identify metabolically active processes, proving more effective in the group of large vessels, such as giant cell arteritis and Takayasu arteritis. Leukocytes, when activated, express glucose transporters who avidly uptake ^{18}F-FDG, justifying it's use for vasculitis. Vasculitis is classified according to the size of vessels that affect. The ^{18}F-FDG-PET/CT is more effective in the group of large vessels. These diseases often present non-specific symptoms and laboratory tests. In studies comparing ^{18}F-FDG-PET/CT with Magnetic Resonance (MRI) for the diagnosis of vasculitis, ^{18}F-FDG-PET/CT detected a higher number of vascular regions affected by inflammation and had greater reliability in after-immunosuppressive therapy patients. The standard uptake value (SUVmax) increases as the inflammation increases, therefore, could serve as a quantitative marker of infection/inflammation.

USE OF FDG-F18 PET/CT TO CONFIRM ISOLATED SUPERIOR MESENTERIC ARTERITIS.

Flores Turk, M. Guadalupe; Facello, Adolfo. Argentina; Claria, Marcelo; Lucino, Sergio; Heinzmann, Monica. Instituto Oulton. Córdoba. Argentina.

ARGENTINA

Acute mesenteric ischemia (AMI) is a syndrome caused by inadequate blood flow through the mesenteric vessels. AMI as arterial disease may be subdivided into non occlusive mesenteric ischemia (NOMI) and occlusive mesenteric arterial ischemia (related to mesenteric arterial embolism or thrombosis). Mesenteric vasculitis causing bowel ischemia is an occlusive rare condition, usually related to immunological and/or inflammatory disorders as rheumatoid arteritis, scleroderma, polyarteritis nodosa, IgG4-related disease, giant cell arteritis, Takayasu disease and others. Isolated superior mesenteric artery (SMA) pathological involvement is quite uncommon. We report a case of a 50-years old man with a chronic history of abdominal pain for irritable bowel syndrome and diverticulitis. He suddenly started with severe abdominal pain, fever and neutrophilia. An enhanced CT scan showed status for localized perforated diverticulitis and strong solid circumferential thickening of SMA wall, from the origin to distal portion, with no signs of dissection and no abnormalities en superior mesenteric vein. A Doppler showed four times increase of intra arterial velocities in SMA. An SMA arteritis was suspected and a no contrast enhanced PET/CT was performed administering intravenous 421.8 MBq of FDG-F18. Images were obtained in routine basis sixty minutes later. Diffuse increase in FDG metabolism (SUVmax 2.6) was observed in the horizontal four proximal centimeters of SMA and then a patchy aspect in the descending portion. No abnormalities were found on aorta and other great vessels in all body. Taking account of PET/CT results, isolated SMA arteritis diagnosis was retained, probably IgG4-related, nevertheless serum IgG serum level and other inmunological markers were normal. Treatment with initial schedule including 40 mg of prednisone was started with improvement of clinical symptoms. Two weeks after, a CT angiography was performed showing significant decrease in solid perivascular infiltrate. In conclusion, FDG-F18 PET/CT is useful for evaluate isolated SMA arteritis and to search other vessels involvement in arterial inflammatory disease.

18F-FDG PET/CT IN THE DIAGNOSIS OF MULTIFOCAL BACTERIAL MYOSITIS IN A PATIENT WITH FEBRILE NEUTROPENIA: A CASE REPORT.

Maidane Luisi Costa Maia Araujo.

BRAZIL

INTRODUCTION : In cases of febrile neutropenia, the determination of the infection site and the assessment of response to treatment are essential to the clinical management. Positron emission tomography/computed tomography with 18F - fluorodeoxyglucose (18F - FDG PET / CT) has an important role in determining the infectious focus.OBJETIVE: Our objective is to report a PET/CT of a patient with febrile neutropenia who had the diagnosis of multifocal bacterial myositis.

CASE REPORT : Man , 42 years old , with acute myeloid leukemia developed febrile neutropenia during hospitalization for consolidation chemotherapy. Blood cultures were positive for methicillin resistant staphylococcus. PET/CT was requested to determine infection site and showed hypermetabolic lesions in multiple muscle groups in the entire body, as well as pulmonary nodules. The diagnostic of multifocal bacterial myositis was considered. After antibiotic therapy, the patient underwent a control PET/CT in which the lesions previously described were no longer observed.

DISCUSSION : The multifocal bacterial myositis is a primary infection of skeletal muscles and occurs most frequently in immunocompromised patients .

CONCLUSION: 18F FDG PET/CT has an important role in the early diagnosis of these patients in order to avoid delays in treatment and progression for suppurative phase, as well as in the evaluation after pharmacological treatment.

GRANULOMA MIMICKING MALIGNANCY IN PET / CT : A CASE REPORT

Maidane Luisi Costa Maia Araujo.

BRAZIL

BACKGROUND: Positron emission tomography / computed tomography with 18F - fluorodeoxyglucose (18F - FDG PET / CT) is

notable for its high accuracy in the assessment of cancer patients . However, some benign lesions may accumulate 18F-FDG, leading to false positive results .OBJECTIVE: Our objective is to report a case of a patient who had a benign lesion mimicking malignancy in a PET/CT.CASE

REPORT : Man, 57 years old, diagnosed with poorly differentiated squamous cell carcinoma of the right lung 6 years ago . Patient underwent pneumonectomy, chemotherapy and radiotherapy and kept asymptomatic after 5 years of follow-up.RESULTS: 18F-FDG PET / CT was performed and showed a markedly hypermetabolic lesion in the right paravertebral region, near to the area of the right 5th rib segmental resection. This fiding was concerned for recurrence of the tumor and was correlated to a CT scan performed 3 years earlier. It was realized that the lesion was already present and remained unchanged , supporting the hypothesis of benign lesion, probably a granuloma.

DISCUSSION : 18F-FDG PET / CT is a very accurate test to detect tumor lesions. However , infectious and inflammatory processes can take up FDG intensely, leading to false positive results . The correlation with the clinical scenario as well as patient follow up can provide information for diagnostic determination. PET/CT interpretation requires knowledge of 18F-FDG physiological distribution, attenuation artifacts, malignant conditions that may be false-negative and benign conditions that may be false positives.

CONCLUSION: In conclusion, the nuclear medicine physician should be alert to the pitfalls of interpretation, which brings impact on staging, and therefore management of the patients .

USEFULNESS OF 99MTC-OCTREOTIDE AND 111IN-DTPA-OCTREOTIDE SPECT/CT FOR EVALUATING SYSTEMIC GRANULOMATOUS INFECTIONS.

Paulo Henrique Silva Monteiro.

BRAZIL

Objectives: To study the usefulness of SPECT/CT with radiolabeled somatostatin analogs (RSA) for the evaluation of patients with systemic granulomatous infections in comparison with gallium-67 citrate scintigraphy.

Materials and methods: Fourteen patients (10 female, 18 to 76 years-old, mean age: 41,4 +- 16.9 years) with active systemic granulomatous infections were studied: tuberculosis (6), paracoccidioidomycosis (4), pneumocystis (2), leishmaniasis (1), infectious vasculites (1). Twelve/14 had started specific treatment 8+- 4 days before imaging. All were submitted to whole-body and SPECT/CT imaging, seven of them 4h post-injection of 300 MBq of 99mTc-EDDA-HYNIC-TOC and, the remaining seven, 24h post-injection of 185 MBq of 111In-DTPA-octreotide. They were also submitted to whole-body and SPECT/CT imaging 48h post-injection of 185 MBq of gallium-67 citrate. Maximum interval between procedures was one week. Uptake was visually classified as mild, moderate or marked.Results: Eleven sites of active infectious disease were detected by both tracers (RSA and gallium-67) in nine patients. Both tracers were negative in five patients. 67Ga uptake was visually higher than RSA uptake in 7 of the 9 patients with positive images.

Conclusions: SPECT/CT with 99mTc-EDDA-HYNIC-TOC or 111In-DTPA-octreotide seems to be a good option for the evaluation of patients with systemic granulomatous infections when compared to 67Ga scintigraphy.

3D SURFACE RENDERED PET-CT IN SUSPECTED OSTEOMYELITIS POST CRANIOPLASTY OF AND AND INFECTED MYOCUTANEOUS FLAPS POST CRANIOFACIAL RECONSTRUCTIVE SURGERY

Shanker Raja , Yasser Orz, Yaser Ajadhai , Sharad George, Larson Sven.

UNITED STATES

Infections are a common occurrence, following cranial-facial surgery (cranSURG). Uncommonly underlying osteomyelitis (Uosteo) may complicate myocutaneous flaps, craniotomies, and skull base surgeries, leading to persistent/recurrent infected grafts or delayed healing of postsurgical bed. It is essential to determine Uosteo complicating infected grafts, since management significantly differs in complicated Vs. uncomplicated Uosteo. Traditionally Tc-99m bone scan, In-111 labeled WBC/Ga-68 and MRI have been used in evaluating osteomyelitis, however, the traditional modalities are limited in the surgically traumatized bone. PET-CT has been increasingly utilized to evaluate osteomyelitis of the diabetic foot and infected prosthesis. We have explored the use of PET-CT in Uosteo complicating post cranSURG.From Oct 2012 to date we have performed 10 PET-CT's in 8 patients for suspected Uosteo complicating cranSURG with/without grafts. When available, concurrent CT and/or MRI and PET were all coregistered and merged into one single common 3D space, the merged data were surface rendered and fused (gray scale –diag CT/MRI, pseudo-color scale -PET). 4/8 pts were neg for Uosteo by PET and clinical f/u, 3/7 pts had proven Uosteo, while 1 pt. had an infected titanium mesh. Of 2 pts pos for Uosteo, f/u PET-CT showed complete resolution in 1 pt, while the other pt had partial resolution on PET and is

on continued treatment.We will demonstrate in an atlas format the correlative findings on multimodality imaging, emphasizing 3D surface rendered images as a tool for tracking the sinuous sinus tracts in 3D space, as well as pre-procedural guidance for planned surgical interventions.

DOES HEPATOSTEATOSIS SIGNIFICANTLY AFFECT SUV MEASUREMENT IN 18F-FDG PET-CT IMAGING? COMPARISON BETWEEN DIFFERENT SUV MEASUREMENT TECHNIQUES

M. Fani Bozkurt Md Febnm, Berfin Temelli Md.

TURKEY

Hacettepe University Faculty of Medicine Department of Nuclear Medicine Ankara.

Objectives: In oncologic PET-CT imaging, liver is generally used as a reference organ for semiquantitative evaluation of 18F-FDG uptake. However, as being an organ which suffers from steatosis frequently, glucose metabolism in liver is expected to be decreased in the state of hepatosteatosis which may cause misleading measurements. The aim of this study is to assess the effect of hepatosteatosis on different SUV measurement techniques in 18F-FDG PET/CT imaging and to find out the most suitable SUV measurement technique for the patients with hepatosteatosis.

Materials and Methods: This is a retrospective study in which 444 patients who are recruited to PET/CT imaging were evaluated. Hepatosteatosis was diagnosed by calculation of the difference of attenuation between liver and spleen in HU (DHU) on non-enhanced CT images from PET/CT and defined as prominent hepatosteatosis, mild fatty infiltration and normal liver density if DHU≤-10, -9<DHU<10 and DHU≥10 respectively. On the basis of non-enhanced CT component of PET/CT imaging, 37 patients were found to have prominent hepatosteatosis, 279 patients showed mild fatty infiltration while the rest 131 had normal liver density. SUVmean measurements from PET images were both normalized to body weight as SUVbw and to lean body mass as SUVlbm and both values were measured in liver, spleen and mediastinum for comparative analysis. Density measurements in HU units from CT component of PET/CT imaging were also done in liver, spleen and mediastinum for regionwise comparative analysis.

Results: There was no significant difference in SUVbw measurements in all 3 sites between 3 groups, while liver SUVlbm measurements in hepatosteatosis group were lower than the other 2 groups showing that the decrease in glucose metabolism in the state of hepatosteatosis can only be measured with SUVlbm technique (p=0,05). Among the groups, only hepatosteatosis group showed significant positive correlation between liver SUVlbm and HU measurements. For the whole group of patients SUVbw measurements displayed significant correlation with body weight, BMI, VLDL, LDL, total cholesterol and trigliseride levels which proves that SUVbw measurement technique is actually affected by all these parameters, while there was no such significant correlation for SUVlbm.

Conclusion:SUVbw measurement technique cannot reflect the changes in liver glucose metabolism thoroughly in case of hepatosteatosis and therefore, SUVlbm as being a more reliable method should be the technique of choice in oncologic 18F-FDG PET/CT imaging when liver is used as a reference organ for semiquantitative analysis.

Federación Mexicana
de Medicina
Nuclear e Imagen
Molecular A.C.

4º Congreso de la Federación Mexicana de Medicina Nuclear e Imagen Molecular

25 al 28 de Junio de 2015·

Hotel Camino Real Monterrey, N.L.

Celebrando los 50 años de la Medicina Nuclear en México

B.P. SERVIMED, S.A. DE C.V.
Tel: + 52 (55) 9171-9570
Fax: + 52 (55) 5660-1903
E-mail: fmmn@servimed.com.mx
Web page: www.servimed.com.mx/fmmn15

NUM 1

VOL 2 • JANUARY - APRIL 2015